Preparation and characterization of engineered antigen presenting cells (APCs) for the generation of cytotoxic response for transplantation-related immunotherapy.

Lia Paola Zambetti

University College London

A thesis submitted to the University College London for the degree of Doctor of Philosophy

I, Lia Paola Zambetti, confirm that the work presented in this thesis is my own. Where information has been derived from other sources, I confirm that this has been indicated in the thesis.

A mamma e papa’

Perche’ senza di voi non ce l’avrei mai fatta.

Grazie.

ABSTRACT:

Expansion and activation of cytotoxic T lymphocytes (CTL) is one of the major goals of immunotherapy but the hurdles in generating a large number of antigen-specific CTL are manifold. One of the limiting factors is the scarce availability of antigen presenting cell (APC) for T cell priming; dendritic cells (DCs) are the best APCs but their generation from adult progenitors is difficult and expensive so there is currently an active research into suitable alternatives.

In this project, three different APCs models, cellular and acellular, were prepared and characterized and their potential use for clinical immunotherapy was explored. One setup was acellular, liposome-based, prepared from material currently used in *in vivo* applications and was tested *in vitro* both in human and murine settings. The other two APC systems were cellular-based; in both cases the antigen-presenting potential of a specific cord blood (CB)-derived cell population was evaluated *in vitro*. In the first case, a DCs-autologous responder culture was set up using whole frozen CB samples as starting material and tested in a peptide-specific model. In the second case, the antigen-presenting potential of γδ T cell in CB samples was evaluated and compared to the same population in adult, as γδ T cells have been recently shown to express antigen presentation-related markers and promote T cell proliferation in adult systems. All the three models were assessed for their practicality of preparation and use, antigen presenting capability and overall feasibility of employment in clinical settings.

ACKNOWLEDGEMENTS:

First of all I thank Prof JA Madrigal for having welcomed me in his laboratory. In these three and a half years I have learnt more than I thought possible. I also thank the late Prof IA Dodi (d. January 2008), my first supervisor, for having initially chosen me for this project and for having helped to set it up. He is greatly missed and this thesis is also dedicated to him. I am also thankful to Prof Sergio Querol for his constant support throughout the project.

A very heartfelt thanks goes to Jim Devitt, Richard Duggleby, Hazel Forde and Aurore Saudemont for their help in the various stages of my project. They have been at my side every day of my PhD and I could not have hoped for better colleagues. Thank you guys, you have been great.

A special thanks goes also to the Marie Curie network, the funding body of my scholarship. The biannual meetings we had around Europe have been brilliant occasions to meet up and share our project and competences together. I would especially thank Professors Ofer Mandelboim, Miguel Lopez-Botet, Stipan Jonjic and Bernard de Bono for their useful feedback and advice and Giuliana, Medya, Hormas and Erich for their friendship and the good time we had together.

I also thank Dr Bala Ramesh, at the Royal Free Hospital, Mr Franco Tavarozzi and his team, at the Anthony Nolan Histocompatibility lab, and Mr Alasdair McWhinnie at the Anthony Nolan Research Institute for their technical help and Prof Steven Marsh and James Robinson for having always come to the rescue when computer crisis arose.

Finally, I would like to thank all my lab mates, in particular Mehri for having taught me a thing or two about the real world outside the lab and Daniel and Sameer for their constant good humour.

TABLE OF CONTENTS:

LIST OF FIGURES:

CHAPTER 1: INTRODUCTION:

CHAPTER 2: MATERIALS AND METHODS:

CHAPTER 3: DEVELOPMENT AND CHARACTERIZATION OF LIPOSOME-BASED aAPCs FOR IMMUNOTHERAPY:

CHAPTER 4: PREPARATION AND CHARACTERISATION OF CB-DERIVED DCs FOR IMMUNOTHERAPY:

CHAPTER 5: CHARACTERISATION OF CB-DERIVED γδ T CELLS AND COMPARISON TO THEIR ADULT HOMOLOGUES:

LIST OF TABLES:

CHAPTER 2: MATERIALS AND METHODS:

CHAPTER 3: DEVELOPMENT AND CHARACTERIZATION OF LIPOSOME-BASED aAPCs FOR IMMUNOTHERAPY:

ABBREVIATIONS:

+ve	positive
-ve	negative
7-AAD	7-Aminoactinomycin D
aa	amino acid
aAPC	artificial antigen presenting cell
APC	antigen presenting cell (*or* allophycocyanin)
APS	ammonium persulphate
ATP	adenosine-5'-triphosphate
β_2m	beta-microglobulin
BCA	bicinchoninic acid
BCR	B cell receptor
BirA	biotin ligase enzyme
B-LCL	B lymphoblastoid cell lines
BP	biodegradable polymers
bp	base pairs
BrHPP	bromohydrin pyrophosphate
BSA	bovine serum albumin
CB	cord blood
CBMCs	cord blood mononucleated cells
CBT	cord blood transplantation
cDCs	conventional DCs
CDP	common DC precursor
CDR	complementarity determining region
CHOL	cholesterol
CLIP	MHC class II-associated invariant-chain peptide
CMV	cytomegalovirus
CMV-IP	cytomegalovirus (related) interstitial pneumonitis
cSMAC	central supramolecular activation clusters
CTL	cytotoxic lymphocyte

Cys	cysteine
DC	dendritic cell
DLI	donor lymphocyte infusion
DMSO	dimethyl sulphoxide
DNA	deoxyribonucleic acid
DNTB	5,5'-Dithio-*bis*-(2-nitrobenzoic acid)
dNTP	deoxynucleotide triphosphate
dSMAC	distal supramolecular activation clusters
DSPE-PEG	1,2-dystearoyl-sn-glycero-3-phosphoethanolamine -N-[methoxy (polyethylene glycol)-2000]
DTT	dithiotreitol
EBV	Epstein-Barr virus
EDTA	ethylenediaminetetraacetic acid tetrasodium salt dihydrate
EGFR	epidermal growth factor receptor
ELISA	enzyme-linked immunosorbent assay
ELIspot	enzyme-linked immunosorbent spot
ER	endoplasmic reticulum
Fab	antigen-binding fragment (of an antibody)
FACS	fluorescence activated cell sorting
Fc	crystallisable fragment (of an antibody)
FCS	fetal calf serum
FITC	fluorescein isothiocyanate
FPLC	fast protein liquid chromatography
FSC	forward scatter
G-CSF	granulocyte colony-stimulating factor
GM-CSF	granulocyte macrophage colony-stimulating factor
GMP	good manufacturing practice
GvHD	graft versus host disease
GvT	graft versus tumour
HEPES	4-(2-hydroxyethyl)-1-piperazineethanesulfonic acid

HIV	human immunodeficiency virus
His	histidine
HLA	human leukocyte antigen
HMBPP	hydroxymethyl but-2-enyl pyrophosphate
HRP	horseradish peroxidase
HSC	hematopoietic stem cells
HSCT	hematopoietic stem cell transplantation
iDC	immature DC
IFN	interferon
IgSF	immunoglobulin superfamily
Ii	invariant chain
IL	interleukin
IPP	isoprenylpyrophosphate
IPTG	isopropyl β-D-1-thiogalactopyranoside
IU	international unit
LB	Luria-Bertani
LMV	large multilamellar vesicles
LPS	lipopolysaccharide
mA	milliampere
MAL	1,2-dystearoyl-sn-glycero-3-phosphoethanolamine -N- [maleimide (polyethylene glycol) - 2000]
mDC	mature DC
MDP	macrophage/DC precursor
MEP	2-C-methyl-D-erythritol-4-phosphate (pathway)
MES	2-(N-Morpholino)ethanesulfonic acid
MHC	major histocompatibility complex
MHSC	mobilized hematopoietic stem cells
MLR	mixed lymphocyte reaction
mRNA	messenger RNA
MWDa	molecular weight (expressed in) Dalton
NEAA	non-essential amino acid

NK	natural killer
nm	nanometre
OD	optical density
ORF	open reading frame
PAMPs	pathogen-associated molecular patterns
PBMCs	peripheral blood mononucleated cells
PBS	phosphate buffered saline
PC	phosphatydilcholine
PCR	polymerase chain reaction
pDC	plasmacytoid DC
PE	phycoerythrin
PEG	polyethylenglycole
PerCP	peridinin chlorophyll protein complex
PFA	paraformaldehyde
PHA	phytohemoagglutinin
PLGA	poly(lactide-co-glycolide)
poly I:C	polyinosinic: polycytidylic acid
PRR	pattern recognition receptor
pSMAC	peripheral supramolecular activation clusters
RHODA	[1,2-dipalmitoyl-sn-glycero-phosphoethanolamine -N-(lissamine rhodamine B sulfonyl)
RNA	ribonucleic acid
rpm	revolutions per minute
RT	room temperature
RT-PCR	reverse transcriptase PCR
SCID	severe combined immunodeficiency
SDS	sodium dodecyl sulphate
SLO	secondary lymphoid organs
SMAC	supramolecular activation clusters
SSC	side scatter
SSP	single specific primer
TAP	transporter associated with antigen presentation

T_{CM}	central memory T cells
TCR	T cell receptor
T_{EM}	effector memory T cells
TEMED	tetramethylethylenediamine
Tet	tetramer
TLR	Toll like receptor
TNF	tumour necrosis factor
TNFR	tumour necrosis factor receptor family
Tris HCL	tris(hydroxymethyl)aminomethane hydrochloride

CHAPTER 1:
INTRODUCTION

1.0.0 INNATE AND ADAPTIVE IMMUNE SYSTEM:

The immune system is a complex organization of cells and molecules specializing in the defense against exogenous infections as well as against self-cells that have become abnormal or cancerous. Vertebrate organisms demonstrate 2 different types of immune responses against pathogens, each mediated by different types of cells and molecular effectors: the *innate* response has the same extent and magnitude every time the pathogen is encountered, while the *acquired* (also called *adaptive*) response improves with every exposure to the pathogen, crucially maintaining memory of past challenges.
The innate response relies on phagocytic cells such as neutrophils, monocytes and macrophages, on cells secreting inflammatory mediators (basophils, mast cells and eosinophils) and on natural killer (NK) cells. The acquired response relies instead on the proliferation of antigen-specific B and T cells; this phenomenon happens after the specialized receptors on their surface engage the antigen (Delves and Roitt, 2000a). Whilst the innate response relies upon germ line-encoded receptors, the adaptive is dependent upon the rearrangement of a small number of gene segments to constitute a large repertoire of receptors each with different specificity (Janeway, 2005).

1.1.0 T CELLS AS KEY PLAYERS IN THE ADAPTIVE IMMUNE RESPONSE:

The components of the acquired immune system are B and T cells. Whilst B cells are responsible for the secretion of antibodies and fulfil a fundamental role in immune response, the focus of this project is on T cells, thus they will be described in more detail. All T cells have a T cell receptor (TCR), which is antigen-specific and whose complex structure will be described in the next paragraphs. T cells can be subdivided into αβ or γδ (Brenner *et al.*, 1986) according to the chains that constitute the TCR. As αβ T cells are the most common every T cell mention in the text will always refer to them unless explicitly stated.

T cells can be divided into 2 subsets, CD4 or CD8, according to the expression of the corresponding co-receptor. CD8 T cells are mainly killer cells whereas CD4 T cells are mainly helper cells, secreting cytokines and with limited direct cytotoxic activity (Delves and Roitt, 2000b). CD4 cells can have various secretion patterns and the most common are named Th1 and Th2 (Mosmann and Sad, 1996). Th1 CD4 T cells are generated in response to pathogens accumulating in intracellular vesicles in macrophages and dendritic cells (DCs). Th1 cells secrete preferentially IL-2 and IFN-γ and elicit a strong cytotoxic response aimed at clearing intracellular pathogens (this kind of response is fundamental for effective eradication of *M. tuberculosis* and *M. leprae* infections, amongst others) and of viral-infected cells. Th1 CD4 T cells stimulate macrophage antimicrobial activity and promote phagocytosis. Th2 CD4 T cells, on the other hand, secrete IL-4, 5, 6, and 10 but not IL-2 or IFN-γ (Delves and Roitt, 2000b). This profile is most effective on parasitic infection and promotes mainly a humoral response with the production of different antibodies isotypes.

1.1.1 T CELL RECEPTOR (TCR):

1.1.2 αβ TCR:

Each T lymphocyte expresses on its surface approximately 30.000 identical T cell receptors (TCR) (Janeway, 2005). Each TCR is composed of 2 different chains, termed TCRα and TCRβ, which are linked by a disulfide chain. The TCR heterodimer is responsible for antigen recognition: the TCR αβ is the most frequent isoform in humans (up to 95% of circulating lymphocytes) and recognizes major histocompatibility complex (MHC) class I-peptide complexes present on the surfaces of all nucleated cells and MHC class II-peptide complexes expressed on the surface of antigen presenting cells (APCs). Antigen presenting cells constitute a specialised subset of various cell types whose main function is to present antigens in an immunogenic form to the cells of the immune system; the most important members of the APC family are dendritic cells (DCs). The topic of APCs and DCs will be discussed in more detail from section 1.1.4 onwards.

A minority of T cells, 2-10% in adults (Otto *et al.*, 2005), expresses a TCR formed by a γδ heterodimer (Brenner *et al.*, 1986). γδ T cells recognize nonclassical MHC-peptide molecules, bisphosphonate antigens and other proteins such as NKG2D. They are important in innate immunity and seem to have a regulatory function as well, however their current physiological role is still unclear and they are the objects of intense investigation.

1.1.2.1 αβ TCR GENE REPERTOIRE:

Both the α and β chains are composed of an NH_2-terminal variable region, a COOH-terminal constant region and a short zipper region containing the Cys that forms the disulfide bond between the chains (Janeway, 2005). Similarly to what happens for antibody chains, both α and β chains are formed from a large number of smaller DNA fragments (Davis and Bjorkman, 1988). Their recombination ensures the large number of antigen specificities that characterizes the T cell potential for antigen recognition. The α chain locus (situated in chromosome 14 in humans) contains between 70 and 80 V (variable) fragments, 61 J (joining) fragments and a single C (constant) fragment, termed respectively V_a, J_a and C_a. The β chain locus (situated on chromosome 7 in humans) contains 52 V fragments, 6 or 7 J fragments in 2 different positions on the chromosome, 2 C regions and 2 D (diversity) fragments, termed respectively V_b, J_b, C_b and D_b (Janeway, 2005).

The rearrangements mediated by these gene fragments can generate up to $\sim 10^{18}$ different TCRs; each TCR will be unique to a single T cell, which will be screened for absence of self-reactivity in the thymus prior to being released into the periphery. After the engagement of a TCR with the ligand it specifically recognizes, T cells will undergo activation and possibly clonal expansion. As the ligand for the TCR is always an MHC-peptide complex, it is logical that the highest variability for the TCR is found in the peptide binding region, which is encoded mainly by the V, D and J gene fragments. The antigen-binding region of the TCR is subdivided into 3 complementarity determining regions (CDR 1, 2, 3). The CDR3 is where the TCR diversity concentrates most, as it where the TCR is in contact with the target peptide (Davis and Bjorkman 1988 and

Jorgensen *et al.*, 1992), while the CDR1 and 2 binds to the MHC protein, surrounding the peptide.

1.1.2.2 αβ TCR GENE REARRANGEMENT:

During the T cell development, the β chain is rearranged and expressed firstly, with the union D_β--> J_β to form DJ_β. This novel gene then rearranges with V_β to form VDJ_β and only at this point a surrogate α chain is attached to the newly formed, rearranged β chain to form a pre-TCR to be expressed on the surface of the maturing T cell (Janeway, 2005). This step also triggers the co-expression of both CD4 and CD8 co-receptors and the end of further recombination for the β chain. Therefore, at this stage, T cells are called double positive and constitute around 80% of total thymocytes (Petrie *et al.*, 1993). A phase of rapid proliferation of double positive cells ensues; at the same time, each cell rearranges independently a functional α chain, following a stepwise process similar to that observed for the β chain (Malissen *et al.*, 1992). During the α chain rearrangement, a complete αβ TCR is expressed for the first time and the T cell selection against autologous MHC-peptide is started. Figure 1.1, below, resumes the genetic recombination steps leading to the production of a functioning αβ TCR in the thymus.

Figure 1.1: scheme of αβ TCR recombination. Modified from Janeway, 2005.

1.1.3 γδ TCR:

γδ T cells constitute a minority in the general pool of T cells in adults. Similarly to αβ T cells, γδ also undergo various stages of chain formation, with γ chains being always assembled via V-J rearrangements and δ chains via V-D-J rearrangements. In contrast, their CDR 1 and 2 regions are longer than their homologs in αβ cells (Hayday, 2000). They also are usually CD4 and CD8-negative, contrarily to conventional αβ T cells. The processes that lead to a formation of the αβ and γδ lineage are still unclear and under active investigation (Archbold, 2009); the signal strength, rather than the type, of the TCR seems to be the most important factor in deciding which type of receptor will be selected and expanded (Hayes *et al.*, 2005).

In healthy adults, the majority of the γδ T cells in peripheral blood –up to 80%- express Vγ9 and Vδ2 chains and are, therefore, termed "Vγ9Vδ2" (Schondelmaier *et al.*, 1993 and Brandes *et al.*, 2009). However, the chain repertoire prevalent in the γδ population depends on the tissue examined and its origin (whether from healthy or infected adult or from adult or child). γδ T cells can be found in blood and other anatomical locations

but, strikingly, they are very rarely found in secondary lymphoid organs such as the lymph nodes or the spleen (Hein and Mackay, 1991)-i.e., the main locations associated with antigen presentation to T cells and where T cell clonal expansion occurs. This important feature suggests that γδ T cells do not rely on professional antigen presenting cells (APCs) for antigen presentation and recognition, but that they rather may recognize antigens directly in tissues. This hypothesis, together with the limited diversity of the γδ TCR, is consistent with a role for γδ T cells in the first line of defence (Janeway *et al.*, 1988) and suggests that γδ T cells recognize directly stress antigens, a hallmark of infected or transformed cells, rather than classical, MHC-presented microbial antigens (Hayday, 2000).

1.1.4 T CELL ACTIVATION:

All types of T cells require a concerted set of signals before being able to fulfil their physiological functions and activities; these signals are usually provided to them by APCs. For the complete activation of naïve CD8 and CD4 T cells, more than one input is required. The first and foremost requirement is antigen complexed to the relevant MHC molecule, leading to MHC-TCR engagement ("signal 1"). Then there is the need for costimulation, provided through the CD28-B7 family of molecules ("signal 2"). However, even the presence of signal 1 and 2 is not enough to fully activate a naïve T cell (Jenkins and Johnson, 1993), as they require in addition a "signal 3" that can be provided by a cytokine, usually either IL-12 (Curtsinger *et al.*, 1999) or type I IFN (i.e. IFN α or β) (Curtsinger *et al.*, 2005). "Signal 3" performs as a molecular switch and its presence determines whether the exposure to antigen will result in tolerance or complete activation and development of memory (Curtsinger *et al.*, 2003).

1.1.5 THE IMMUNOLOGICAL SYNAPSE:

T cell activation requires, in most cases, physical contact between T cell and APC to bring the TCR and the MHC complexes together. This contact is defined by the sizes of the complexes involved (MHC and TCR), which at roughly 13 nm requires widespread

interdigitation of the glycocalyx of both T cell and APC (Dustin, 2008). The interaction between T cells and APCs causes the formation of specialized signalling areas, termed immunological synapses. Immunological synapses were first defined as such in the late 1990's (Grakoui *et al.*, 1999), even if their existence as conjugate or cell pairs was first described and studied in the late 1970s. Micrometer-scale molecular complexes that form within minutes after the T cell-APC interaction are present at the immunological synapse; they are called supramolecular activation clusters or SMACs (Monks *et al.*, 1998). A SMAC is composed of 2 concentric regions: the inner one is termed central SMAC (cSMAC) and is the region with the highest concentration of TCR, while the outer one is called peripheral SMAC (pSMAC) and is enriched in the integrin LFA-1 (on the T cell side) and in its ligand ICAM-1 (on the APC side). Also a distal SMAC (dSMAC) has been characterized and the signature molecule of this region is CD45 (Freiberg *et al.*, 2002). The immunological synapse fulfils various useful functions for T cell activation, among them:

- It acts as a braking mechanism, effectively ceasing rapid T-cell migration and allowing T cells to remain in contact with APC or target cells for hours.
- It is important as a spatial marker, setting up an actin-depleted central secretory domain allowing membrane traffic in both directions from the centre of the synapse. It also acts as a gasket surrounding the secretory domain, retaining macromolecular complexes in the SMAC.
- It contributes to set an axis of asymmetry, which may be important for prolonged signal transduction and asymmetric cell division, such as occurs during differentiation processes.
- The immunological synapse stability may finally play a role in deciding other aspects of T cell fate, like Th1-Th2 switch (Monks *et al.,* 1998 and Dustin, 2008).

The role of cSMAC and pSMAC in the immunological synapse is still the subject of active debate. When it was first discovered it was thought that the peculiar molecular segregation observed could be linked to T cell activation. In particular it was speculated

that the cSMAC would boost signalling and allow a few MHC-peptide complexes to promote T cell activation (Monks *et al.*, 1998). This very reasonable hypothesis was challenged by the fact that TCR signalling begins in the periphery and is precedent to TCR clustering in the cSMAC. It was then proposed that molecular segregation in the SMAC reflected another type of functional distinction, with the peripheral area (pSMAC) corresponding to an area of productive signalling and the central area (cSMAC) not contributing to the signalling, but rather being a site for TCR internalization and degradation (Lee *et al.*, 2003 and Varma *et al.*, 2006). This hypothesis was initially suggested since the intensity of signalling was lower in the cSMAC than in the pSMAC (Lee *et al.*, 2003). Recently this model has been amended taking into account the strength of the antigen binding as a factor. Shaw's group *(*Cemerski *et al.*, 2008) found that a weak antigenic stimulus (for example, a suboptimal concentration of antigenic peptide or a peptide-MHC complex with a short half-life, therefore unable to form sustained interaction with the TCR) triggered sustained TCR signalling, as measured by protein tyrosine phosphorylation, in the cSMAC. Using a strong antigenic stimulus (in this case, optimal peptide concentration), the readout system gave a lower signalling level, possibly due to TCR down-regulation. However, when TCR down-regulation was blocked, signalling markers were detected in the cSMAC. This and other data suggested that the cSMAC could work as an adaptive controller of T cell activation and promote enhancement of weak signals and attenuation of strong ones (Cemerski *et al.*, 2007). The evidence from Cemerski *et al.*, 2008, suggests that, although TCR signalling is initiated in the immunological synapse periphery, its continuation evolves differently according to the strength of the antigen. If the antigen stimulus is strong the TCR will be rapidly degraded. As such, although productive signalling occurs in the cSMAC, its effective readout will be hampered by the rapid degradation of the signalling pathway components. If the antigen stimulus is weak, instead, the rate of TCR degradation is slow and signalling is more easily detected in the cSMAC. A representative example of immunological synapse between a DCs and a T cell is presented below in Figure 1.2.

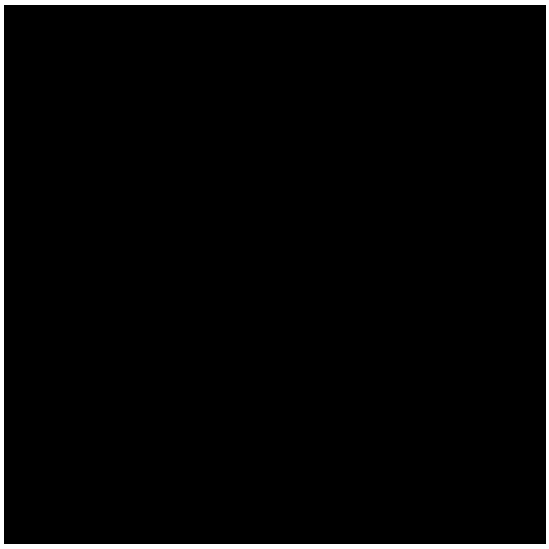

Figure 1.2: representation of an immunological synapse between a T cell (in blue) and a dendritic cell (in grey, in the lower part of the picture). The immunological synapse is in the centre of the figure (red = adhesion, bright green = foreign antigen). This is a composite image of a scanning electron micrograph and a fluorescence image. Picture taken by Michael Dustin.

T cells can be subdivided into various subsets according to their phenotype and functionality. "Naïve" T cells are cells that have not yet encountered their cognate antigen; once they have been activated by antigen-specific APCs they will undergo a robust expansion, resulting in the generation of a large "effector" T cell population. After the rapid expansion, and the clearance of the infection, the effector population will contract (up to 95% of effector cells die by apoptosis) and the surviving pathogen-specific T cells form the "memory" population (Obar and Lefrançois, 2010). The generation and phenotype of these subsets will be discussed in more detail in section 1.1.7.

1.1.6 THE IMPORTANCE OF COSTIMULATION:

Effector T cells can be activated simply by TCR engagement with the specific MHC-peptide complex. Once the TCR is engaged with the MHC molecule, it is complexed with an ensemble of molecules acting as coreceptors and collectively termed CD3. The CD3 is a signal transmission complex and its components are one CD3γ, one CD3δ and two CD3ε chains, together with a disulphide-linked ζ chain homodimer. When TCRs

cluster, which happens when the TCR molecules engage the peptide-MHC complexes on the cell surface, the activation signal cascade is initiated via the phosphorylation of the tyrosines in the cytoplasmic segments of the CD3 complex. The activation of the CD3 leads to a downstream signal to the nucleus that initiates various transcriptional responses including the up-regulation of cytokines that stimulate proliferation and survival of T cells.

Naïve T cell activation occurs only if additional signals, such as costimulatory molecules ("signal 2") and cytokines ("signal 3") are present. In fact, costimulatory molecules (either positive or negative) are crucial players in all stages of T cell response. The majority of the costimulatory molecules belong to one of three groups: immunoglobulin superfamily (IgSF), tumour necrosis factor receptor (TNFR) family and integrin family.

The IgSF superfamily is also known as B7 family and counts six members: the fundamental CD80 (also known as B7-1) and CD86 (B7-2), then B7-H1/PDL1, B7-DC/PDL2, B7-RP-1 and B7-RP-2. Various ligands for the B7 molecules have been identified on T cells but the most important are CD28 (for positive costimulation) and CTLA-4 (for negative costimulation) recognized by both CD80 and CD86 (Song *et al.*, 2008). CD80 and CD86 share about 25% sequence homology and, while interacting with their receptors, the binding of CD80 is stronger, as measured by equilibrium dissociation constant (Van Der Merwe and Davis, 2003). CD80 and CD86 also differ in their presentation on the cell surface, with CD80 reported to exist as a dimer (Ikemizu *et al*., 2000), while crystallographic data indicate that CD86 is unlikely to form a stable dimer (Collins *et al*., 2002). While CD80 and CD86 are generally considered to have overlapping roles, data from Davis's group (Collins *et al*., 2002) suggest that CD80 is likely to be a more potent ligand for CTLA-4, based on both higher affinity and avidity, thereby resulting in an inhibitory effect/phenotype. Conversely, CD86 is probably a more effective ligand for CD28 than CD80, at least in some circumstances, as its effects seem to be less opposed by CTLA-4 (Sansom *et al.*, 2003). These considerations suggest that cells expressing both CD80 and CD86 (i.e., APCs) have the potential to

promote stimulation of T cells as well as its opposite-tolerization. Therefore, the possibility of a tolerogenic phenotype when generating APCs should be evaluated.

The TNFR family, expressed on T cells, includes 4-1BB ligand (also known as CD137) and OX40 (CD134) and bind Tumour necrosis factor (TNF) molecules expressed by APC. Finally, integrin molecules, which are a family of heterodimers formed by two chain (α and β) covalently linked, forming LFA-1, are a fundamental component of the immunological synapse (Song *et al.*, 2008). Costimulatory signals can have many different functions, including increasing IL-2 production, promoting progression through the cell cycle or inducing cytokine synthesis and secretion. The CD28-B7 binding provides the most important effect of costimulation, which is the increase of IL-2 production via both mRNA stabilization and activation of nuclear transcription factors AP-1 and NF-kB (Zhou *et al*., 2002). When T cells engage their TCR without concomitant CD28-B7 binding, IL-2 production is very limited and T cells do not proliferate, becoming anergic instead. The crucial relevance of IL-2 in acquired immunity is well explained by the immunosuppressive drugs used to prevent transplant rejection: cyclosporin A and tacrolimus both inhibit IL-2 production by blocking the TCR-transmitted signals, while rapamycin inhibits the signal transmission mediated by IL-2 receptor (Janeway, 2005). A scheme summarising the signals required for full T cell activation is shown below in Figure 1.3.

Figure 1.3: scheme resuming all the signals required for full T cell activation. Modified from Steenblock *et al.*, 2009. The numbers on the arrows refer to the type of signal mediated by the indicated molecules.

1.1.7 CD8 AND CD4 T CELL SUBSETS:

CD8 T cells can be subdivided into various types according to their maturation -effector vs memory T cell, for example. All T cells, when they leave the thymus after their education (positive and negative selection), are naïve- i.e. they have not encountered any antigen yet. Naïve CD8 T cells usually migrate through secondary lymphoid tissues, the location where they come across their cognate antigen and the appropriate costimulatory molecules (both provided by a professional APCs), to be primed. This occurrence triggers clonal expansion, which mediates an enormous increase in a given antigen-specific T cell population during the subsequent effector phase and also results in the generation of T cells subpopulations with different phenotypes and distinct functions (Williams and Bevan, 2007). Effector cells are predominant in the clonal

expansion and they are characterized by a cytotoxic potential and by the secretion on IFN-γ, TNF-α, and/or IL-2.

Following clearance of the pathogen and contraction of the overall T cell population a small percentage of long-lived cells can survive for a long time. Those cells are generically termed "memory cells" and, in contrast to naïve cells, can reactivate specific effector functionality extremely quickly when challenged, even within minutes. Moreover, an effector cell population can expand rapidly starting from memory T cells (Stemberger *et al.*, 2007). The "readiness" of memory T cell to respond to secondary infections results from their persistence in a pro-growth state, with high levels of cyclin-dependent kinase 6 (CDK6)-cyclin D3 complex (Badovinac *et al.*, 2002), and from the maintenance of mRNA expression of cytotoxic proteins, cytokines and chemokines.

CD4 T cells can also be subdivided in various subsets, according to their cytokine secretion pattern and function. Historically, Coffman's group described 2 subsets of CD4 T cells according to the secretion of IFN-γ or IL-4 (Mosmann *et al*., 1986), however it is now acknowledged that naïve CD T cells have at least 4 different fates that are determined by the combination of signals they receive upon the initial interaction with the antigen and are termed Th1, Th2, Th17 and induced regulatory (iTreg) cells (Zhu and Paul, 2008). Th1 cells mediate responses against intracellular pathogens and have a fundamental role in the response to mycobacterial infections in humans. The predominant cytokines secreted by Th1 cells are IFN-γ, IL-2 and lymphotoxin α (LT-α) (Mosmann and Coffman 1989). Th2 cells mediate the adaptive immune response against extracellular pathogens (including multicellar parasites such as helminths) and have been implicated in playing an important role in the induction and persistence of asthma and allergic diseases. Their main cytokine products are IL-4, IL-5, IL-9, IL-10, IL-13, IL-25 and amphiregulin (Zhu and Paul, 2008). Th17 cells promote the immune responses against extracellular bacteria or fungi (Weaver et al., 2006), but are also important in the induction of many organ-specific autoimmune diseases. They secrete IL-17a, IL-17f, IL-21 and IL-22. Finally, iTreg cells secrete TGFβ, IL-10 and IL-35; like all Tregs, irrespective of their origin, they are fundamental

both in maintaining self-tolerance and regulating the immune response (Sakaguchi, 2004). An increase in their numbers or suppressive activity could be beneficial to treat autoimmune pathologies and to prevent allograft rejection (Zhu and Paul, 2008).

1.1.8 KINETICS OF T CELL ACTIVATION:

T cells become activated following their interaction with an APC presenting a peptide-MHC complex and costimulatory molecules of the B7 family, able to bind to the CD28 expressed on T cells. The number of naïve T cells specific for each distinct epitope is very low (1 in 10^6-10^7), so each T cell must contact and interrogate many different APC to find the one presenting its cognate antigen on its surface (Henrickson and von Andrian, 2007). To maximize a positive antigen encounter, the half-life of T cells in the bloodstream is limited (approx 30 min) as circulating lymphocytes are continuously recruited into the secondary lymphoid organs (SLO), where the professional APCs reside. SLOs include the spleen, which collects antigens from the blood, lymph nodes, which collect antigens from the skin and solid organs, and Peyer's patches, where antigens from the gut lumen are collected and presented. T cells remain in the SLOs for approximately one day before returning to the bloodstream and during this period they crawl in an amoeboid manner displaying a cellwalk-like behaviour (Miller *et al.*, 2003). It has been calculated that the average speed of naïve T cells is approx 12 μm/minute (Mempel *et al.*, 2004b). Assuming a 23h/day permanence in the SLO, each T cell would cover more than 6 meters/year.

In an experiment aimed to elucidate the kinetics and timings of antigen presentation in an *in vivo* model (Mempel *et al.*, 2004a), it was found that T cells priming in lymph nodes occurs in three distinct phases. After DCs and T cell injections in recipient mice, and following injection of anti L-selectin (that blocked further lymphocyte homing to the lymph nodes), the first phase of T cell priming lasted approximately 8 hours and was characterized by brief T cell-DC encounters where T cells moved rapidly and scanned many APC. Phase two covered the period between 8 and 24 hours after the adoptive cell transfer. In this phase the T cell-DCs conjugates became more stable and

lasted for more than 1 hour. T cell velocity slowed down and by the 20th hour T cell started secreting IL-2 and IFN-γ: expression of activation marker was abundant but no cell division occurred yet. Phase three started 1 day after T cell homing; in this phase T cells detached from the DCs, started a massive proliferation and left the lymph nodes (Mempel *et al.*, 2004a). The expression of the activation markers CD25 and CD69 diminished, whilst CD44 expression remained high. T cells still made contacts with DCs at late time points (44-48 hours), but it is not clear if such interactions are productive, as DCs may not have any more antigenic peptide at that time. This pattern was followed also when DCs did not present any antigen, even if in this case phase two was shorter than with antigen-bearing DCs (Mempel *et al.*, 2004a).

1.1.9 MEMORY T CELL EXPANSION:

Lanzavecchia's group showed the difference between effector and naïve T cells in their requirements for activation during a study aimed at highlighting the importance of the duration of antigen stimulation in determining the fate of naïve and effector T cells (Iezzi *et al.*, 1998). They found that naïve T cells require a very long antigenic stimulation (20 hours) to become committed. In contrast effector T cells require 1 hour only (Iezzi *et al.*, 1998). However, the latter undergo activation-induced cell death if stimulation is prolonged. High levels of antigens and the presence of CD28 costimulation shortened the time required by naïve T cells for commitment. However, even under the best conditions, there is a 20-fold difference in the time required for commitment between effector and naïve T cells. Also their reaction to high antigen dose is different; it increases activation-induced cell death for effector T cells, while costimulation reduces it. Costimulation via CD28 has been shown to enhance massively the response of naïve T cells to low doses of antigen, where no T cell activation could be detected even in the presence of maximal TCR engagement. It has been shown that IL-2 also plays an important role in T cell activation but, even in presence of IL-2 in the culture medium, naïve T cells still have a minimum 6 hr commitment time. In fact, the 6 hours required for commitment correlate with the slow kinetics of IL-2 receptor α chain

expression, whose up-regulation occurs indeed after 6 hours of antigenic stimulation (Iezzi *et al.*, 1998).

1.1.10 THE PHENOTYPE OF MEMORY T CELLS:

Memory cells can be subdivided into 2 different types: effector memory T cells (T_{EM}) and central memory T cells (T_{CM}). T_{EM} are preferentially found in peripheral tissue, they have immediate effector functions upon encounter with an antigen but have poor proliferative potential. T_{CM}, on the other hand, usually reside in lymphoid organs, can produce large amounts of IL-2 and are able to expand massively upon antigen encounter (Sallusto *et al.*, 2004). The various classes of effectors cells can be discriminated according to the expression of CD62L, the lymph node homing receptor, CD127, the α chain of the IL-7 receptor, and CD27, a member of the TNF receptor superfamily. The expression of the said markers correlates well with the functional properties of the cells types they are expressed on: T_{CM} are CD127/CD27^{high}CD62L^{high} and T_{EM} are CD127/CD27^{high}CD62L^{low}. Memory T cells can also be subdivided according to the expression of C-chemokine receptor 7 (CCR7), which is present on various lymphoid tissues and promotes the activation of B and T cells. CCR7 expression correlated with CD62L expression, and they are both expressed by T_{CM}, while T_{EM} are negative for both markers (von Andrian and Mackay, 2000).

1.1.11 THE EFFECTOR MECHANISMS OF T CELLS:

How do cytotoxic T cells exert their action? The cytotoxic activity of T cells is mediated either by the secretion of proteins by the T cells or by the activation of specific pathways in the target cell. Cytotoxic molecules belong to two groups: cytotoxins, which are stored in lytic granules in the cytosol, and cytokines, which are synthesized *de novo* by all effector T cells (Janeway, 2005).

Cytotoxins are the main effector molecules and their release needs to be tightly controlled as their actions are unspecific and can exert their cytotoxic effects on any cell within their range of action, not necessarily on the target only. Cytokines, on the other

hand, have a receptor-specific effect. The principal cytokine released by CD8 effector cells is IFN-γ (Harty *et al.*, 2000), which can block viral replication and even eliminate the virus without killing the cell hosting it.

Cytotoxic T cells can kill directly their target cell or induce its apoptosis. The first mechanism is mediated by the release of the proteins stored in the lytic granules, following the recognition of the antigen in the surface of the target cells. Lytic granules are modified lisosomes and contain three different classes of cytotoxic proteins (perforin, granzymes and granulolysin). The perforin, as the name suggests, polymerises and creates pores in the membrane of the target cells, leading to water entry and disruption of cell integrity. Granzymes and granulolysin can both induce apoptosis once in the target cells and the same effect is mediated by the Fas ligand (CD178) (Shresta *et al.*, 1998), which induces apoptosis of target cells expressing the Fas receptor (CD95) (Harty *et al.*, 2000).

1.2.0 ANTIGENS AND EPITOPES-DEFINITION:

The immune system in humans is able to mount a protective response against anything that can be bound by the receptors of either the innate or adaptive immune system. A compound is generically termed “immunogen” if the cells of the immune system can mount a response against it, regardless of the subtype of cell involved. An “antigen” is any compound or substance that can bind an antibody. Antigen size and chemical composition can vary greatly. An antigen that triggers an immune response is called immunogenic, but there are also antigens, called haptens, that are not immunogenic (Delves and Roitt, 2000a). Haptens need to be coupled to larger immunogenic molecules termed carriers to be rendered immunogenic (Mitchison, 1971). Large proteins are usually immunogenic on their own; carbohydrates, on the other hand, require often to be joined to proteins to elicit an immune response, for example in vaccine preparation. In the case of T cells, the overall length of the antigen recognized by the TCR is usually between 9-15 aa. As such, T cell receptors recognize only a part

of a complex antigen (such as a whole viral protein, as it might be the case of cytomegalovirus pp65), which is called an epitope.

1.2.1 MHC:

The αβ TCR –and, by extension, any CD4+ve or CD8+ve T cell- can mount a response against an antigenic peptide only if this is presented by a molecule of the MHC family. As a consequence, every pathogen able to evolve and escape MHC presentation would have a strong selective advantage. However MHC genes, which in human are called Human Leukocyte Antigen (HLA), are polygenic and extremely polymorphic. In fact, they are the most polymorphic set of genes in the entire human genome and this marked variability results in complete MHC escape being more difficult. The number of HLA alleles is continuously growing and, up to October 2010, there are 5,674 total class I and class II HLA alleles divided in HLA-A, B and C (class I HLA alleles) and HLA-DP, DQ, DR (class II HLA alleles). Any individual can either be homozygous or heterozygous for each of the alleles stated above. Peptides bind to a MHC molecule according to their origin, as follows:

- Peptides coming from the cytosol, derived from intracellular pathogens, are presented by MHC class I molecules, which are expressed on every nucleated cell in the organism, to CD8 T cells. The MHC class I pathway provides a system to display a sample of the proteome synthesized by every cell at any given time. This enables CD8 T cells to kill cells that express viral proteins as a result of viral infection and tumour antigens as result of cancer transformation.
- Extra-cellular peptides, which have been internalized and processed, or peptides derived from pathogens proliferating in intracellular vesicles, are instead presented on MHC class II molecules to CD4 T cells. The expression of MHC class II molecules is restricted to APCs such as DCs, B cells, macrophages and thymic epithelial cells. Since CD4 T cells can stimulate other subsets of the immune system, it seems appropriate that only cells that can regulate an immune response (ie. APCs) can activate them. In fact, the surface presentation of MHC

class II molecules and the expression of costimulatory molecules are tightly regulated processes, reflecting the importance CD4 T cells have in adaptive immunity (Jensen, 2007).

According to this model extracellular peptides should not be presented on MHC class I molecules for recognition by CD8 T cells: however, dendritic cells (DCs) are able to present extracellular peptides on MHC class I molecules (cross presentation) for recognition by CD8 T cells (cross priming) (Albert *et al*., 1998, and Mellman and Steinman, 2001).

1.2.1.1 MHC CLASS I AND II:

The MHC class I protein is a heterodimer formed by 2 different polypeptidic chains. The larger one is termed MHC class I heavy chain and is coded on the MHC locus on chromosome 6; the variability imparted to the MHC molecule derives from the heavy chain. The second and smaller polypeptidic chain is termed β_2-microglobulin (β_2m), is coded on chromosome 15 and is conserved. The MHC heterodimer consists of 4 protein domains, 3 of which (α1, 2 and 3) are derived from the heavy chain, while the 4th is formed by the β_2m. The α1 and α2 domains form the peptide-binding groove and, not surprisingly, are also the sites where the polymorphisms are mostly concentrated (Bjorkman *et al*., 1987).

The MHC class II molecules are heterodimers as well. They are formed by 2 chains (α and β), both coded on the MHC locus on chromosome 6. The crystallographic conformation is quite similar to that of MHC class I: in this case, as well, the polymorphism is maximal on the peptide binding groove, which is formed by the domains α_1 and β_1 (Fremont *et al.*, 1996).

With both MHC class I and II molecules, the bound peptides constitute an integral part of the correctly folded molecule and are buried in the peptide-binding groove, held in place by noncovalent interactions, mainly hydrogen bonds. In MHC class I proteins the

length of the bound peptide is limited to 8-10 residues by conserved hydrogen bonds at each end of the peptide-binding groove. However, some bulge in the middle of the peptide-binding groove is allowed. In MHC class II molecules the peptide is instead not restricted to a specific length as the ends of the peptide-binding groove are open (Rammensee, 1995).

1.2.1.2 NON-CLASSICAL MHC:

In addition to MHC class I and II molecules there are also other proteins that are very similar to MHC class I and II but display less polymorphisms and usually have a far more restricted tissue distribution. These proteins have been called, collectively, MHC class Ib and are also currently termed nonclassical MHC. Between the nonclassical MHC, the proteins expressed from the MIC genes are peculiar, as they are not constitutively expressed, as the classical MHC class I molecule is, but instead is induced upon cellular stress. Moreover, if they bind peptide products they tend not to be the classical microbial products as seen with MHC class I and II. MICA and MICB, for example, are heavily glycosylated proteins with low homology (18-30%) with MHC class I molecules, but a relatively high level of polymorphisms. Their expression is limited to epithelial surfaces, mainly gastrointestinal system and thymic cortex, and their expression is up-regulated upon heat shock, cell transformation and infection (Braud *et al.*, 1999). MICA and MICB are recognized by NK cells via their NKG2D receptor and can activate them to kill the MICA-expressing cells. Other MHC Ib molecules, such as HLA-G, result instead in an inhibitory signal, so that NK cells do not kill the uterine cells expressing them. HLA-E is the least polymorphic of all MHC class Ib genes and is also has the widest tissue distribution, albeit with a lower level of expression than classical MHC molecules. It preferentially, but not exclusively, binds peptide sequences derived from MHC-class-I derived leader peptides. HLA-E can produce inhibitory responses, when interacting with CD94-NKG2A, or activating responses, when interacting with CD94-NKG2C and TCR, thus exerting a wide range of actions depending on the cellular context (Sullivan *et al.*, 2008).

Finally, CD1 molecules are similar to MHC proteins in structure, as they share both limited sequence homology and domain organization (a heavy chain composed of three distinct α1, 2 and 3 parts, non-covalently associated with β_2m). However, they have a very distinct functionality as they bind and present lipid antigens to elicit T-cell mediated immunity (Odyniec *et al.*, 2010). Recently DC-expressed CD1b and CD1c have been shown to mediate the recognition of lipid A, the most conserved membrane anchor of LPS, by γδ T cells, promoting their proliferation (Cui *et al.*, 2009). Figure 1.4, below, represents the three types of MHC molecules (class I and II plus CD1 as an example for class Ib) described in this chapter.

Figure 1.4: MHC molecules, classical and nonclassical. Modified from Porcelli, 2005.

1.2.2 MHC CLASS I PRESENTATION:

MHC class I molecules bind their peptide in the endoplasmic reticulum (ER). The peptide supply is generated in the cytosol via the proteasome degradation of endogenous proteins. The peptides are then carried into the lumen of the ER by the transporter associated with antigen processing (TAP). However, the peptides generated by the proteasome are between 2 and 25 aa in length, so they may exceed the maximum length admitted by MHC class I molecules (Kloetzel, 2004). A further trimming step is then performed in the ER by the ubiquitously expressed ER aminopeptidase ERAAP (also called ERAP1). ERAAP recognizes the COOH-end of the peptide and trims the

NH_2-end to form 8-10mer (Chang *et al.*, 2005). The chaperone is then released and the MHC class I molecule, still without peptide, is joined to the MHC class I peptide loading complex for loading and exposure on the cell surface. This complex comprises many different proteins, including TAP, tapasin, the chaperone calreticulin, protein disulfide isomerase (PDI) and ERp57 and has two distinct functions, as it both regulates the final assembly MHC class I-peptide and provides quality control for the MHC-class I loaded molecules to be exported. TAP associates to the MHC class I heavy chain via tapasin and provides a topological advantage (i.e. it brings peptide and MHC heavy chain in close proximity) but it does not seem to be a necessary part of the peptide-loading complex (Flutter and Gao, 2004). On the other hand, tapasin is a fundamental player in the formation of the peptide-loading complex, its role being a bridge between TAP and the yet-unloaded MHC class I. Calreticulin is both an essential effector in intracellular calcium homeostasis (its deletion is lethal in embryogenesis, (Mesaeli *et al.*, 1999)) and an important ER chaperone involved in glycoprotein -such as MHC class I- folding (Flutter and Gao, 2004). ERp57 is a thiol oxidoreductase whose role is to form a disulfide bond with tapasin (Dick *et al.*, 2002). In fact, tapasin acts as a sink for ERp57 sequestration: when tapasin is absent, ERp57 catalyses the reduction of a disulfide bond in the MHC class I heavy chain (Kienast *et al.*, 2007). PDI is the latest candidate for addition to the peptide-loading complex and its general function is catalysing the formation of native disulfide bonds in the initial phases of protein folding in the ER (Jensen, 2007). A scheme resuming the main players in class I presentation is presented below in Figure 1.5.

Figure 1.5: scheme of MHC class I presentation. Taken from Jensen, 2007.

1.2.3 MHC CLASS II PRESENTATION:

The peptide loading of MHC class II monomers relies on the action of a specialized chaperone protein termed the invariant chain (Ii) for its assembly in the ER (Watts, 2004). Ii mediates the stable assembly of MHC class II in the endoplasmic reticulum via a protein fragment that fits into the MHC class II peptide-binding groove and acts as a surrogate peptide to stabilize the protein. Ii release from the MHC class II involves a series of proteolytic cleavages, the key one being mediated by cathepsin S, which leaves only a short peptide (MHC class II-associated invariant-chain peptide or CLIP) in the peptide-binding groove. This results in each MHC class II molecule starting with the same self-peptide -CLIP- that needs to be displaced and substituted by other peptides for the antigen presentation system to work. Without enzymatic help the rate of dissociation of CLIP from most MHC class II molecules is too slow to allow effective peptide substitution before presentation on the cell surface. A fundamental role in MHC class II presentation is, therefore, performed by the chaperone protein HLA-DM. This accelerates the rate of CLIP release and peptide exchange in the MHC class II compartment. HLA-DM is a nonpolymorphic MHC class II heterodimer: it does not

directly bind peptides itself but interacts with peptide-MHC class II molecules and facilitated peptide exchange. It is also thought that HLA-DM has a role in peptide editing by catalyzing multiple events of peptide exchange, possibly with a bias towards the most stable complexes (Jensen, 2007). Class II MHC molecules, following their association with Ii, are concentrated in multivesicular, late endosomal compartments called "MHC II compartments" (Vyas *et al.*, 2008). As such, the MHC class II peptide supply must be able to access this compartment. Extracellular material including antigens and whole microorganisms is taken up by the APC cells and enclosed in a phagosome, a membrane-bound compartment to confine ingested material. The phagosome then undergoes various modifications, whose nature can depend on the content of the phagosome itself, and fuses with a lysosome to form a phagolysosome (Vyas *et al.*, 2008). At this stage the phagolysosome can interact with the MHC class II molecules for peptide loading. Figure 1.6, below, summarizes some of the possible sources of materials for loading on MHC class II molecules.

Figure 1.6: scheme resuming the various possible sources of antigen for MHC class II presentation. Taken from Vyas *et al.*, 2008.

The final step in MHC class II antigen presentation requires the transportation of the vesicles containing the MHC class II peptide-loaded molecules to the cell surface. This process is thought to involve the transformation of MHC class II-containing vesicles into tubular structures directed towards the plasma membrane in the site of the interaction with the T cell (Vyas *et al.*, 2007). Such a targeting is thought to enhance MHC class II clustering at the site of T cell contact and might play a role in the formation of the immunological synapse.

1.2.4 CROSS PRESENTATION:

For a long time MHC class I and II pathways of antigen presentation have been considered strictly distinct, with antigens of exogenous origin (i.e., phagocytosed or otherwise acquired by the cells and not naturally present in the cytosol) presented only on MHC class II molecules. The need for such a tight regulation of MHC class I restriction to endogenous antigens only appear clear when considering that otherwise healthy cells might become a target for CD8 cytotoxic T cells. However, if MHC class I presentation was indeed completely restricted to endogenous antigens, this would raise the question on how it would be possible to mount a cytotoxic response against pathogens that do not infect APCs. If APCs were not infected, in fact, they would not present the pathogen's antigen on their MHC class I and, therefore, it would not be possible to mount a cytotoxic response against any other cell infected/transformed in the same way. Such a response is made possible by the cross presentation pathway, where DCs present exogenous antigens on MHC class I molecules.

Cross presentation is fundamental to triggering a cytotoxic response against bacteria, tumour, and certain viruses, and for the tolerance to self-antigens (Savina and Amigorena, 2007). *In vivo* cross presentation has been attributed mainly to DCs, however *in vitro* experiments have shown that also other cell types including B cells and macrophages can cross present, albeit with a low level of efficiency (Reis e Sousa and Germain, 1995). There are many pathways available for cross-presentation, with

phagocytosis and macropinocytosis being the main routes for antigen uptake. However, the intracellular compartments responsible for cross presentation are still not well defined, even in DCs. Some antigens are presented through the so-called "cytosolic pathway"; following internalization in endosomes, protein antigens are partially digested to form large fragments, which are then exported in the cytosol and subjected to further degradation in the proteasome. Finally they are bound by TAP, transported into the ER and loaded onto MHC class I molecules (Ackerman and Cresswell, 2004). However, a "vacuolar pathway", similar to MHC class II presentation and presumably independent from any cytosolic step, has also been reported (and reviewed in Ramachandra *et al.*, 2009). As for the type of antigens used in cross-presentation, peptides derived from particulate antigens (cell- or particle- associated) are much more efficiently presented than soluble ones. This and other evidences suggest that phagocytosis enhances antigen delivery into the MHC class I pathway (Ackerman and Cresswell, 2004). It has also been demonstrated that export to the cytosol in DCs is more rapid for small than for large molecules (Rodriguez *et al.*, 1999). While the evidence for phagosome/endosome-contained antigens being released in the cytosol is quite strong (Kovacsovics-Bankowski and Rock, 1995), the fusion of ER with the phagosome system has been a topic of hot debate for some years. This was consistently clarified by Cresswell's group (Ackerman *et al.*, 2006), as they published that a bead-bound protein with a specific site for N-glycosylation underwent glycosylation after phagocytosis from DCs while still being attached to the bead. As N-glycosylation is a peculiar feature of the ER, this provides quite strong evidence for ER-phagosome interaction in DCs. To summarize, cross presentation is still very much an open field and new substantial developments are to be expected.

1.3.0 ANTIGEN PRESENTING CELLS:

A critical factor, possibly the most important factor for the generation of effective T cell lines, is the interaction between the T cell and the antigen–presenting cell (APC), in which peptides derived from the antigen are loaded on MHC molecules and presented on the APC surface to the TCR. Controlling and fine-tuning the APC functionality is

hence fundamental for any therapeutic strategy requiring T cells stimulation, either *in vitro* or *in vivo* (Oelke *et al.*, 2005). Many types of cell in the body can exert APC function; in fact, virtually any cell carrying an HLA molecule loaded with a peptide would be able to elicit a memory T cell response. However, only professional APC– mainly dendritic cells (DCs)- are able to prime effectively naïve T cells to promote a full primary response (Banchereau *et al.*, 2000). The success of any adoptive transfer immunotherapy protocol requires that the lymphocytes be presented the relevant antigen(s) and that, after antigen presentation, they mature and undergo activation, expansion and differentiation.

1.3.1 B CELLS, MACROPHAGES:

While DCs are the most efficient APCs in humans other cell types, mainly B cells and macrophages, can have antigen-presenting activity. B cells, in particular, show a constitutive expression of MHC class II that begins during B cell development and is maintained throughout differentiation and maturation (Chen and Jensen, 2004). However, the expression of CD80 and CD86 is very low upon B cell maturation, thus rendering them unable of providing normal co-stimulation during antigen presentation. This feature is consistent with B cells at this stage being able to induce T cell tolerance rather than activation (Chen and Jensen, 2008). B cells are not very efficient in the capture and processing of pinocytosed or endogenous antigens which, combined to their lack of costimulatory molecules prior to activation, renders them poor presenters of non-specific antigens compared to, for example, DCs or macrophages (Chen and Jensen, 2008). However, once they encounter a specific antigen via their BCR they are then able to present with very high efficiency.

Macrophages were initially identified by E. Metchnikoff in the early 1900 as highly phagocytic cells that were able to eliminate pathogens and perform general housekeeping functions in a wide range of organisms (Martinez *et al.*, 2009). Later on it was discovered that IFN-γ, which is secreted by both NK and T cells, can convert macrophages in cells with a clear antigen presenting activity, an increased rate of synthesis of proinflammatory cytokines and an increase in phagocytosis too (Martinez

et al., 2009). However, both the cell types described above cannot match dendritic cells in terms of efficacy of antigen presentation.

1.3.2 DENDRITIC CELLS:

DCs are the most potent APCs and they have a unique ability to stimulate naïve T cells (Banchereau and Steinman, 1998). DCs are present in low numbers throughout the body, both in lymphoid and nonlymphoid tissues. In peripheral tissues they reside particularly in skin and mucosae, the sites of interface with the external environment. Their distribution -they are abundant in pharynx, upper oesophagus and gastrointestinal system, vagina and anus, in brief at all sites where exogenous pathogens could be present- makes them the predominant cell to respond to disease-related stimuli (Steinman and Banchereau, 2007). DCs are also able to extend their processes –and as such their antigen-sampling ability- through the tight junctions of the epithelia without altering its barrier function (Rescigno *et al.*, 2001). This feature probably enables the silencing of the immune system towards harmless environmental pathogens.

DCs are involved in the establishment of both innate and adaptive immunity (Banchereau *et al.*, 2000) and can promote Th1 (Pulendran *et al.*, 1999) and Th2 differentiation in helper T cells. They are able to induce memory in specific T cell clones, thus allowing its long-term persistence and a rapid response upon re-exposure to the original antigen (Badovinac *et al.*, 2005). The key features DCs possess regarding their antigen presentation and T cell activation potential are summarized in Figure 1.7, below.

Figure 1.7: main features of DCs. Taken from Steinman and Banchereau, 2007.

However, DCs also contribute to the differentiation of regulatory T cells required for the maintenance of self-tolerance (Steinman and Nussenzweig 2002) and/or to the dampening of an immune response, as it will be described also in sections 1.3.2.1 and 1.3.2.2. DCs can be tolerogenic in their immature state, as explained in section 1.3.2.2, but this phenotype can also be induced by exposing them to various immunosuppressive and anti-inflammatory agents such as IL-10, TGF-β1 or compounds as prostaglandin E_2 (Morelli and Thomson, 2007). DCs can also induce tolerance, rather than activation, upon capture of harmless self-antigens, environmental antigens, or in some cases antigens from dying cells (Morelli and Thomson, 2007).

1.3.2.1 MAIN DCs SUBTYPES:

DCs are a unique subset of cells and their heterogeneity is partly reflected by their widespread distribution in the body. All human DCs are leukocytes arising from the bone marrow and DCs and DCs precursor make up around 1% of circulating PBMCs (Sato and Fujita, 2007).

The main subdivision in DCs subsets is between conventional (cDCs) and plasmacytoid (pDCs) DCs. There is also a subset of cells termed follicular DCs, but these are non-haematopoietic in origin, do not express MHC class II on their surface and reside in follicles and germinal centres (hence the name). They have long dendrites but do not

process the antigen, carrying it intact on their surface instead, and are not related to classical dendritic cells.

Human DCs are defined as lineage-ve MHC class II+ve cells; moreover, all human DCs express CD4. cDCs are defined as CD11c+ve while pDCs are CD11c-ve in humans, whereas in mouse all DCs are CD11c+ve regardless of the subtype (Sato and Fujita, 2007). pDCs derive their name by their cytologic similarities with antibody-producing B (plasma) cells, can be involved in tolerance when in their immature state and, contrarily to cDCs, are long-lived. Upon maturation, they express Toll-like receptor (TLR) 7 and 9 and are known to express large amounts of type I IFN (Steinman and Banchereau, 2007) in response to viral infections, which is their main physiological role. They can also act as APC and control T cell responses once they have undergone maturation (Colonna *et al.*, 2004); however, as the level of MHC and costimulatory molecules is not as high as in classical cDCs, this is probably the reason for their minor efficiency in T cell priming (Villadangos and Young, 2008). pDCs have also been shown to be able to induce Tregs (Moseman et al., 2004).

cDCs are more common than pDCs, are highly mobile between various body compartments and can be further sub-divided according to the tissue of residency. cDCs in the epidermis, for example, are called Langerhans cells and express langerin and CD205, while some of the DCs in the dermis express CD209 and can activate antibody-producing B cells (Steinman and Banchereau, 2007). Dendritic cells in the intestine are characterized by the common marked CD11c and can be divided into two further subsets according to CD103 or CX3CR1 expression (Laffont and Powrie, 2009). DCs of either type are closely related to macrophages and monocytes so it is not surprising that DCs are derived from a macrophage/DCs precursor population (MDPs) residing in the bone marrow, which subsequently differentiates into monocytes and common DCs precursors (CDPs). CDPs would then differentiate into DCs but not into monocytes. Of note, in fact, while differentiation of DCs from monocytes is well-established *in vitro* (Sallusto and Lanzavecchia, 1994) and is possibly the preferred technique for DCs

generation in laboratories worldwide, *in vivo* this seems not to be the preferred pathway for DCs differentiation (Fogg *et al.*, 2006).

1.3.2.2 PHENOTYPE OF IMMATURE AND MATURE DCs:

When in non-lymphoid tissues, DCs are in an 'immature' state ie. they do not express the costimulatory signals required for T cell activation. During their time in non-lymphoid tissues, in fact, DCs tend to sample their environment and display a phenotype characterized by high phagocytosis and continuous internalization of antigens (Banchereau *et al.*, 2000), either particulate or soluble, via phagocytosis, endocytosis or macropinocytosis. They can also acquire microbial pathogens, dead or dying cells, and immune complexes (Rossi and Young, 2005). DCs are actually able to recognize different pathogens through the expression of pattern recognition receptors (PRR), which interact with specific microbial structures called pathogen-associated molecular patterns (PAMPs). Immature DCs can present antigens to T cells but this presentation is inefficient and results either in an abortive T-cell activation and induction of anergy (Sotomayor *et al.*, 2001) or differentiation of regulatory T cells (Jonuleit *et al.*, 2001). In fact, it has been shown that immature mDCs, characterised by a low expression of costimulatory molecules (CD80, CD86 and inducible costimulatory ligand or ICOSL) have the potential to induce suboptimal T cell priming, thus often leading to T cell tolerance (Steinman and Nussenzweig, 2002), and to inhibit alloantigen-specific T cell responses. These immature DCs are able to improve the survival of grafted organs after their transfer across an MHC barrier (Fu *et al*., 1996). Therefore, the full maturation of DCs prior to its interaction with T cells is an important requisite for T cell activation.

Antigen uptake, together with exposition to inflammatory cytokines, provokes DCs maturation, which is usually completed in 24 hours. The maturation of DCs involves downregulation of antigen uptake and processing, upregulation of antigen presentation and migration to the local draining lymphoid tissue. DCs maturation is also characterised by an increase in the expression of MHC I and II molecules on the cell

surface. This feature results from both an increase in the efficiency of antigen processing for both MHC class I and II pathways (Guermonprez *et al*., 2002) and a longer persistence on the cell surface for the peptide MHC class II complexes, which would be otherwise rapidly recycled (Shin *et al*., 2006). The costimulatory molecules CD80 and CD86 and the marker of cell activation CD83, required for T cell activation, are also up-regulated (Banchereau *et al.*, 2000). The extent and type of innate and adaptive immune response elicited by the activated DCs depends on the type of signal that activated them. The maturation of DCs involves several stages each with its specific kinetic of expression of cytokines and surface molecules critical for initiation and control of both innate and adaptive immune responses (Langenkamp *et al.*, 2000 and Granucci *et al.*, 2001). In particular, inflammatory molecules such as the tumour necrosis factor (TNF) are strongly upregulated immediately after bacteria stimulation, but subsequently downregulated. This suggests that inflammatory activity of DCs takes place, in its main part, early after activation, before DCs left the inflammatory site.

1.3.3 γδ T CELLS AS APC FOR STRESS-RELATED RESPONSES:

The antigen presentation system in which the key players are DCs and macrophages provides a good description of the immune surveillance targeting microbial/viral pathogens. However, the immune surveillance dealing with nonmicrobial stress is less well known, at the moment, and is the focus of active investigation. While DCs and monocytes should be able to mount a response against some stress signals released from dying cells, such as ATP (Rock and Kono, 2008), they may not be able to recognize a more diverse range of molecules such as MICA, which is up-regulated on epithelial cells following various physicochemical perturbations, is expressed by tumour cells and is present at inflammatory sites (Groh *et al.*, 1996 and Groh *et al.*, 1999). These antigens are recognised by NK cells and "nonconventional" T cells, of which γδ T cells are the main representatives (Hayday, 2000). After one of their receptors, including the TCR, is engaged with a stress-related antigen, γδ T cells are able to initiate a fast-acting lymphoid stress-related response that is not constrained by either clonal expansion or *de novo* differentiation (Strid *et al.*, 2008). Such a quick response would necessitate a high

frequency of γδ T cells ready to react upon activation mediated by autologous stress antigens, common pathogens, or a combination of both. The full range of ligands able to engage the TCR γδ receptor has not been fully established; however, it has been ascertained that most of the ligands are not β_2m-dependent. Two murine MHC-I-related proteins termed T10 and T22 have been shown to ligate two independently derived γδ TCR (Adams *et al.*, 2008).

Better known, at the moment, is the reactivity of human Vγ9Vδ2 cells to low molecular mass phosphoantigens (Hayday, 2000). In accordance with the stress surveillance model, phosphoantigens can be either of autologous origin, such as isoprenylpyrophosphate (IPP), which is accumulated in virus-infected and transformed cells (Hayday, 2000), or pathogen-derived such as hydroxymethyl but-2-enyl pyrophosphate (HMBPP), an intermediate of the MEP pathway of isoprenoid synthesis shared by many prokaryotes and pathogens (Eberl *et al.*, 2003), including the malarial parasites. Of interest, aminobisphosphonates, which are currently used in therapy against osteoporosis and myeloma, inhibit farnesyl pyrophosphate synthase in patients and this results in IPP accumulation and Vγ9Vδ2 activation (Kunzmann *et al.*, 1999). A scheme summarising all the known ligands for γδ T cells, together with the possible activation outcomes, is presented below in Figure 1.8.

Figure 1.8: scheme resuming the main activatory ligands, and possible outcomes of activation, for γδ T cells. Modified from Hayday, 2009.

γδ T cells are able to exert a wide range of functions. They are effector cells and among the first IFN-γ-secreting cells both in mice and human and as such are essential contributors to host survival in early life (Gibbons *et al.*, 2009). In fact, in adults γδ T cell exert a cytotoxic effect towards various malignancies, including leukaemias (Lamb *et al.*, 2001), and respond to virus, parasites and bacteria (Boismenu and Havran, 1998). It was recently shown that γδ T cells produced IFN-γ and proliferated in response to a *M. tuberculosis*-derived antigen (Li and Wu, 2008). An effector/cytotoxic phenotype has been suggested in CB as well (Engelmann *et al.*, 2005 and Campos Alberto *et al.*, 2009). Finally, Moser's group showed unequivocal antigen presenting activity for the Vγ9Vδ2 subset in adults, thus broadening γδ T cell functionality (Brandes *et al.*, 2005 and Brandes *et al.*, 2009).

1.4.0 ARTIFICIAL APCs:

As described above, DCs are the most effective APCs and as such they would be ideal candidates for immunotherapeutic applications. However, preparing DCs cells for clinical use is extremely challenging (Kim *et al.*, 2004). DCs generation is cumbersome in itself due to the need for autologous cells. The task is also technically difficult due to the requirement of a sufficient number of activated cells, suitably differentiated and rapidly and reproducibly generated (Oelke *et al.*, 2003). This is a more acute problem in patients with advanced disease (Steenblock *et al.*, 2009). Moreover, the APCs should be unaffected by tumour and viral immune evasion strategies responsible either for the disease itself or the malfunctioning of the physiological APC in the first place.

An artificial system for antigen presentation would solve many of the problems presented by DCs generation. Ideally an artificial APC (aAPC) platform should have the following characteristics: it should be able to traffic the human body safely, it should be biodegradable, cell compatible, inert (non toxic and non tumourigenic), it should be capable of forming T immunological synapse and delivering adequate T cell signal and finally be as small as possible and yet traceable *in vivo*. Another ideal requirement would be the "one-type-fits-all" quality, i.e. it should be possible for the same aAPC to be loaded with different peptides/molecules and therefore be used for a large variety of diseases (Oelke *et al.*, 2005). These requisites would be best satisfied by a non-cell based aAPCs system, which would also offer the further advantage of ensuring its efficacy is unaffected by the pathology, whatever may happen to the endogenous APC. Non-cell based systems offer also complete "off-the-shelf" availability, while it is more difficult envisaging a way to avoid the culture requirements of any cell-based aAPC. There are many features of a T cell that should be elicited by an ideal aAPC: the signals received from T cells during the *ex vivo* expansion affect their specificity but also the potential survival, their tropism, their differentiation into functional subsets and the generation of memory cells. Ideally all these characteristics should be elicited by an aAPC.

1.4.1 CELL-BASED ARTIFICIAL APCs:

A number of cell-based and acellular APCs systems fulfil part of the requirements quoted in the paragraph above. Mouse fibroblasts, engineered to express an HLA molecule and 3 costimulatory molecules (CD58, CD80, CD54), proved to be as effective as autologous APCs (Latouche and Sadelain, 2000). Insect APCs cells from *Drosophila melanogaster*, pulsed with a melanocyte-derived peptide, were able to generate 10^9 cytotoxic T lymphocytes within one month starting from 10^{10} PBMCs (Mitchell *et al.*, 2002). A human leukemia cell line, K32, has been transformed in a potent amplifier cell following transfection with CD32 (low affinity Fcγ receptor) and subsequent incubation with anti-CD3 and anti-CD28 antibodies: these cells were capable of promoting a 1,000 fold increase in the T cell population, getting up to 10^{10} polyclonal T lymphocytes after starting from 500 ml of blood (Maus *et al.*, 2002). More recently, Barber *et al.*, 2006, developed a cell-based APC system where Daudi B cells, which do not naturally express HLA class I, were coated with fixed amount of HLA class I monomers and used to stimulate PBMCs *in vitro*. These modified Daudi cells promoted the expansion of CMV epitope-specific CD8 T cells from 0.03% to 30.6% in two weeks, a result comparable to the use of peptide-loaded dendritic cells (Barber *et al.*, 2006).

All the systems here described, although effective, would not be appropriate for an *in vivo* use due to the origin of the cells employed. In fact, any cell-based aAPC system would be unsuitable for an *in vivo* destination, regardless of the origin of the APCs cells employed, as there would be a rejection of the exogenous cell product once transferred in the patient. A more appropriate option for an *in vivo* compatible aAPC would then be an acellular platform. In the next paragraphs an overview on the state-of-the-art aAPC will be presented. Exosomes will be presented first, as they are at the interface between physiological and artificial APC.

1.4.2. NON-CELL-BASED ARTIFICIAL APCs:

1.4.2.1 EXOSOMES:

A possible aAPC acellular system is represented by exosomes, small (30-100 nm) cell-derived vesicles enclosed by a lipid bilayer and secreted in the extracellular space (Thery *et al.*, 2002b and Thery *et al.*, 2009). There is a wide range of vesicles that can be secreted either directly from the plasma membrane or after the fusion of cytosol compartments that contain intraluminal vesicles with the plasma membrane. The term exosome has been specifically used since 1987 for only this second group of vesicles – i.e., exocytosed vacuoles of endosomal origin (Pan *et al.*, 1985 and Thery *et al.*, 2009). Exosomes are secreted exclusively by living cells (Thery *et al.*, 2001). Moreover, exosomes derived from various cell types (murine DCs, human intestinal epithelial cells and EBV-transformed B cells) displayed similar characteristics; all were enriched in MHC class II molecules and contained heat shock proteins, annexins, integrins, cytoskeleton proteins and MHC class I molecules (Mignot *et al.*, 2006). True exosomes share physical and chemical characteristics with the late endocytic compartments, however the precise nature of the intracellular location/organelle from which they derive is still unknown. Their secretion by the parent cell depends on the type of cell involved; while in T (Blanchard *et al.*, 2002) and resting B lymphocytes (Saunderson *et al.*, 2008) the secretion is inducible, in DCs (Zitvogel *et al.*, 1998) and EBV transformed B cells (Raposo *et al.*, 1996) it is constitutive, as it is in most tumour cell lines. In the case of DCs, it has been shown that exosome secretion is more relevant in immature rather than mature DCs (Thery *et al.*, 1999). This suggests that exosome secretion is modulated by both cell types and environmental changes; it is possible that such a feature is one of the means cells use to adapt to these changes (Thery *et al.*, 2009).

As both antigenic material and MHC-peptide complexes are present on the exosome surface, they have sparked the interest of immunologists regarding their possible role in eliciting immune responses. Exosomes purified from tumour cell lines (Wolfers *et al.*, 2001) can induce the activation of antigen-specific T cells *in vitro* in presence of

recipient DCs, even if the professional APCs have not encountered the antigen previously. This indirect activation of recipient DCs has also been shown in the case of bacterial infection, for both *M. tuberculosis* and *M. bovis* (Giri and Schorey, 2008) and CMV (Walker *et al.*, 2009). In some circumstances, moreover, the MHC-peptide complexes on the exosomes surface can be directly presented to T cells.

Minami's group, among others, reported that DCs-derived exosomes were able to activate CD8+ve T cell clones on their own (Utsugi-Kobukai *et al.*, 2003), while Zitvogel's group showed the same outcome even when exosomes were incubated with DCs bearing allogeneic MHC class I complexes, thus indicating that the exosomes-derived MHC molecules were functional (Chaput *et al.*, 2004). However, tumour-derived exosomes seem to be able to activate CD8+ve T cells only when incubated with recipient DCs bearing the correct MHC haplotype (Wolfers *et al.*, 2001). When derived from a B cell, exosomes can provoke $CD4^+$ T cell proliferation, *in vivo,* but the efficiency is not optimal (Raposo *et al.*, 1996). More interestingly, purified exosomes can be loaded with antigenic peptides and tumour-derived exosomes can be used for immunization, resulting in a better efficiency than immunization with irradiated tumour (Wolfers *et al.*, 2001).

1.4.2.2 OTHER ACELLULAR OPTIONS:

The aAPCs described in literature so far belong to four different types: latex beads, magnetic beads, biodegradable polymers and liposomes (Steenblock *et al.*, 2009).

1.4.2.3 LATEX BEADS:

Latex beads are rigid spheres that can be coated, via nonspecific interactions, with different ligands and as such perform as aAPCs. They are non-physiological and do not have a fluidic interphase, but despite these main disadvantages they have been proven very useful to study APC-T cell interactions (Curtsinger *et al.*, 1997). Latex bead-based aAPCs were first used to prove that the size of the antigen-presenting particle is a

crucial factor for T cells stimulation (Mescher, 1992). Latex microbeads covered with either MHC class I molecules or tumour cells-derived membranes were used to activate splenocytes and it was found that the degree of activation depended on size, with 4-5 μm diameter aAPCs resulting the most effective (Mescher, 1992). Crucially, it was also discovered that T cell responses were dependent on the density of ligands per bead, rather than to the number of beads presenting at lower densities (Deeths and Mescher, 1997). It was discovered, as well, that T cells responses were dependent on exogenous cytokines for a sustained proliferation, despite acquiring effector phenotype after three days of stimulation (Deeths and Mescher, 1999). Oosten *et al.*, 2004, used latex beads coated with costimulatory molecules and minor histocompatibility antigens-MHC complexes to expand peptide-specific CTL cell lines while Whitelegg *et al*., 2005, employed CD54, CD80 and MHC class I coated-latex beads to study peptide-independent allorecognition. Finally, latex bead-based aAPCs were also used for clinically relevant studies: the stimulation of PBMCs from healthy donors with latex beads covered with MHC and a glioma epitope, CD28 and CD83 lead to an expansion of glioma antigen-specific cells of 50-60 folds over 4 weeks (Jiang *et al.*, 2007).

1.4.2.4 MAGNETIC BEADS:

When the aAPCs are large (5 μm or more) their separation from the expanded T cells becomes a fundamental step to prevent *in vivo* complications such as embolism. This size prerequisite makes magnetic beads very attractive; in addition to the ease in coupling T cell ligands via biochemical techniques, they can be removed from the cell suspension simply using a magnet.

Non-antigen-specific CD4+ve and CD8+ve expansion was obtained when cells were stimulated with magnetic beads coated with anti-CD3 and anti-CD28 particles (Levine *et al.*, 1997). Magnetic beads also showed potential in an antigen-specific system, where influenza-specific tetramers coupled to the beads were able to maintain antigen specificity in CD4+ve sorted cells over 9 weeks of culture (Maus *et al.*, 2003). When MHC dimers coupled to magnetic beads were used in a melanoma-specific system, up to 10^9 MART-1 specific cells were obtained in less than 2 months (Oelke *et al.*, 2003).

1.4.2.5 BIODEGRADABLE PARTICLES:

While biodegradable polymers (BPs) are particularly suitable as vehicles due to their flexibility in size and to the ability of encapsulating cytokines, they present a particular challenge for antigen presentation, as their biodegradable nature compromises long-term surface ligand presentation. This may result in insufficient time of ligands being exposed on the surface to attain successful antigen presentation. However, the most widely used polymers -aliphatic polyesters- have a degradation rate ranging from days to months (Steenblock *et al.*, 2009).

Three years ago it was published that the stimulation of unsorted murine splenocytes using poly(lactide-co-glycolide) (PLGA) particles that presented anti-CD3 and anti-CD28 and released IL-2 resulted in a marked skewing to 100% CD8+ve cells by day 4 (Steenblock and Fahmy, 2008). This population expanded 45-fold in one week and this effect was not observed without encapsulation of IL-2. Few studies have used any of the aAPC platforms described above, or liposome-based systems, as APC *in vivo*. Among these studies, the focus has been on latex and magnetic beads and on biodegradable polymers as aAPC. Very little has been accomplished when using liposomes as aAPC *in vivo* (Steenblock *et al.*, 2009).

1.4.3 LIPOSOMES:

The fourth acellular APCs system is based on liposomes, small (up to 150 nm) vesicles made up of a lipid bilayer. Liposomes are similar to very small empty cells, having a cell membrane with a hydrophilic-based internal cavity but no organelles. The lipid molecules used to build liposomes are usually phospholipids with or without additional additives. For example, cholesterol is a common component as it improves the lipid bilayer' characteristics: it helps increasing the microviscosity of the lipidic vesicle and stabilizing the membrane (Vemuri and Rhodes, 1995). Liposomes' long-standing popularity as biological vehicles can be ascribed to their ease of preparation; they self-assemble easily in aqueous buffers and their sizes can be adjusted from 60 nm to 1 μm via mechanical methods (Steenblock *et al.*, 2009).

The first research involving liposomes date back to the late 1970s when they were studied to encapsulate and deliver chemotherapy (Gregoriadis, 1976). Although liposomes were not defined nanoparticles at that time and despite their dimensions being slightly bigger than what would qualify them as nanotechnology (minor or equal than 100 nm), their research was propelled by the current "nanotechnology moment". Today a significant portion of nanotechnology research in biomedicine is focused on liposomes (Kim *et al.*, 2004).

1.4.3.1 LIPOSOMES AND DRUG DELIVERY:

Recently liposomes have been widely employed for drug delivery purposes (Park, 2002 and Mamot *et al.*, 2003, review the topic), where the drug is enclosed in the liposome thus increasing its half-life in the organism. Among the best characterized uses for liposomes is the encapsulation of doxorubicin, a member of the anthracyclines class of drugs, whose use is severely limited by systemic toxicity (Park, 2002). In particular, pegylated liposomal doxorubicin (Doxil®) is characterized by a prolonged circulation in the organism, with a terminal half-life of 55 hours, due to the reduced interaction with plasma protein and phagocytes conferred by the pegylated lipids on the surface (Park, 2002). Liposomal daunorubicin (DaunoXome®) too has been approved for cancer treatment. Manipulating their lipid formulation, the liposomes can be made temperature or pH sensitive, to allow controlled release of their content. Mills and Needham, 2004, managed to construct temperature-sensitive liposomes that released their drug content in tens of seconds at clinically feasible hyperthermia (39-42°).

1.4.3.2 IMMUNOLIPOSOMES:

Immunoliposomes –liposomes in which fragments of monoclonal antibody (Fab) are conjugated to the surface- are an important component in the development of new, molecularly-targeted drug delivery systems. They can be engineered to promote specific binding to a target antigen followed by receptor-mediated endocytosis (Mamot *et al.*, 2005). In addition to targeting, the drug delivery is also rendered more efficient by the

immunoliposome and a drug delivery in the cytoplasm can potentially overcome the chemotherapeutic resistance due to membrane efflux system (common in cancer settings). So far, immunoliposomes have been used mainly for drug delivery purposes. Promising results have been achieved targeting the liposomal doxorubicin to specific receptors; immunoliposomes targeted to HER-2 overexpressing tumour cells show increased therapeutic efficacy in delivering the drug in preclinical model (Park, 2002) and they can be prepared from existing liposomal doxorubicin. Immunoliposomes have also been directed against the epidermal growth factor receptor (EGFR) and *in vitro* experiments showed a massive internalization in the cytoplasm of EGFR-overexpressing cells. The same immunoliposomes showed also a marked cytotoxicity when encapsulating a chemotherapeutic drug such as doxorubicin or methotrexate (Mamot *et al.*, 2003). Also, non-antibody mediated targeting of liposomes have been attempted: one example is folate targeting, pursued conjugating liposomes to folic acid and then exploiting the folate receptor pathway in cancer cells. Studies in a murine resistant lung carcinoma model showed that folate-targeted liposomal doxorubicin had a superior efficacy compared to non-targeted doxorubicin when assayed in an *in vivo* model (Goren *et al.*, 2000).

1.4.3.3 LIPOSOMES AND ANTIGEN PRESENTATION:

The enhanced efficiency of molecular interactions, when occurring within fluid biological membrane, was first highlighted by A. Delbrueck (1968). It has also been shown that antigen presentation is more efficient if the antigens are taken up within particles rather than from a solution (Shen *et al.*, 1997). As the formation of the immune synapse requires that the molecular interaction progress in an orderly configuration of which the lipid bilayer is an essential component, it can occur also via liposomes. The first mention for liposome-based antigen presentation dates back to 1978, when Burakoff's group prepared liposomes derived from cell membranes and used them as an aAPC for the stimulation of polyclonal murine lymphocytes (Engelhard *et al.*, 1978). Subsequent works used liposomal aAPCs prepared using different lipids formulations and tumour cells or viral membranes (Finberg *et al.*, 1978 and Weinberger *et al.*, 1985).

As already seen for magnetic beads, it was found that the level of stimulations depended on the density of T cell antigens on the liposome' surface.
Albani's group embedded MHC class II molecules in unilamellar liposomes and mixed it with CD4+ T cells; this resulted in IL-2 secretion (Prakken *et al.*, 2000). Moreover, the MHC clusters induced on liposome-stimulated cells were very similar to the physiological clusters induced by natural APCs (Prakken *et al.*, 2000). It was also shown that the preliminary clustering of T cells antigens into microdomains in the liposomes improved aAPC function (Giannoni *et al.*, 2005). In fact, when incubated with human T cells for polyclonal expansion, liposome-based aAPC where antigens had been previously clustered in microdomains achieved preferential CD8+ve T cells expansion and avoided terminal differentiation *in vitro*. Moreover, a robust expansion of MelanA-specific T cells was observed after 2 weeks of stimulation using liposome-based aAPCs and IL-2 and IL-15 in the culture; however, the aAPCs themselves were not antigen-specific and the cells had been incubated with MelanA-pulsed T2 cells prior aAPC expansion (Zappasodi *et al.*, 2008).

1.5.0 ARTIFICIAL ANTIGEN PRESENTATION AND ITS CLINICAL APPLICATION:

This PhD project will focus on the development and characterization of artificial antigen presentation systems to be used in clinical settings. In particular, it will concentrate on hematopoietic stem cell transplantation (HSCT) and on how to target post-transplantation infections and improve the outcome via immunotherapy. Therefore, a brief overview of HSCT, immunotherapy and cytomegalovirus infection, which is one the main complication occurring after HSCT, will be now presented.

1.6.0 HEMATOPOIETIC STEM CELL TRANSPLANTATION (HSCT):

Hematopoietic stem cell transplantation (HSCT) is now the most effective treatment for a variety of haematological diseases, such as myelomas, non-Hodgkin's lymphoma, acute and chronic myeloid leukaemia, acute lymphoblastic leukaemia, aplastic anaemia,

Fanconi's anaemia and SCID (Copelan, 2006). Prior to undergoing transplant, patients who are eligible for HSCT –regardless of the underlying disease- need a preparatory treatment, or regimen, which can consist of chemotherapy, total body irradiation, or a combination of the two. This is performed in an attempt to remove the underlying condition and, in the case of allogeneic HSCT, to establish the immunosuppressed state that will allow a successful engraftment. Once the transplantation has been performed, T cells from the recipient will recognize donor antigens (especially MHC molecules – see below) and this can cause graft failure. On the other hand, donor T cells will recognize recipient MHC-mismatched antigens; this process is responsible for both graft-versus-host-disease (GvHD) and graft-versus-tumour (GvT) activity, which are tightly related effects.

Both graft failure and GvHD are the clinical manifestation of the immune response to allogeneic cells (i.e, cells that have different alleles at one or more loci, especially MHC). Cells of donor origin can be recognised by the B, NK and T cells of the recipient as they do not express the same MHC alleles and this can result in graft failure, while the recognition of recipient cells by the donor effector cells (mainly T cells) is responsible for the beneficial GvT/L effect. T cells are the most relevant players in alloreactivity (i.e, an immune response against cells with a mismatched MHC), as shown by the fact that T cell suppression is the main approach to control alloreactivity in transplant patients (Whitelegg and Barber, 2004). During thymic maturation, T cells are selected to form a repertoire of lymphocytes that interact preferentially with the MHC molecules expressed by the same individual (Kisielow and Von Boehmer, 1995). The phenomenon where T cells recognise MHC molecules they have not been previously exposed to is termed allorecognition and could be considered a paradox in the context of thymic selection. Alloreactive T cells (around 1-10% of total T cells, Suchin *et al*., 2001) are able to elicit a very strong immune reaction; the phenomenon was firstly shown by the protocol of mixed leukocyte reaction, or MLR, where T cells from two different individuals are co-cultured to assess the proliferation of the T cells from one donor against the other (Janeway, 2005).

GvHD is highly detrimental, while GvT/L is very effective in eradicating the malignancy and is the main mechanism accounting for the use of transplant as a therapy. GvHD is one of main complications when performing HSCT; it can be localized and easily treated or develop into a multisystemic syndrome affecting skin, gut and liver. When not prevented by appropriate prophylactic chemotherapy (methotrexate and cyclosporine, for example) almost all HSCT recipients are affected by GvHD (Sullivan *et al.*, 1986). The main risk for GvHD occurrence is HLA mismatch, however it can occur also in HLA-matched patients and despite preventative measures. Depleting T cell in the graft prior transplantation can reduce GvHD, but this results in an increased rate of graft failure, opportunistic infections and relapse (Wagner *et al.*, 2005), so the disease-free survival rate is not improved. The GvT/L effect can explain the reduced rate of relapse after either allogeneic HSCT (as compared to HSCT where the donor is an identical twin) and in patients who develop GvHD compared to those who do not (Horowitz *et al.*, 1990).

The source of stem cells available for HSCT is varied. Traditionally stem cells of bone marrow origin (obtained by repeated aspiration from the iliac crests while the donor is under local or general anaesthesia) were the first to be employed. Moreover, stem cells can also be found in peripheral blood, due to their recirculation between blood and bone marrow. The number of stem cells can be estimated from the expression of CD34+ve cells and in peripheral blood they are very few, less than 0.06% of total nucleated cells (Korbling and Anderlini, 2001). However, stem cells can be successfully mobilized from the bone marrow into the blood using the granulocyte colony-stimulating factor (G-CSF). Compared with bone marrow-derived cells, stem cells of peripheral blood origin contain more T cells, resulting in a more rapid reconstitution but increasing the incidence of chronic GvHD (Cutler *et al.*, 2001). However, both these sources rely on adult donors; it is estimated that international registries (for all patients who do not have an HLA-matched sibling or relative) can find a suitable donor for more than 50% of the patients. As such, there is a dire need for alternative sources of stem cells to find a match for the remaining patients awaiting transplantation.

1.6.1 CORD BLOOD TRANSPLANTATION:

Cord blood (CB) has been used as a source of hematopoietic stem cells (HSC) alternative to bone marrow and mobilized peripheral stem cells for a variety of diseases. The proof of principle for CB-derived HSCT came in 1988, when E. Gluckman and her team successfully transplanted an 8-years-old boy suffering from Fanconi's anaemia, reaching complete chimerism one month after transplantation (Gluckman *et al.*, 1989). This first milestone proved that one CB contained enough HSC to guarantee engraftment, at least in paediatric patients. Since then, CB has now been used to transplant more than 20000 patients both adults and paediatric (data referred to 2009).

Three potential advantages of CB use in HCST were clear from the beginning: firstly, CB was most likely to be free from herpes virus contamination. Secondly, CB collection could be targeted –a feasible and practical strategy to increase the representation of ethnic minorities samples in the registry- and, most importantly, HLA-typed, frozen CB was ready to use as and when required, without the delays required for typing and collecting compatible adult donors samples (Wagner and Gluckman, 2010). The lack of collection-related risks for the donor (i.e. the mother/baby after delivery) was another attractive feature (Gluckman, 2009), as it was the ease of collection. So far cord blood transplantation (CBT) has been shown to have a delayed engraftment and lower GvHD compared to HLA-identical sibling transplant (Rocha *et al.*, 2000). This is possibly due to the low number of CD34+ve cells in CB (if compared with adult HSC) (Rocha et al., 2000); this feature is a limitation to the use of CB in transplantation, especially in adult patients. However mismatched CB, if compared with matched unrelated bone marrow, can promote a similar long-term leukaemia-free survival in both children (Rocha *et al.*, 2001) and adults (Takahashi *et al.*, 2007). Improvements in adults transplantation were also obtained with strategies designed to increase the CD34+ cell dose, such as the use of double CB transplant (Ballen et al., 2007) and the combination of single-unit CB transplant with the co-infusion of mobilized haematopoietic stem cells (MHSC) from a third party donor (Bautista *et al.*, 2009; Martin-Donaire *et al.*, 2009).

As general features, the decrease in GvHD observed in CB transplantation is accompanied by a higher rate of post-transplant infections, especially CMV reactivation, and by a slowed immune reconstitution when compared to HSCT using adult-derived stem cells. More specifically, neutrophils and NK cells return to physiological levels in the first 2 months after transplantation but CD4 and CD8 T cells remain low for 6-12 months (Komanduri *et al.*, 2007), resulting in a longer period of immunodepression compared to adult HSC recipients. CB transplanted patients also experience a slower engraftment when compared to adult-derived HSCT. The increased naivety/immaturity of CB cells may account for all these observations.

To summarize, HSCT is more effective in establishing cure and remission than alternative chemotherapy-based treatments, but is also responsible for a substantial treatment-related morbidity and mortality (Wagner and Gluckman, 2010). Even if the transplant-related mortality of some allogeneic HSCT is less than 10%, there will be an approximate rate of 40% fatality among the patients with established malignancy who undergo HSCT, and this will depend on complications related to the transplant. Transplant-related infections, mainly of fungal and viral origin, play a major role in this; therefore, any treatment against them (including immunotherapy) has great importance in HSCT.

1.6.2 IMMUNOTHERAPY:

Immunotherapy is defined as a treatment that elicits therapeutic responses against a disease primarily through the host immune defence mechanisms, either innate or adaptive (Kim *et al.*, 2004). The aim of immunotherapy may vary depending on the ongoing pathology: it can be elimination of damaging cells, either cancer or virus-infected ones, or protection of healthy tissue from immune destruction, as can happen in graft rejection or autoimmune diseases. These objectives can be reached via either cells- and/or cytokines-mediated action, as shown below in Figure 1.9. Concentrating on cellular-mediated immunotherapy only, broadly speaking it can belong to one of two categories: the *active* one aims at the introduction of antigens into the patient in an

immunogenic form, either to break tolerance or to activate T cell subsets; vaccination is a well known and very successful form of active cellular immunotherapy (Mocellin *et al.*, 2004). In the *adoptive* immunotherapy immune cells are instead collected, stimulated and expanded *ex vivo* and then infused in the patient. Figure 1.9, below, is a scheme resuming all the main types of immunotherapy available, with examples for each major subtype.

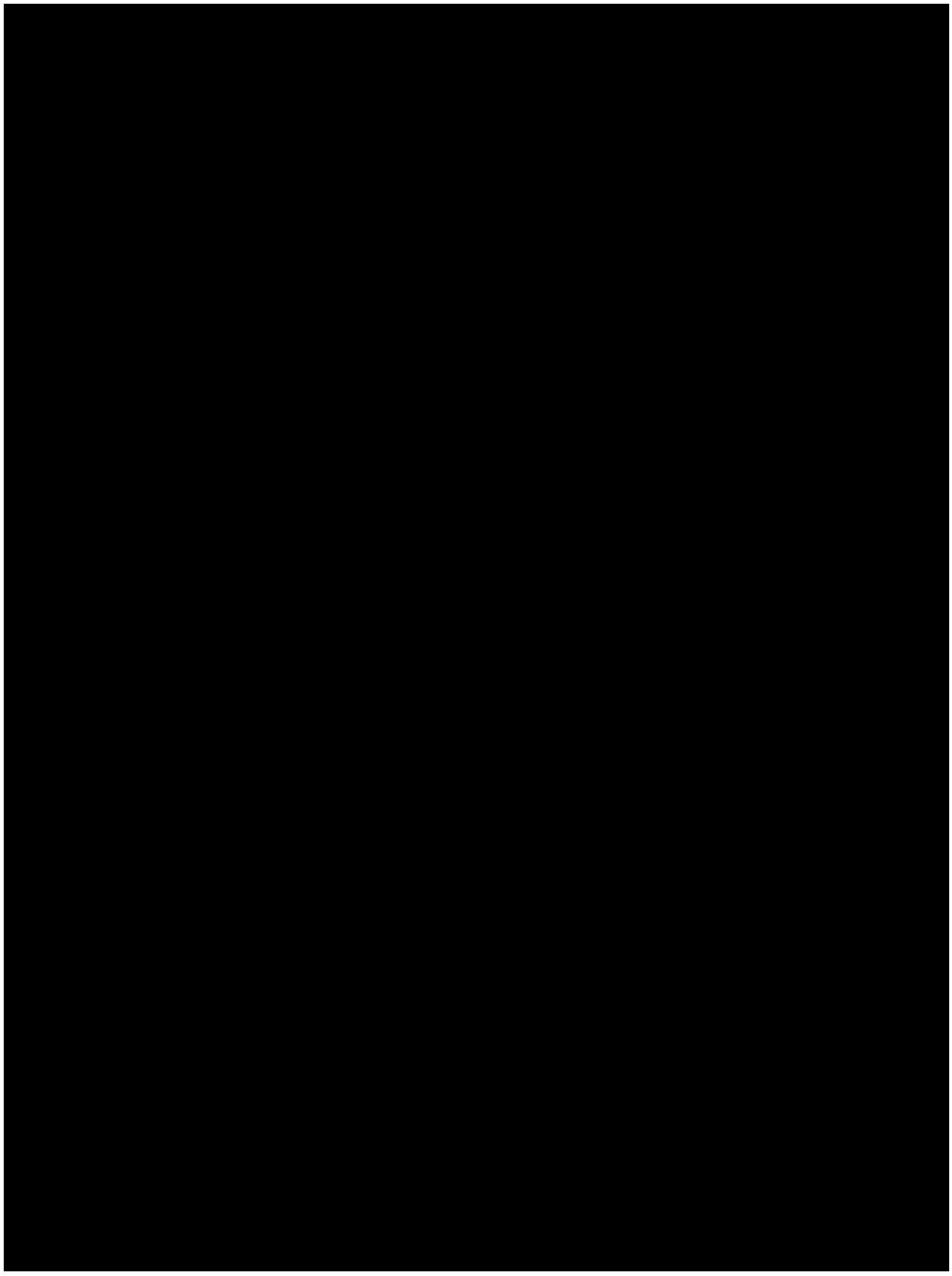

Figure 1.9: scheme of all types of immunotherapy. Modified from Van Den Bosch *et al.*, 2006.

1.6.3 CYTOMEGALOVIRUS (CMV):

CMV is one of the largest and most complex viruses known so far. Belonging to the herpes virus family, CMV is a double stranded DNA virus whose genome (230 Kb), enclosed in an icosahedral nucleocapsid, is surrounded by both a matrix and a lipid bilayer containing a variety of viral glycoproteins. A large proportion of the matrix proteins are phosphorylated and potently immunogenic; the most abundant are pp150 (UL32) and pp65 (UL83) that is one of the main CMV antigens. pp65 is synthesized early in the lytic cycle and the regulation of its production is likely to play a major role in controlling the latent state (Peggs, 2009). CMV is a species-specific ubiquitous pathogen and the co-evolution occurred within its human host led to the development of a number of immune evasion strategies that allow the survival of a significant viral reservoir in infected individuals, mainly in the mononuclear leukocytes subset. Around 50 to 80% of the USA adult population is infected with CMV by the 40th year of life (from http://www.cdc.gov/cmv/facts.htm), yet the infection is asymptomatic in the majority of cases. Despite its lack of clinical symptoms in healthy patients, the percentage of the host immune system devoted to CMV control is remarkable, as up to 1-2% of both the CD4 and CD8 compartments in young samples' cohort and up to 30-40% in elder cohorts are CMV-reactive (Pourgheysari *et al.*, 2007).

1.6.4 THE IMPACT OF CMV IN HSCT:

In some cases, symptoms that are indistinguishable from those of infectious mononucleosis occur in the host upon primary CMV infection. However, viral replication is in most cases not clinically relevant in healthy patients. This may allow the virus to spread both horizontally and vertically but, even so, systematic dissemination events remain rare in immunocompetent hosts, as the virus is kept in check by both innate and adaptive immunity.

However, the virus-host existence is severely altered when the host immune system is suppressed, for example following HIV infection or allogeneic HSCT. In these circumstances CMV disease -defined as viral dissemination with end-organ disease- has

a lethal potential and at the very least is a significant cause of morbidity. As the main reservoir for CMV is the leukocyte cell subset in blood, the use of leukocyte-depleted blood or blood products can diminish the risk of primary CMV infection upon HCST. However, viral replication and dissemination takes place in 60-70% of CMV-seropositive transplant recipient, while the rate of primary infections for CMV-seronegative recipients with CMV-seropositive donors is between 20 and 40% (Peggs, 2009). Once viral replication occurs, if left untreated, it leads, in 40-50% of the total cases, to a symptomatic disease whose most common manifestations are interstitial pneumonitis (CMV-IP), hepatitis or gastrointestinal disease (Van Den Bosch *et al.*, 2006). Among all the clinically relevant symptoms, CMV-IP is the most important as it has an associated mortality of around 90%; antiviral drugs (ganciclovir, foscarnet) are available, but their limited efficacy once CMV-IP is established and the relevant morbidity associated with their use (renal toxicity and suppression of myelopoiesis) urgently call for alternative ways to control CMV infection. In this light, the reconstitution of pathogen-specific immune protection via immunotherapy is an attractive and promising strategy.

1.6.5 IMMUNOTHERAPY FOR CMV IN HSCT SETTING:

One of the main objectives in immunotherapy is to generate an effective cell-mediated immune response, particularly in the case of CMV infection where the virus persists in a latent state. In HSCT setting, CMV reactivation occurs rapidly after the immunosuppressive treatment is started. Moreover, it is possible that alloreactive immune responses play an important role in CMV reactivation, as the incidence of CMV-related morbidity is higher in allogeneic transplantation than in syngeneic setting (Soderberg-Naucler and Nelson, 1999).

The transfer of antigen-specific T cells from the stem cell donor to the patient takes place several weeks after the HSCT has been performed and is a feasible and attractive option to restore effective antiviral immunity in patients. Kolb *et al.*, 1990, produced the demonstration that this strategy was effective in clinic, when they performed donor

lymphocyte infusion (DLI) in patients to decrease the rate of relapse boosting the GvT effect. Some years later Gadner's group demonstrated that cellular immunity could be transferred via DLI when they showed a CMV-specific response in a patient after leukocyte administration from a CMV-seropositive donor (Witt *et al.*, 1998). These approaches, despite being promising, were not pursued further due to two main reasons; firstly, DLI is still associated with a significant GvHD rate and, most importantly, it was not intended to restore viral immunity in the first place, as it is a non-specific treatment (Van den Bosch *et al.*, 2006). Indeed, the advent of DLI has revolutionised HSCT protocol but its main application remains the treatment of a malignant disease, rather than infections. However, the transfer of viral-specific cells holds more potential and considerably less drawbacks.

In fact, the finding that CMV-specific CD8 T cells conferred protection against lethal CMV challenge in mice (Reddehase *et al.*, 1985) encouraged the development of adoptive transfer protocols in humans. Greenberg's group performed the first adoptive transfer of *in vitro*-expanded CMV-specific T cells lines and, upon reinfusion in the patients, CMV-specific cytotoxicity was shown (Riddell *et al.*, 1992). Peggs *et al.*, 2001, introduced a modification in the *in vitro* protocol for CTL generation eliminating the need for live virus and using viral lysate instead (Peggs *et al.*, 2001). Using this approach, half of the patients treated did not require antiviral drugs (Peggs *et al.*, 2003). Of particular relevance in this study was the large *in vivo* expansion registered in the T cell compartment; tetramer-mediated analysis showed that the clonal expansion of T cells was in the order of 1 X 10^3-1 X 10^5 fold. Hebart's group showed that CMV-specific, polyclonal T cell lines containing both CD4 and CD8+ve cells were effective against viral reactivation even when the adoptive transfer was performed very late after HSCT (median 120 days, Einsele *et al.*, 2002). The use of NLV peptide, rather than CMV lysate, to pulse the DCs used subsequently for T cell expansion, resulted in a skewing towards CD8 T cells with a high efficiency (62% NLV-specific T cells compared to 0.2-6.5% CMV specific CD8 T cells when using lysate) (Micklethwaite *et al.,* 2007). A direct selection approach (i.e. effectors cells that are not expanded *ex vivo*) is also arriving in clinical settings; Cobbold *et al*., 2005, published their findings about a

cohort of nine HSCT patients receiving cells selected by HLA-peptide tetramers of various specificities. While total numbers of infused cells were low (between 1.2 and 33 X 10^3 cells/kg) the purity was very high (median over 95%), making the absolute numbers of CMV-specific cells comparable to the ones published in Peggs *et al*., 2003 (Cobbold *et al*., 2005). Multi-specific immunotherapy has also been employed; an approach using DCs transduced with pp65-encoding adenoviruses to expand CTLs, which are then infused prophylactically after transplantation, led to an increase in ELISPOT analyses in 7 out of 10 patients and in an increase in tetramer-specific cells in 4 of the 7 patients above (Leen *et al*., 2006). Finally, a preclinical trial involving the preparation of CMV specific, TCR transgenic T cells showed promising results in an *in vitro* setting (Schub *et al*., 2009).

1.7.0 SUMMARY OF THE PROJECT:

This PhD project will describe the characterization of three engineered aAPC systems developed with the long-term objective of using them to generate antigen-specific CD8+ve T cells for immunotherapy. Two of the systems are cellular-based (DCs and γδ T cells of CB origin) while the third is liposome-based, completely artificial and prepared starting from data previously generated in the Anthony Nolan Research Institute and published in De La Peña *et al.*, 2009. The main antigens used in this project are NLV (a CMV-derived peptide) as a model for immunotherapeutic treatment of HSCT-related viral infections and Melan A (a melanoma-derived peptide) as a proof-of-concept for cancer-directed immunotherapy. Chapter 3 will describe the preparation and use of the liposome system in two *in vitro* models (a CMV human system and an ovalbumin murine one). Chapter 4 will describe the set up and characterization of the CB-derived DCs model and its use to generate CD8+ve T cells in an *in vitro* MelanA system. In Chapter 5 the data regarding the analysis of γδ T cells from CB and their APC potential will be presented and discussed. While in the case of γδ T cells from CB the generation of antigen-specific CD8+ve T cells was not accomplished, this experiment was set up in both the other two systems under examination (DCs and liposomes).

CHAPTER 2:
MATERIALS AND METHODS

2.1.0 BIOCHEMISTRY:

2.1.1 LIPOSOME PREPARATION:

2.1.1.0 MATERIALS:

Five different lipids (Avanti Polar Lipids, INC) were used for the lipid mix to prepare liposomes: phosphatydilcholine (PC), cholesterol (CHOL), 1,2-dystearoyl-sn-glycero-3-phosphoethanolamine-N-[methoxy (polyethylene glycol)-2000] (DSPE-PEG), 1,2-dystearoyl-sn-glycero-3-phosphoethanolamine-N-[maleimide (polyethylene glycol)-2000] (MAL), [1,2-dipalmitoyl-sn-glycero-3-phosphoethanolamine-N-(lissamine rhodamine B sulfonyl) (RHODA). The lipids were mixed together according to the following published ratio (Pagnan *et al.*, 2000, Pastorino *et al.*, 2000 and De La Peña *et al.*, 2009):

PC: CHOL: DSPE-PEG: MAL = 2: 1: 0.02: 0.08.

RHODA, when used, was added at 1% of PC amount, resulting in a lipid mix/batch as follows:

PC	76 mg
CHOL	19.33 mg
DSPE-PEG	4.20 mg
MAL	11.76 mg
RHODA	0.76 mg

2.1.1.1 PREPARATION:

The lipids were dissolved in a round-bottomed flask using chloroform as solvent. Following complete solubilisation, the chloroform was evaporated under a stream of liquid nitrogen using a rotor evaporator (many thanks to Dr Ramesh, Royal Free Hospital, for his technical assistance). The resulting dry lipid mix was hydrated using freshly made hydration buffer (4-(2-hydroxyethyl)piperazine-1-ethanesulfonic acid or

HEPES ($C_8H_{18}N_2O_4S$) 25 mM + NaCl 140 mM, pH 7.4, filtered and degassed) to obtain multilayer "onion" vesicles. The preparation was then vortexed for one hour at room temperature (RT) prior to extrusion taking care not to overheat the mixture. The extrusion step required to cut the liposome at the desired dimension (100 nanometers (nm)) was accomplished using a manual mini extruder kit (Avanti Polar Lipids, INC): using two 1-ml syringes, the hydrated onion vesicles were then passed 10 times through a 100 nm pore filter. The liposomes were then kept at 4°C in the dark until use; they can be stored for a maximum of one week (as from indication of the lipid manufacturer) but were usually used the day after preparation, following loading and Fast Protein Liquid Chromatography (FPLC) purification. An overview of liposomes' preparation is reported below in Figures 2.1 and 2.2.

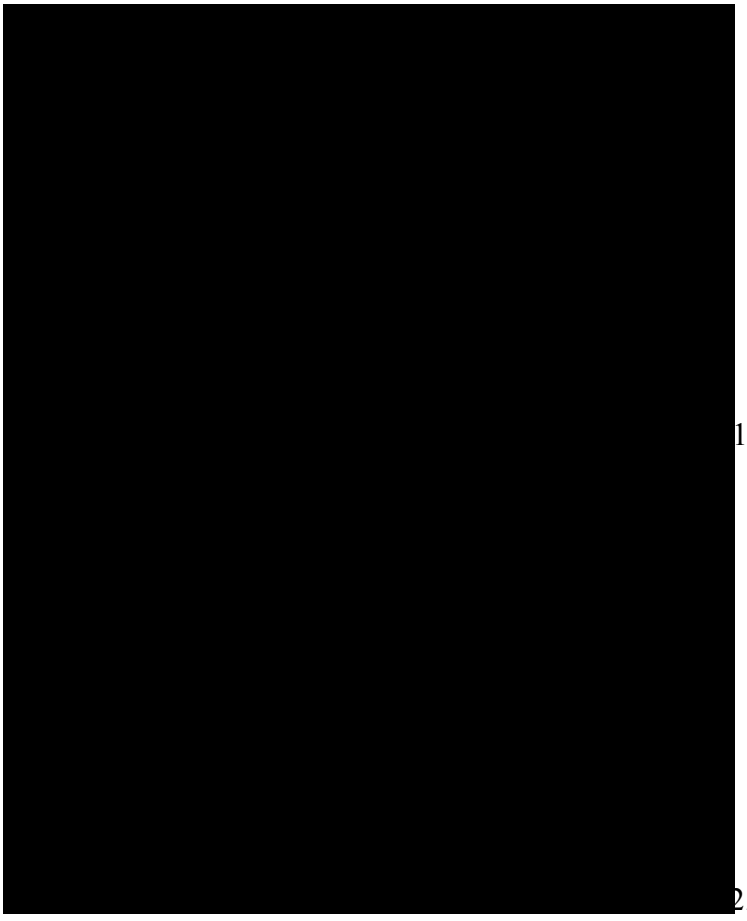

Figure 2.1: scheme of liposome formation. The figure summarizes the steps leading to liposome formation starting from the swelling and detachment of the dry lipid sheet to form large, multilamellar vesicles (LMV). LMV's size is then reduced via either mechanical energy (extrusion, as in figure 2) or sonication. Figure courtesy of http://www.pharmainfo.net/reviews/liposome-versatile-platform-targeted-delivery-drugs. **Figure 2.2: mini-extruder.** It was used to reduce the LMV's dimensions, as detailed by the manufacturer. Figure courtesy of Avanti Lipids.

2.1.1.2 CHROMATOGRAPHIC PURIFICATION:

Following their coupling with MHC molecules (see paragraph 2.1.2.10) the liposomes underwent FPLC to remove all the unbound protein monomers from the preparation. The chromatography was performed also on "naked" liposomes (i.e. without any protein coupled) to provide a suitable control in downstream experiments. All FPLC experiments were performed on an AKTA purifier (Pharmacia Biotech) using sepharose CL-4B beads (40-165 μm diameter, Pharmacia) packed in XK column (16 mm diameter, 20 cm length) from Amersham Biosciences. The buffer used for the chromatography was the same HEPES buffer used for the hydration of the lipid film. Liposomes, both loaded and unloaded, usually fell around fraction 2-3 (see Figure 2.3B, below), while unbound protein was usually retrieved in fraction 6-7 (see Figure 2.3B, below), or, in any case, approximately 4-5 fractions after the liposomes.

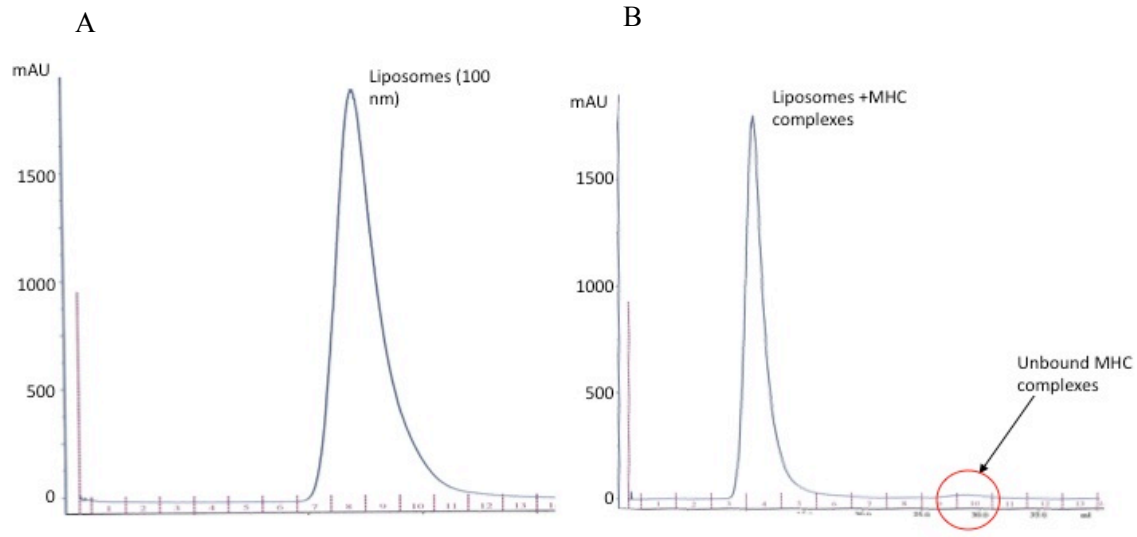

Figure 2.3: chromatographic purification of liposomes. The chromatographic plots of purification of A, an unloaded liposome and B, an MHC-loaded liposome (the shoulder highlighted in the red circle represents the unbound MHC complexes) are shown. Fractions 7-10 and 3-5, for A and B respectively, were collected for liposome concentration and recovery. A chromatographic purification step was performed at every liposome preparation. mAU, milli absorbance unit.

2.1.1.3 CONCENTRATION, FILTRATION AND STORAGE:

Following chromatographic purification the liposomes (usually 1 or 2 fractions of 3 ml each) were concentrated to a final volume of approximately 3 ml using Vivaspin tubes (Vivascience) with a molecular cut-off of 10000 Dalton as molecular weight unit (MWDa), as the expected weight of the loaded liposomes was around 43000 MWDa. Centrifugation was performed at no more than 2200 revolutions per minute (rpm) or 687.5g not to damage the liposomal membrane and for the shortest time possible. If they were to be used *in vitro,* they were then filtered using single-use filters with 0.20 μm pores (Minisart) and stored aseptically.

2.1.1.4 FLOW CYTOMETRY OF LIPOSOMES:

Liposomes were blocked with 1/10 of final volume of human serum (BioWhittaker) for 30 minutes at RT. The relevant antibodies (anti-HLA A2/fluorescein isothiocyanate (FITC); Abcam, anti-HLA class I (clone W6 32) FITC; Bioscience, and /allophycocianin (APC); Biolegend) were then added to the blocked liposomes and incubated for 30 minutes more at the same conditions prior to run the samples. Liposomes, when analyzed by flow cytometry on their own (i.e. when they were not added to cell cultures), were not washed (as in regular flow cytometry staining protocol) due to the poor tolerance of liposomes to centrifugation.

2.1.2 MHC/PEPTIDE COMPLEXES SYNTHESIS:

2.1.2.0 CLASS I HEAVY AND LIGHT CHAIN, PEPTIDES:

Two MHC heavy chain were used in this project: HLA-A*0201 (exon 2, 3 and 4 only, corresponding to the exoplasmic portion of the protein) and H2-K^b (exoplasmic part only). Both heavy chains were refolded with the human β_2m light chain. All the above molecules were already available in the laboratory before the start of this project as open reading frames (ORFs) inserted in the pET3D expression vector.

Two peptides were used for the human HLA-A*0201 heavy chain and one for the murine H2-K^b heavy chain. Their full sequence is presented in Table 2.1, below. The NLV peptide is a well-known immunodominant CMV epitope derived from the viral protein pp65 (Solache *et al.*, 1999). The MelanA-Mart1 peptide (from now on called MelanA) is an HLA-A*0201 restricted melanoma-related antigen. Naïve MelanA-specific CD8+ve T cells can be detected in up to 60% of the healthy, HLA-A*0201 positive population (Pittet *et al.*, 1999). The ovalbumin peptide was chosen as a model to be used in the OT-1 transgenic mouse strain (see Table 2.3, paragraph 2.2.1.5) kindly made available by Prof H. Stauss (Royal Free Hospital, London). All the peptides were bought from Alta Bioscience, Birmingham.

Name	**Sequence**	**Gene/protein of origin**
NLV	NLVPMVATV	pp65 (cytomegalovirus)
OVA	SIINFEKL	Ovalbumin
MelanA-Mart1	ELAGIGILTV	MelanA gene

Table 2.1: **list of the peptides used in this project.**

All the peptides above were used to refold monomers, in combination with the relevant heavy chain. HLA-A*0201-NLV and HLA-A*0201-MelanA monomers only were also used for tetramerization, when required.

2.1.2.1 INCLUSION BODIES PREPARATION:

Glycerol stocks of the bacterial strains containing the protein of interest were plated on Luria-Bertani (LB) medium plates (Sigma) with 100 mg/ml of ampicillin, then incubated overnight at 37°C. A single colony was then used to inoculate 5 ml of ampicillin-supplemented LB medium, as above, and following an overnight incubation the whole culture was used to inoculate a litre of XYT medium (10 g of tryptone and 5 g yeast extract, both Sigma, and 5 g NaCl, AnalaR BDH) supplemented with ampicillin as above. The cultures were incubated at 37°C with constant mixing until they reached an optical density (OD) of 0.4-0.6 at 550 nm. This usually required between 4 to 6 hours. The expression of the protein was induced by adding to the cultures 1 mg of

isopropyl β-D-1-thiogalactopyranoside (IPTG, Alexis Biochemicals) and the culture was continued for 4 more hours to maximize protein expression. Aliquots of the culture were collected at hourly intervals to assess the induction efficiency. At the end of the incubation period, the bacteria were collected via centrifugation (30 minutes at 4000g, 4°C). The resulting pellet was resuspended in the minimum amount possible of ice-cold PBS and frozen at -70°C overnight.

2.1.2.2 PURIFICATION OF INCLUSION BODIES:

The bacterial pellets were defrosted and sonicated 8 times for 45 seconds each time at maximum amplitude, taking particular care not to heat the mixture (sonication was performed with the tube containing the inclusion bodies always immersed in ice). The resulting solution was washed 3 times with freshly made Triton wash buffer (50 mM Tris HCl pH 8, 100 mM NaCl, 1 mM EDTA ($C_{10}H_{16}N_2O_8$) pH 8, 0.1% sodium azide (NaN_3), 0.5% Triton X-100, 1 mM dithiotreitol (DTT, $C_4H_{10}O_2S_2$) added just before use) spinning at 15000 rpm (4700g), 4°C, between each wash and ensuring to break up the pellet thoroughly at each wash. A further wash step was performed using freshly made resuspension buffer (50 mM Tris HCl pH 8, 100 mM NaCl, 1 mM EDTA pH 8, 1 mM DTT added just before use), prior to a final spin using the same condition as above. The resulting pellet was dissolved in the minimum volume possible of a urea-based buffer and left to dissolve at 4°C and rolling.

The composition of the urea buffer for β_2m chain was 8 M Urea (CH_4N_2O), 0.1 M NaH_2PO_4, 0.01 M Tris HCl pH 8, 0.1 mM EDTA pH 8, 0.1 M DTT, while the buffer for the heavy chains was 8 M urea, 50 mM 2-(N-Morpholino)ethanesulfonic acid (MES, $C_6H_{13}NO_4S$) pH 6.5, 0.1 mM EDTA pH 8 and 0.1 M DTT. For both buffers, all the components except the DTT were added, then the solutions were deionized at 4°C using Amberlite beads (Merck). The solution was left stirring, adding more beads if necessary, until some of the beads retained their blue colour (while the majority turned yellow). The solutions were then filtered on filter paper to remove the beads. DTT was added immediately before use. After the overnight incubation any insoluble material

was removed with a centrifugation at 3300 rpm (1031g), 4°C, for 10 minutes. The concentration of the protein in the solution was then assessed, either via a BCA assay or using a Nanodrop spectrophotometer using appropriate settings.

2.1.2.3 BCA ASSAY:

The bicinchoninic acid (BCA) assay (Pierce) is a robust assay that allows the colorimetric detection and quantification of an unknown protein by spectrophotometer absorbance at 562 nm. Protein concentrations were determined comparing them to a standard curve prepared using bovine serum albumin (BSA) at known concentrations. A series of dilutions of albumin were prepared and assayed alongside the test protein. A titration curve was prepared aliquoting BSA from 0 to 8 μg in 500 μl of water. The test protein was instead aliquoted at 1, 2.5 and 5 μl in 500 μl of water. 500 μl of the A, B, C solution of the BCA kit (Pierce) mixed in a 1 : 0.96 : 0.04 (A:B:C) ratio were then added to all the experimental and standard curve samples. All the samples were mixed manually and incubated at 60°C for 1 hour to allow colorimetric development and then immediately read on a spectrophotometer at 562 nm. The protein concentration was assessed comparing the OD values against the ones of the standard curve. Figure 2.4 is an example of a BCA standard curve.

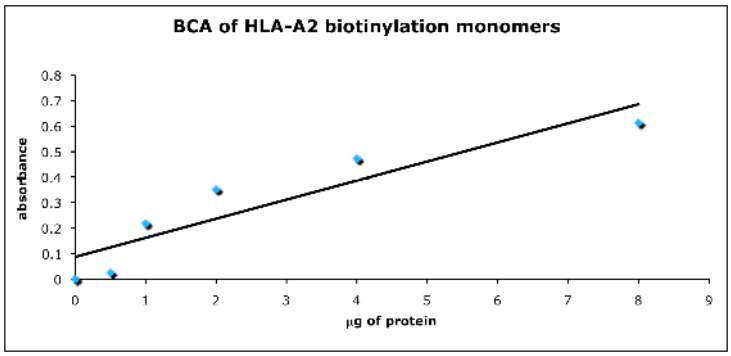

Figure 2.4: BSA standard curve. The blue dots represent the actual spectrophotometric readings for each BSA sample while the black line is the approximate curve obtained via linear regression.

2.1.2.4 SDS-PAGE GEL:

A denaturing protein gel was run using the samples collected during the induction with the two aims to assess the efficacy of the induction and the size of the proteins retrieved after purification. The SDS PAGE gel formula was as follows:

- Running gel: 0.375 M Tris HCl pH 6.8, 0.1% sodium dodecyl sulphate (SDS, $CH_3(CH_2)_{11}OSO_3Na$), 30% acrylamide (C_3H_5NO), 0.03% ammonium persulphate (APS, $(NH_4)_2S_2O_8$), 0.15% tetramethylethylenediamine (TEMED, $C_6H_{16}N_2$) (added in this order).
- Stacking gel: 0.125 M Tris HCl pH 6.8, 0.1 % SDS, 5% acrylamide, 0.1% APS, 0.1% TEMED (added in this order).

10 µl of the samples preserved before and during the induction were loaded on the gel together with an equal volume of loading buffer (1 M Tris HCl pH 6.8, 10% SDS, 0.1% bromophenol blue, 10% glycerol, 1 M DTT). The samples+loading buffer were denatured for 3 minutes at 98°C and then loaded on a gel together with a molecular weight standard (Biorad Laboratories). The gel was run for 1 hour at 150V and 400 milliAmpere (mA) in a running buffer composed of 25 mM Tris HCl, 250 mM glycine and 0.1% SDS. At the end of the run the gel was stained in Coomassie blue (0.1% Coomassie blue (BDH, catalogue number 44248) in 40% methanol (CH_4O) and 10% acetic acid ($C_2H_4O_2$)) for 30 minutes, de-stained overnight in methanol and acetic acid buffer (10% methanol, 7% acetic acid) and dried. Figure 2.5 shows an example of heavy chain induction on SDS gel.

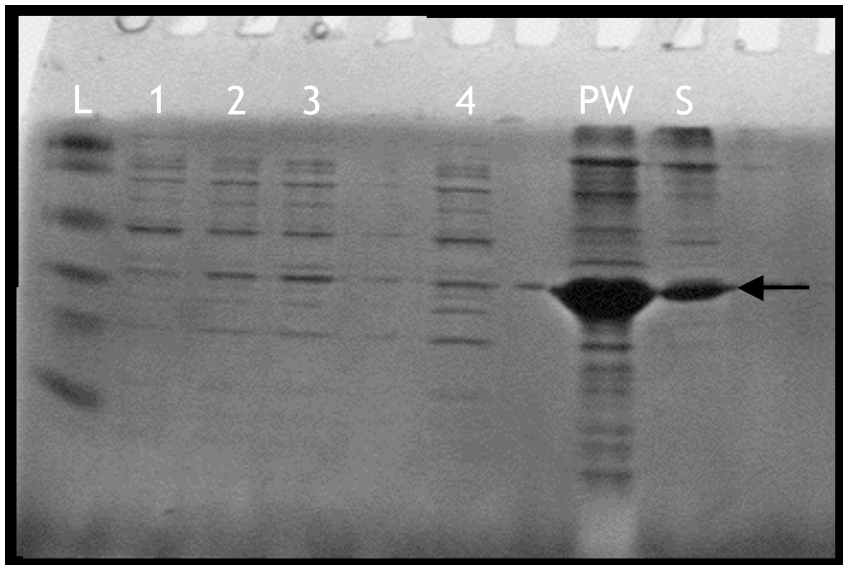

Figure 2.5: SDS gel run to assess the size and concentration of HLA-A*0201 molecules prepared via inclusion body purification. L, molecular weight ladder (BioRad Broad Range), 1-4, 10 μl aliquots of the HLA-A*0201 heavy chain collected at 1-4 hours post IPTG induction, PW, 1 μl aliquot of HLA-A*0201 heavy chain post wash and solubilization, S, 1 μg of known HLA-A*0201 heavy chain preparation used as standard. The black arrow indicates the band of interest (45 KDa).

2.1.2.5 MHC-PEPTIDE REFOLDING:

In this project, the rapid dilution method for the refold of MHC-peptide complexes was selected among the various protocols available in literature. Working at 4°C, 4.8 mg of β_2m, 6.2 mg of heavy chain and 2 mg of peptide (corresponding to a 2 μM: 1 μM: 10 μM ratio) were added drop by drop, in this order, to 200 ml of refolding buffer (100 mM Tris HCl, 400 mM arginine monohydrochloride ($C_6H_{14}N_4O_2 \cdot HCl$, Sigma), 1 mM EDTA pH 8, 5 mM reduced glutathione, 0.5 mM oxidised glutathione, Sigma). The pH of the refolding solution was the single most important factor for the success of the refold and varied according to the peptide and heavy chain used: for HLA-A*0201-NLV and HLA-A*0201-MelanA the optimal pH was 8.0, for H2-K^b-OVA was 8.5 (optimization not shown). The solution was left stirring at 4°C for 48-60 hours and then spun at 4°C for 20 minutes at 3300 rpm (1031g) to remove any insoluble aggregate.

The refolding protocol detailed above was followed for HLA-A*0201-NLV and H2-K^b-OVA only. A slightly different protocol, as provided by Drs Mandruzzato and Della Santa (University of Padova, Italy), was chosen for HLA-A*0201-MelanA. The

decision to use a modified refold protocol was taken as Drs Mandruzzato and Della Santa had already an optimized procedure for HLA-A*0201-MelanA refolding, while there was no previous experience in our laboratory; therefore, it was considered that a protocol already tried and tested, rather than a *de novo* optimization, would have guaranteed better chances of success. In this case the amount of the single components were the same, but peptide and β_2m were added first in one aliquot, while the heavy chain was added in three aliquots over a total period of 36 hours. After this period the HLA-A*0201-MelanA refold was concentrated and treated as described below.

The refold solution was then concentrated to 2 ml using sequentially the Amicon (Millipore) UltraFiltration Cell system and Vivaspin tubes, keeping it always at 4°C. The concentration process from 200 to 2 ml (the maximum amount that could be loaded for FPLC) usually required some hours. The concentrated solution was stored at 4°C until the moment of performing FPLC, usually immediately after the concentration step. Low salt buffer (10 mM Tris HCl, 5 mM NaCl, filtered and degassed) was used in the chromatography step and the fractions containing the correctly refolded peptide-MHC complexes were collected and stored at 4°C (see Figure 2.6 below).

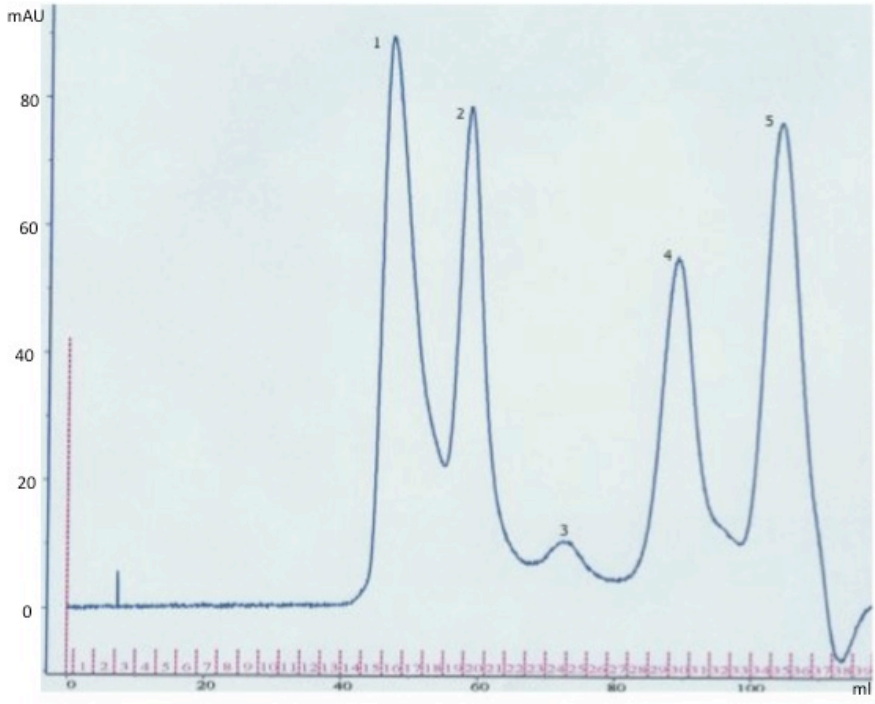

Figure 2.6: Chromatography plot of an HLA heavy chain-β_2m-peptide refold. 1: aggregate peak. 2: peak containing the refold of interest. 3: irrelevant shoulder. 4: peak of unrefolded β_2m molecule. 5: peak containing arginine (from the refold solution) and unrefolded peptide. mAU, milli absorbance unit.

The fractions of interest were then concentrated to 1 ml using Vivaspin tubes as above and the amount of protein was assessed via either BCA assay or Nanodrop spectrophotometer measurement. The refolded protein was then stored at 4°C for short-term use (i.e. up to 2-3 days maximum) or aliquoted and stored at -70°C for long-term use.

2.1.2.6 QUALITY MONOMER ASSESSMENT: DOT BLOT AND ELISA:

Two different protocols (dot blot and Enzyme-Linked Immunosorbent Assay or ELISA) were used to assess the correctness of the MHC-peptide refolding following FPLC. As detection antibodies W6/32 (anti-HLA class I, recognizes the HLA monomer only if it is correctly refolded including the presented peptide) for HLA-A*0201 monomers and 25.D1/16 (anti-H2-K^b-OVA) for the OVA-presenting H2-K^b monomer were used. The 25.D1/16 antibody was a kind gift from Dr Reis E Sousa, Cancer Research UK, London.

For the dot blot, a nitrocellulose membrane (Hybond ECL-Amersham) was "dotted" with the samples (either 1 μg of protein or 5 μl of water as negative control). The membrane was blocked by soaking it in blocking buffer (5% BSA in 0.05% Tween, 20 mM Tris HCl, 150 mM NaCl, pH 7.5) for 30 minutes. The membrane was then incubated for one hour with the primary antibody (3 μg total) diluted in the same buffer as above but with 0.1% BSA instead of 5%. The membrane was then washed 3 times, 5 minutes each time (same buffer as above, without BSA), and a secondary antibody – anti-mouse peroxidase for W6/32, anti-goat peroxidase for 25.D1.16- was added to the membrane after dilution in phosphate buffered saline (PBS) solution (Lonza) and incubated for one hour. The sample was then washed 4 times (same conditions as above) and the detection was performed using the ECL detection kit (Amersham) according to the manufacturer's instructions. The samples were detected as dark dots on Kodak films 18X24 cm. Figure 2.7, below, shows a representative dot blot performed using H2-K^b-OVA monomer.

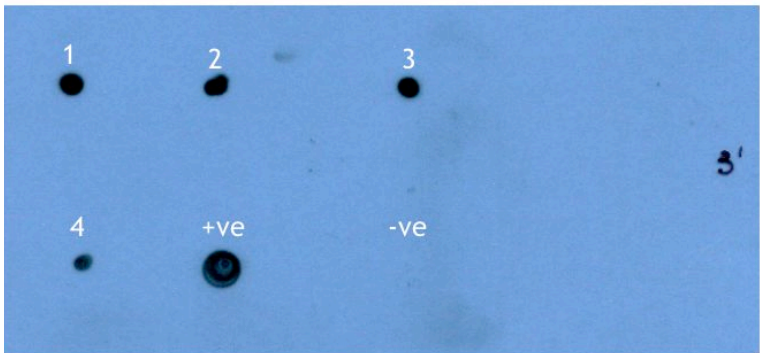

Figure 2.7: H2-K^b dot blot. Various aliquots of H2-K^b-OVA refold to be tested were dotted on a nitrocellulose membrane (1-4), alongside a 1 μg aliquot of a previously checked H2-K^b-OVA molecule as positive control (+ve) or water as negative control (-ve). Different exposure times were tested and only the best one (three minutes) is shown.

In figure 2.7, above, water only was used as –ve control. Other suitable -ve controls would have included either single heavy chain or β_2m molecules and irrelevant human (or irrelevant murine) MHC molecules; these controls would also have provided a measure of the cross-reactivity of the primary antibody used.

For the ELISA, an ELISA plate (Nunc-Immuno/MaxiSorp Surface, Gibco) was coated with a primary antibody (5 μg/ml W6/32 or 25.D1/16 antibody diluted in PBS or PBS only as negative control) and left for 2-3 hours at 37°C; the antibody was then flicked off. The plate was blotted on a tissue to drain and blocking buffer (1% BSA in PBS) was added to the wells and incubated overnight. Wells were then washed 6 times with PBS and a serial dilution of the protein to be tested was performed and incubated at RT for 1 hour. The plate was washed for 6 times with PBS and then a 1:5000 dilution of rabbit anti-human β_2m (secondary antibody, Sigma) was added to the wells and incubated for 20 minutes at RT. The plate was then washed 6 times with PBS and a 1:3300 dilution of horseradish peroxidase (HRP)-conjugated goat anti-rabbit Ig (Dako) was added to the wells and incubated for 20 minutes. The plate was then washed 6 times with PBS and developed colorimetrically using the Substrate Reagent Pack (catalogue number DY999, R&D) for 20 minutes at RT in the dark. The reaction was stopped using Stop solution (catalogue number DY994, R&D) and the plate was immediately read on an ELISA plate reader (Biotek) at 450 nm. Figure 2.8 shows an ELISA result plot.

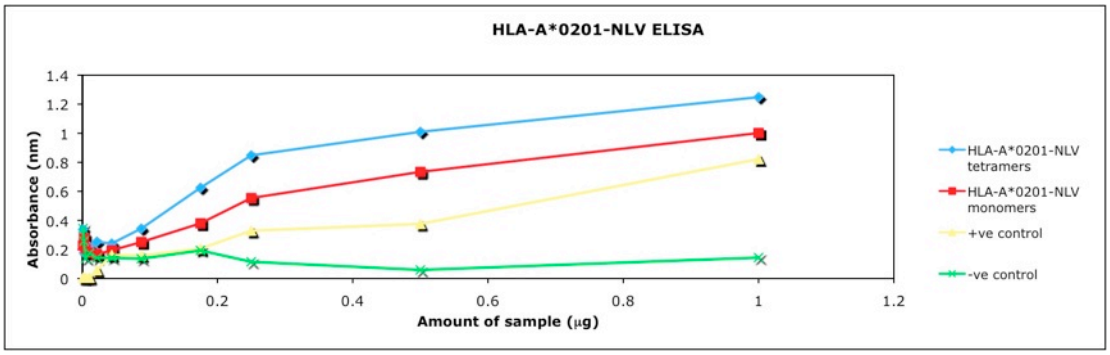

Figure 2.8: ELISA results. The assay was performed to check 2 different aliquots of HLA-A*0201 monomers (blue and red line, respectively tetramerized and monomeric molecules) compared to a known HLA-A*0201 refold used as standard (yellow line) and to PBS used as –ve control (green line).

In figure 2.8, above, PBS was used as –ve control. Other suitable -ve control would have included either single heavy chain or β_2m and irrelevant human (or irrelevant murine) MHC molecules; these controls would have provided also a measure of the eventual cross-reactivity of the primary antibody used.

2.1.2.7 MONOMER BIOTINYLATION:

After testing for a correct refold, the monomers were conjugated with biotin for subsequent tetramerization, if required. The HLA-A*0201 expression vector carried the AviTag sequence for biotinylation mediated by the biotin ligase (BirA) enzyme (Avidity, Colorado), thus allowing the reaction to be performed *in vitro*.

Briefly, the refolded protein was concentrated down to approximately 170 µl; a small unbiotinylated aliquot was taken and stored at –20°C to assess the efficiency of the reaction later on. 25 µl each of Biomix A and B were then added to the bulk of the refolded protein, followed by protease inhibitor and 0.5 µl of BirA enzyme (all from Avidity, Colorado). The reaction was incubated overnight at RT. The day after an FPLC step was performed to remove the excess of biotin in the reaction. This procedure was required, as biotin excess would have considerably hampered the efficiency of the successive tetramerization step. For biotin removal FPLC was performed using high salt buffer (150mM NaCl, 20 mM Tris HCl, filtered and degassed) and the fractions containing the biotinylated refold were promptly collected and concentrated as previously done. Figure 2.9, below, shows a chromatographic plot of the FPLC step to remove excess biotin.

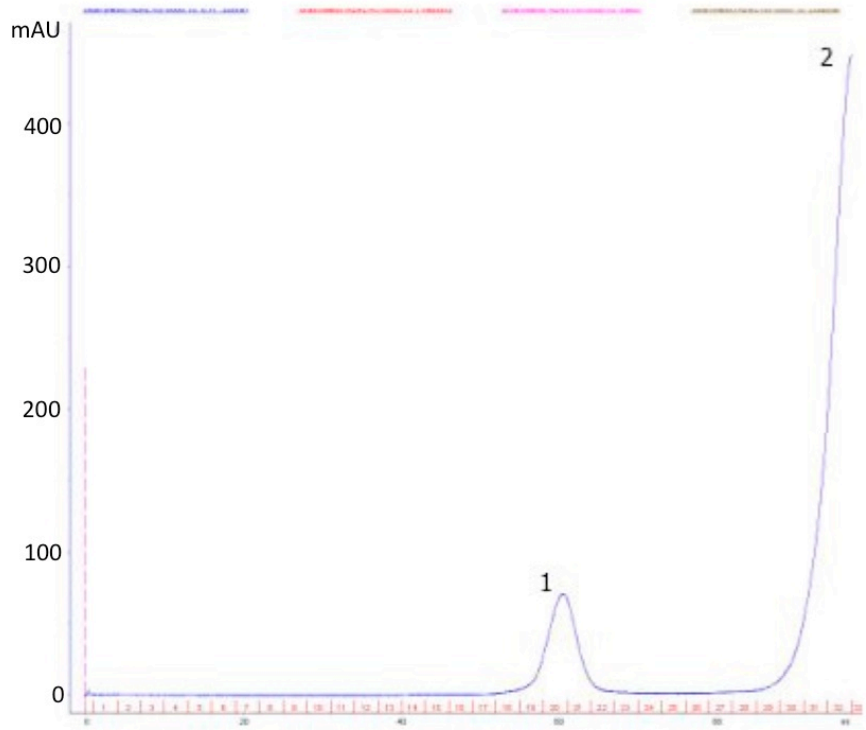

Figure 2.9: chromatography plot of the biotinylated HLA-A*0201-NLV monomer. Peak 1, around fraction 19-20, represent the biotinylated monomer (confront with figure 2.6), while peak 2, from fraction 29 onwards, represents unbound biotin (which is always added in excess to the reaction to improve its kinetics). mAU, milli absorbance unit.

Protein concentration was assessed either by BCA assay or by Nanodrop spectrophotometer reading using appropriate settings. A small aliquot was used for a native gel shift assay and the rest was either kept at 4°C for immediate tetramerization or aliquoted and stored at –70°C for long-term storage.

2.1.2.8 NATIVE GEL SHIFT ASSAY:

This assay is aimed to assess the efficiency of the biotinylation reaction. Pre-incubating biotinylated samples with extravidin (1 mg/ml stock, Sigma), biotin-conjugated HLA molecules will associate with the avidin molecule and will be heavier than unconjugated ones when run on a non-denaturing polyacrylamide gel. The difference in molecular weight results in a shift on the gel, as visible in Figure 2.10 below-confront lane 1 vs 2 and 3 vs 4.

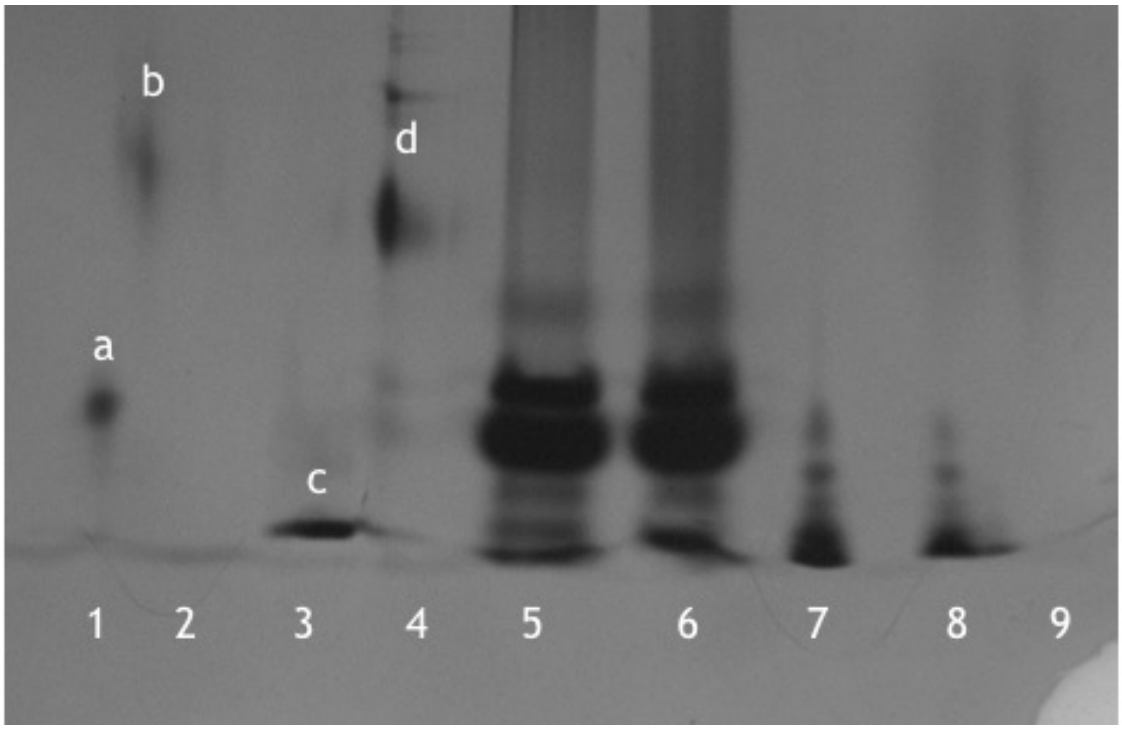

Figure 2.10: native gel shift assay. Lane 1: biotinylated monomer without extravidin. 2: biotinylated monomer after incubation with extravidin. 3: biotinylated commercial control without extravidin. 4: biotinylated commercial control after incubation with extravidin. 5 and 6: unbiotinylated monomer with (5) and without (6) extravidin. 7 and 8: unbiotinylated commercial control with (7) and without (8) extravidin. 9: extravidin loaded alone.

Lanes 1 and 2 show the biotinylated preparation without and with extravidin, respectively. While both samples are quite blurred (this is possibly due to the non-denaturing conditions of the gel; see as a comparison, for example, the clear bands showed in Figure 2.5), it is still possible to see a shift between extravidin-conjugated and unconjugated sample (as can be seen by a comparison of bands a and b). A similar shift can be observed between lanes 3 and 4, a commercial biotinylated sample without and with extravidin, respectively (compare bands labelled c and d). Between lanes 5, 6, 7 and 8, no shift can be detected; as these were the unbiotinylated samples, extravidin could not associate with the protein and, therefore no change in molecular weight was observed.

In the example shown above molecular weight markers were not included. However, when run in parallel, it should be possible to confirm that the bands of interest contain proteins of the correct size. Note however that the migration properties of proteins in

non-denaturing conditions can vary such that the relationship between size and molecular weight is not necessarily linear.

All the monomers that showed a successful native gel shift were subsequently used for tetramer production; of those, only tetramers producing a definitive stain (as seen in example Figure 2.12A) were then used for experiments.

This assay is performed in strictly non-denaturing conditions, with no SDS in the gel, loading or running buffer. The native gel was prepared as detailed in Table 2.2 below.

Reagents	**Running gel**	**Stacking gel**
30% acrylamide	8 ml	1.7 ml
Distilled H_2O	14.5 ml	6.8 ml
1.5M Tris HCl pH 8.8	7.5 ml	-
1M Tris HCl pH 6.8	-	1.25 ml
APS	100 µl	100 µl
TEMED	20 µl	10 µl

Table 2.2: **reagents required for a native gel**.

Once cast, the gel was pre-run at 150V for at least 30 minutes to remove any excess salt that may influence separation in a running buffer made of 24.8 mM Tris base and 192 mM glycine. Samples to be tested were incubated for 1 hour at RT with 3-6 µl of extravidin, then an equal amount of native loading buffer (50 mM Tris HCl pH 8.8, 0.1% bromophenol blue, 10% glycerol) was added to the samples and they were then run at 150V until the blue dye reached the bottom of the gel. The gel was then stained with Coomassie blue, destained with methanol solution as detailed before and examined (see Figure 2.10 above).

2.1.2.9 TETRAMERIZATION:

Following biotinylation and the assessment of its efficiency, the monomer sample was concentrated down to approximately 100-200 µl depending on the starting amount. Tetramerization was routinely performed on small aliquots of monomers and only when tetramers were needed to avoid long-term storage of fluorescent tetramers. For

tetramerization, a 4:1 molar ratio of monomers: fluorescent streptavidin is required (see Figure 2.11, below).

Figure 2.11: scheme of the tetramerization process. For this project both Pe- and APC-conjugated streptavidin was used.

Once the required amount of streptavidin was determined, it was added in $1/10^{th}$ aliquots at 20 minutes intervals to the biotinylated monomer, which was maintained in gentle agitation at 4ºC at all times. After the last addition of streptavidin, 0.05% of NaN_3 was added to each tetramer aliquot to prevent any bacterial growth. The tetramers were stored at 4ºC wrapped in foil. It was found that ready-to-use tetramers often degraded if stored long-term (i.e.>2 months) at 4ºC (data not shown); as such, it was preferred to store at -80ºC small aliquots of the biotinylated monomers, ready for tetramerization, and add the fluorescent streptavidin whenever required.

Figure 2.12A, below, shows the tetramer titration performed on an HLA-A*0201, CMV+ve donor. The same donor was also stained using commercial HLA-A*0201, CMV specific pentamers (ProImmune) (Figure 2.12B).

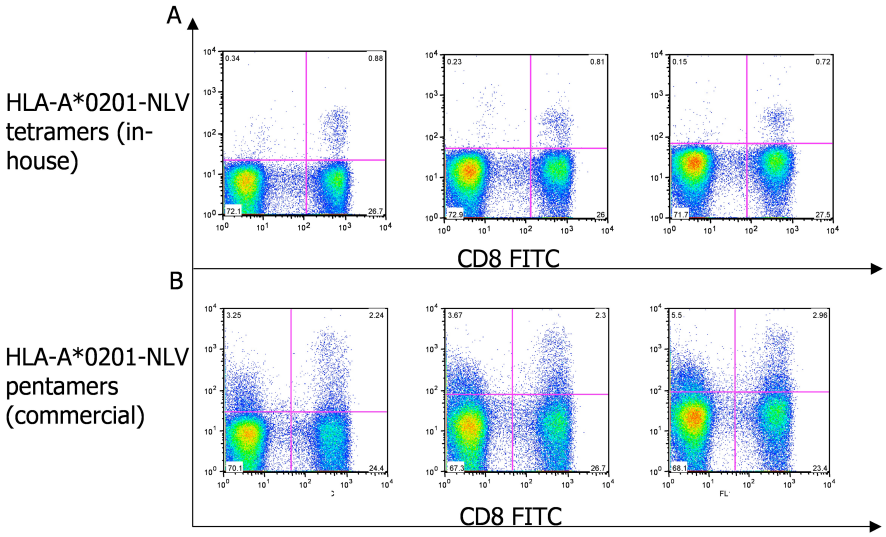

Figure 2.12A: titration of HLA-A*0201-CMV tetramers. Fresh PBMCs from a CMV+ve, HLA-A*0201+ve donor were stained with increasing amounts of tetramers (from left to right, 1, 2.5 and 5 μl respectively). The cells shown above were gated on lymphocytes.
Figure 2.12B: titration of HLA-A*0201-CMV commercial pentamers (ProImmune). Fresh PBMCs from a CMV+ve, HLA-A*0201+ve donor were stained with increasing amounts of commercial pentamers (from left to right 2.5, 5 and 10 μl respectively). The cells shown above were gated on lymphocytes.

It was found that the use of in-house tetramers was more effective compared to the commercial pentamers. Evidence of this is shown by the presence of a discrete CD8+ve tetramer+ve population with reduced unspecific labelling (CD8-ve tetramer+ve population) in Figure 2.12A. The staining with the commercial pentamers did not result in a discrete CD8+ve tetramer+ve population at any of the concentrations used and unspecific binding was more evident (see Figure 2.12B). Therefore, in-house tetramers were used in all the subsequent experiments.

Below (Figure 2.13A) the tetramers were used on a HLA-A*0201+ve, CMV–ve adult donor to check for unspecific staining. HLA-A*0201-MelanA tetramers were also tested on a MelanA-specific cell line (see Table 2.3) to ensure that the binding was TCR specific (Figure 2.13B).

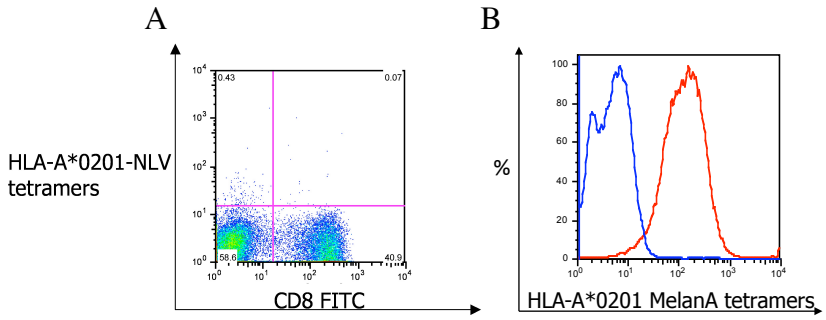

Figure 2.13A: assessment of tetramer-related unspecific staining. HLA-A*0201-CMV in-house tetramers were used to stain fresh PBMCs from a CMV-ve, HLA-A*0201+ve adult donor. Any unspecific staining should appear as a population in the upper right quadrant. Cells were gated on lymphocytes.
Figure 2.13B: assessment of HLA-A*0201-MelanA tetramers staining. An aliquot of J-RT3 cells (cell line transgenic for the HLA-A*0201-MelanA TCR) was stained with an aliquot of in-house tetramers. (—) unstained, (—) tetramer-stained (3 μl).

It was found that the use of HLA-A*0201-NLV in-house tetramers did not result in unspecific staining. The HLA-A*0201-MelanA tetramers were tested on the J-RT3 cell line, which provided a MelanA+ve control, and produced a good-quality staining (see above Figure 2.13B).

2.1.2.10 MONOMER ACTIVATION FOR LOADING ON LIPOSOMES:

The two monomers HLA-A*0201-NLV and H2-K^b-OVA were used in their native form for loading on the liposome surface. At the beginning of this project all the polypeptide chains to be loaded on the liposomes were treated with Traut's reagent (2-Iminothiolane Hydrochloride-C_3H_7NS•HCl Pierce) to add more –SH groups and thus facilitate the binding on MAL-containing liposomes.
The desired amount of protein (the highest amounts used in De La Peña *et al*., 2009, (7.98 and 10.64 μg) were used as references for this protocol) was dissolved in the same HEPES buffer used for hydrating the liposomes at a pH of 8.0. A stock solution prepared dissolving 8.5 mg of Traut's reagent in 1.5 ml of HEPES buffer was used to add an approximate 10-fold molar excess of reagent to the protein (whose volume was typically a few μl). The protein-Traut's solution was then taken to a final volume of 1 ml using HEPES buffer as above and incubated at RT for 1 hour. At the end the excess

Traut's reagent was removed using PD-10 desalting columns (GE Healthcare) according to the manufacturer's instruction. Cys-tagged monomers were treated in the same way omitting the Traut's reagent. The activated protein was concentrated to a final volume of 200-300 μl using Vivaspin tubes and immediately aliquoted onto 1 ml of liposome in a 12-well plate. The liposome plus the activated protein were then left mixing overnight at RT to promote loading of the protein. At the end of the incubation period, the monomer-conjugated liposomes underwent a chromatographic purification step (see Figure 2.2).

2.1.2.11 ELLMAN'S ASSAY:

The degree of activation (here defined as the amount of SH groups newly introduced in the protein) was assessed using the Ellman's reagent (5,5'-Dithio-*bis*-(2-nitrobenzoic acid)-DNTB, $C_{14}H_8N_2O_8S_2$, Pierce), which is recommended by the Traut's activation protocol as the best way to determine the free sulphydryl content in peptides and complex proteins. The Ellman's assay was performed according to the manufacturer's instructions: briefly, a buffer containing 1 mM EDTA, pH 8.0, and 0.1 M monobasic sodium phosphate ($Na_2HPO_4 \bullet H_20$) was prepared and used to dilute fixed amount of both Ellman's reagent and the sample to be tested (Traut's treated and untreated monomer), which were then combined. All the samples were incubated at RT for 15 minutes, then immediately read at 412 nm with a spectrophotomer. The amount of sulphydryls in each sample was then measured from the absorbance starting from the known DNTB extinction coefficient (14,150 $M^{-1}cm^{-1}$) and compared between Traut's treated and untreated samples. The results for this experiment are presented in Figure 2.14 below.

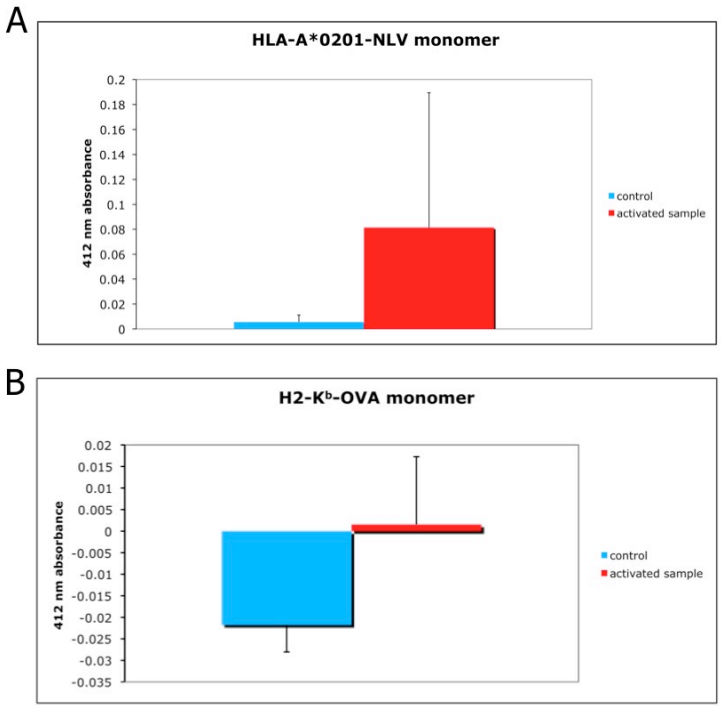

Figure 2.14: Ellman's assay on activated MHC monomers. Following the activation of MHC monomers with Traut's reagent for Cys introduction they were then assessed for their new level of thiol groups, as examined by measurement of absorbance at 412 nm. N=1, column represent the mean results of triplicate wells. Error bars correspond to standard deviation.

2.2 CELL BIOLOGY:

2.2.1 CELL SOURCES AND GENERAL CELL CULTURE PROTOCOLS:

2.2.1.0 BLOOD CELLS SOURCES:

The adult volunteer donors required for experiments were chosen among the cohort of voluntary blood donors in the Anthony Nolan Research Institute. Their HLA typing and CMV serology, when appropriate, was assessed in the Anthony Nolan Histocompatibility Laboratories and each volunteer signed an informed consent to the use of his/her blood for research purposes. Buffy coat samples were obtained from the Sheffield NHS blood bank.

Cord blood was used in the project either fresh as a whole cord blood sample (from the Anthony Nolan Cell Therapy Centre based in Nottingham, or from the Banc de Sang i

Teixits, Barcelona, Spain) or as frozen cord blood aliquot after ficoll treatment (from the Anthony Nolan Cell Therapy Centre based in Nottingham). Frozen aliquots were always shipped as double bags, one of 5 ml one of 20 ml, which could be processed independently (see Figure 2.15 below).

Figure 2.15: **segmented bag used for cord blood cryopreservation**. Image courtesy of www.cordlife.com/images/cryobag2.

Whenever possible, fresh samples were used within 24 hours from collection as it was found that time significantly affected monocyte viability (data not shown and Drs Richard Duggleby and Francesc Borras, personal communication). Whole fresh cord blood samples were shipped at 4ºC and as such, upon receiving, they were always diluted in the same volume of fridge-cold transport medium (RPMI supplemented with 5 mM β-mercaptoethanol (C_2H_6OS) and 3.3% sodium citrate ($Na_3C_6H_5O_7$), dissolved in deionized water and filtered) and left to equilibrate at RT. This process usually required 1-2 hours. Fresh cord blood samples were always processed on the day of arrival to use cells as viable as possible.

2.2.1.1 PBMCs PURIFICATION FROM ADULT BLOOD:

A small amount of heparin (200-300 μl for up to 50 ml starting blood) was added to fresh blood immediately after collection to prevent clotting. The heparinized blood could be maintained at RT for up to 24 hours without any adverse effect, if necessary, but it was always aimed to use it immediately after collection. The blood was layered over an equal amount of Lympholite (Cedarlane Laboratories Limited) and centrifuged

at 2200 rpm (687g) for 20 minutes at RT. The brake was not applied during the slowing down of the centrifuge to avoid any disturbance in the phase separation. The interphase containing the leukocytes was collected in a fresh tube and washed twice with RPMI 1640 medium (BioWhittaker) supplemented with 1% of penicillin/streptomycin solution (pen/strep), BioWhittaker (from now on called wash medium), or 1X PBS. The first wash was at 1800 rpm (562.5g) for 10 minutes, the second at 1800 rpm (562.5g) for 5 minutes. The brake was applied in both washes. The supernatant was then poured off, pellet was re-suspended by flicking and viable cells were counted. Cells were then maintained in wash medium until re-suspension and plating out as soon as possible after purification. The same procedure was applied to Buffy coat samples.

2.2.1.2 CBMCs PURIFICATION FROM CORD BLOOD:

Cord blood (mixed with the same amount of transport medium) was layered over Ficoll-Paque Premium (GE Healthcare) in a 50-ml Falcon tube using the following ratio: 15ml Ficoll-Paque: 35ml blood + transport medium. Cells were centrifuged at 2000 rpm (625g) for 30 minutes at RT. Brakes were not applied during the slowing down of the centrifuge not to disturb the phase separation. The pellet was re-suspended in two steps; firstly, the pellet was re-suspended in a few drops of media and then the suspension was diluted in x25 wash buffer and washed twice, as with adult cells (see 2.2.1.1).

If cell clumps occurred upon resuspension or during washing –a sign of early cell lysis- a DNAse treatment was performed. Briefly, a suitable amount of DNase I (CalBiochem, 1 X 10^6 U/ml, resuspended in PBS 1X) –the quantity varied for each sample according to total cell number and pellet size- was added to the resuspended cells and the solution was then incubated in a water bath at 37ºC with constant mixing until complete clumps disappearance or for up to three minutes maximum. Following a DNase treatment, cells were washed with 50 ml of warm wash medium and centrifuged for 5 minutes at 1700 rpm (531g) in addition to the two washes performed during the Ficoll-Paque treatment. Cells were then counted with Trypan Blue and/or Turk's stain. Following Ficoll-Paque

treatment cells were then re-suspended in wash medium until use, if they were to be used in the same day. If not, they were cryopreserved.

2.2.1.3 CELL COUNTING:

Cells were counted using two different methods in function of the red blood cell percentage of the sample. Trypan Blue (Sigma) 0.4%, a vital stain, seeps inside the cells (hence making them blue) when the cell membrane is damaged i.e. when cells are dead or apoptotic. Viable cells are not coloured by Trypan Blue appearing bright pink. Trypan was used in a 1:1 volume ratio to cells to assess the number of total viable cells. Trypan Blue cannot however discriminate between nucleated and anucleated cells. To accomplish this, Turk's staining was used (acetic acid 1% V: V in water and bromophenol blue) in a ratio 9 Turk's solution: 1 cell volume/volume. Turk's solution stains only nucleated cells, hereby allowing the removal of erythrocytes from the count of the total white cells as retrieved by Ficoll-Paque protocol. Turk's solution was used primarily for cord blood samples due to the higher number of red blood cells present. Nucleated cells appear as very bright and compact spots using Turk's staining.

2.2.1.4 CRYOPRESERVATION AND THAWING:

If cord blood or adult PBMCs were not used on the day of collection they were cryopreserved for long-term storage. Briefly, cells were pelleted by centrifugation at 1700 rpm (531g) for 5 minutes, resuspended in a solution made of 90% heat-inactivated fetal calf serum (FCS) and 10% dymethylsulphoxide (DMSO, C_2H_6OS) and transferred into cryovials (Nunc). No more than 10 X 10^6 cells/ml and/or 1.5 ml of cells/freezing mix were added to a single cryovial. They were immediately transferred on ice and stored at -80°C in a polystyrene box (for a gradual lowering of the temperature) for up to 3 days. The cryovials were then transferred into liquid nitrogen tanks for long-term storage.

To thaw adult PBMCs, the cryovials were warmed in a water bath at 37°C until no ice clumps were seen. The cell suspension was then quickly transferred to a 15-ml Falcon

tube containing 10 ml of warm RPMI medium and centrifuged at 1700 rpm (531g) for 5 minutes. The supernatant was poured off and the cell pellet was resuspended in RPMI medium for cell counting.

Frozen cord blood samples were thawed using a different protocol to minimize the temperature shock, as firstly described by Querol *et al.*, 2000. Briefly, the bags containing cord blood were warmed in a water bath at 37°C as seen above. Immediately upon complete thawing, the cell suspension was collected and added to an equal volume of chilled dextran buffer (dextran/gentran 40, Baxter, 5% heat-inactivated FCS, 0.63% sodium citrate, 5 mM $MgCl_2$, 1000 IU/ml DNase-I). This mixture was left at 4°C for 5 minutes. At this point more dextran was added (1 ficolled frozen cord blood: 4 dextran, or 1 unprocessed frozen cord blood: 6 dextran in volume) and the cells were spun for 20 minutes, 450g, at 10°C. The pellet was resuspended in RPMI medium and at this point a DNAse treatment was performed if cell clumps appeared. Otherwise, cells were counted and used.

2.2.1.5 CELL LINES AND GENERAL CULTURE CONDITIONS:

In addition to the primary cells (PBMCs from adult donor and CBMCs from cord blood), various cells lines were also used in this project. They are listed in Table 2.3 below.

Name:	Growth conditions:	Source/Owner:	Propriety:
RF 33.70	RPMI+10%FCS, 1% PS 1% l-glutamine, 1% NEAA (non-essential amino acids), 1% Hepes	Prof K. Rock, Umed, Massachussets	T cell hybridoma; it secretes IL-2 in the supernatant if its TCR is specifically engaged with an H2-K^b-OVA molecule.
J-RT3	RPMI+ 10% FCS	Prof P. Romero, Lausanne, Switzerland	T cell line (Jurkat-derived)-TCR-ve on its own, it has been transfected with an HLA-A*0201 MelanA-specific TCR.
K562	RPMI+ 10% FCS	Lab collection	Lymphoblast cell line of bone marrow origin; it is MHC class I-ve.
OT-1	RPMI+ 10% FCS	Prof H. Stauss, Royal Free Hospital	CD8+ve T cell line; it expresses only H2-K^b and derives from a transfected $RAG^{-/-}$ mouse.
RMA	RPMI + 10% FCS	Prof H. Stauss Royal Free Hospital	Murine T cell tumour line; it is an H2-K^b-expressing cell line and was used as an H2-K^b cDNA source

Table 2.3: **cell lines used in this project, their source and the main characteristic for which they have been chosen**.

2.2.2 FLOW CYTOMETRY:

2.2.2.1 ANTIBODIES:

The commercial antibodies used in this project for flow cytometry, their optimal staining dilution, their clone and company are listed in Table 2.4 below.

Antibody specificity:	Clone	Dilutions	Company	Cat no:	Isotype
CD8 FITC	SK1	1/10	BD	345772	IgG1
CD8 PerCp	SK1	1/10	BD	345774	IgG1
CD3 Pe	HIT3a	1/17	Pharmingen	555340	IgG2a k
CD3 PerCp	SK7	1/17	BD	345766	IgG1
CD3 FITC	HIT3a	1/10	Pharmingen	555339	IgG2a k
CD45 APC	HI30	1/16	Pharmingen	555485	IgG1, k
CD 45 FITC	HI30	1/10	Pharmingen	555482	IgG1, k
HLA-DR FITC	HL-39	1/12.5	Immunotools	21279993	IgG3, k
CD 80 PE	L307.4	1/5	BD	340294	IgG1, k
CD11c APC	B-ly6	1/25	BD	559877	IgG1, k
CD83 PE	HB15e	1/5	Pharmingen	556855	IgG1, k
CD14 FITC	MEM-15	1/5	Immunotools	21279143	IgG1
CD86 PerCP	Bu63	1/20	Abcam	ab77131	IgG1
CD40 FITC	5C3	1/5	BD	555588	IgG1, k
FITC isotype IgG3	MG3-35		Biolegend	401305	IgG3
HLA-A2 FITC	BB7.2	1/5	Abcam	ab27728	IgG2b
HLA-A, B, C APC	W6-32	1/100	Biolegend	311401	IgG2a, k

Table 2.4: **monoclonal antibodies and isotype controls used in this project, with the unique clone, company and catalogue number.**

2.2.2.2 SURFACE STAINING:

Whole PBMCs/CBMCs, selected populations and/or cell lines were stained as follows: 200 μl of cells (up to 1 million cells/staining) were aliquoted into a flow cytometry tube (fluorescence-activated cell sorting (FACS) tubes BD, catalogue number 352052) and spun at 1800 rpm (562.5g) for 3 minutes at 4ºC. If a pellet was visualized the supernatant was poured off and the cells were resuspended in 50 μl PBS 1X + 0.5% of heat-inactivated FCS (from now on FACS buffer) already containing the relevant antibody and/or tetramer and the tube was incubated in the dark for 10 minutes at 4°C. Following the incubation, tubes were spun as before and washed twice using 200 μl of FACS buffer. Samples were washed three times if tetramers were used to minimize the unspecific binding due to free fluorescent streptavidin. The sample was then resuspended in 100 μl of FACS buffer, or PBS, for immediate analysis. If the sample was to be stored before analysis (for up to 4 days) it was resuspended in PBS+4%

paraformaldehyde (PFA) for 30 minutes at 4^0C; the cells were then pelleted via centrifugation, the PFA solution was removed and the sample was resuspended in PBS until analysis. For DCs the same protocol was followed but the staining was performed in PBS 1X+10% mouse serum to achieve a better blocking, given the very high number of Fc receptor present on the surface of DCs.

2.2.2.3 ANTIBODY TITRATION AND ISOTYPE CONTROLS:

Most of the recommended dilution in table 2.4, above, were obtained titrating the relevant antibody against a suitable cell population. Moreover, most of the monoclonal antibodies used to stain DCs were compared to the staining of the corresponding isotype control prior experimental use to be certain to keep the unspecific binding to a minimum. Figure 2.16A shows the antibody titration for CD86 while Figure 2.16B shows an example of titration of CD83 with isotype control.

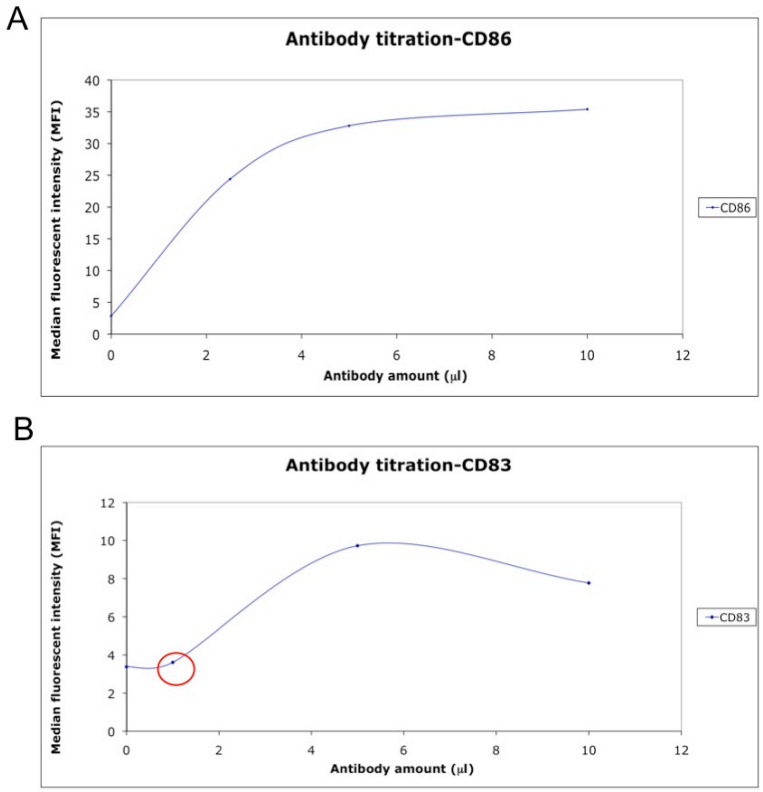

Figure 2.16A: saturation curve of the titration of the anti-CD86 antibody. The DCs cells were gated and the median fluorescent analysis (MFI) for each staining was plotted on the Y-axis against the corresponding amount of antibody (on the X-axis) used each time.
Figure 2.16B: saturation curve of the titration of the anti-CD83 antibody. The DCs cells were gated and the median fluorescent analysis (MFI) was plotted on the Y-axis against the corresponding amount of antibody (on the X-axis) used each time. In this case an isotype control was used as well; its MFI value was plotted in the curve as second value (highlighted by a circle in the plot). In both cases, a final volume of 50 µl per staining was used.

The amount of CD86 antibody chosen for a 50 µl-staining volume was 2.5 µl; initially, an MFI analysis was not performed during titration and a slightly suboptimal amount was chosen, as 2.5 µl is on the edge of the plateau and therefore more vulnerable to dilution errors. The amount of CD83 antibody chosen for a 50 µl staining was 10 µl (the maximum amount tested). The amount of antibody in the total volume of the staining, rather than the more precise concentration, was used in this case as neither supplier provided a working concentration for its product (only indications of dilutions were given).

2.2.2.4 IFN-γ INTRACELLULAR STAINING:

Intracellular staining, when required, was performed using the Cytofix/Cytoperm Fixation/Permeabilization kit (BD Biosciences) following the manufacturer's instructions. Briefly, the samples to be stained intracellularly were firstly incubated with 5 μg/ml Brefeldin A for 4-5 hours prior staining. Brefeldin A interferes with the protein transport from the endoplasmic reticulum (ER) to the Golgi and its use results in protein accumulation inside the ER. Following Brefeldin A incubation, the samples were surface-stained in FACS tubes and then washed twice using intracellular staining wash buffer (PBS 1X, 1% heat-inactivated FBS, 0.09% NaN_3). After the second wash, samples were incubated for 20 minutes at 4°C with 250 μl of Fixation/Permeabilization solution, then washed twice using 1 ml of 1X Perm/Wash buffer (all provided in the kit). This step caused cell membrane permeabilization; from this point on, the cells were maintained in permeabilization buffer to the end of the protocol. After the permeabilization step cells were incubated with the IFN-γ antibody (1 μl/staining) at 4°C for 30 minutes in the dark. Following the incubation with the antibody, cells were then washed 3 times using 1 ml of 1X Perm/Wash buffer each time, centrifuging at 1800 rpm (687.5g) for 5 minutes at every wash. The longer and harsher centrifugation condition, compared to a standard surface staining, were required as due to the permeabilization cells are swollen and much looser than their intact counterparts and as such harder to pellet. Following the last wash, cells were resuspended in 200 μl of 1X Perm/wash buffer for FACS analysis.

2.2.3 CELL LINES GENERATION AND CELL-BASED ASSAY:

2.2.3.0 PREPARATION OF DCs:

Monocytes were purified from PBMCs via CD14+ve selection kit (Miltenyi) according to the indications of the manufacturer. The purified monocytes (and the –ve fraction) were then routinely stained as follows to check purification efficiency and viability:

- Monocytes (CD14+ve fraction): CD14, 7-AAD

- Flowthrough (CD14-ve fraction): CD45, 7-AAD

The CD14–ve fraction (flowthrough) was frozen down for future use when required. The CD14+ve fraction (monocytes) was incubated at 0.5 X 10^6 cells/ml/1 well of a 24-well plate in RPMI medium supplemented with 1% AB serum (FCS was not used to avoid aspecific DC maturation) supplemented with 70 ng/ml of GM-CSF (it stimulates growth and differentiation of monocytes) and 35 ng/ml of IL-4 (it stops macrophage growth) at 37°C. On day 2 and 4, half of the medium was changed adding full amount of cytokines. On day 5, monocytes were pulsed with the relevant peptide (if necessary) for 3 hours and matured overnight. Cells were matured either with 10 μg/ml of polyinosinic: polycytidylic acid (poly I:C) or 1 μg/ml of lipopolysaccharide (LPS, from *E. coli*, serotype 055:B5, Sigma). Poly I:C is a toll-like receptor (TLR)-3 stimulant and can be considered a synthetic analogue of a double stranded RNA, a common viral feature, while LPS is a bacterial constituent derived from the outer membrane of Gram-negative bacteria and it interacts with the CD14/TLR4/MD2 receptor. Both mature and immature DCs were used the day after the incubation with the maturing stimulus. One aliquot of differentiated monocytes was always left immature to provide a suitable control for flow cytometry and further experiments.

2.2.3.1 DCs-RESPONDER STIMULATION ASSAY:

Two different protocols for the DCs-responder stimulation assay were used according to the source of the cells employed (CB or adult samples). The conditions that follow apply to HLA-A*0201+ve, HLA-B*0702-ve, CMV+ve PBMCs derived from healthy adult donors. When used for tetramer-specific expansion one well of the DCs prepared as above was washed twice with 1X PBS, to remove both dead cells and any LPS/poly I:C residues, then 1.5 X 10^6 autologous responders (from the CD14-ve fraction of the monocyte purification), resuspended in 1 ml RPMI+10% AB serum, were added to the DCs. The culture was incubated at 37°C for 1 week and then stained with the relevant antibodies and tetramers.

When cord blood-derived DCs and responders were used, a protocol using stronger stimulation conditions was followed due to the higher naivety and hyporesponsiveness of cord responders. The cord blood optimized protocol was based on previously published evidence (Salio *et al.*, 2003). In this case, DCs were pulsed for 3 hours and responders were added as above. However, recombinant IL-2 was added from day 4 to 7 at 10 U/ml and cells were then expanded with 500 U/IL-2 until analysis (at days 10-15) via surface and intracellular staining and tetramer staining.

2.2.3.2 APCs STIMULATION CONDITION:

In addition to DCs-mediated expansion, adult PBMCs were also expanded using the liposomal aAPCs described in chapter 3 in a HLA-A*0201+ve, HLA-B*0702-ve, CMV+ve system. Briefly, 100,000 PBMCs resuspended in 100 μl RPMI+10% AB serum were aliquoted in a round-bottomed 96-well plate and 60 μl of liposomes (corresponding to the best ratio as optimized in De La Peña *et al.*, 2009) were added to the wells, together with +ve controls (NLV peptide or HLA-A*0201-NLV monomer) and –ve controls (cells left without stimulus). 20 ng/ml IL-7 was added to the culture at day 0 (to promote CD8 memory cell expansion), 50 ng/ml IL-2 was added at day 1 (and not at day 0 to prevent aspecific CD8 expansion). Cells were incubated at 37°C for 7-10 days or longer (up to 21 days maximum) and examined with the relevant antibodies and tetramers.

2.2.3.3 MLR STIMULATION ASSAY:

A stimulation assay was employed to establish the alloreactivity of CB-derived APCs (immature (iDCs) and mature DCs (mDCs)) and compare them to adult APCs obtained using the same protocol. Briefly, 5,000-10,000 APCs (stimulators) were irradiated (30 grays for 7 minutes) to stop proliferation and aliquoted in 100 μl RPMI+10% AB serum in a round-bottomed 96-well plate. For CB-derived DCs it was found that an irradiation step was not necessary as the level of proliferation (as assessed by thymidine uptake) was negligible and comparable with the one of irradiated cells. Varying amount of

allogeneic PBMCs or CD14-ve fraction-derived cells (termed "responders", 10,000, 25,000, 50,000 cells/well) were resuspended in 100 μl of RPMI+10% AB serum and added to the stimulators. As positive controls responders were incubated with Dynabeads (Dynal Biotech anti-CD3 anti-CD28 microbeads, 0.15 μl/100 μl cells), while all the cell types co-cultured in the MLR were also added alone and used as negative control. No cytokines were added and the culture was incubated at 37°C and 5% CO_2 for 5 days. At day 5 H^3-thymidine was added to each well (0.074 Mbq/well) and the plate was incubated for a further 16 hours at 37°C. Cells were then harvested using an Harvester 96 Mach III M (Tomtec) and transferred on a paper filter (Printed Filtermat, Wallac), scintillant was added to the filter (Betaplate Scint, Wallac) and the H^3-thymidine was counted using a 1450 Liquid Scintillation Counter Microbeta Plus (Wallac).

2.2.3.4 γδ T CELLS PROTOCOLS:

For all experiments involving gamma-delta (γδ) T cells an expansion protocol was devised in order to overcome their very low number in both adult and cord blood. Briefly, whole PBMCs or CBMCs were plated in 24-well plates at 1 X 10^6 cells/well/ml of RPMI+10% human AB serum and supplemented with 60 ng/ml of IL-2. The cells were checked daily and half of the medium was changed twice weekly, together with IL-2. If cells were too dense (i.e. reaching over 2-2.5 X 10^6 cells/well) they were collected by gentle scraping and re-seeded at the conditions above. The rate of γδ T cells enrichment in the preparation was measured by weekly staining with an appropriate antibody. γδ T cells expansion was performed for 2 to 3 weeks, then all cells were collected and if appropriate positively selected using the Anti-TCR γδ Microbead kit (Miltenyi) according to the manufacturer's instructions.

For some of the experiments described, positively selected γδ T cells were incubated for three days with different stimuli to boost their HLA-DR expression level. In addition to Dynabeads (anti-CD3 anti-CD28 microbeads, as seen in section 2.2.3.3), used at the same concentration employed for MLR, irradiated K562 cells (in a 1:1 ratio to γδ T

cells) and isopentenyl pyrophosphate (IPP, Sigma), alone, or in combination, were used. IPP is a classic γδ TCR ligand and was added to the cells at 50 μM, the concentration most commonly used in literature (Brandes *et al.*, 2005, Brandes *et al.*, 2009 and Campos Alberto *et al.*, 2009).

2.2.3.5 RF 33.70 CELL LINE STIMULATION FOR ELISA-MEDIATED IL-2 DETECTION:

The T cell hybridoma, RF 33.70, was used to investigate whether the H2-K^b-loaded liposomes were able to present the OVA peptide effectively. Briefly, 50,000 RF 33.70 cells/well were resuspended in RPMI+10% FCS and added to a 96-well plate (effectors) and liposomes (either loaded with H2-K^b molecules or left unloaded, as a –ve control) were added to the effectors. As a +ve control for the reaction, OT-1 splenocytes - resuspended in the same medium, pulsed overnight with the OVA peptide, then irradiated and washed prior adding them to the effectors- were used as stimulators. RF 33.70 cells alone, and OT-1 splenocytes unpulsed, were used as –ve control. The plate was incubated overnight at 37°C and the day after 50 μl of supernatant/well were collected and either used immediately for an ELISA or stored at –20°C for later use. The Mouse IL-2 DuoSet ELISA kit (R&D systems, DY402) was then used according to the manufacturer's instructions. Briefly, the capture antibody (rat anti-mouse IL-2) was aliquoted onto an ELISA plate and incubated overnight at RT. The plate was then washed three times, blocked with 1% BSA in PBS 1X for a minimum of 1 hour, then the experimental sample (and the standard provided in the kit) was added to the plate and incubated for 2 hours. Following three washes, the detection antibody (biotinylated goat anti-mouse) was added to the plate and incubated for a further 2 hours. After extensive washing, the horseradish-peroxidase (HRP)-conjugated streptavidin was added to the plate for 20 minutes and then the plate was colorimetrically developed using the Substrate Solution (R&D systems, DY999) at RT in the dark for 10-15 minutes until a pale blue colour appeared in the wells. The reaction was then stopped using 50 μl/well of Stop Solution (R&D systems, DY994) and the plate was immediately read at 540 nm on a BioTek EL-X 800 reader.

2.3 DNA AND MOLECULAR BIOLOGY WORK:

2.3.0 IN-HOUSE HLA-TYPING:

As the MelanA antigen is an HLA-A*0201-restricted epitope, only HLA-A*0201+ve cords could be employed. To this purpose, cord blood-derived DNA was extracted and typed in-house. Briefly, 200 μl of whole CB were used for DNA extraction using the QIAamp DNA Blood mini kit (QIAGEN, 51104), according to the manufacturer's instructions. DNA yields of 100 ng/μl or more, as assessed via Nanodrop spectrophotometer measurement, were routinely obtained and the DNA was stored at 4°C for immediate use or at –20°C for long-term storage. Typing was performed using the SSP HLA-A low resolution-bulk kit (Olerup, Sweden) according to the manufacturer's instructions. Briefly, 23 primer-specific reactions and one –ve control were set up using the primer set and master mix provided in the kit. The reactions were then run on a thermal cycler (MJ Research, PTC 200 Peltier Thermal Cycler) using the following PCR cycling parameters:

1. 1 cycle:	94°C for 2 minutes	Denaturation
2. 10 cycles:	94°C for 10 seconds	Denaturation
	65°C for 60 seconds	Annealing and extension
3. 20 cycles:	94°C for 10 seconds	Denaturation
	61°C for 50 seconds	Annealing
	72°C for 30 seconds	Extension

The PCR reaction were then loaded on a 2% agarose (Invitrogen) gel, after addition of 2 μl/sample of DNA loading buffer (10% glycerol + 0.1% bromophenol blue) and run in 1X TBE buffer (Lonza) at 150V until the dye reached the bottom of the gel. The typing outcomes were analyzed with the help of Mr Tavarozzi and his team (Anthony Nolan Histocompatibility Laboratories). Out of 10 samples analyzed 6 were HLA-A*02+ve and 3 were HLA-A*02-ve; one sample showed maternal blood contamination and was discarded.

2.3.1 IN-HOUSE SEQUENCING AND OUTPUT ANALYSIS:

All the sequencing required for the re-cloning of HLA-A*0201 and H2-K^b heavy chains sequences was performed and analysed in-house. Briefly, the DNA of interest was extracted from the bacterial strains used for cloning or expression using the QIAprep Spin Miniprep kit (QIAGEN) according to the manufacturer's instructions. Yields up to 1 μg/μl of DNA were routinely obtained and, if not used immediately, the DNA was stored at –20°C until use. At the moment of sequencing, DNA was thawed, diluted up to 0.5 μg/μl if necessary, and the sequencing reaction was prepared. For each sample to be analysed, 1 μl of ready reaction mix (BigDye Terminator v3.1 Cycle Sequencing RR-100, Applied Biosystems), 2 μl of 5X buffer (supplied with the reaction mix, Applied Biosystems), 1 μl of the relevant primer (1.6 mM), 0.5 μg of DNA and, if necessary, deionized water up to 10 μl final volume, were added in a well of a 96-wells sequencing plate. The plate was then sealed and the cycling protocol was performed on a Perkin Elmer Cetus 9600 thermocycler as follows:

1. 1 cycle:	96°C for 1 minute	Denaturation
2. 25 cycles:	96°C for 10 seconds	Denaturation
	50°C for 5 seconds	Annealing
	60°C for 4 minutes	Extension

At the end, reactions were either immediately precipitated or stored at 4°C for up to 48 hours. For the precipitation protocol, 2.5 μl of 125 mM EDTA were added to each well and the plate was quickly spun. Then 30 μl of 100% ethanol were added to each well and the plate was vortexed thoroughly, incubated at RT for 15 minutes and then spun at 3200 rpm (1000g) at RT for 30 minutes. The plate was quickly inverted to remove the supernatant, 30 μl of 70% ethanol were added to each well and the plate was spun again at 3200 rpm (1000g), RT, for 10 minutes. The plate was then inverted as above, spun in an inverted position briefly to remove all the supernatant and air-dried for 5 minutes. The samples were then resuspended in 10 μl of HiDi Formamide (Applied Biosystems) -10 μl of water were also added to any empty well- and either sequenced immediately or stored at -20°C until loading on the sequencing machine (3730 DNA Analyzer,

Applied Biosystems). The sequencing output was collected using Sequencing Analysis 5.2 software and analyzed. An example of sequencing outcome is reported in Figure 2.17.

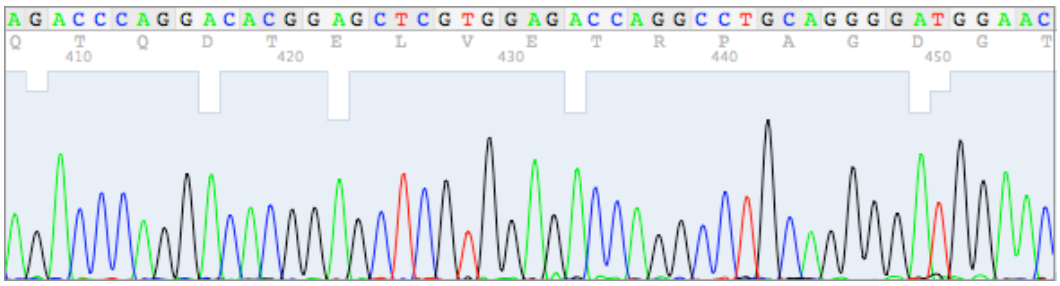

Figure 2.17: an example of sequencing output.

The sequencing results were analysed using the 4Peaks software, to assess the quality of the sequencing, and the Seaview software to perform alignment and highlight any point mutation occurring in the sample.

2.3.2 DNA CLONING AND VECTOR-RELATED WORK-GENERAL:

During this project, it was required to re-clone the heavy chains of both the HLA-A*0201 molecule (exoplasmic part only) and the H2-K^b molecule (exoplasmic part only), to add a Cys in the 3' end position. For a starting source of HLA-A*0201 cDNA, the corresponding expression vector was used. However, the same could not be done for H2-K^b and as such a suitable H2-K^b-expressing cDNA had to be produced. Various H2-K^b-expressing cell lines were tested and the process of RNA extraction and reverse transcriptase are described in paragraph 2.3.4. The primers used in this project are listed in Table 2.5, below.

Primer name:	Sequence:
Actin FW	5'-GCTCCGGCATGTGCAA-3'
Actin RW	5'-AGGATCTTCATCAGGTAGT-3'
Oligo-dT	5'-TTTTTTTTTTTTTTTTT-3'-
A2 FW cloning out	5'-ATGGCTCTCACTCCATGAGG-3'
A2 RW cloning out	5'-TTAACACCCATCTCAGGGTC-3'
H2-K^b FW cloning out	5'-GGATCCATCGGCCCACACTCGCTG-3'
H2-K^b RW cloning out	5'-GGATCCTTAACAAGGCTCCCATCTCAGGGT-3'

Table 2.5: **the main primers used in this project, with their sequence and the name that has been used in the text**. All the primers used were ordered at ThermoElectron (Ulm, Germany).

2.3.3.0 GENERAL PCR CONDITIONS, OPTIMIZATION AND MATERIALS:

2.3.3.1 HLA-A*0201 CLONING: PRIMER OPTIMIZATION:

The Cys-cloning for the HLA-A*0201 molecule was performed using the HLA-A*0201-pET3D vector for monomer expression already available in the laboratory and specific primers. Upon arrival the primers were optimized for best PCR conditions using a temperature and Mg^{2+} gradient. This optimization step is used when receiving previously untested primers (or primers that yet have to be tested on a new template source) and was performed for all primer pairs used in this project (data not shown). The two factors tested in any optimization protocol were Tm (temperature of annealing of the primers to the template) and amount of Mg^{2+} in the reaction. Tm affects primer binding to the template (the higher Tm is, the more specific the binding primers/template is), while the Mg^{2+} form complexes with the dNTPs, and those complexes (rather than the dNTPs alone) are the actual substrate for the DNA polymerase. Each reaction was set up as follows:

DNA (up to 100 ng/μl)	1 μl
Taq polymerase (Bioline)	0.2 μl
Mg^{2+} (Bioline, 50 mM)	1 to 3 μl /reaction
DNTPs (Promega, 1mM)	1 μl
10X buffer (Promega)	3 μl
FW primer (10 mM)	1 μl
RW primer (10 mM)	1 μl

H_20	up to 30 μl

The PCR protocol used is detailed below:

1. 1 cycle:	95°C for 5 minute	Denaturation
2. 35 cycles:	95°C for 30 seconds	Denaturation
	45°C to 50° for 1 minute	Annealing
	72°C for 1 minutes	Extension
3. 1 cycle:	72°C for 10 minutes	Final extension

An example of primers optimization is shown in Figure 2.18 below.

Figure 2.18: primer optimization. From left to right: L: molecular weight ladder (Hyperladder 4, Bioline). Lanes 1-6: optimization of primer A2 FW cloning out and A2 RW cloning out, using a gradient temperature (45° to 50°) and 1 μl of $Mg2^+$. Lanes 7-11: optimization of primer A2 FW cloning out and A2 RW cloning out, using a gradient temperature (45° to 49°) and 2 μl of $Mg2^+$. In this case all temperatures and $Mg2^+$ concentrations tested allowed amplification of the desired band (expected weight 840 bp).

2.3.3.2 INSERT PRODUCTION:

After primer optimization, a large-scale PCR reaction was set up (final reaction volume 50 μl) in order to have enough material to perform a gel-extraction and retrieve the band of interest. Briefly, after performing the PCR, the whole reaction product was loaded on an ethidium-bromide-free gel in 2 aliquots: 2-3 μl were loaded immediately alongside the molecular weight marker, while the remaining product was loaded in the adjacent well. When the dye reached the bottom of the gel, the run was stopped and the gel portion containing the molecular weight marker and the small aliquot of PCR product cut out, placed in a 50 ml Falcon tube filled with TBE buffer and 10 μl of ethidium

bromide (10 mg/ml), and incubated for 10 minutes. At the end the gel cut-out was examined on UV transilluminator (UVP, Inc) and the height of the band was localized and used to cut out the bulk of the PCR product from the ethidium-bromide-free portion of gel. This procedure was employed for every gel extraction where the product was to be used in a ligation, to minimize the impact of DNA mutagenic agents, and therefore the chance of mutations, in the sequence of interest. Once cut out of the gel, the band was agarose-extracted using the QIAquick Gel Extraction Kit (QIAGEN) according to the manufacturer's indications, its concentration was estimated via Nanodrop reading and, if not used immediately, the DNA was stored at –20°C until use.

2.3.3.3 TRANSFORMATION IN CLONING VECTOR AND SCREENING:

The PCR product was then cloned in a cloning vector; for this project the pDRIVE Cloning Kit ligation (QIAGEN) was used (the map of the vector is reported in the Appendix section). Briefly, the pDRIVE cloning vector is a linear vector with a Uracil overhang at each 3' end. This allows its efficient hybridisation with PCR products containing an Adenine overhang, such as those generated by Taq or other non-proofreading DNA polymerases. The cloning of the HLA-A*0201 insert was performed in two steps; firstly the insert was amplified from a suitable template (as seen in sections 2.3.2, 2.3.3.2 and 2.3.4) and ligated into pDRIVE via A-U hybridisation. The ligation was then used to transform *E.coli* competent cells and the transformation products analysed for orientation/points mutations of the inserted sequence; once a clone carrying the desired sequence was detected, the insert was transferred into an expression vector via restriction enzyme digestion (as detailed in section 2.3.3.4).

When choosing the insert-to-vector ratio it was decided to always use the maximum amount of insert allowed by the reaction, up to 10:1 molar excess, as it was observed that this promoted a more efficient reaction (data not shown). A ligation reaction was set up as follows:

pDRIVE Cloning Vector (50 ng/μl)	1 μl
PCR purified product	4 μl

Ligation Master Mix 2X	5 μl

The reaction was mixed by reflux pipetting then incubated for 30 minutes at 10°C in a thermocycler. The reaction was then immediately used to transform an aliquot of chemically competent cells (TOP10, Invitrogen) according to the indications of the manufacturer. Briefly, for each transformation an aliquot of TOP10 cells was thawed on ice, paying attention not to overheat the bacteria, then 5 μl of the ligation mixture were added to the cells and the tube was gently flicked to ensure mixing. The cells were incubated on ice for 30 minutes, then placed at 42°C in a pre-heated thermoblock for exactly 30 seconds and placed on ice again briefly. 250 μl of pre-heated SOC medium (Invitrogen) was added to each transformation and the vial was placed in a 37°C-heated shaking incubator (225 rpm) for 1 hour prior to plating out on antibiotic-supplemented LB plates and incubating overnight. The following day, plates were observed for the presence of colonies and, if they were present, they were immediately screened for the presence of the insert. The PCR protocol was the same described above (see paragraph 2.3.3.1, using an annealing temperature of 50ºC and 1 μl of Mg^{2+}/reaction) with the only difference that the source of DNA in this case was a small part of a single colony, collected with a tip and dipped in the PCR reaction tube (where all the other components were already added) prior to be transplanted on a fresh LB plate for storage.

2.3.3.4 FURTHER CLONING STEPS:

Wherever a positive insert was amplified via PCR, the relevant bacterial culture was inoculated for small-scale DNA extraction and sequencing to confirm the presence and orientation of the insert. When a positive clone was identified via sequencing it was then inoculated for large-scale DNA extraction, restriction digestion and ligation in the expression vector. The restriction digestion was performed incubating the DNA in a final volume of 50 μl as follows:

DNA (variable volume, up to 10 μg)	X μl
Restriction enzyme	1 μl each

10X buffer	5 μl
H_20	up to 50 μl

The reaction was incubated for up to 4 hours at 37°C and then the whole of the digestion was loaded on an ethidium bromide-free agarose gel.

In parallel, the expression vector pET3d was prepared for ligation as well. pET3d is a commercially available expression vector derived from the pBR322 plasmid (the map is shown in the Appendix). It carries an N-terminal T7 tag and it had been used previously in this laboratory to express various MHC class I molecules. It was, therefore, a natural choice for the Cys-recloning of HLA-A*0201 and H2-K^b. The restriction enzymes used for cloning were BamHI and NcoI for HLA-A*0201 and BamHI and XbaI for H2-K^b.

Following a large-scale DNA extraction (performed using the QIAfilter Plasmid Maxi kit according to the manufacturer's instructions) the vector was digested with the same set of restriction enzymes used for the insert, then dephosphorylated prior ligation. The dephosphorylation step, while not being fundamental for a successful ligation, is often performed to avoid re-circularisation of the vector on itself. This is prevented via the enzyme-mediated removal of the 5' phosphate group, which is a required substrate by all DNA ligases, from the linearized vector DNA. Dephosphorylation was performed post gel extraction using the Antarctic Phosphatase (NEB). Briefly, to 1 μg of DNA 1/10 of the final reaction volume (depending on the DNA volume) of 10X reaction buffer and 1 μl of phosphatase were added, then the reaction was incubated for 15 minutes at 37°C. The enzyme was inactivated by incubating the reaction at 65°C minutes for 5 minutes, and then the dephosphorylated vector was used for ligation. In this case, as well, an insert-to-vector ratio of 10:1 or more was used in each case and the reaction was performed overnight at 10°C in a thermocycler using T4 DNA ligase (1U/μl, Invitrogen). The ligation was then used the day after for transformation into TOP10 competent cells and screened as seen above. Once a positive clone was identified, the DNA was extracted and transformed into a suitable expression competent strain; BL21 competent cells (laboratory collection, kindly provided by Ms Forde), an *E. coli* strain optimized for protein expression, and AVB 101 (Avidity) cells were both

used. Both these strains are chemically competent and the transformation protocol was the same as seen for TOP10 competent cells. An overview of the full cloning process for the HLA-A*0201 is presented below in Figure 2.19.

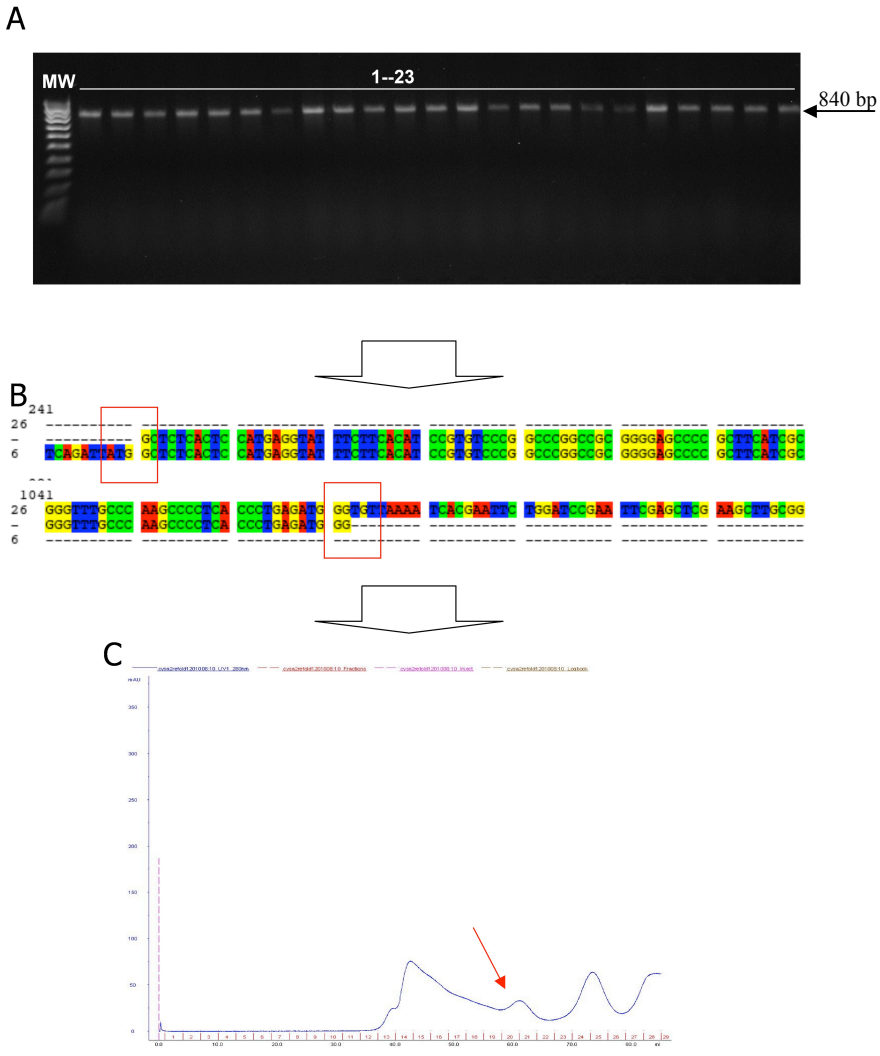

Figure 2.19: overview of HLA-A*0201-Cys cloning and heavy chain production. A, colonies transformed with a pDRIVE-HLA-A*0201-3'-Cys heavy chain (exoplasmic region only) were PCR-screened for the presence of the insert. The expected band was 840bp (MW, DNA ladder, 1-23, colonies). B, sequencing output of one of the colonies showing the insert. Orientation, 3'-Cys presence and eventual point mutations were checked; the initial ATG and the Cys insertion are shown in the red rectangles. C, chromatographic plot of the 3'-Cys refolded monomer (the red arrow highlighting the peak containing the correctly-refolded molecule).

As seen above, the HLA-A*0201 heavy chain was first PCR-amplified and then cloned in a cloning vector. Following PCR screening to detect the presence of the insert (Figure 2.19A), 10 colonies showing the presence of a band at the right height were

then sequenced using primers annealing to the middle of the amplified fragment (Figure 2.19B). It was decided to sequence a reasonably large number of samples in order to have more than one perfect (i.e. right orientation, no point mutations at all and 3' Cys presence) clone to be stored and used in further cloning steps if necessary. One positive clone was then cut out of the cloning plasmid and into the expression vector, re-checked by PCR and expressed for heavy chain purification. The purified heavy chain was then used for a MHC refold (Figure 2.19C) whose correctness was subsequently checked by ELISA using a conformation-specific antibody.

2.3.4 H2-K^b RT-PCR:

Total RNA was extracted from 3-5 X 10^6 H2-K^b expressing cells (RF 33.70 or RMA cells) using the RNAeasy mini kit (QIAGEN) according to the manufacturer's instructions. Yields of 3-5 μg/μl total RNA were routinely obtained, as assessed via Nanodrop spectrophotometer reading. If not used immediately, RNA was stored at -20°C. Given the fragility of RNA and the ubiquitous presence of RNAses, particular care was taken to maintain an RNAse-free environment when working with RNA (in addition to good laboratory practice, dedicated filter tips and RNAse-free plastic-ware were used and surfaces and equipment were wiped with RNAse Zap, QIAGEN, prior to use). Total RNA was then retro-transcribed using the M-MuLV Reverse Transcriptase (New England Biolabs-NEB) according to the manufacturer's instructions. Briefly, 2 μg of RNA solution, 2 μl of oligo-dT (40 mM, see Table 2.5), 4 μl of dNTPs mix (2.5 mM each diluted in deionized water) and nuclease-free water up to a final volume of 16 μl were added in a PCR tube. The tube was heated for 5 minutes at 70°C in a Grant BT1 Block Thermostat, then spun briefly and placed on ice. 2 μl of 10X RT buffer (supplied with the M-MuLV Reverse Transcriptase), 1 μl of Rnase inhibitor (NEB) and 1 μl of M-MuLV Reverse Transcriptase were added to the tube and the reaction was incubated at 42°C for one hour. The enzyme was inactivated by incubating the reaction at 90°C for 10 minutes; if not used immediately, the cDNA was stored at -20°C until use. In addition to the H2-K^b amplification, an actin band was also amplified in a separate PCR reaction to ensure the retrotranscribed cDNA had been produced correctly. Figure 2.20

below, shows an example of PCR performed using H2-K^b primers (experimental reaction) and actin primers (control reaction).

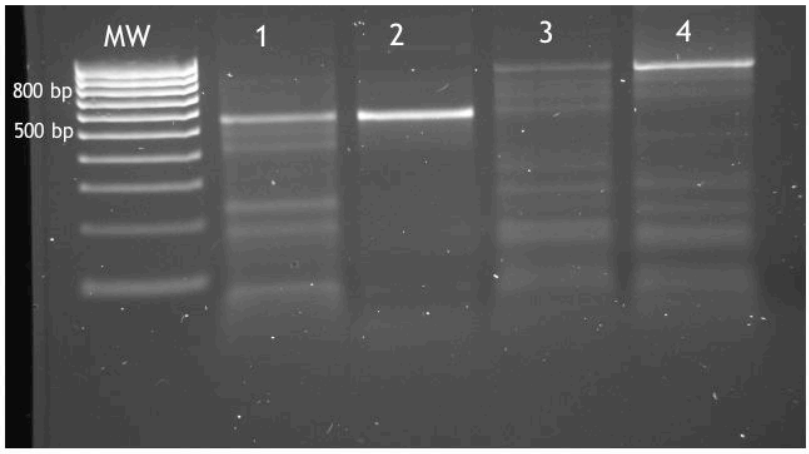

Figure 2.20: H2-K^b RT-PCR. This reaction was performed using cDNA (extracted from RMA cell line, lanes 1 and 3, or from BL/6 splenocytes, lanes 2 and 4) as template. Lanes 1 and 2 show the amplification of an actin band (control reaction, expected height: 542 bp); while in lanes 3 and 4 the experimental samples (H2-K^b exoplasmic region, expected height 840 bp) were loaded. Next to the molecular weight ladder (Hyperladder 4, Bioline) the size of the relevant bands has been highlighted.

After retrieving a good quality H2-K^b cDNA, the Cys-recloning of this molecule was performed with the same protocol and steps seen above for HLA-A*0201. The main passages of this process are summarized in Figure 2.21 below.

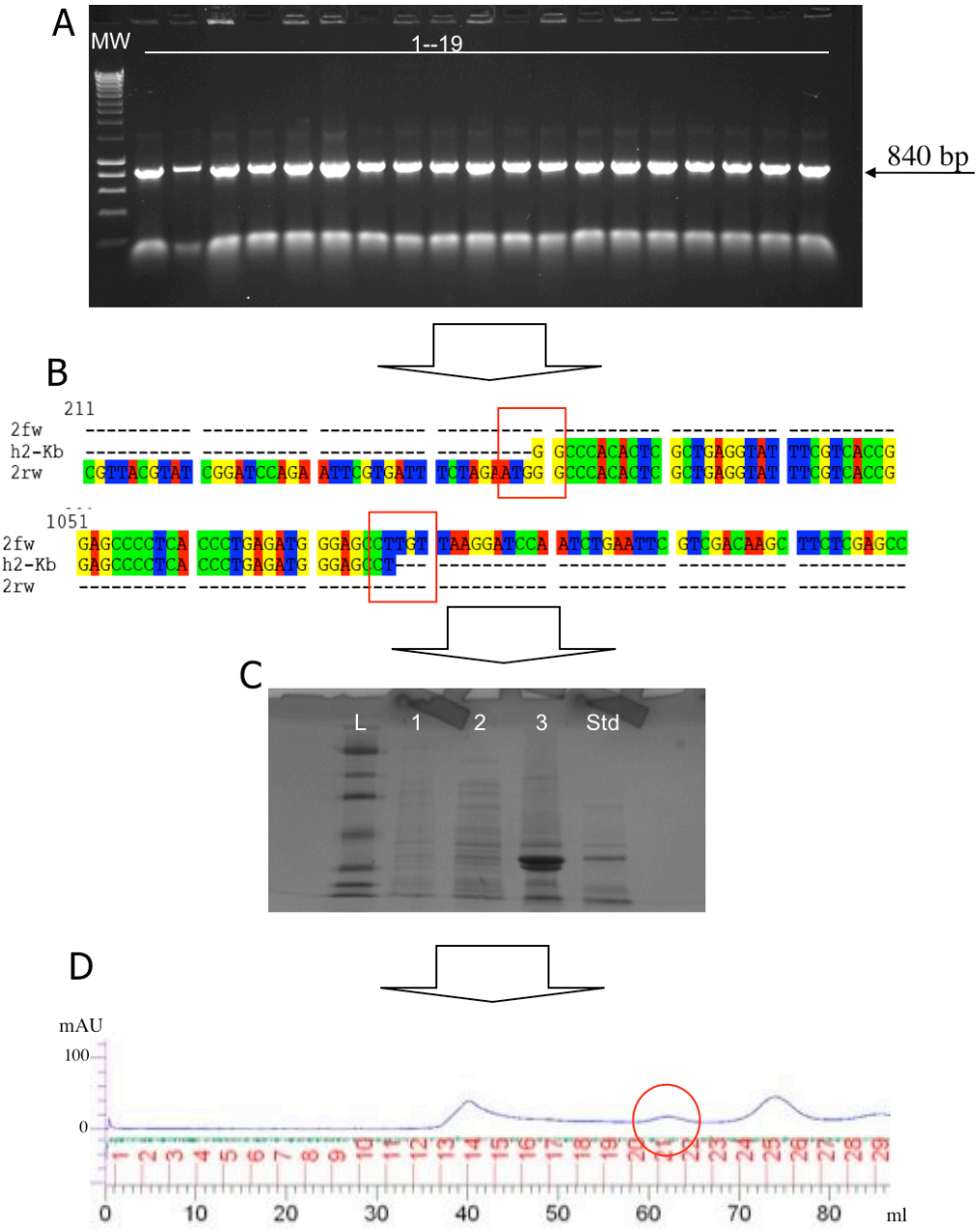

Figure 2.21: overview of H2-K^b-Cys cloning and heavy chain production. A, colonies transformed with a pDRIVE-H2-K^b-3'-Cys heavy chain (exoplasmic region only) were PCR-screened for the presence of the insert. The expected band was 840bp (MW, DNA ladder, 1-23, colonies). B, sequencing output of one of the colonies showing the insert. Orientation, 3'-Cys presence and eventual point mutations were checked, the initial ATG and the Cys insertion are shown in the red rectangles. C, SDS gel showing the H2-K^b-Cys heavy chain pre-induction (lane 1), post induction (lane 2), post induction and inclusion body purification and wash (lane 3), as compared to a standard (Std) and to a molecular weight ladder (L). D, picture of the chromatographic plot of the 3'-Cys refolded monomer (the red circle highlighting the shoulder containing the correctly-refolded molecule). mAU, milli absorbance unit.

2.4.0 CONFOCAL MICROSCOPY:

For confocal microscopy only freshly prepared PBMCs were used. It was found that the use of frozen PBMCs, or Buffy coats, had a negative effect on the sample preparation and as a result the quality of the images that could be acquired decreased markedly (data not shown). Cells were cultured in PBS+1% heat-inactivated FCS instead of complete medium. This was due to the high level of autofluorescence imparted by the RPMI medium (data not shown) and required cells to be prepared just before the setting up of the liposome-cells co-cultures, to reduce the time in minimal culture conditions. Cells were plated at 300,000 cells/100 μl volume in a 48-well plate, then fluorescent, unloaded liposomes were added at different time points (0, 2, 4 and 8 hours and overnight) in a 500 μl final volume. The –ve control was provided by the same cells plated without liposomes. The cells+liposomes co-cultures and the –ve control were then pelleted at 1700 rpm (531g) for 5 minutes at RT and the pellet was resuspended in 4% PFA for 20 minutes in the fridge. The cells were then pelleted again and the PFA was replaced with PBS, then the preparation was stored at 4°C overnight. The day after the cells were mounted on glass slides and fixed. Briefly, 100 μl of cells were loaded on a glass slide using a cytospin (speed 030, 6 minutes-the equipment was generously made available by Dr Steele and Mr Reed, Royal Free Hospital). Once all the slides were prepared they were left to dry for 20 minutes at RT. Cells were then rehydrated by adding a drop of PBS and leaving it for 5 minutes, then the PBS was washed off and a drop of 4% PFA was added on each sample. The PFA was left for 20 minutes and then the slides were washed twice in PBS. After removing as much PBS as possible, the slides were left to dry for 20 minutes (or until no more liquid could be seen on the glass) then 10 μl of Prolong Gold fixative (Invitrogen) was dotted on each sample to help maintain the fluorescence. A cover slide was then mounted on the samples and the slides were stored at RT in the dark until use. Images were acquired with an Olympus FV-1000 and FluoView v2.0 software microscope using an Olympus Plan super Apochromat 60X/1.35 NA oil objective (many thanks to Dr Garcon, Babraham Institute, Cambridge, for technical help and assistance with image acquisition) and the results were analysed using ImageJ software for preparation of stacked pictures.

2.5 STATISTICAL ANALYSIS:

All the statistical analyses showed in this work were performed using the GraphPad software. A student t-test was performed in every case; whenever possible, a paired t-test was performed (i.e. when the samples to be assessed were perfectly paired, for example being the same samples assessed at different time points), otherwise an unpaired t-test was used. P values were considered significant when they were less than 0.05; P values at 0.001 or less were usually reported in the text.

CHAPTER 3:
DEVELOPMENT AND CHARACTERIZATION OF LIPOSOME-BASED aAPCs FOR IMMUNOTHERAPY:

3.1.0 INTRODUCTION:

A number of immunosuppressive treatments are performed in preparation to HSCT; however, these leave patients susceptible to the reactivation of latent viruses such as CMV and this is one of the main causes of morbidity and mortality in HSCT (Van Den Bosch *et al.*, 2009), during the post-transplant period. While antiviral agents, such as ganciclovir, are available and effective, their side effects can be substantial; therefore, the development of immunotherapy-based protocols, where the patient's immune system is manipulated to restore CMV cellular immunity, is an attractive option (Van Den Bosch *et al.*, 2009). Whilst a T cell-mediated response would be very effective against CMV reactivation, this would require CMV-specific CD8+ve T cells. The generation of these cells presents more than one challenge, as they would have to be HLA-specific and there may be a requirement for a suitable CMV-pulsed APC to expand the autologous lymphocytes. DCs are the most efficient physiological APCs and as such they would be the best choice as APCs for CD8+ve T cells production but their generation *ex vivo* is long and labour-intensive. Other cell populations, such as macrophages and B cells, display APC properties both *in vitro* and *in vivo*, but not as effectively as DCs and, as with DCs, would be required to be generated from the patient or donor. A different way to tackle this issue would be developing an off-the-shelf artificial antigen presenting cell (aAPC) which would be ready whenever required and would not involve extensive manipulation and expansion prior to use. Whilst such an aAPC could be cellular or acellular an acellular-based option would offer the greatest flexibility and ease of use. It would also, arguably, provide fewer obstacles for clinical approval than any engineered cell line. MHC-coated liposomes would fit well the aAPC identikit described so far and their production, characterisation and testing, in both human and murine models, is the topic of this chapter.

Liposomes have been used for many years in clinical and biological practice for a wide range of applications. In therapy, they are mainly used for gene delivery, transfection and drug delivery, especially in cancer settings (see Park, 2002 and Mamot *et al.*, 2003, for a review on the subject).

When used as "transporter" liposomes, there is generally not a requirement for proteins or peptides to be loaded onto their surface. However, there are a number of exceptions such as when targeting the liposomes to a specific subset of cells, such as tumour cells. As such, various approaches to add proteins to the surface of liposomes, and maintain their orientation whilst doing so, are reported in literature (Koning *et al.*, 2006, Hussain *et al.*, 2007 and Baum *et al.*, 2007 among others).

The loading of antibodies, for example, has been achieved by adding thiol groups to the protein and coupling it with liposomes enriched with maleimide or thiol groups (Hansen *et al.*, 1995). Generally speaking, the binding of the protein on the liposome surface is achieved via chemical cross-linking between reactive groups on the protein and a suitable reactive molecule incorporated into the lipids that constitute the liposome (Altin and Parish, 2006). Other possibilities include a biotin-avidin-mediated interaction, or, in the case of Fab binding, a hydrazone-mediated binding following Fc oxidization (Hansen *et al.*, 1995), a detergent-mediated preparation (Prakken *et al.*, 2000) and the insertion of a metal chelator into the liposomes, for the binding of His-tagged proteins (Altin and Parish, 2006).

There are two examples in the literature that might support the concept of liposomes as aAPC. The first was published by Prakken *et al.* (Prakken *et al.*, 2000); in this work, liposomes were loaded with MHC class II in order to study the immunological synapse. The second involves the exosome model proposed by the groups of Amigorena (Thery *et al.*, 2002b) and Zitvogel (Mignot *et al.*, 2006). In this model small lipid vesicles, loaded with MHC class I and co-stimulatory molecules, are shed by various cell types, including cancerous cells, and elicit an immunological response. This model might be considered to be describing a naturally occurring example of what is being attempted with liposomes.

The aim of this PhD project is the generation and characterisation of aAPCs to be used in immunotherapy. This research line has been an important object of investigation at the Anthony Nolan Research Institute in the last years; this PhD started from the data obtained previously in the laboratory and published by De La Peña *et al.* in 2009. De La

Peña *et al.* described the construction of a nanotechnology-engineered aAPC in the form of an MHC-loaded liposome, or artificial exosome, and its use as an immunotherapeutic tool in a human memory/recall response (De La Peña *et al.*, 2009). Both in the paper and in the work described in this chapter, CMV was chosen as antigen due to its importance in transplantation. Moreover a new, murine-based system was introduced in this project, to substantiate the findings obtained in the CMV context and as a preliminary set up for future *in vivo* experiments.

3.1.1 STRUCTURE OF THE LIPOSOME-BASED aAPC:

Figure 3.1, below, describes the liposome-based aAPC used in this project. The represented model is a modification of a previously published system (Pastorino *et al.*, 2003 and De La Peña *et al.*, 2009) and is essentially a polyethylenglycole (PEG)-modified liposome with MHC monomers covalently linked to its surface.

Figure 3.1: **model of the liposome-based APC.** A lipid bilayer formed by cholesterol and phosphatidylcholine encloses an aqueous centre (— in the figure above). In the lipid bilayer are interspersed rhodamine-conjugated, fluorescent (red triangles) and PEG-conjugated (grey triangles) lipids. Maleimide-conjugated lipids (blue triangles) are used to couple MHC proteins (yellow double rectangles) on the liposome' surface.

The main structure of the liposome is composed of cholesterol and phosphatidylcholine (PC and CHOL, depicted as a turquoise ring in the picture above). Three other lipids (DSPE-PEG, RHODA and MAL) are interspersed in the main structure, each one of which has a distinct function. DSPE-PEG prevents the liposomes' clearance from the monocytic cell system by reducing the liposomes' interaction with opsonizing proteins (Allen, 1994), thus prolonging its *in vivo* persistence from minutes to up to 5-10 hours (Klibanov *et al.*, 1990). RHODA renders the whole liposome fluorescent, allowing it to be tracked *in vivo* and *in vitro* via flow cytometry analysis and/or fluorescent microscopy. MAL is a maleimide-conjugated lipid that allows covalent binding of proteins to the liposome surface, wherever a reactive thiol group on the protein is free to form a disulphide bond with the corresponding thiol group on the liposome surface.

3.2.0 EXPERIMENTAL AIMS:

The aims of the work performed in this chapter are the preparation, characterisation and assessment of the antigen presenting potential of MHC-loaded liposomes using both human (HLA-A*0201-NLV)- and murine (H2-K^b-OVA)-based models. Two different loading strategies and the various techniques used to assess the liposome loading will be described.

3.3.0 RESULTS:

In the data presented in this chapter, two different approaches were followed to load each of the proteins of interest (see Table 3.1, below) onto the liposomes' surface. The first method involved random introduction of SH groups into the MHC molecules - thereafter called "activation"- performing a thiol-exchanging reaction (using Traut's reagent) as published by De la Peña *et al.*, 2009. It was then decided to engineer a thiol group into the 3'-end of the heavy chain of both MHC molecules to be bound on the liposome, as was done by the Schwendener group (Marty *et al.*, 2001). This second step had two main objectives: firstly, to improve efficiency of loading by ensuring that a high percentage of the MHC molecules were presented on the liposome surface in an orientation favourable for interaction with the TCR and secondly, if possible, to reduce

the amount of monomers required for each loading. The range of MHC class I monomers (mouse H-2 and human HLA) bound on the liposomes' surface was also broadened compared to De la Peña *et al.*, 2009, and Table 3.1, below, lists the systems used and the main characteristics for each.

MHC model:	Cell type	Response type	Readout	Chosen because:
HLA-A*0201-NLV	PBMCs from adult donors	Memory	Tetramers	Previous results were published in this model and we sought to reinforce them+strong expertise and materials available
H2-K^b-OVA	RF 33.70 hybridoma (cell line)	Recall (only TCR engagement is required)	ELISA	Cleaner readout (one cell population compared to mixed cultures in PBMCs), more robust than primary cells+used as a pilot model for *in vivo* upgrade.

Table 3.1: the MHC class I models used and their main characteristics.

The liposome system employed in this thesis possesses two modifications from the one described by De La Peña *et al.*, 2009. While performing the first flow cytometry experiments using fluorescent liposomes prepared as published in De La Peña *et al.*, 2009, it became apparent that the extreme intensity of the rhodamine dye used in the lipid mix made instrument compensation very difficult. Moreover, it limited the choice of antibodies that could be used in conjunction with liposomes. It was therefore decided to modify the published protocol and RHODA was excluded when liposomes were to be examined by flow cytometry or ELISA in co-cultures with cells. Instead, RHODA was used when liposomes were detected by fluorescent microscopy or when they were examined by flow cytometry without being added to cells. Secondly, it was decided to focus experiments in setting up the liposome model *per se,* using systems that did not require further co-stimulation in addition to TCR engagement. Therefore, no Fab molecules were added to the liposomes in conjunction with MHC molecules at any point of the protocol.

3.3.1 MHC ACTIVATION AND LOADING ON LIPOSOMES:

All the proteins of interest need to bind the exposed SH groups on the MAL lipid with a free SH lateral chain in order to be loaded onto the liposome surface. The only amino acid with a sulphydryl group at the end is cysteine (Cys), unfortunately MHC molecules contain only 6 Cys groups, all of which are occupied forming intra-molecular bonds. Consequently, to allow binding to the liposome surface, the MHC molecules are required to be activated by addition of SH groups to surface exposed residues. The first liposome preparations were designed, therefore, to assess the efficacy of activation of the MHC monomers. Following activation, the presence of SH groups in the treated protein was evaluated by performing an Ellman's assay. The assay was successful and its results are shown in Materials and Methods, Figure 2.14; however, it was performed only once as the amount of monomers required for each experiment was extremely high (around 1/3 of the total stocks available for each protein) and a relevant noise was registered.

Following the Ellman's assay, the next experimental question was to assess whether the activated monomer was being loaded on the liposome surface and, more importantly, if a sufficient amount retained an orientation conducive to antigen presentation. To achieve this result, the best technique was to use MHC class I-specific conformational antibodies (such as W6/32 for HLA-A*0201) and a suitable system of secondary detection on the loaded liposomes. Therefore, the assessment of the efficiency of monomer loading on the liposome surface was initially performed via dot blot. To this aim, different amounts of liposomes were aliquoted onto a nitrocellulose membrane, incubated with W6/32 and detected using a secondary antibody (see Figure 3.2). Dot blots were performed either on the same day of liposome preparation (i.e. after chromatographic purification following MHC coupling) or the day after (see Materials and Methods paragraph 2.1.1.1).

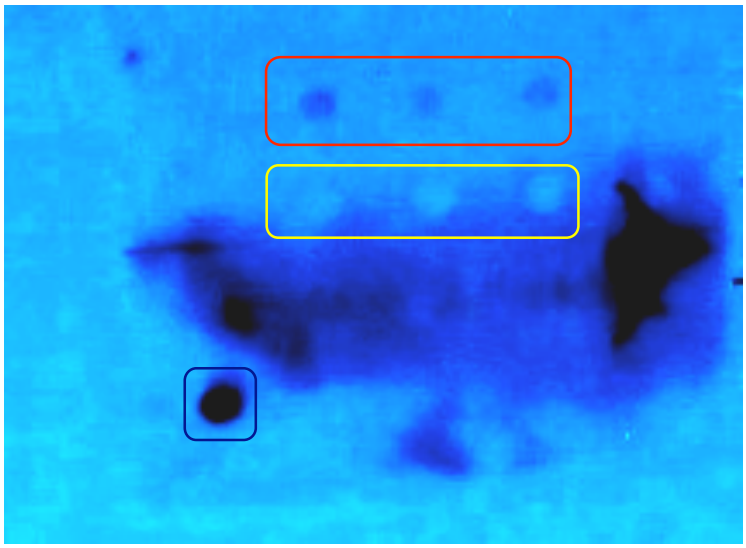

Figure 3.2: Dot blot. MHC loaded (red rectangle) or unloaded (yellow rectangle) liposomes were dotted in triplicate on a nitrocellulose membrane, subsequently incubated with W6/32 antibody. MHC monomers alone were used as +ve control (blue rectangle). N=1.

In Figure 3.2, above, the positive control is shown in blue and the negative control in yellow. In red, a series of positive dots marked the position where the loaded liposomes were added on the membrane, thus confirming the presence of a detectable amount of MHC molecules on the liposome' surface. This experiment showed that at least a fraction of the activated monomers was being loaded on the liposomes. However, the relatively faint signal and most importantly, the lack of consistency between different liposome batches while performing the dot blot suggested the need to look into new, more adequate and sensitive ways to assess the efficiency of liposome loading.

3.3.2 FLOW CYTOMETRY OF MHC-LOADED LIPOSOMES:

Following the dot blot evidence and the reproducibility issues encountered while performing it, it was decided to use flow cytometry to detect loaded liposomes. It was speculated that flow cytometry would provide both sensitivity and increased reproducibility. The first such attempt was performed on liposomes alone (see Figure 3.3A and 3.3B, below).

The aim of this experiment was to elucidate the FSC-SSC appearance of liposomes; in this case, they were prepared with the addition of RHODA as the rhodamine fluorochrome was meant to be the only channel of detection. As expected given the small diameter of the liposomes (100 nm after extrusion) their dimension was very small, as assessed by the low forward side scatter (FSC) value. Two different populations (one with high SSC the other with low SSC, see Figure 3.3A and 3.3B) were detected when examining the liposomes by flow cytometry. While it was not possible to ascribe this finding to a specific feature, one hypothesis is that the liposomes in suspension, when left untouched, tend to clump into different-sized micelles that have varying SSC properties when analysed via flow cytometry. The higher density of events in the population with high SSC (as represented by the brighter colour in the plot) could indicate that in this case the density of the liposomes is higher, possibly as a result of clumping. This theory was in some part substantiated by fluorescence microscopy of the liposomes in the absence of cells; on two independent occasions fluorescent spots of very different dimensions were detected when liposomes alone were observed (data not shown). Once it had been established that liposomes could be detected by flow cytometry a loaded batch was prepared and stained with W6/32 antibody. The W6/32 labelling was then detected with a fluorescent conjugated secondary antibody. Unloaded liposomes treated in the same way provided the required negative control. Figure 3.3C shows a small but detectable shift between loaded and unloaded liposomes, suggesting the presence of MHC class I on the surface of the examined liposomes and reinforcing the evidence obtained with the dot blot (Figure 3.2).

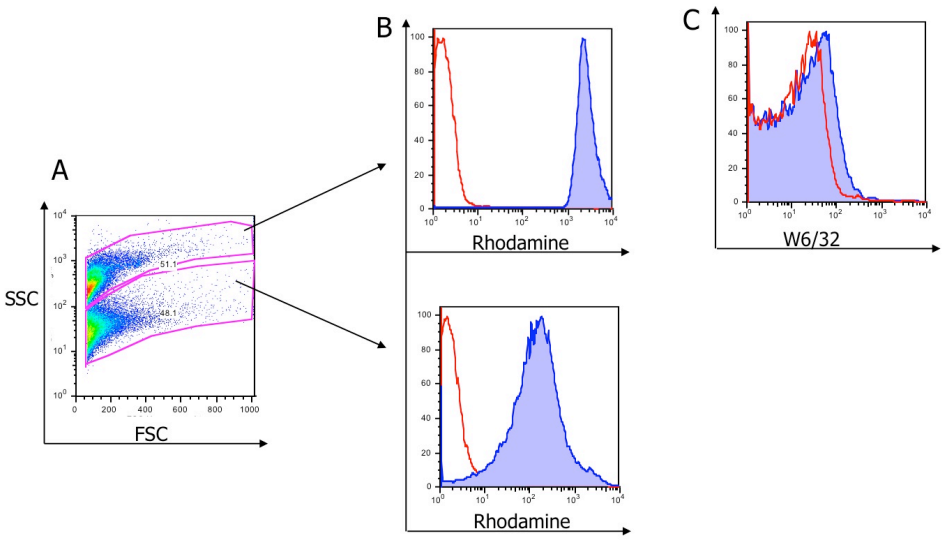

Figure 3.3: analysis of liposomes by flow cytometry. A, Liposomes by themselves were examined via flow cytometry, resulting in two discrete population having high and low SSC (representative of 4 experiments). B, When fluorescent liposomes were examined, both subpopulations were clearly positive for rhodamine (—) compared to unfluorescent population (—). C, liposomes were loaded with MHC class I molecules and the level of W6/32 was examined in the loaded (—) and unloaded (—) population. B and C, representative of 2 experiments, each time performed in duplicate.

3.3.3 FLOW CYTOMETRY OF LIPOSOMES-CELLS CO-CULTURES:

One of the issues that emerged during the experiments of flow cytometry performed on liposomes alone was the difficulty encountered during the staining protocol that resulted from the inability to centrifuge the liposomes. The usual washes to remove unbound antibody could not be performed and, therefore, high degree of unspecific binding was common. In an attempt to circumvent this problem HLA-A*0201–ve cells were cultured with HLA-A*0201-NLV monomers. Liposomes that have been successfully loaded with the HLA-A*0201-NLV monomer should be taken up by the HLA-A*0201-ve cells. This should then be theoretically be detected using an HLA-A*0201-specific antibody. Any HLA-A*0201 labelling detected in the cell culture would be liposome-derived.

For the first cellular-based experiment, the first cell type selected to co-culture with liposomes was HLA-A*0201-ve DCs. Professional APCs were selected as it was considered that their marked phagocytic capacity might enhance the uptake and

presentation of liposome-loaded HLA-A*0201 monomers on the cell membrane. Figure 3.4 shows the results of this experiment.

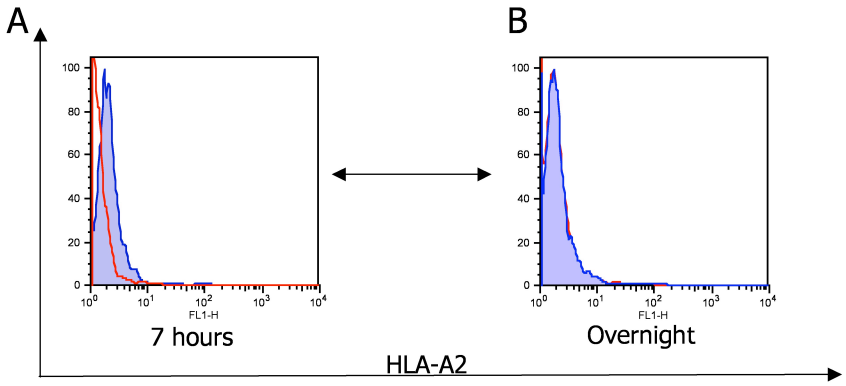

Figure 3.4: flow cytometry analysis of DCs-liposomes co-cultures. DCs from an HLA-A*0201-ve donor were prepared, incubated with nonfluorescent liposomes A, for 7 hours, or B, overnight, and the HLA-A2 expression (—) was then measured by flow cytometry for each sample within the DC gate and compared to a liposome-free DC preparation (—). N=1.

As seen in Figure 3.4, above, a small shift in HLA-A*0201 labelling was observed in the liposomes-DCs co-culture after 7 hours (Figure 3.4A), but not after an overnight incubation (Figure 3.4B). Two possible conclusions could be drawn from these data; either that the absorption of liposomal MHC molecules by cells reached a saturation point in a few hours or that the half-life of liposomes in culture with cells was limited to a short period. In any case, the outcome of this experiment suggested that the incubation time (in particular overnight or longer cultures) was an important variable in the system used and that prolonged incubation times might have affected liposome detection.

Performing intracellular staining for HLA-A*0201 might have served to localize the MHC molecules from the liposomes after uptake. However, it is also possible that uptake of the MHC molecules would then lead to degradation/digestion. Therefore, such labelling might not quantify functional or intact HLA-A*0201.

3.3.4 IMPROVING THE LOADING VIA CYSTEINE CLONING:

Whilst all the data up until this point suggested that monomer had indeed been loaded onto the liposomes, the results were subtle with no clear indication of success. One

possibility is that the activation of the monomers was too stochastic and led to a high degree of variability in the extent of SH group introduction into the molecules.

To reduce this variability it was planned to re-clone the existing heavy chain molecules adding a 3'-Cys residue and re-express the newly Cys-modified heavy chains to use them for monomer refolding. This Cys residue would eliminate the need for random activation prior to loading on the liposomes' surface, as MHC molecules would already have a Cys-based anchor for the liposomes in the best possible position for correct loading. The whole process is summarized in Figure 3.5, below.

Figure 3.5: new mechanism of monomer loading. A, monomers are at the moment loaded randomly on the liposomes' surface. The introduction of a Cys at 3' in the monomer, B, should promote a better orientation of the monomers on the liposomes' surface, C.

The re-cloning of both heavy chains (HLA-A*0201 and H2-K^b) was then undertaken according to the procedure detailed in Materials and Methods and shown in Figure 2.19 (for HLA-A*0201) and Figure 2.21 (for H2-K^b). Both molecules were successfully cloned in an expression vector, expressed in a prokaryotic system and used for refolding together with the appropriate peptides.

3.3.5 LIPOSOME-MEDIATED CMV EXPANSION:

Once the Cys-modified HLA-A*0201 monomer was produced, it was decided to test the potential of HLA-A*0201-NLV-loaded liposomes as aAPC. This was performed by setting up a liposome-PBMC co-culture, as previously published (De La Peña *et al.*, 2009). To this end, both versions of the monomer (with and without added 3'-end Cys) were loaded on different aliquots of the same batch of liposomes. The effectiveness of these liposomes in expanding an HLA-A*0201-NLV tetramer-specific population was assessed using freshly purified, unselected PBMCs from an HLA-A*0201+ve, CMV positive donor.

Firstly it was decided to test the liposome-mediated expansion and compare it to as many positive controls as possible (NLV peptide and HLA-A*0201-NLV monomer). Whilst peptide-mediated expansion is the commonest choice in literature, monomers have also been used. By using monomers as a control the influence of loading the monomers onto liposomes could be assessed. Two negative controls, cells incubated without any stimulus and cells incubated with unloaded liposomes, were also used. The ratio of liposomes-to-cells and the cell culture conditions previously optimized in De La Peña *et al.*, 2009, were used throughout the whole series of liposome-mediated expansions. Figure 3.6A, below, shows a representative result from one of the liposome-mediated expansion performed, while Figure 3.6B summarizes as a column graph the results obtained in all the expansions performed.

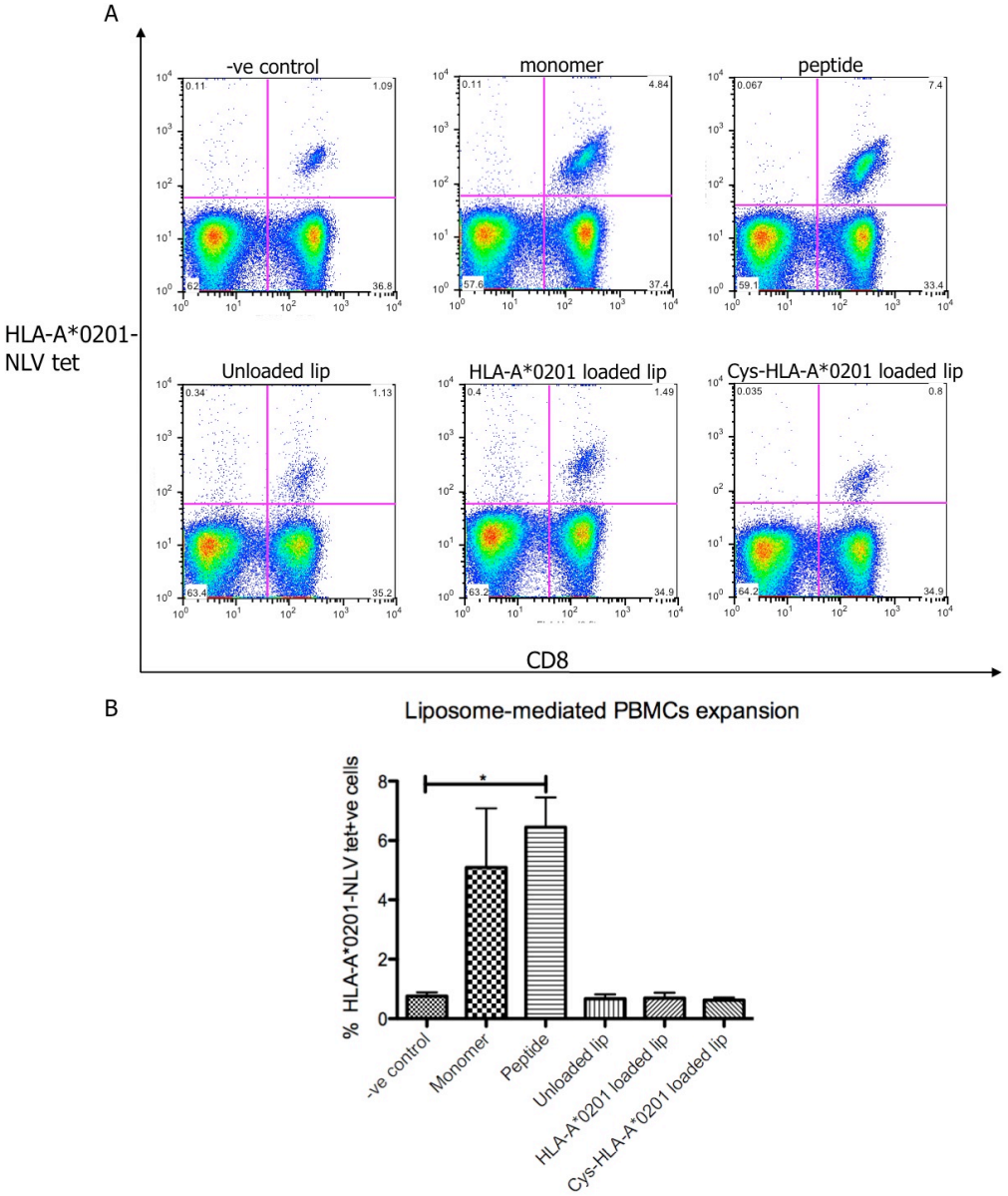

Figure 3.6A: flow cytometry analysis of PBMCs-HLA-A*0201-NLV loaded liposomes co-cultures. PBMCs from an HLA-A*0201+ve healthy donor were incubated with HLA-A*0201-NLV loaded, nonfluorescent liposomes for 7-10 days and analysed for their HLA-A*0201-NLV tetramer specific expansion. NLV peptide and HLA-A*0201-NLV monomer were used as +ve controls, cells incubated without antigenic stimulus were used as -ve control. In all cases lymphocytes were gated and the CD8+ve tetramer+ve population was shown. Results shown are representative of 5 independent experiments on 2 different donors.

Figure 3.6B: graph summarizing the results from all the liposome-mediated PBMCs expansion performed. Data are expressed as columns representing the mean of the CD8+ve HLA-A*0201-NLV-tetramer+ve population for each condition tested, while the error bars represent the standard deviation. Mean values ± standard deviation are also quoted in the text. Data were analysed using the student paired t-test; N=5, P*<0.05.

A small but clear tetramer+ve population was detected in all cases in the unstimulated aliquot, thus providing a starting point for the assessment of HLA-A*0201-NLV tetramer-specific expansion. The positive controls used promoted relevant tetramer expansion in the donors tested (see figure 3.6A above, upper row, for a representative example). No comparable or consistent expansion was detected when using HLA-A*0201-NLV-loaded liposomes in any of the conditions tested (see Figure 3.6A bottom row and 3.6B last two columns on the right). In the representative case shown above in Figure 3.6A there is a slight expansion between the loaded- and unloaded-liposome cultures (1.49% vs 1.13% of CD8+ve HLA-A*0201-NLV tetramer+ve cells, as shown in the lower row of figure 3.6). In contrast, the level of CD8+ve HLA-A*0201-NLV tetramer+ve cells in the Cys-loaded liposomes is 0.8%, which is below the correspondent amount of cells in the negative control (unstimulated cells- Figure 3.6A, upper row, left quadrant). Loading the monomers through a Cys anchor did not appear to improve the aAPC potential of the liposomes.

A plot summarising all the liposome-mediated expansion experiments is presented in figure 3.6B. A significant difference in the percentage of CD8+ve HLA-A*0201-NLV tetramer+ve cells was detected when comparing unstimulated cells versus peptide-stimulated cells (0.76±0.1% versus 6.4±1%, respectively; P=0.004). There was a trend of expansion with the monomers over unstimulated cells but this expansion was too inconsistent to be significant with this sample size. No significant difference was observed between the unstimulated control (Figure 3.6B; -ve control) and PBMCs stimulated with unloaded and loaded liposomes, regardless of the loading protocol used (Figure 3.6B first and last three columns).

The results presented above may suggest that liposomes inhibited responses rather than expanding tetramer-specific cells. The results in Figure 3.6 were obtained in five independent experiments using two different donors and did not change with different batches of monomer-loaded liposomes, different batches of monomers as stimulators and different culture times (the longest one attempted was 21 days).

This series of experiments suggested firstly that the cell culture conditions by themselves were compatible with PBMCs' survival and growth, as a tetramer-specific expansion was detected in all of the positive controls. Even if not statistically significant, the use of HLA-A*0201-NLV monomers as stimulus resulted in a tetramer-specific expansion, thus ruling out any MHC-related role in the absence of expansion observed with monomer-loaded liposomes. However, the lack of expansion and possible liposome-mediated inhibition observed in the cell/liposome co-cultures prompted further investigation into the effect of liposomes (loaded and unloaded) on cells.

3.3.6 QUALITY CONTROL AND LIPOSOME-MEDIATED EFFECT ON PBMCs CULTURES:

Up to this point the experimental evidence suggested that liposomes were not promoting tetramer-specific cell expansion when incubated with primary cells, in contrast with previously published data. The priority now was to understand the action of liposomes on PBMCs. Firstly it was determined whether the presence of unloaded liposome could affect expansion in the peptide and monomer driven positive controls and secondly the effect of liposome alone on the amount of tetramer+ve cells was assessed in the absence of stimuli. The effect of empty liposome on peptide and monomer driven expansion is shown below in Figure 3.7.

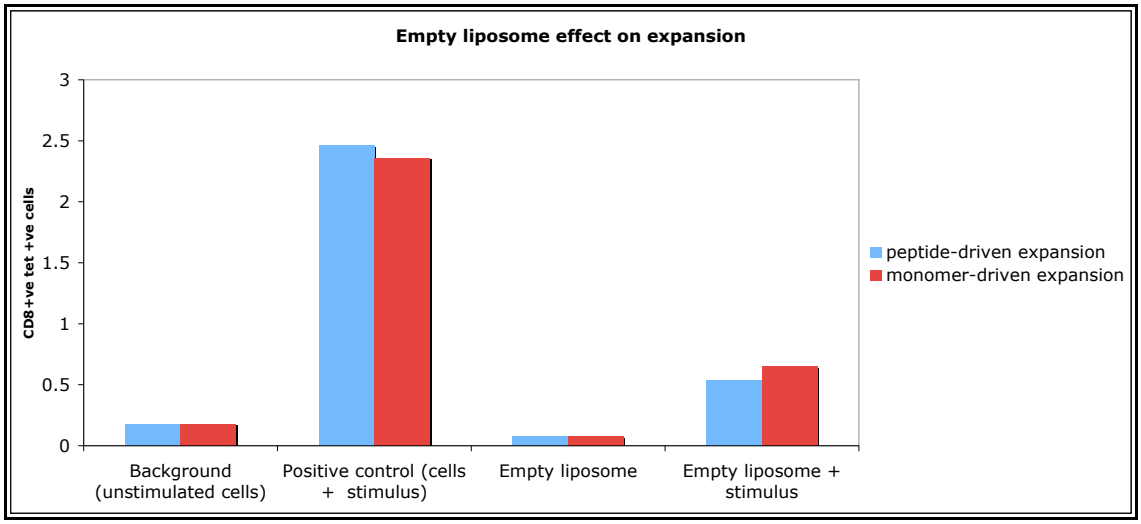

Figure 3.7: the effect of empty liposomes on peptide- and monomer-driven HLA-A*0201-NLV PBMCs expansion. PBMCs from an HLA-A*0201+ve healthy donor were incubated with unloaded, nonfluorescent liposomes and either NLV peptide or HLA-A*0201-NLV monomer as stimulus. HLA-A*0201-NLV tetramer specific expansion was analysed at day 7. Bars show the CD8+ve HLA-A*0201-NLV tetramer+ve population. Results shown are representative of 3 independent experiments on 2 different donors.

As before, stimulating cells with positive controls produced a convincing expansion of the tetramer-positive population (2.41% tetramer+ve cells from 0.18% in the unstimulated control) whilst cells co-incubated with liposomes see the same population drop below the level of the negative control (0.07%). The presence of liposomes in the peptide and monomer cultures resulted in a much smaller expansion (0.59% tetramer+ve cells), than that registered in the sample stimulated in the absence of liposomes. This pattern of reduced tetramer-specific expansion when cells are co-incubated with liposomes was, therefore, observed in two independent series of experiments.

The effect that liposomes, both loaded and unloaded, had on PBMCs cultures without any other exogenous antigen was then examined. In this case, different amounts of liposomes were added to PBMCs and the percentage of tetramer+ve cells was assessed and compared to cultures without liposomes (-ve control). Results for this experiment are shown in Figure 3.8.

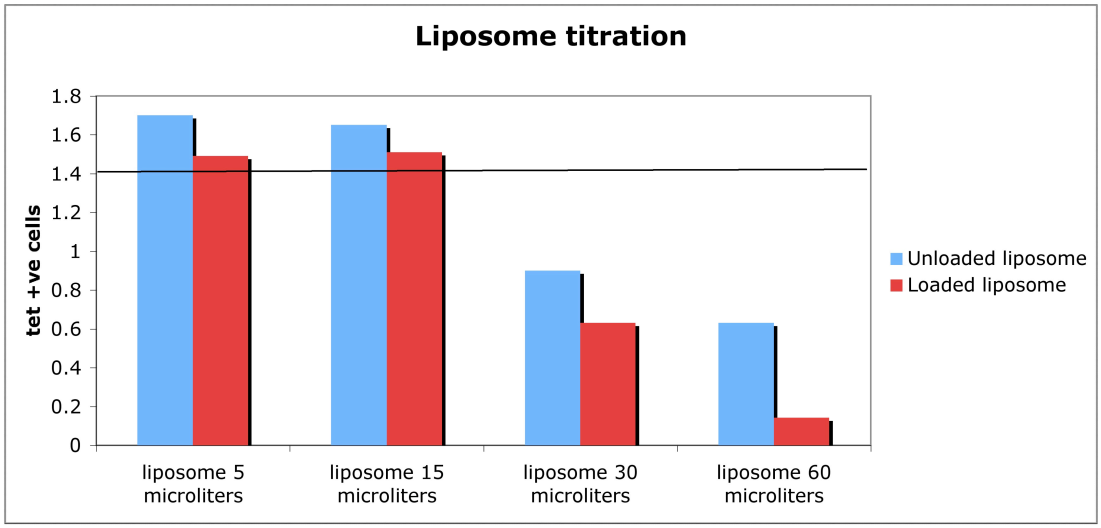

Figure 3.8: the effect of liposomes on HLA-A*0201-NLV tetramer+ve cells. PBMCs from an HLA-A*0201+ve healthy donor were incubated with different amounts of loaded and unloaded, nonfluorescent liposomes for 7 days, then analysed for their HLA-A*0201-NLV tetramer specific population. Bars show the CD8+ve tetramer+ve population; the black line across the graphs marks the level of tetramer+ve cells in the -ve control (PBMCs incubated without either liposome). Results shown are representative of 2 independent experiments on 1 adult donor and 1 Buffy coat sample.

Figure 3.8, above, compares the percentage of tetramer+ve cells in PBMCs incubated with various amount of liposomes with the same cells without liposomes. Results suggested that large amounts of liposomes, from 30 microliters upwards, corresponding to the condition used in Figure 3.6, have an inhibitory/toxic effect on culture, as demonstrated by the drop in number of tetramer+ve cells (less than 0.8% of tetramer+ve cells). Conversely, small or very small volumes of liposomes, up to 15 microliters, have no effect on the percentage of tetramer+ve cells and presumably on cell viability, as tetramer+ve cells remained above 1.4%. Unfortunately, such limited amounts of liposomes may be ineffective in promoting a cellular response.

The effect of unloaded liposomes on viability was also tested on Buffy coat samples, which were stained for 7-AAD following incubation with increasing amounts of liposomes and the buffer used for liposome preparation (HEPES buffer). The results are shown below in Figure 3.9.

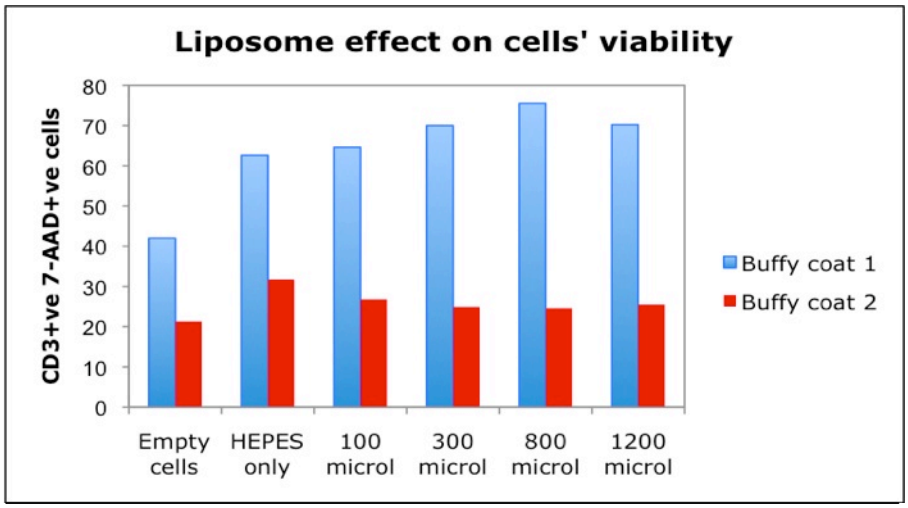

Figure 3.9: the effect of liposomes on Buffy coat cells' viability. PBMCs from 2 Buffy coat samples were incubated with different amounts of unloaded, nonfluorescent liposomes and with the buffer used to resuspend them (HEPES only) for 7 days. The cultures were then analysed for their CD3+ve 7-AAD+ve population for a general assessment of the effect that liposomes and buffer had on the viability of T cells. Empty cells (PBMCs without any liposomes or buffer) provided the negative control. Bars show the CD3+ve 7-AAD+ve population. In this case large wells, and consequently larger amounts of liposomes, were used due to the availability of a large number of cells from the Buffy coats. N=1.

The first conclusion from the results is that the co-culture of unloaded liposomes with Buffy coat cells results in an increase in the percentage of CD3+ve 7-AAD+ve cells (marked for Buffy coat 1, more moderate in the case of Buffy coat 2). The decrease in viability was observed with every liposome amount; however, it does not seem to be dose dependant for liposomes. An increase in the CD3+ve 7-AAD+ve population is also seen with the buffer used to prepare the liposome, suggesting it is not compatible with Buffy coat viability in the conditions and system used. Buffy coat 1 and 2 had different background non-viable lymphocyte populations (CD3+7-AAD+) as shown by the percentage of dead cells in the empty cells condition. However, the trend of increase in the CD3+ve 7-AAD+ve population when in the presence of liposomes or HEPES buffer is similar in both samples.

3.3.7 PBMCs/LIPOSOME CO-CULTURES, PRELIMINARY CONCLUSIONS:

All the evidence presented so far suggested that liposomes were being prepared and loaded correctly. However, their prolonged (i.e. >overnight) co-incubation with PBMCs

resulted in a lack of expansion of tetramer-specific cells, in contrast with previously published data, suggesting that there were intrinsic issues with the liposome system. The data suggested the liposomes were apparently exerting an inhibitory/toxic effect when incubated with cells. However, it was important for the project to assess the general feasibility of using liposomes in the *in vitro* PBMCs system employed in this work, assuming the toxicity issues could be resolved. In particular, it needed to be clarified whether liposomes retained their integrity in co-culture with PBMCs long enough to exert an antigen presenting effect. Among the explanations proposed for the data in Figure 3.4 was that liposomes are taken up by the cells at very early time points; if this were the case, it would affect the capability of these MHC-loaded liposomes to act as aAPC (being sequestered inside cells). Therefore, it was decided to assess the PBMCs-liposomes interaction via fluorescent and confocal microscopy, to determine if all the liposomes were internalized.

3.3.8 FLUORESCENT MICROSCOPY OF LIPOSOMES-CELLS CO-CULTURES:

Fluorescent microscopy and a PBMC-fluorescent (rhodamine) liposome co-culture was used to determine the extent of liposome uptake by cells at early time points (Figure 3.10). To rule out any membrane localization of the liposomes, confocal images were taken for some of the most relevant time points to have a stack of images for any given slide section examined (Figure 3.11). The results for these experiments are shown below.

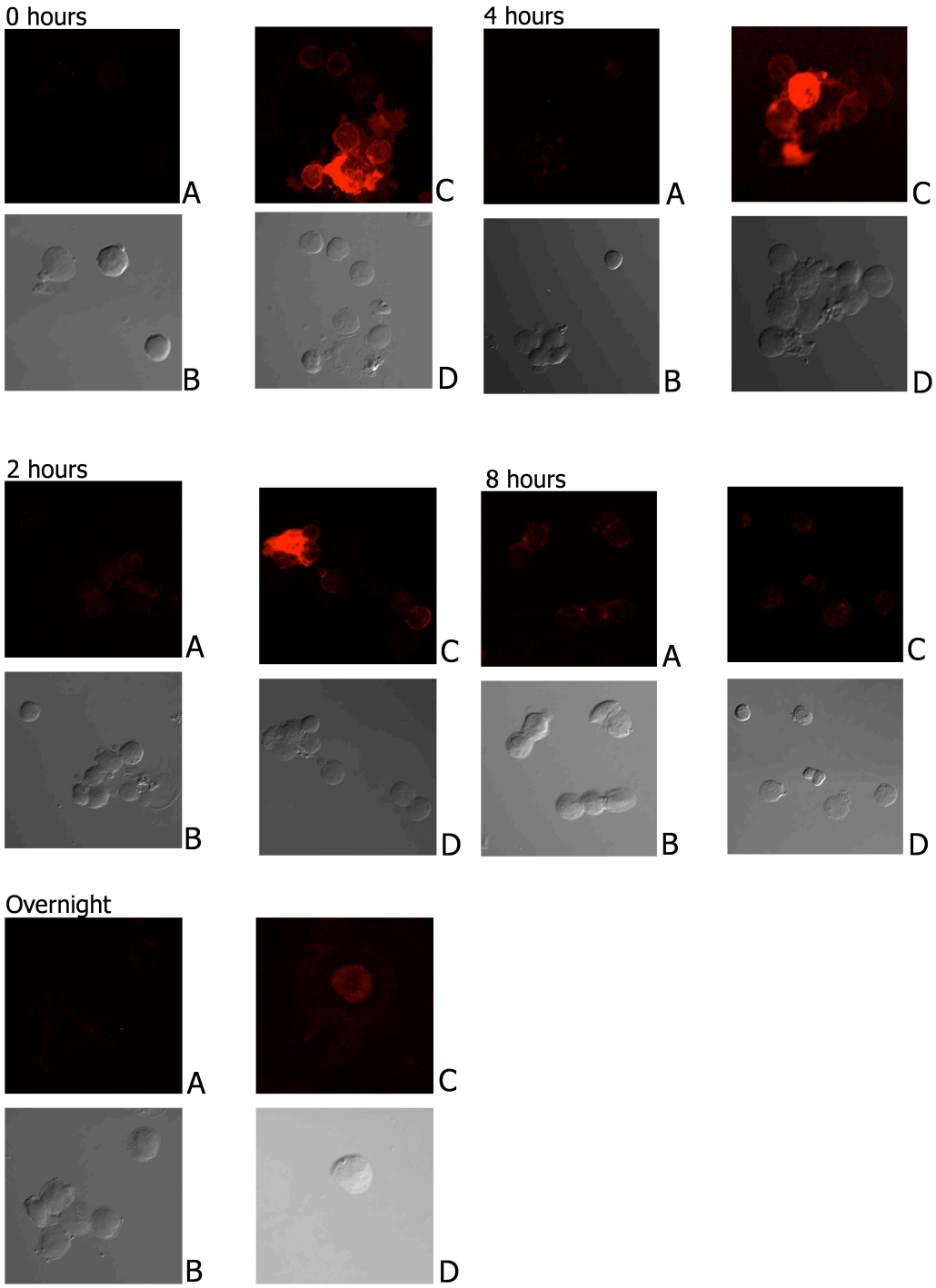

Figure 3.10: Fluorescent microscopy analysis of liposome-PBMCs co-culture. Unloaded, fluorescent liposomes were added to fresh PBMCs and the rhodamine-derived fluorescence was examined at various time points, as indicated in each figure. For each time point: PBMCs alone were examined for autofluorescence, A, and in bright field, B, and PBMCs-liposomes co-culture were examined for rhodamine fluorescence, C, and in bright field, D. Results shown are representative of 2 independent experiments.

As seen in Figure 3.10, above, rhodamine fluorescence can be detected in all samples; it is brightest at 0, 2, and 4 hours and a fainter fluorescence can be detected at 8 hours and overnight too. At 0 and 4 hours the liposome-mediated fluorescence appears concentrated on the edges of some cells, whilst at 2 hours the brightest spot in the focal slide examined belongs to a single cell, even if edge fluorescence is still detectable around the brightest point. All samples (with the exception of hour 8) show that the respective –ve controls are autofluorescence-free so the signal observed in the rhodamine-fluorescence channel can be genuinely attributed to the liposomes. While it is not possible to detect a gradient of pigmentation in the samples between 0 and 4 hours it appears that, in the system in use, liposomes are present on the cell surface and are possibly internalized at early time points, as better shown in the next figure. Figure 3.11, below, shows stacked images for some of the same time points photographed in one-plane in figure 3.10.

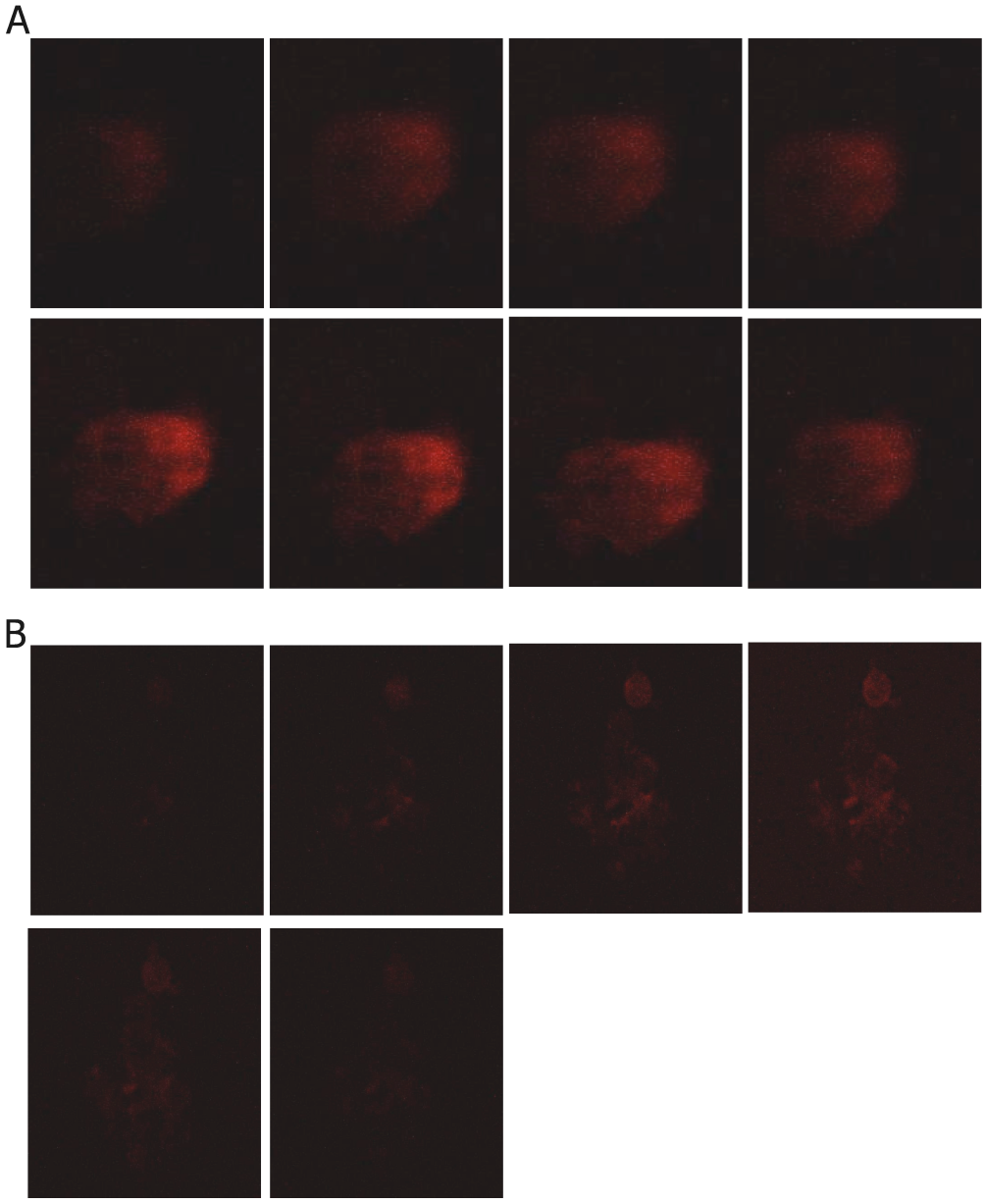
A
B

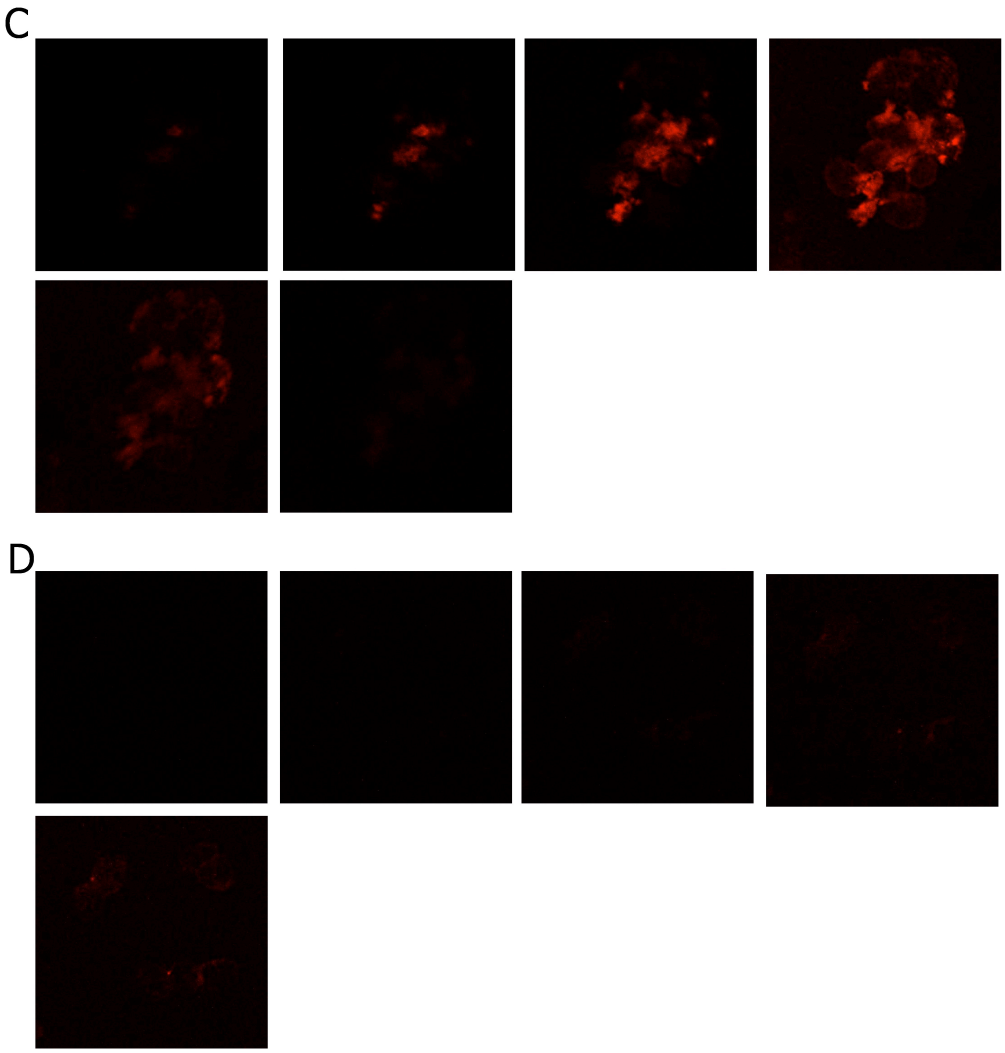

Figure 3.11: Confocal microscopy analysis of liposome-PBMCs co-culture. Unloaded, fluorescent liposomes were added to fresh PBMCs and the rhodamine-derived fluorescence in stacked slides of the same image was examined at 0 (A, B) and 8 hours (C, D). A and C, PBMCs+liposomes, B and D, PBMCs alone (as a control for autofluorescence). For each image a representative series of stacked slides was reported, except for D where all the available slides were shown.

In the case of confocal microscopy it was decided to focus on 0 and 8 hours time points as examples for very early and late uptake, respectively. As it can be observed in Figure 3.11A, the rhodamine fluorescence is clearly detectable in all the focal slides of the single cell examined at t = 0. This suggests that at least a fraction of the liposome preparation is entering into the cells immediately after establishment of the co-culture. The low level of autofluorescence detected in the negative control (cells alone in Figure 3.11B) is most likely due to fixing procedure. The fluorescence signal is more intense in

the 8-hour samples (Figure 3.11C-D), which show a high level of rhodamine fluorescence inside many cells in the majority of the focal slides examined, and little or no autofluorescence in the control. Taken together, the confocal microscopy results shown in Figure 3.10 and 3.11 strongly suggest that liposomes are taken up early by PBMCs when co-cultured. This finding might affect their employment as aAPC; uptake by cells could affect the ability of the liposome to form an immunological synapse, to present the MHC monomer to the TCR on the T cells and/or have an impact on TCR signalling. Moreover, high levels of liposome inside the cytosol might have a cytotoxic effect by themselves by affecting intracellular osmolarity. However, it has to be pointed out that such effects might be cell-dependent, with different cell types uptaking the liposomes at different rates. Ideally, liposome uptake should be assessed independently in each cell system used.

3.3.9 SETTING UP THE RF 33.70 READOUT:

In parallel to the liposomes-PBMCs experiments, the ability of the liposomes to function as aAPCs was also tested using a murine model. This involved using the OVA restricted RF 33.70 non-lytic CD8 T cell hybridoma (see Materials and Methods section 2.2.1.5) as responding cells; murine H2-K^b-OVA monomers (see Table 3.1) were employed as stimulus. As was done with HLA-A*0201-NLV, a re-cloning step was undertaken to add 3'- end Cys residues.

H2-K^b-OVA-specific RF 33.70 cells release IL-2 upon successful TCR engagement, consequently the readout for this system was IL-2 in the culture supernatant, measured by ELISA. The first experiment performed was an ELISA test on the RF 33.70 cells incubated with OVA peptide alone, to ensure that no cross-presentation of peptide was occurring in the absence of exogenous monomer or antigen presenting cells. No detectable IL-2 secretion was recorded and the background from unstimulated cells was very low (data not shown). This confirmed that the system in use was "clean"-i.e., peptide alone could not exert an effect. Consequently even if peptide were to become detached from the liposomes' surface, this would not interfere with a genuine liposome-mediated antigen presentation.

A suitable positive control was then established using H2-K^b-expressing splenocytes from OT-1 mouse, pulsed overnight with various concentrations of OVA peptide and irradiated. They were then co-incubated with two different amounts of RF 33.70 cells to evaluate which was the combination promoting the best IL-2 secretion. Results for this experiment are shown in Figure 3.12, below.

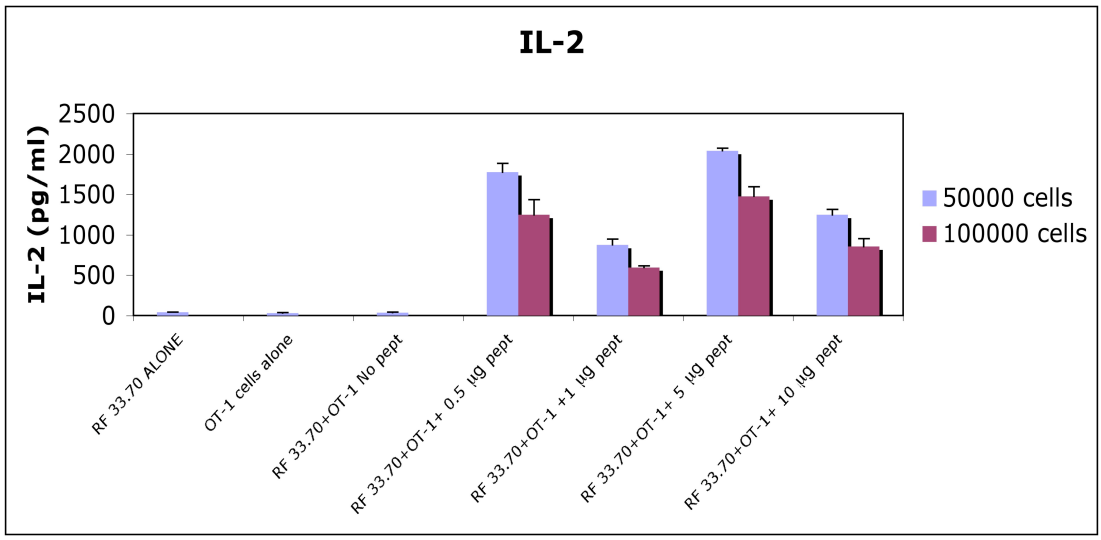

Figure 3.12: RF.33.70 cell line ELISA optimization. 2 different amounts of RF 33.70 cells (H2-K^b-OVA specific hybridoma) were incubated overnight with a fixed number of unpulsed OT-1 splenocytes (third from left) or splenocytes pulsed with increasing amount of OVA-peptide (fourth to seventh from left). Both cells types alone (first and second from left, respectively) were used as -ve controls. IL-2 in the supernatant was then detected by ELISA and plotted as a column (each column is the mean result of values from triplicate wells; standard deviation is plotted as error bars). Results shown are representative of 2 independent experiments.

Figure 3.12 shows marked secretion of IL-2 only when the responder RF 33.70 cells were incubated with pulsed OT-1 splenocytes. Neither type of cells alone, nor RF 33.70 incubated with unpulsed OT-1 splenocytes, resulted in significant amounts of IL-2 being released in the supernatant. However, all the concentrations of peptide tested resulted in consistent IL-2 secretion with both amounts of RF 33.70 cells used. There was no correlation between increasing amount of peptide and increased secretion of IL-2. Instead, a relatively low peptide dose (0.5 µg) gave one of the best responses, while the next increment -1 µg- gave the poorest response registered. It was decided that 0.5 µg of peptide gave the most consistent response from the RF 33.70 cells. However, it is possible that a more optimal peptide concentration existed at a lower dose. If the

optimal dose had been needed, a dose response curve from dose of 0.5 μg and lower would have been required to elucidate it.

3.3.10 LIPOSOME MEDIATED IL-2 SECRETION IN THE RF.33.70 SYSTEM:

After setting up all the controls (see Figure 3.12) the antigen presenting potential of H2-K^b-OVA-loaded liposomes was tested in the RF 33.70 system. To this end, a batch of H2-K^b-OVA-loaded liposomes was prepared and incubated with RF 33.70 cells, together with OVA-pulsed OT-1 splenocytes as controls. Liposome doses that had been shown to be optimal by De La Peña *et al*., 2009, were used. A RF 33.30-liposome specific titration was not performed, as the amount of liposome required to form an increasing dose titration was impractical (approximately half the culture volume was required to be liposomes to achieve the De La Peña *et al*. doses used in this experiment).

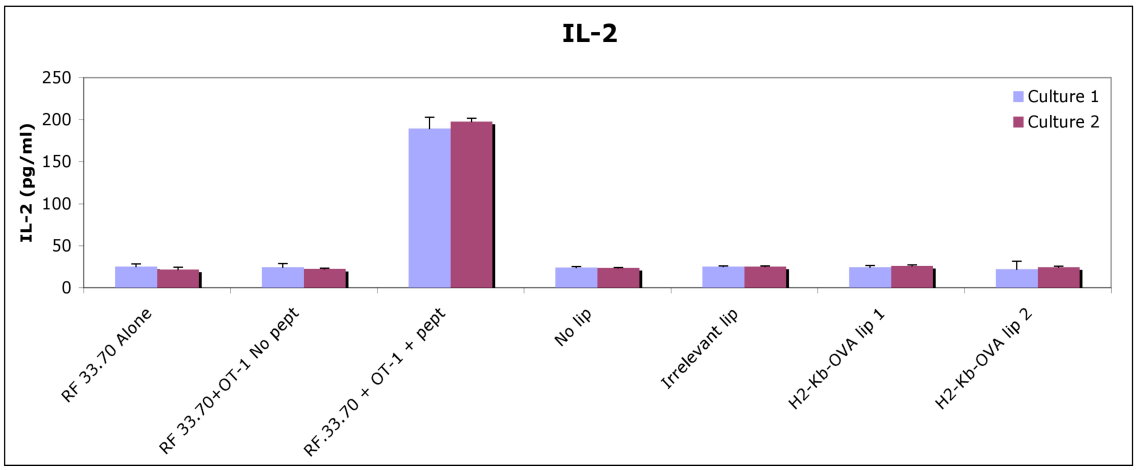

Figure 3.13: RF.33.70-liposomes ELISA. 2 independent cultures of RF 33.70 cells were incubated overnight with unloaded liposome (empty lip), with liposome loaded with an irrelevant human monomer (irrelevant lip) or with two different H2-K^b-OVA loaded liposomes (H2-K^b-OVA lip 1 and 2). As -ve controls, RF 33.70 cell alone or RF 33.70 cells incubated with unpulsed splenocytes (RF 33.70 + OT-1 no pept) were used, while as +ve control RF 33.70 cells incubated with pulsed splenocytes (RF 33.70+OT-1+pept) were employed. Results shown are representative of 2 independent experiments using both H2-K^b-OVA- and Cys- H2-K^b-OVA-loaded liposomes. Columns represent the mean values from triplicate wells, while the standard deviation is plotted as error bar.

In this case the IL-2 secretion for the +ve control (Figure 3.13, third column from left) was not as marked as shown in Figure 3.11, however it was still enough to produce a

clear positive result. None of the negative controls (RF 33.70 cells on their own and incubated with unpulsed splenocytes) showed any IL-2 secretion. However, neither did any of the liposome-stimulated samples. In addition to two independent batches of H2-K^b-OVA-loaded liposomes, an unloaded liposome and a liposome loaded with an irrelevant human monomer (HLA-B*0702) were used and in no case was a significant amount of IL-2 was detected. Similar results were obtained when using Cys-H2-K^b-OVA-loaded liposomes (data not shown). These findings suggested that the H2-K^b-OVA-loaded liposomes were not exerting an antigen-presentation effect in this system, or were not being correctly recognized by the cells.

3.4.0 DISCUSSION:

The initial aim of the work described in this chapter was to produce a liposome-based aAPC to be used for immunotherapeutic applications, following the results obtained previously in the laboratory and published in De La Peña *et al.*, 2009, during the course of this PhD project. In this work, it was decided to focus on T cell systems involving memory responses only. This should have reduced the need for co-stimulatory molecules on the liposomal surface; signal 1, i.e. TCR-MHC/peptide engagement, should have been the only requirement for an immune response. During the project, however, unforeseen and persisting standardization issues were encountered during the preparation and MHC loading of the liposomes. Moreover, results that were not consistent with the previous reports emerged in the more functional, cellular-based experiments. In the next sections some possible explanations for these results will be discussed and various hypotheses to explain the discrepancies between the published data and these findings will be presented.

3.4.1 MONOMER ACTIVATION:

The first objective to be accomplished in this project was the correct loading of each type of monomers on the liposomal surface. Due to the requirement for a Traut's reagent-mediated activation step, it seemed natural to employ the Ellman's assay to assess whether the introduction of novel SH groups had been successful or not. It was

discovered, however, that it was not possible to quantify exactly how many new thiol groups were introduced; Ellman's assay would have provided only an overall quantitative assessment of the increase in SH groups in the activated protein. The first attempt was successful but it was performed only once as the method was very inefficient. A single experiment required 1/3 of the total refolded monomer stocks available for each protein and a high experimental noise was registered. To continue with the Traut's reagent protocol would likely require the titration of different amounts of the reagent to the monomers and the evaluation of activation via Ellman's assay. Optimization would have to have been performed independently for each of the substrate used in the project-i.e. the HLA-A*0201-NLV and H2-K^b-OVA molecules. However, this approach was abandoned on the basis of both the very high amounts of monomers required for each Ellman's assay and the difficulties in detecting correctly loaded monomers on the liposome surface using only biochemical methods. In fact, these preliminary results and considerations prompted the question whether a biochemical assay was the best choice to evaluate liposome quality, or if there were other possible options available.

3.4.2 MONOMER LOADING AND DETECTION:

3.4.2.1 BIOCHEMISTRY METHODS:

Some technical issues were also encountered during the next step in liposome preparation, the evaluation of loading efficiency. Initially this was assessed via biochemical methods, as previously published by De La Peña *et al.*, 2009, but very poor consistency between different assays and batches of liposome was experienced. The reported sensitivity of a dot blot i.e., the minimum amount of protein that can be detected, is around 1 μg. As each batch of liposome was loaded with a maximum of 10 μg protein, pre-chromatography, the maximum amount of MHC-loaded liposome that could be added to a blot membrane was likely to contain approximately 0.9 μg of protein. Whilst this should have been in the range of detection it would have been at the lower end. However, more sensitive biochemistry-based assays such as silver staining of polyacrylamide gel (which can detect nanogram amounts of protein), Western Blots,

or ELISA, were not viable options. For silver stains and Western Blots, the difficulty was loading a sufficient amount of whole liposomes on a gel (data not shown) without a denaturation step that would have most likely affected the loaded monomer. In the case of the ELISA, the liposome cannot be adhered to the plate, making washing to remove detection antibody difficult to impossible.

3.4.2.2 FLOW CYTOMETRY METHODS:

Taking into account all these considerations it was decided to use flow cytometry-based techniques to further elucidate the efficacy of loading, as it was considered that flow cytometry detection would provide a good balance between practicality and sensitivity. Initially, flow cytometry experiments performed on liposomes alone showed positive results. However, it was discovered that the staining of liposomes led to very high non-specific binding, amplified or possibly caused by the inability to wash the preparation. The flow cytometry analysis was complicated further by the very high level of fluorescence imparted to the liposome preparation by the rhodamine-fluorescent lipid. This was an unavoidable requisite when liposomes were examined alone. To circumvent both these problems, it was decided to examine liposome-cell co-cultures. In this case, liposomes did not need to be fluorescent and staining and washing could be performed as normal, resulting in an improved clarity on whether monomer loading was successful or not. Regardless of its detection level, however, it could well be possible that the scarce amount detected as correctly loaded on the liposomes' surface is more than enough to exert a cellular action. As such, a poor detection did not necessarily imply a poor liposome-mediated expansion in the PBMCs system.

3.4.3 MONOMER LOADING OPTIMIZATION:

Even after having ascertained that monomer molecules were present on the liposome surface and could be detected, albeit at a low level, the orientation issue still remained. It was perfectly possible that the amount of randomly-activated monomers loaded on the liposome surface was enough to elicit a response from cells. However, the orientation of single proteins on the liposome surface was impossible to control as there

was no way to add cysteines preferentially on one part of the molecule rather than the other. To improve monomer loading and decrease the intrinsic variability of the process, it was decided to insert one Cys at the 3'-end of each heavy chain molecule (HLA-A*0201 and H2-K^b). The addition of a single amino acid, rather than a string as has been described in the literature (Marty *et al.*, 2001 and Marty *et al.*, 2002), was chosen to avoid self-annealing of SH reactive group from contiguous cysteine amino acids. Moreover, it was speculated that the addition of a single amino acid, rather than a string, was less likely to affect the tertiary structure of the refolded protein. In fact, the addition of a single Cys at the 3'-end position did not impact on the refold of the monomer, as assessed by conformation-specific ELISA in both HLA-A*0201-NLV and H2-K^b-OVA monomers (data not shown). Finally, it was considered that, in the case of HLA-A*0201 at least, the addition of a single Cys could have had a significant impact on loading. As there are only other 6 cysteines in the entire protein, all used for inter-protein binding, (Bjorkman *et al.*, 1987), it was predicted that one more Cys at the 3'-end of the molecule would provide a good anchor for liposome attachment without affecting the structure of the protein.

Another reason to optimize the monomer loading was the possibility to reduce the amount of protein that resulted unused during the attachment to the membrane. With the activation protocol it was very likely that a relevant amount of the monomer used for loading ended up in an unfavourable orientation. However, there was no way to recover and reuse such misloaded molecules. Therefore, after the appropriate optimization, a more rational procedure of monomer attachment would have reduced the amount of protein required for each loading, improving greatly the efficiency of the protocol. The overall amount of monomers available was in fact one of the limiting factors of the system. Indeed, the preparation and optimization of a monomer-producing cell line, starting from a tricistronic vector transfected in a eukaryotic expression system, was considered at the beginning of the project but abandoned due to time considerations. However, a larger amount of monomer available from the start would have been beneficial for the aAPC-liposome system, as it would have allowed the testing of a larger number of conditions.

3.4.4 TOXICITY AND EXPANSION:

Following liposome preparation and characterisation, it was decided to test the antigen presenting potential of HLA-A*0201-NLV loaded liposomes in an *in vitro* system. PBMCs from CMV+ve, HLA-A*0201+ve healthy adult donor and optimized conditions described in De La Peña *et al.*, 2009, were used in the experiment.
The controls for this system, both positive and negative, worked consistently well; indeed, in some experiments a better tetramer-specific expansion was seen when using HLA-A*0201-NLV monomer rather than NLV peptide as +ve control (data not shown). This was explained with the fact that, while the peptide was prepared and used aseptically across the whole procedure, this was not the case for the monomers. In fact, heavy and light chain were obtained by bacteria inclusion bodies and, despite lengthy washes and chromatography, the resulting preparation could not be completely sterile- i.e., completely free of bacteria-derived components. Therefore, it is likely that some PAMPs or other immunogenic bacterial byproducts survived in the monomer preparation. This could have promoted general T cell activation, resulting in an increased percentage of tetramer-specific cells if compared to the peptide-stimulated PBMCs.

In the experimental samples, however, it was not possible to detect the same level of HLA-A*0201-NLV liposome-mediated expansion described in the published data. Instead, a small but noticeable decrease of tetramer+ve cells often occurred when the PBMCs were co-incubated with the liposomes. In the first experiments this effect was detected when using Cys-modified MHC-loaded liposomes. If this trend had been observed in all the expansions performed a possible conclusion would have been that only the Cys-modified loaded liposomes were, for some reason, ineffective and possibly promoting cytotoxicity. In further experiments, however, whenever liposomes (unloaded or loaded with either protocol) were used, the percentage of CD8+ve HLA-A*0201-NLV tetramer+ve cells in the corresponding co-cultures tended to either remain at the same level of the unstimulated culture or to diminish slightly. These results were observed in more than one donor and with different incubation times (including longer time points than those described in De La Peña *et al.*, 2009). This

finding lead to an interruption in further PBMCs-liposome expansion experiments, as it was necessary to assess the effect of liposomes on cells in the system used in this project. Judging from the experimental evidence, it was speculated that liposomes might be taken up by cells at early time points in the co-culture and such an uptake might have resulted in the inhibition/mild toxic effect observed.

The effect of unloaded liposomes was also assessed using Buffy coat cultures; a decrease in cell viability upon co-incubation with liposomes (as evaluated via direct 7-AAD staining) was observed. Some possible mechanisms of action were hypothesised as explanation for this finding. Firstly, the formulation of the liposomes' suspension is not at a physiological concentration. More accurately, the concentration of NaCl in the buffer used for re-suspension and chromatography is 140 mM, whilst the physiological solution used in medical practice is 154 mM. Whilst the osmotic difference is slight, it may have a damaging effect on PBMCs, leading to potential loss of viability. The HEPES buffer might have also have had an adverse effect, as the Buffy coat samples had a slight increase in overall mortality when incubated only with the re-suspension buffer. Secondly, without access to GMP facilities, it was not possible to maintain complete sterility during liposome preparation. Liposomes were filtered just before use and subsequently maintained aseptically but there is still the possibility they will not be suitable for prolonged *in vitro* use. Even in the absence of obvious contamination (such as bacterial or fungal growth during cell culture) the possibility of contamination remains which may negatively impact on cell viability.

3.4.4.1 THE TIME INCUBATION EFFECT:

The most relevant determination of toxicity is likely to be a combination of primary cell use with relevant amounts of liposomes (i.e.>30% of total culture volume) and prolonged incubation. Analysing the studies reported in the literature reveals few details of the exact amounts of liposomes added to a specific number of cells (one of the few examples is reported by Marty and Schwendener, 2005). The liposomes-cell incubation times vary greatly, ranging from 30 minutes (Marty and Schwendener, 2005) to 1 (Koning *et al.*, 2006, Huth *et al.*, 2006 and Baum *et al.*, 2007), 2 (Copland *et al.*, 2003)

and 6 hours (Mercadal *et al.*, 1999). The longest incubation described was up to 48 hours (Ignatius *et al.*, 2000). Albani's group (Prakken *et al.*, 2000) used liposome-based aAPCs as a stimulus for the measurement of IL-2 production in a setting similar to that presented in this work, and described a cell-liposome co-incubation time of 8 hours.
Exosomes are a physiological analogue of the liposome system presented in this project. Amigorena's team (Thery *et al.*, 2002a) employed exosomes in a 4 day thymidine-based assay while the Zitvogel group (Andre *et al.*, 2004) used them in a 2-hours co-incubation with either DCs or peripheral blood lymphocytes. Finally Admyre *et al.*, 2006, added them as stimulators of CD8+ve T cells for 48 hours for a subsequent ELIspot assay. With the exception of De La Peña *et al.*, 2009, there are no studies published involving incubations greater than one week.

In addition to the much shorter incubation times, all the liposome papers quoted above described experiments performed with immortalized cell lines. In most cases, tumour-derived cell lines and not primary human cells (such as the PBMCs used in the present work) were employed. Ultimately, it was speculated that the combination of primary cells combined with long incubation periods with large volumes of liposomes resulted in overall "extreme" culture conditions. This could have lead to the lack of PBMCs expansion observed in the tetramer-specific expansion and PBMCs/liposome co-incubations and the possible liposome-mediated decrease in viability observed in the Buffy coat experiments.

3.4.4.2 LIPOSOME UPTAKE BY CELLS:

In addition to an inhibitory liposome-mediated effect on tetramer+ve specific expansion, evidence for early uptake was also detected. The first indication of its occurrence in PBMCs-liposome co-cultures was suggested by the DCs-liposome experiment. Here, liposome associated HLA-A*0201+ve fluorescence was detected after 7 hours, but not after an overnight incubation, suggesting the possibility of DC uptake since DCs are characterized by high phagocytosis. However, this feature is not extensively shared by other cell populations within the PBMC fraction. Therefore, phagocytosis and liposome uptake is likely to have been more relevant for DCs than for

PBMCs. The experiment above was performed only once, and as such, no stand-alone conclusions can be derived. However, its results were further substantiated by time courses performed on HLA-class I negative cell lines. These also showed liposome absorption (as measured by HLA-A*0201+ve cells) at very early time points (data not shown).

Stronger evidence of liposome absorption and uptake by PBMCs was indicated by the microscopy results. All the slides required fixation; this, in addition to the slide preparation protocol, possibly resulted in the limited degree of autofluorescence observed in some samples. However, the strong rhodamine fluorescence that was detected in all samples (albeit fainter at 8 hours or overnight) was considered to be genuine. Single-plane fluorescence microscopy does not provide information on whether the fluorescence is on the membrane or inside the cells. Consequently, stacked images were also taken at some of the time points considered. The stacked images at t=0 showed rhodamine fluorescence in all the slides of the single cell in the field, strongly suggesting that liposomes are internalized in the cytosol rather than merely being absorbed on the cell membrane. This was confirmed by the same result obtained after 8 hours of co-incubation, further demonstrating that part of the liposome is internalized by PBMCs shortly after setting up the culture.

The results obtained in the microscopy experiments supported the evidence for early liposome uptake presented in the chapter. In the microscopy case, it is not known which particular cell type mediated the phagocytosis, as a mixed cell population was used. However, considering that DCs and other highly phagocytic populations are usually a minority within PBMCs, it could be inferred that liposome uptake is a feature shared by all cells in PBMCs.

While the requirements for T cell activation and immune synapse formation are under active investigation, it is known that DC-T cell interactions leading to activation are stable and may last several hours (Bousso, 2008). Also, T cells may demonstrate immunological synapses lasting 90-minutes and are characterised by continuous recycling within this time (Dustin, 2008). Considering the long and stable contact between APC and T cells required for T cell activation, and the important liposome

internalization observed, it is possible that the loaded liposomes do not remain in solution long enough, or are stable enough, to effectively present antigen.

Other liposome preparations reported have been formulated with the specific aim to study the immunological synapse. These studies all utilized some mechanism to cluster the antigen on the liposome surface (Giannoni *et al.*, 2005 and Zappasodi *et al.*, 2008). This is a factor that might have had a strong impact, as it is known that the antigen density on the aAPCs surface is crucial for a good T cell stimulation (Zappasodi *et al.*, 2008). However, it would have been impossible to determine the exact amount of monomers on the surface of our liposomes when using the activation method (i.e. random introduction of SH molecules). In fact, antigen clustering was achieved in these previously reported studies using quite complicated systems of neutravidin/streptavidin rafts and/or cholera/tetanus binding sites (Giannoni *et al.*, 2005 and Zappasodi *et al.*, 2008). These methods are not neither physiological nor compatible with an *in vivo* model.

3.4.5 THE MURINE MODEL:

All the results presented and discussed so far were obtained in a human model using primary cells. However, a murine, *in vitro* model was also employed. This system had fewer variables to be accounted for; a single cell population and an easier readout technique (ELISA vs tetramer-specific expansion) were used. It was expected that the use of the RF 33.70 cell line would not pose any toxicity issue. Moreover, any results obtained with the hybridoma cell line would have been easier to interpret as a purified population was being employed. Another main advantage of the RF 33.70 hybridoma was the sensitivity of its readout. According to the manufacturer, the ELISA kit in use would have reliably detected concentrations of IL-2 of less than 20 pg/ml. This would allow for even minimal liposome-mediated TCR engagement to be detected. However, these advantages were somewhat counterbalanced by the increased difficulties in obtaining the murine protein. The H2-K^b-OVA heavy chain production and refolding required extensive optimization, with the maintenance of a correct pH throughout being critical. Also the complete monomer had much lower stability than the HLA-A*0201-

NLV monomer. Consequently, the overall yield of H2-K^b-OVA monomer available for liposome loading was consistently less than that for HLA-A*0201-NLV (data not shown). Moreover, flow cytometry analysis could not be performed on this monomer as the conformational specific antibody 25.D1/16 was not fluorescently conjugated and using a secondary antibody prevented by the high non-specific binding shown by liposomes. When testing the antigen presenting potential of H2-K^b-OVA-loaded liposomes, results were similar to those encountered in the human model ie. no liposome-mediated antigen presentation could be detected. In this case as well the presence or absence of a 3'-end Cys on the monomer was irrelevant in terms of antigen presentation efficacy.

3.4.6 CONCLUSIONS:

Considering the issues described so far in terms of liposome preparation, standardization and loading, if the research work had continued on this topic the focus of this project would have had to shift radically from an immunological focus to a biochemical one. At this point, in fact, the only way to cast some light into the poor standardization/lack of expansion issues seemed to be the step-by-step assessment of the liposome preparation protocol using all techniques available and an assessment of the effect each component had on the PBMCs (and, as a control, more robust cell lines).
It still remains an open question as to why it was not possible to reproduce the previously published results; all aspects of the liposome preparation and loading were verified by the first author of De La Peña *et al.*, 2009. All stimulation and cell culture conditions were as previously optimized (as published in De La Peña *et al.*, 2009). There was, however, one important condition that was not reproducible; the access to the same CMV+ve donors. Therefore, previously untested donors had to be used. All the newly selected donors were checked for the resting HLA-A*0201-NLV-tetramer-specific population and all of them were tested for both peptide and monomer-driven expansion (as shown in Figure 3.6). In some cases, they were also tested for NLV-pulsed, DCs-mediated expansion (data not shown) as a further control to ensure the CMV response was maintained. In all cases a marked tetramer-specific expansion was

obtained, effectively ruling out a general hypo-response to CMV stimulation as cause for a lack of liposome-mediated tetramer expansion.

To conclude, the issues of standardization and reproducibility encountered using the models presented in this chapter would suggest a stop against their further use as immunotherapeutic tool until all the questions related to loading, cytotoxicity and degree of response have been addressed. To maintain an immunological focus in the PhD project, other forms of antigen presentation were subsequently explored.

CHAPTER 4:
PREPARATION AND CHARACTERISATION OF CD-DERIVED DCs FOR IMMUNOTHERAPY

4.1.0 INTRODUCTION:

In addition to the liposome-based aAPC, various possible cellular-based APCs and the source of these cells were also evaluated in this project. Of these sources cord blood (CB) was the primary focus due to its increasing importance in all aspects of HSCT. Of the cells types available, CB-derived DCs were likely to be the most potent APCs, as they are professional APCs, able to stimulate naïve and resting T cells more effectively than monocytes, macrophages or B cells (Steinman, 1991).

4.1.1 DCs FROM CB:

Several studies have assessed the properties of DCs either present in CB or differentiated from CB-derived stem cells/or monocytes. These studies could be divided in two distinct groups involving either a phenotypical characterization, often in comparison with adult-derived DCs, or establishment of DCs-cytotoxic T cell (CTL) models using various antigens.

Takahashi's group compared DCs generated from fresh and frozen CB-derived CD34+ve cells, and reported that both cell types expressed markers relating to antigen presentation, had DCs-like morphology, and were more effective than peripheral blood mononucleated cells in promoting MLR (Sato *et al.*, 1998). In contrast Lau's group reported reduced expression of HLA-DR, but not of CD86 and CD11c, on monocyte-derived DCs from CB compared to their adult counterparts. Importantly, they also showed reduced alloreactivity by T cells stimulated with CB-derived DCs as compared with adult-derived DCs (Liu *et al.*, 2001). These results were confirmed and expanded upon by the Cairo lab showing that monocyte-derived DCs from CB were less effective than their adult counterparts in an allogeneic MLR, despite being phenotypically similar (Bracho *et al.*, 2003). It was also recently published that CB-derived DCs, either differentiated from monocytes or freshly purified, induced less IFN-γ secretion but induced more IL-4 production when compared to adult peripheral blood DCs and suggested that CB-derived DCs were more prone to Th2 rather than Th1 T cell priming

(Naderi *et al.*, 2009), confirming similar results published earlier (Langrish *et al.*, 2002). It would therefore seem, on this basis, that whilst stem cell derived DCs from cord blood are fully functional, that isolated or monocyte-derived DCs have reduced antigen-presenting activity.

Whilst there is evidence of reduced antigen presenting activity by CB monocyte-derived DCs there is also evidence that they can support naïve T cell responses. In 2003 Cerundolo's group showed that priming of CB-derived T cells by autologous DCs could be achieved in a MelanA-specific system (Salio *et al.*, 2003). Using the same antigen model, it has been recently shown that MelanA-specific CD8 T cells of CB origin could be expanded also with peptide expansion/polyclonal stimulation, and that these cells displayed an effector phenotype (Merindol *et al.*, 2010). In 2004, Her2/*neu*-specific CTLs were generated using a CB-derived DC autologous system and repeated administration of peptide (Wang *et al.*, 2004). Szabolcs's group showed the successful production of CB-derived, CMV-specific T cells following priming with autologous DCs pulsed with CMV lysate. These T cells were able to lyse CMV-pulsed autologous targets and secreted IFN-γ and TNF-α (Park *et al.*, 2006). Recently, Bollard's team reported they were able to generate virus-specific T cells starting from non-adherent cells as responders and viral-transduced DCs and EBV-transformed B cell lines as APCs (Hanley *et al.*, 2009). They focused on CMV, adenovirus, and EBV-specific T cells due to the importance of these viruses in HSCT. Importantly, they used only frozen CB samples throughout their entire protocol, the only source of CB actually available for clinical transplantation.

Taken together, the evidence in the literature supported the choice to explore the APC potential of monocyte-derived DCs from CB and their use for the generation of a DC-CD8+ve T cells autologous system using a model peptide. Since there was also evidence of alloreactivity and, in some cases, reduced DCs-markers expression but effectiveness in CTL generation the CB derived DCs would be thoroughly assessed for both phenotype and alloreactivity prior to development of an antigen-specific CD8 T cell response system.

4.2 EXPERIMENTAL AIMS:

The work described in this chapter aimed to generate a CB-derived, peptide-specific DC-CD8 T cell system, using a MelanA peptide as a model antigen and conditions as shown in Salio *et al.*, 2003; success would be measured by both IFN-γ intracellular staining and evidence of tetramer-specific expansion. To achieve this, DCs were generated from CB CD14+ve cells, characterized and compared to adult monocyte-derived DCs. The cells were assessed for the expression of DC-specific markers and to highlight any eventual difference between the two subsets. Cultured DCs from CB and adults were then assayed using an MLR to evaluate their overall antigen presentation potential. Finally, a peptide-specific expansion system was set up.

4.3 RESULTS:

DCs (from CB and, as a control, from adults) were differentiated from CD14+ve precursors. DCs of either origin were then characterized for relevant markers (the most important were HLA-DR, CD11c, CD80, CD86) and their potential to elicit an allo-reaction was measured in an MLR. When using cells from HLA-A*0201+ve, HLA-B*0702-ve, CMV+ve adult individuals it was only necessary to demonstrate that the DCs could mediate an NLV tetramer+ve expansion to indicate APC functionality. MelanA expansion was then assessed in adult and CB samples.

4.3.1 DCs GENERATION:

4.3.1.1 ADULT-DERIVED DCs:

4.3.1.1.1 PHENOTYPE:

The first step in the protocol was the preparation and characterization of DCs of both adult and CB origin. It was decided to set up the adult system first to have a solid control base for any CB-derived results. Summarized in Figure 4.1 is a representative example of adult-derived DCs preparation and characterization.

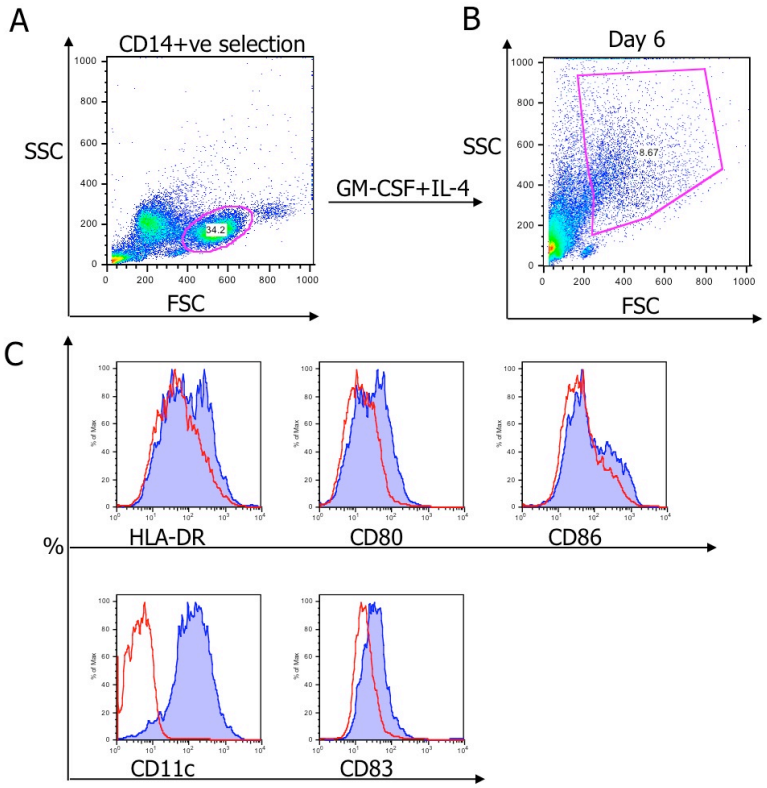

Figure 4.1: **flow cytometry analysis of DCs generated from adult monocytes.** A, monocytes were isolated (via CD14 selection) from healthy adults PBMCs and analyzed by flow cytometry. They were cultured for 5 days with GM-CSF and IL-4, then pulsed with the relevant peptide if necessary and matured with LPS. On day 6, mature and immature DCs were analysed by flow cytometry. B, DCs were selected on the basis of FSC and SSC and C, the relevant markers were analyzed within the DC-gated population ((——) immature DC (——) mature DCs, with the only exception of CD11c where (——) is mature unstained and (——) mature stained DCs). Representative of 8 independent experiments.

Figure 4.1 shows the outcome of the CD14+ve selection from freshly prepared adult PBMCs (Figure 4.1A, circled population) and their change in morphology (indicated by their increase in FSC-SSC) following differentiation into DCs after the 5 days of culture with GM-CSF and IL-4 (Figure 4.1B, gated population). Adult DCs were then matured with LPS and the relevant markers were analysed and compared between immature DCs, as control, and the mature DCs population (in the histograms in Figure 4.1C).

All gated cells were CD11c+ (the αX subunit of integrin CR4), both matured (shown here) and immature (not shown), indicating that the cells are myeloid or conventional DCs. A subset of the DCs (<50% of gated cells) showed an increase of HLA-DR and CD80 expression upon maturation. The proportion of CD86 expressing cells remained similar but a total population shift was observed with CD83 expression. This indicates that a signification proportion of the DCs had a mature DC phenotype. The results

shown above suggested that the system in use generated DC-like cells in terms of morphology and phenotype starting from a CD14+ve population.

4.3.1.1.2 TETRAMER-SPECIFIC EXPANSION:

Since CB T cells are naïve they will, therefore, require professional APCs to elicit a response to antigens. Consequently, before using them to generate CD8 T cell lines it was important to demonstrate that the DCs, in additional to having an APC-like phenotype, were functional. Therefore, to assess whether adult-derived DCs were also effective APCs, it was determined if they could support the expansion of an NLV-tetramer+ve population. This system, used as positive control, was chosen to check the general conditions of culture and assess the degree of tetramer-specific expansion in a well-known model (as done in De La Peña *et al.*, 2009). Shown in Figure 4.2, below is a representative, NLV-specific, expansion from an adult donor.

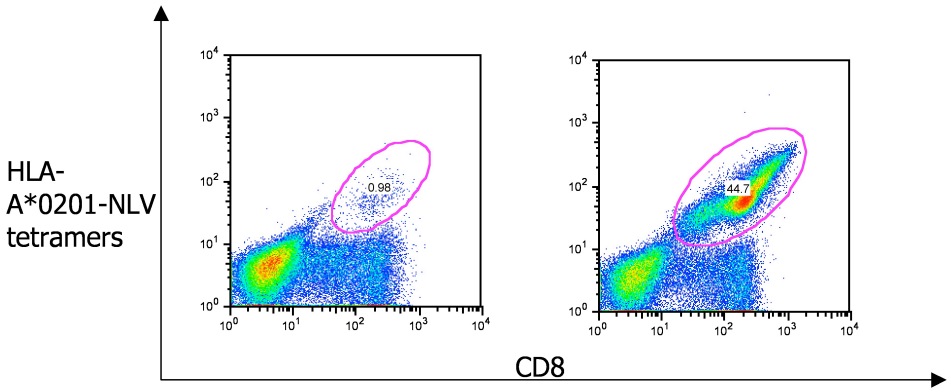

4.2. **Flow cytometry analysis of DCs-mediated tetramer expansion**. Following generation of DCs as shown in Figure 1, autologous responders (frozen CD14-ve fraction) were added to the DCs culture and the mixed culture was incubated for a further week to promote peptide-specific CD8 T cell expansion. In the figure above, the lymphocyte population was selected and the CD8+ve HLA-A*0201-tetramer+ve double +ve population within the lymphocyte gate was shown above. On the left, -ve control (responders incubated without DCs), on the right responders incubated with pulsed DCs. Representative of 2 experiments.

As shown above, a high percentage of HLA-A*0201-NLV-tetramer+ve cells (>40%) was obtained when PBMCs were incubated with NLV-pulsed DCs as compared to the control (<1%), thus confirming the effectiveness of our protocol in generating DCs capable of promoting peptide-specific T cell expansion in an adult system.

4.3.1.2 CB-DERIVED DCs:

4.3.1.2.1 PHENOTYPE:

Having set up the DC generation and CD8 cell expansion system in adults the work we then progressed to CB samples beginning with the differentiation of DCs from CB CD14+ cells (Figure 4.3).

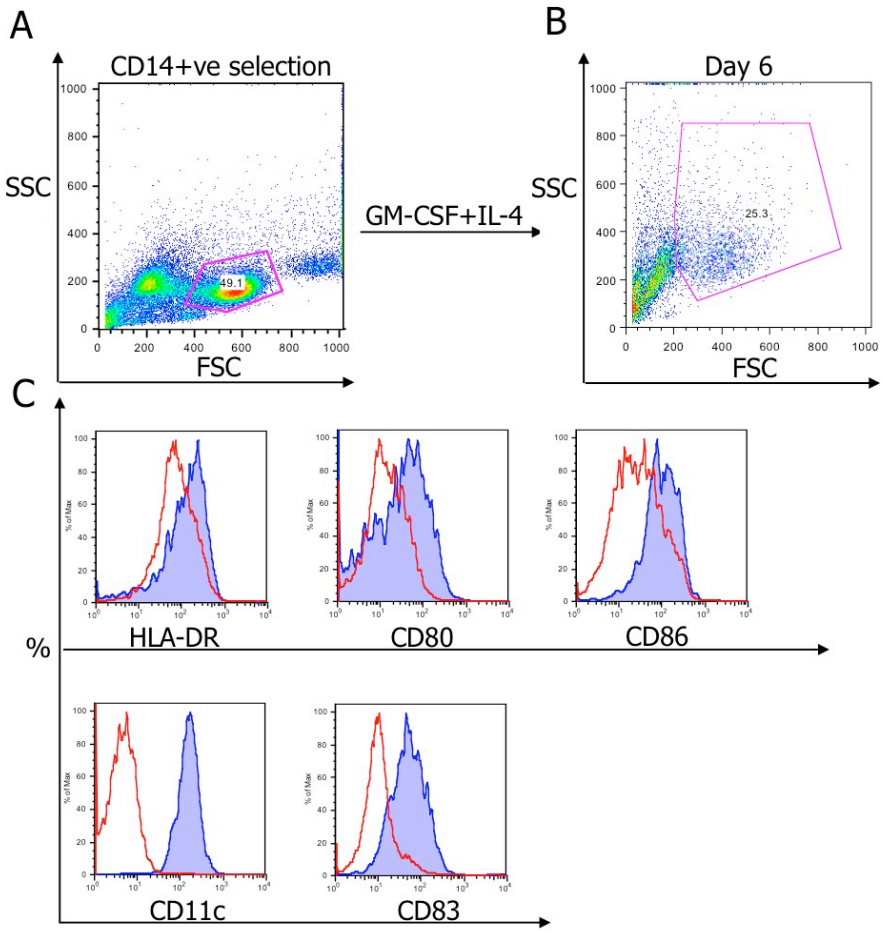

Figure 4.3: **flow cytometry analysis of DCs generated from CB monocytes.** A, monocytes were isolated (via CD14 selection) from CBMCs and analyzed by flow cytometry. They were cultured for 5 days with GM-CSF and IL-4, then pulsed with the relevant peptide if necessary and matured with LPS. On day 6, mature and immature DCs were analyzed via flow cytometry. B, DCs were selected on the basis of FSC and SSC and C, the relevant markers were analyzed within the DC-gated population ((——) immature DCs, (——) mature DC, with the only exception of CD11c where (——) is unstained and (——) stained DCs). Representative of 8 experiments.

Figure 4.3 shows the outcome of the CD14+ve selection from whole fresh CBMCs (Figure 4.3A, circled population) and their change in FSC-SSC appearance following their differentiation into DCs after the 5 days culture with cytokines (Figure 4.3B, gated population), as seen for their adult counterparts. CB-derived DCs were then matured with LPS and compared with immature DCs for surface marker expression (in the histograms in Figure 4.3C). As seen in the adult culture all cells were CD11c+ve (myeloid DCs) and showed an increase in CD83. However, unlike the expression that was observed in the adult cultured DCs, HLA-DR, CD80 and CD86 expression was seen to increase for the whole population, rather than a subset.

To summarise the results presented in Figures 4.1 and 4.3, an analysis of the median fluorescent intensity (MFI) for each label is reported below as a column plot (Figure 4.4).

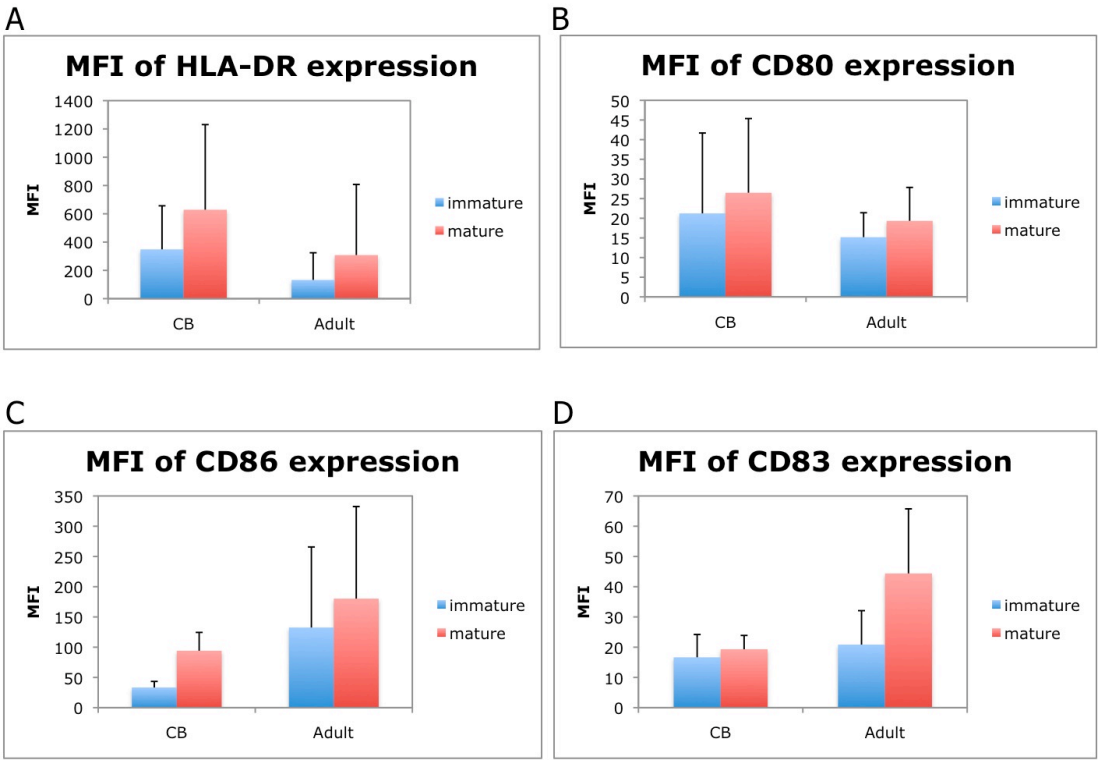

Figure 4.4: **column plot of the median fluorescent intensity (MFI) of HLA-DR, CD80, CD86, CD83 in the adult and CB samples subsets.** The MFI for each marker/sample was calculated and the columns represent the average of all MFI values; the error bars represent the standard deviation. N=6.

All the results shown above were analysed using the student t-test, to detect significant differences in the MFI of each marker between immature and mature samples of the same origin (paired t-test) or to compare the expression of the same marker between adult and CB samples (unpaired t-test). While no significant differences were detected, Figure 4.4 shows that in both the CB and adult subsets there is a trend of increase in the expression of each marker between immature and mature DCs. MFI values for HLA-DR and CD80 are higher in CB than in adult samples, while the opposite is seen for CD86 and C83. Moreover, MFI values were on average higher for HLA-DR and CD86 than for CD80 and CD83, regardless of the subset examined. Following these findings, it was concluded that both adult and CB-derived DCs were successfully generated and that there were not any significant differences in the expression of the markers examined. It was also concluded that CB-derived DCs exhibited a mature phenotype that should be compatible with effective antigen presentation.

4.3.1.2.2 FUNCTIONALITY OF CB-DERIVED DCs:

Following CB-derived DC generation and phenotypical characterization, the next objective was the assessment of their functionality. It was chosen not to set up a peptide-specific response system as a control for the CB system functionality (as done for adults in the HLA-A*0201-NLV-tetramer expansion). The CB sample used would need to be HLA-A*0201+ve, however typing of a cord sample before receipt was not practical. As an alternative option, it was decided to assess their alloreactivity potential compared to adult-derived DCs. With a relative short incubation time (compared to a lengthy expansion and re-stimulation for peptide specific expansion) this would provide a quick and clear readout. Finally, as literature results were quite discordant on the antigen presentation potential of CB-derived DCs (describing either a delayed alloreactivity for CB-derived DCs or effective antigen presentation and successful CD8 T cells generation in different publications) it was important to evaluate the behaviour of the CB DCs in this system.

A successful CB-DC-mediated MLR was considered a preliminary step for all subsequent experiments and a general proof of principle that CB-DCs could act as

antigen presenting cells and promote cell proliferation. To this end, an MLR assay comparing immature and mature DC from both adults and CB was set up and results are presented below in Figure 4.5.

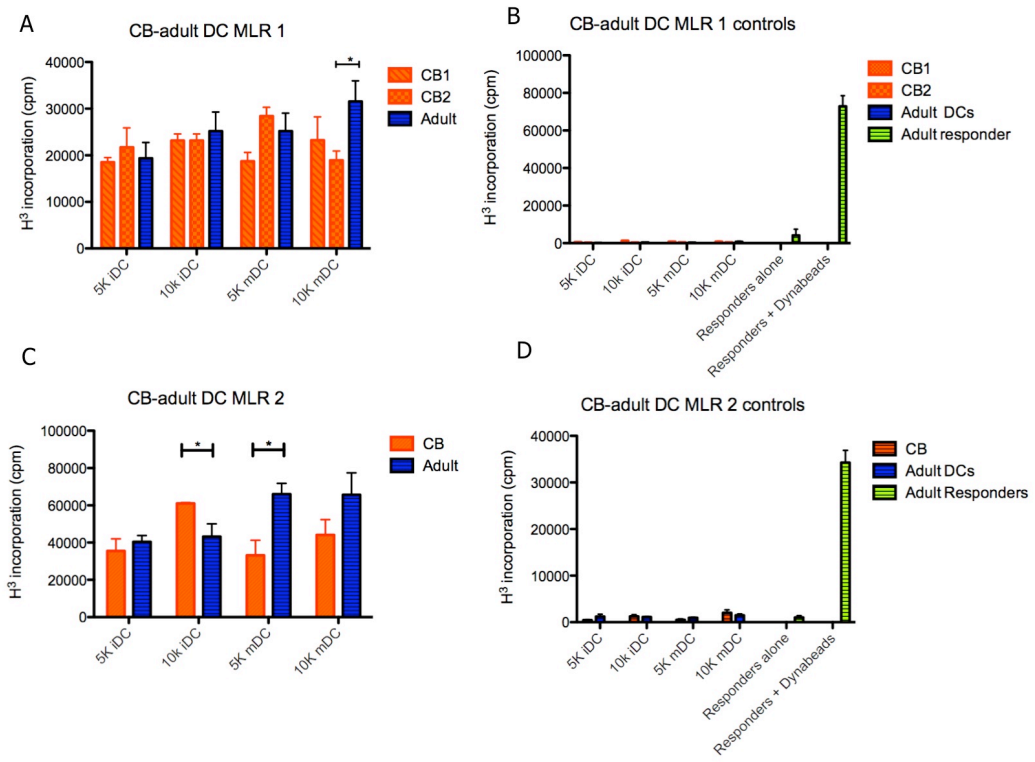

Figure 4.5: **comparison of alloreactivity between CB and adult-derived iDC and mDC-mixed lymphocyte reaction**. CB- and adult-derived iDC and mDC were assessed for their alloreactive potential against responder cells (unselected adult PBMCs). A, C experimental samples; B, controls for samples shown in A and D, controls for samples shown in C. DCs and responders by themselves as -ve controls and responders incubated with Dynabeads (anti-CD3CD28 beads) as +ve controls were used. P*<0.05 (t-test in all cases), N=3 independent experiments using different CB samples and adults. Results are expressed as the mean of triplicate wells (columns), while the error bars represent the standard deviation.

In figure 4.5 A and C adult and CB derived iDCs and mDCs (5000 or 10,000) were used to stimulate adult PBMCs. All DCs used, irrelevant of their origin or amount employed in the assay, elicited proliferation. Overall, the levels of proliferation induced by iDCs of three different CB and adult iDCS appeared to be similar; only one CB, at 10,000 cells, showed a significant difference with the same number of adult iDCs (Figure 4.5C 10k iDCs, P*0.01). With mDCs significant differences were detected between responses to adult and CB DCs in two out of three CB samples used (Figure 4.5A, 10k mDCs CB2, P*0.011 and Figure 4.5C, 5k mDCs CB, P*0.047). Overall,

when mDCs were used as stimulators, a trend of lower proliferation compared to that elicited by adult was detected (although this was not statically significant in all cases).

All the different cell types employed in the MLR as stimulators and the responders were also incubated alone, as a negative control, and showed no significant proliferation (Figure 4.5B and D). As a positive control, responders were co-incubated with anti-CD3CD28 Dynabeads and a robust proliferation was observed (Figure 4.5B and D, last column on the right).

From the data presented in Figure 4.5 it seems that, overall, the CB-derived mDCs examined here were not as effective as adult-derived cells in eliciting an allogeneic response; this difference was not observed in the iDC subset, where CB-derived iDCs appeared as effective as or, in one case, more effective than their adult counterparts. Regardless, the results of this experiment confirmed that CB-derived DCs were able to stimulate a robust proliferation in an MLR assay. Therefore, it was concluded that CB-derived DCs could demonstrate reasonable APC activity and that as such it was appropriate to test them for peptide-specific expansion in further experiments.

4.3.2.1 MELAN-A TETRAMER-SPECIFIC EXPANSION IN ADULT DONORS:

Following the generation and characterization of monocytes-derived DCs in both adults and CB, the next step was to generate CD8 T cell lines from a responder population stimulated with autologous DCs. The peptide model selected for the CB-derived CD8 T cells generation was MelanA, using a protocol published by Salio *et al.*, 2003. As a preliminary step to the expansion in CB, the level of MelanA-specific CD8 cells in resting healthy adult humans and the expansion of this subset that could be obtained was assessed. Unfortunately we had no access to melanoma patients and therefore could not compare the response with a MelanA positive control (MelanA is a tumour antigen). As the MelanA antigen is HLA-A*0201-specific, only healthy adults carrying the HLA-A*0201 allele were chosen for assessment and peptide expansion. The results from this experiment are shown below in Figure 4.6.

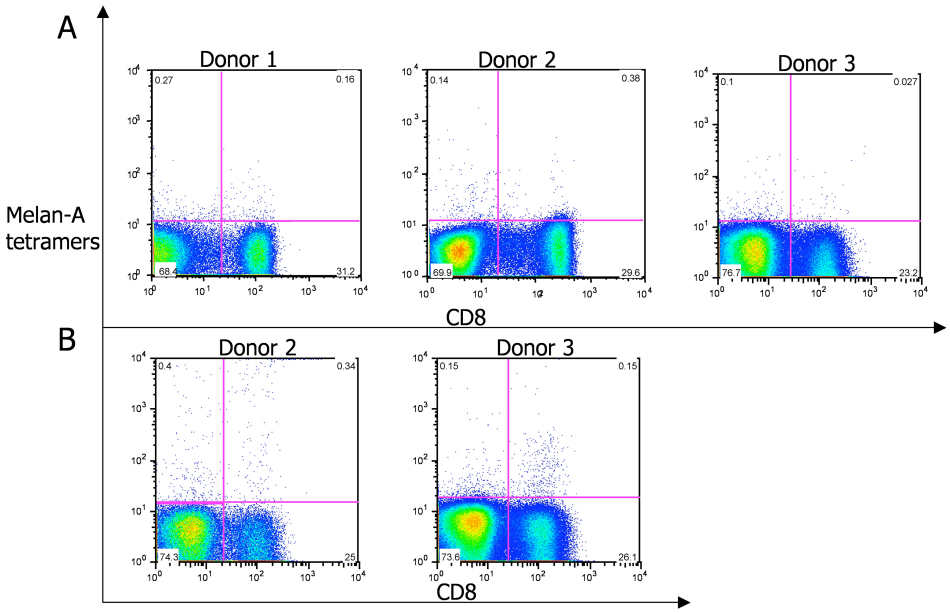

Figure 4.6: MelanA expression in adult samples. PBMCs from HLA-A*0201+ve donors were analyzed by flow cytometry for their expression of Melan-A specific CD8 T cells with (B) or without (A) peptide-specific expansion. A, lymphocytes were stained at day 0 (donor 1 and 2) or after one week culture in the absence of antigenic stimulus, to provide a time-matched control for the tetramer-specific population (donor 3). The results are representative of 7 experiments on 4/5 different donors. B, lymphocytes were stained after 1 week of peptide-specific expansion. Results are representative of 3 independent experiments.

All the available donors were tested for presence and amount of CD8 HLA-A*0201-MelanA tetramer+ve cells. In all cases a very small percentage of tetramer+ve cells was detected (0.16±0.09, see Figure 4.6A for three representative stainings), comparable to the 0.07±0.06 % reported by Pittet *et al.*, 1999. Having detected a putative tetramer+ve population in resting PBMCs, an expansion protocol was then performed to have a comparison model for the planned generation of CB-derived CD8 T cells and to assess whether it was possible to obtain a more defined tetramer+ve population after expansion. PBMCs were incubated with the MelanA peptide and the tetramer+ve population was assessed after 1 week (Figure 4.6B) to check for expansion. Tetramer+ve staining was also performed after 2 weeks of culture but no expansion was registered (data not shown).

In only one of the donors used a moderate expansion in the CD8+vet tetramer+ve subset was detected after 1 week (donor 3, see Figure 4.6B right panel and compare with the same sample in the row above), registering an increase of 0.12% in the tetramer+ve

population. This expansion, however, was accompanied by an increase in the proportion of CD8-ve, tetramer+ve labelling. It is, therefore, debatable whether it was a genuine, tetramer-specific expansion. One of the most important conclusions from this experiment was that not every stimulated adult sample resulted in a clear, MelanA-specific population. If this also occurs in the CB samples, it is possible that we will be unable to detect a tetramer specific expansion in the CB cohort.

4.3.2.2 MELAN-A TETRAMER-SPECIFIC EXPANSION IN CB SAMPLES:

Following the results obtained in adults, a MelanA specific expansion protocol was set up in CB samples. As with adults, the CB needed to be HLA-A*0201+ve to present MelanA peptide.

Each cord unit has a 20ml and a 5ml section; the 5-ml section from frozen CB samples was used for typing (see Materials and Methods paragraph 2.2.1.0). When a HLA-A*0201+ve CB sample was encountered, CD14+ve cells were selected, from the 20ml section, DCs were prepared as described in Figure 4.3 and the CD14-ve fraction obtained after selection was frozen for future use. When DCs reached the maturation point, they were pulsed overnight with the MelanA peptide, the responders were added the morning after and the culture was incubated until the tetramer+ve expansion was assessed (day 10-12). In addition to the tetramer+ve expansion, IFN-γ intracellular staining was also performed as a general assessment of T cells activation. Figure 4.7, below, shows the results for this experiment.

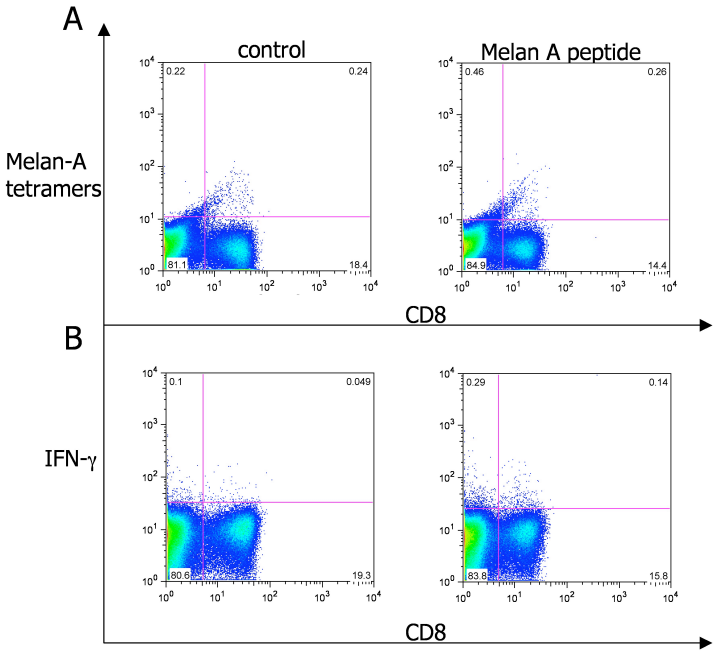

Figure 4.7: analysis of MelanA expression in CB samples. DCs from CB samples were prepared and pulsed with the MelanA peptide (as in Figure 4.3) and at day 6 autologous responders were added. Co-cultures were then incubated and analysed by flow cytometry at day 9-10 for A, tetramer expansion and B, IFN-γ expression as a general activation marker. Results are representative of 2 independent experiments.

The figure above reports the results of a CB-derived expansion performed following the protocol published by Salio *et al.*, 2003. No significant difference could be detected between the control (responders incubated with unpulsed DCs) and the experimental samples (Figure 4.7A). Figure 4.7B shows the IFN-γ intracellular staining performed on the MelanA expanded samples and on the control. In this case, a moderate increase in IFN-γ producing cells was detected in the experimental sample compared to the control (0.14% over 0.049%); however, an increase was registered in both the CD8+ve and CD8-ve subsets of the experimental sample so it appears unlikely to be peptide-specific.

Overall, these results suggested that a moderate degree of activation was taking place in the MelanA expanded sample, as measured by IFN-γ intracellular staining, but a relevant tetramer+ve specific expansion in the CB samples examined could not be recorded, even if a background population of HLA-A*0201-MelanA+ve cells was detected. Following these results, an optimization of the expansion protocol (checking

all culture conditions, starting with the dose of peptide used to pulse the DCs and its repeated administration during DCs-responders incubation) was planned. However, while setting up the CB system described in Figure 4.6, issues concerning its overall viability were detected.

4.3.3 VIABILITY:

4.3.3.1 RESPONDERS (CD14-VE FRACTION):

When frozen CB samples began to be routinely used as a cell source, as required by the need of typing for HLA-A*0201 positivity, issues concerning cell numbers and/or viability in the cell populations of interest (the CD14+ve fraction, to be isolated immediately upon thawing, and the CD14-ve or responders fraction, which was collected after CD14+ve selection and frozen again prior its final use) were registered. Figure 4.8, below, provides an overview on the total amount, viability and general phenotype by flow cytometry of the responder fraction upon collection after CD14+ve selection.

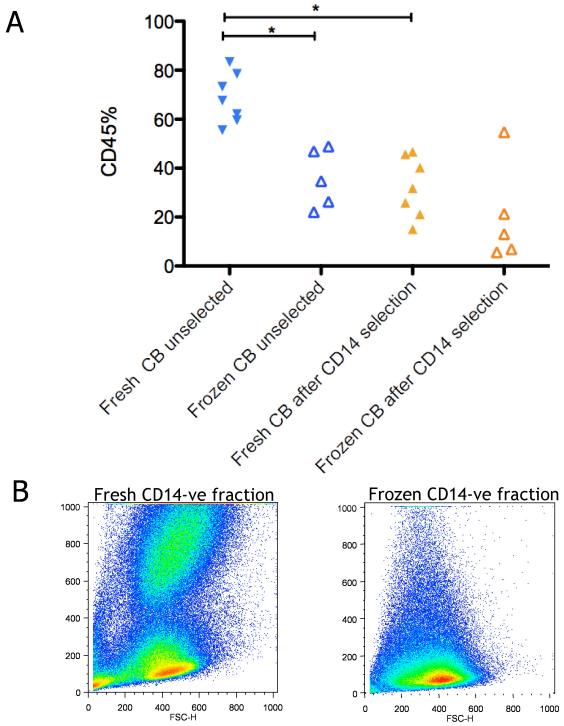

Figure 4.8: analysis of the fresh vs frozen CB samples-responders fraction. CB samples, both fresh and frozen, were examined immediately after thawing to assess numbers and overall quality as responders. A, graph showing the percentages of CD45+ve cells in various CB populations and B, representative example of FSC-SSC appearance of fresh vs frozen CB sample. Representative of 5 frozen and 7 fresh CB samples. Student t-test was performed (paired between the same CB samples, unpaired between fresh and frozen), P*<0.05 was considered significant.

Figure 4.8A, above, shows the percentage of CD45+ve cells (used in this context as an approximate indication of the total numbers of responders available) in the CB used for CD8 T cells generation. A significant difference between fresh and frozen unselected cells (68.6±3.9 vs 35.8±5.4 respectively, P*0.0003) was detected. A statistically significant difference was also found in fresh CB between selected and unselected samples (68.6±3.9 vs 32.4±4.7, respectively, P*<0.0001). This difference is still present, albeit not significant, in frozen CB (32.3±4.7 for unselected vs 20.3±9 for selected samples, respectively). This evidence seems to suggest a damaging effect of the selection process on the percentage of CD45+ve cells retrieved in the negative fraction, regardless whether the sample had been freeze-thawed. Another important result was the extremely low percentages of CD45+ve cells obtained in these samples (regardless fresh or frozen) after selection; retrieving around 20% from whole frozen-thawed CB after selection meant that often only a few millions cells were available for use. Finally, a relevant point to be considered is that all the data presented in Figure 4.8 refer to the

first thawing only –i.e., when the whole frozen CB sample is thawed for the CD14 selection and DCs differentiation. The CD14-ve fraction then needs to be re-frozen until the DCs are ready to be pulsed, when they are thawed again and finally used. Figure 4.8B shows a representative example of flow cytometry analysis for the CD14-ve samples from fresh and frozen samples, respectively. While in the fresh sample a clear lymphocyte population can be outlined, this is not the case in the frozen one-in fact, cells in this case have an unusual appearance where no lymphocytes, granulocytes or other blood populations can be discerned.

4.3.3.2 MONOCYTES (CD14+VE FRACTION):

While overall low numbers and the effect repeated freeze-thawing procedures were having on the CD14-ve fraction were the main concerns regarding the responders, a viability issue emerged when working with the CD14+ve fraction. Figure 4.9, below, shows the main results obtained when CD14+ve cells were selected from fresh and frozen CB samples.

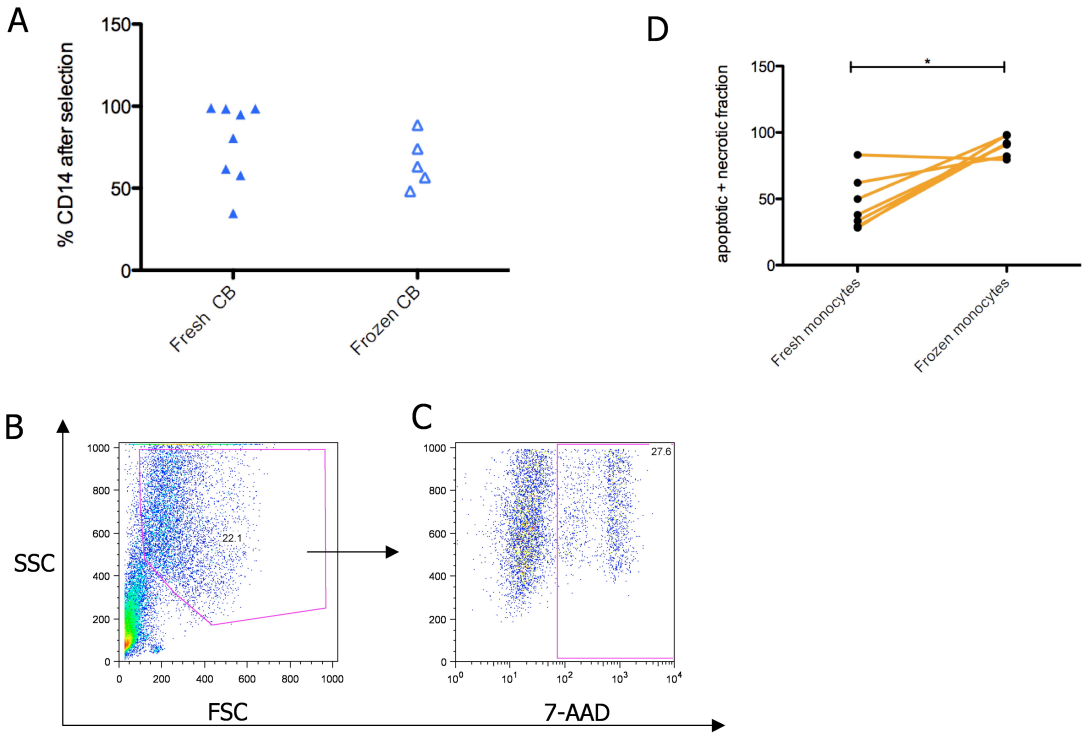

Figure 4.9: analysis of the fresh vs frozen CB samples-CD14+ve fraction. CB samples were selected for CD14 using microbeads. A, The CD14+ve fraction was further analyzed to assess purity of selection (frozen CB N=5, fresh CB N=8). CD14+ve cells from frozen CB, plated out for DCs maturation, were stained with 7-AAD at day 4 to assess their overall viability. B, cells were firstly gated on maturing DCs according to FSC and SSC and C, the 7-AAD+ve cells were quantified within this gate (N=1). D, graph plotting the sum of annexinV+ve 7-AAD-ve (apoptotic) and annexinV+ve 7AAD+ve positive (necrotic) monocytes before and after thawing in a cohort of CB samples from the Anthony Nolan Cell Therapy Centre (courtesy of CB Bank and Dr RC Duggleby). Paired student t-test, P*<0.01; the values are expressed in the text as average ± standard deviation.

Figure 4.9A shows the purity of CD14+ve selection between fresh and frozen CB samples; no significant difference was detected. It was observed that a purity around or above 90% was obtained most often in fresh rather than frozen CB, however this finding might be explained with the relatively small size of both set of samples and in any case even a purity below 80%, as was most often retrieved from frozen samples, did not adversely affect the DCs preparation. Figure 4.9B and 4.9C show the flow cytometry analysis of a differentiating monocyte culture (at day 4 after plating out the monocytes, so one day before DC maturation), showing that in the DCs gate the percentage of 7-AAD+ve cells was around 30%. While this experiment was performed on one CB sample only, at least 2 more DCs cultures showed a similar suboptimal viability (data not shown).

Figure 4.9D (data kindly provided by Dr RC Duggleby and the Anthony Nolan Cell Therapy Centre, Nottingham) shows the percentage of both necrotic and apoptotic monocytes (by CD45high SSChigh phenotype) in a small cohort of CB samples examined fresh and upon thawing. While usually apoptotic (annexinV+ve) and necrotic (7-AAD+ve) cells are kept separate during results evaluation, as they constitute different subsets with different properties, it was decided to group them in a single analysis here as both fractions affect the final percentage of viable monocytes in the culture. While the percentages of necrotic and apoptotic monocytes in fresh CB is quite variable but the average value is still below 50% (46.3±20.3), the same subsets in the same samples after freezing and thawing record an average of 90.3±7.1 of necrotic and apoptotic monocytes, resulting in an overall viability (for the monocytes subset) of around 10%. Of note, the variability range for the thawed samples was much reduced compared to the fresh one, being consistently over 79% vs 28-83% in frozen vs fresh respectively, and the difference in the overall percentage of necrotic and apoptotic cells in fresh and frozen samples was significant (P* was 0.0045). The results presented in Figure 4.9D suggested that, despite viability in monocytes selected from fresh CB being variable but still high enough to support productive DCs generation, the same parameter in frozen-thawed monocytes was not, resulting in possible problems with the use of frozen monocytes for DCs generation.

4.3.3.3 DCs-RESPONDERS CO-CULTURES:

The results shown in Figure 4.8 and 4.9 raised questions about the overall feasibility of a DCs-responder co-culture set up using frozen CB samples as starting material. An annexin staining was performed on the DC-responders co-culture in expansion and Figure 4.10, below, shows the results for this experiment.

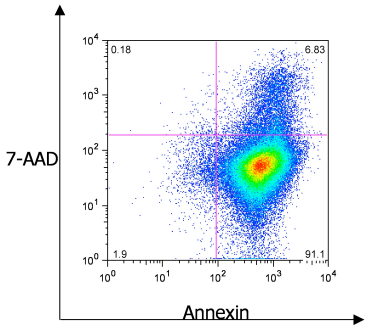

Figure 4.10: viability of a frozen CB-derived DCs-responder culture. Frozen CB-derived, DCs-responder co-culture was stained with annexin V and 7-AAD at day 7 to assess viability. CD45+ve cells were gated and the viability was assessed within this gate (N=1).

As shown above, the percentage of apoptotic (annexin+ve) and necrotic (7-AAD+ve annexinV+ve) cells exceeded 90% in the culture. This experiment was performed only once as it was decided not to establish more DC-CD8 T cells cultures after experiencing the technical issues described above (poor monocyte-DCs viability, low responder numbers and overall appearance upon second thawing, or both). The results described from Figure 4.8 onwards suggested a thorough reassessment of the feasibility of CD8 T cells generation in the system described so far.

4.4 DISCUSSION:

This chapter describes the preparation and characterization of DCs from CB and their use in generating peptide-specific CD8+ve T cells in an autologous system. While the controls and setting up in adults worked as expected and gave consistent positive results, various problems were experienced in the DCs-CD8+ve T cells system in CB, particularly regarding monocytes viability and responder numbers. These issues, together with a comparison of the results obtained in this project with the current literature, will be discussed below.

4.4.1 DCs FROM CB AND THEIR PHENOTYPE:

The choice of CB as source material for this project was logical due to its increasing importance in HSCT. As the immunosuppression required prior each transplant leaves the patient severely immunocompromised and exposed to opportunistic infections, a DLI is often performed. This is even truer in the case of CB transplants, which are characterized by later engraftment compared to adult donors, but in which a DLI is not possible as the whole of the CB is used in transplantation. Adoptive immunotherapy in the form of CD8+ve cells infusion would then constitute a suitable alternative to DLI.

To assess the potential of CB-derived APC and their use for development of an autologous APC-CD8 T cell system, the first step was to select which APC was to be employed. DCs were then chosen, partly because they are *the* professional APCs and the only cell type capable to elicit a full CD4 and CD8-mediated response, from naïve cells. It was decided from the start of the project not to focus on the DCs already differentiated in CB. This was due to their low number, the finding that their viability starts decreasing after CB collection (data not shown) and the difficulty in selecting simultaneously all the subtypes of DCs. The focus was instead on the ones that could be differentiated from precursor populations.

In the literature two approaches for the generation of DCs from precursor populations were reported, one starting from CD34+ve cells (Sato *et al.*, 1998, Kobari *et al.*, 2006 and Balan *et al.*, 2009) and one starting from CD14+ve cells or mononuclear cells selected by plastic adherence (Liu *et al.*, 2001, Bracho *et al.*, 2003 and Hanley *et al.*, 2009). The second approach was selected for two reasons; not only CD14+ve cells are more abundant than CD34+ve in CB blood, but most importantly it is possible to select large numbers of CD14+ve cells from adults without previous treatment, while the CD34+ve cells circulating in healthy adults are negligible. Moreover, the use of CD34+ve cells would have had most likely required an expansion step, thus complicating the whole protocol, while working with CD14 cells was much more straightforward. Initially a plastic adherence step was performed, but as a microbeads

CD14+ve selection resulted in much more consistent and high yield results (data not shown), this option was preferred in all the experiments described in this chapter.

Once DC generation from CB was successfully accomplished, as seen from their DC-like phenotype, their APC potential was assessed. As discussed previously, the state-of-the-art literature on CB-derived DCs seemed quite discordant on this point. Some papers suggested CB-derived DCs were less functional than their adult counterparts, especially in terms of alloreactivity and Th1-skewing/polarizing (Liu *et al.*, 2001, Langrish *et al.*, 2002, Bracho *et al.*, 2003 and Naderi *et al.*, 2009). However, other publications (Salio *et al.*, 2003, Park *et al.*, 2006, and Hanley *et al.*, 2009) reported that CB-derived DCs were able to elicit a Th1-skewed response and CD8 expansion, thus suggesting that DCs of CB origin did not show any functional difference from their adult counterparts and could be as effective as adult DCs.

The results presented in this chapter seemed to be halfway between these two options: on one hand no relevant difference in DC-related marker expression was seen between CB- and adult-derived DCs, however some significant differences in alloreactive proliferation were detected when using DCs of CB origin rather than adult.
In terms of DCs-related markers, it was speculated that the similar level of expression between adult and CB-derived DCs (and especially the expression of CD83, a marker indicative of DCs maturation) was not likely to correlate with a phenotype of tolerogenic DCs; it is, however, not possible to exclude the presence of this subset within the CB-derived cultures presented here (especially since suppression assays were not performed). In fact, if the study of CB-derived DCs were to be continued, a thorough analysis of all molecules of the CD80-CD86 family should be performed on the samples, to elucidate whether their phenotype is more tolerogenic or activatory in the conditions used. Moreover, an unbiased evaluation of their functionality (i.e. CD8 T cell expansion and suppression assay using the same CB sample as DCs source) would be useful to have a definitive assessment of the *in vitro* activity of CB-derived DCs.

In terms of allogeneic proliferation, while the difference in DC-mediated proliferation between the adult and CB samples used in the MLR was statistically significant, it was

reasoned that the degree of proliferation obtained was still high enough to suggest an effective APC activity. Therefore, DC-CD8 T cell antigen-specific cultures were then developed.

4.4.2 ANTIGEN-SPECIFIC SYSTEM:

When selecting a model peptide and a readout technique for the DC-CD8 T cell system described in this chapter, MelanA (also known as Mart-1) and tetramer expansion were chosen, respectively. The preference for this particular antigen, rather than the CMV-derived peptide used in the previous chapter, was driven by two different motivations. While being aware of the relevance that CMV, a classical cause of death following HSCT, has in hematopoietic transplant-related immunotherapy, it was considered that a tumour antigen would have provided a stronger stimulus than CMV in the naïve system employed in this work, and thereby be easier to detect and to interpret. Moreover, there was pre-existent literature describing the expansion of MelanA tetramer+ve cells from CB (described in Salio *et al.*, 2003). Even if a potentially important difference in the experimental set up was the source of CB (fresh for Salio *et al.*, 2003, frozen in this work), it was speculated that for a complex procedure such as antigen-specific CD8 T cells generation from CB, the most practical option was to start from already published protocols. Before starting this project, there were not any published data on the generation of CMV-specific, CB-derived CD8+ve cells. However, in the first months of 2009 Bollard's group published the generation of virus (CMV, EBV and adenovirus)-specific T cells starting from CB in an autologous system and using frozen CB as starting material (Hanley *et al.*, 2009). This publication would have provided an ideal initial protocol for moving onto a CMV system once the preliminary MelanA experiments had been successful. Finally, while tetramers as a preferred choice to judge successful CD8 T cell line generation was probably the most difficult route (due to the low numbers of precursors and consequently the low levels of expansion) they were still considered the most appropriate readout for peptide-specific cells with a prospective use in immunotherapy. However, IFN-γ intracellular staining both in adults (data not shown) and in CB was also set up as a control.

MelanA expression and expansion was assessed in the largest cohort possible of adult donors, i.e. all healthy donors having an HLA-A*0201 allele. Even if a tetramer-specific population was detected in most of them, thus confirming the finding published by Romero's group (Pittet *et al.*, 1999), a MelanA expansion was registered in only one of the donors tested. It is difficult to compare the expansion results obtained in this project with the published reference on this topic, as Romero's team first sorted the HLA-A*0201-tetramer+ve cells using FACS and then expanded the positive fraction with a strong protocol including cytokine, PHA and autologous irradiated fraction (Pittet *et al.*, 1999), reaching around 10% of tetramer+ve cells after 15 days of expansion. Such a relatively moderate amount of tetramer+ve cells after 2 weeks of strong stimulation in healthy adults donors suggested that the level of expansion in the adult samples examined in this work could have also been lower. As such, the expansion detected in the adult donor was considered successful. Moreover, if not all healthy HLA-A*0201+ve donors are able to expand a MelanA-specific population, a small number of samples can influence the total number of expansions obtained due to stochastic effects. Finally, if such low expansion levels were detected in adults, it was speculated that in CB they would have probably reach even lower levels. Salio *et al.*, 2003, published a percentage of tetramer+ve cells of around 2% after expansion (starting from <0.1% on average in resting CB) so this value was taken as reference. When the MelanA DC-responder system was set up according to Salio *et al.*, 2003, the MelanA-specific CD8 T cells levels did not match the published results (data not shown). This might have been due to the stimulation conditions, that needed to be stronger -i.e., repeated administration of peptide, increased amount of cytokines in the culture, or repeated rounds of DC-peptide presentation- or to unpredictable effects such as the starting number of tetramer+ve cells being too low to support a successful expansion in the CB samples examined. Before repeating the experiment to optimize the expansion conditions, however, viability issues when using frozen CB samples to set up the culture were detected.

4.4.3 VIABILITY AND OTHER LIMITATIONS:

The decision to choose a peptide-specific system meant that only HLA-A*0201+ve CB samples could be used and that each CB available should be typed to detect if it was suitable for use. To effectively mimic the CB samples used in clinical settings, frozen samples were used in this project. Out of the 10 samples tested, 6 were HLA-A2 positive, 3 negative and one showed signs of maternal blood contamination and was, therefore, discarded (data not shown).

When the selection of monocytes from the CD14+ve fraction was performed, low viability, both at selection and during the DCs differentiation, was experienced. In fact, of all the 4/5 frozen CB examined, only one had overall good monocyte/DCs viability. More precisely, while DCs generation was achieved more than once when using frozen CMBCs as starting material, only from one sample was possible to freeze an aliquot of monocytes and, after thawing, use them to successfully prepare DCs (as would have been required for a second DC-mediated stimulation of the expanding CD8 T cells). It has to be stressed that monocyte viability was generally low upon thawing, while this was not necessarily the case with fresh samples; as such, it was impossible using the viability data from the fresh sample to predict the outcome after thawing.

On the other hand, there were issues also when using the CD14-ve or responders fraction, as the overall number of cells available was sometimes very low after thawing and selection. Moreover, all the results shown in this chapter refer to cells that were then re-frozen to be re-thawed when the cultured DCs became available. Even if CD45 staining was not performed on this second occasion, it is conceivable that the percentages would have been even lower- indeed, it was possible to set up a DC-CD8 T cell culture only from one of the frozen samples used. The two issues described above - the poor monocyte viability and the low number of CD45+ve cells in the responder fraction- suggested a reassessment for the whole approach to antigen-specific CD8 T cells generation. The analysis and evaluation of viability for various cell types within the frozen CB cohort is object of active investigation by various members of the group.

As for the MelanA-specific response elicited in the CB system, it was not possible to detect a convincing tetramer-specific expansion in the samples tested, thus indicating that future experiments would need to address stimulation conditions. However, a moderate IFN-γ secretion was detected in the CD8 subset, suggesting that a certain degree of CD8 activation is promoted by the actual culture conditions.

4.5 FUTURE EXPERIMENTS:

The easiest way to solve the viability issues described in this chapter would be the use of fresh, rather than frozen, CB. An alternative option would be to divert some blood at collection for CD14+ve selection and DC generation, freeze the rest and use the frozen aliquot as responders. However, against both these solutions is the consideration that fresh CB samples are not the best match for clinical transplantation-frozen CB is. Therefore, every effort should be devoted to optimize the culture conditions in frozen samples.

A straightforward way to reduce the need for freeze-thawing procedures would be to freeze the CB sample as currently done, saving, however, at this stage an aliquot for HLA typing (15-20 X 10^6 cells would be enough). This would prevent the need to use the 5-ml segment of the frozen CB for this operation, as it had to be done in this project; one would prepare DCs from this aliquot, discard the CD14-ve fraction at this stage, and use the 20-ml section as and when required as responders. This would not likely solve the monocyte viability issue, but should help avoid low responder numbers affecting the outcome of the expansion. To solve the monocyte issues, one could envisage two possible routes: either give priority to monocytes/DCs as APC, and as such try every possible strategy to optimize viability, or go for another type of APC. In the first case, all the viability data available (as generated by Dr RC Duggleby and the Anthony Nolan Cell Therapy Centre) should be analysed to select only CB with exceptionally high monocyte viability at fresh. Even better, if it emerged that a correlation between viability upon thawing and any other of the parameters analysed these informations should be used too. In the second case, the best candidate would

probably be a B-LCL cell line. Lymphoblastoid cell lines offer some advantages; they are more robust than DCs, while still exerting a reasonable antigen presenting activity and crucially, they can be expanded to high numbers. B-LCL generation from frozen CB was attempted but difficulties were experienced in establishing a self-replicating cell line (data not shown); however, once a CB-specific protocol is established, this should be a viable and reasonably easy option. In fact, as Bollard's group used B-LCL in conjunction with DCs for subsequent stimulation following DCs priming (Hanley *et al.*, 2009) it would be worth generating B-LCL even when DCs are used as the primary APC, as B-LCL could provide a good restimulation tool.

The readout system employed could also be modified. While tetramers are a relatively difficult option, due to their high specificity, they should still be included in the protocol as they are possibly the most sensitive readout of antigen-specific CD8 T cells generation. In addition to tetramer+ve assessment and IFN-γ intracellular staining, an attractive choice would then be ELIspot in response to MelanA peptide, as done by Hanley *et al.*, 2009. While this approach would arguably require some optimization prior its use in CB samples, it would then present the great advantage of requiring a low number of cells for its setting up, thus enabling the testing of more stimulation conditions (such as different amount of peptide) even with small samples.

CHAPTER 5:
CHARACTERISATION OF CB-DERIVED γδ T CELLS AND COMPARISON TO THEIR ADULT HOMOLOGUES

5.1 INTRODUCTION:

The aim of this project was to generate and characterise antigen-presenting systems that could be used in immunotherapy. After the assessment of the liposome-based artificial antigen presenting cell (aAPC) system, it was decided to expand the analysis of the antigen presenting cell potential of cord blood (CB)-derived cell populations. CB-derived dendritic cells (DCs) were evaluated first but other CB-derived cells with APC potential were also considered for examination and the focus was on γδ T cells. The main γδ T cell subpopulation in adults, called Vγ9Vδ2 cells from the TCR sub-chains they express, has been recently shown to possess robust APC activity *in vitro* both in human (Brandes *et al.*, 2005, Moser *et al.*, 2006 and Brandes *et al.*, 2009) and animal (bovine, Collins *et al.*, 1998 and murine, Cheng *et al.*, 2008) models. These could then, potentially, replace CB-derived DCs in the absence of a viable monocyte population.

Moser's group (Brandes *et al.*, 2005) reported that freshly isolated γδ T cells (from tonsil) expressed HLA-DR, CD80, CD86, as did IPP-expanded, but not resting, peripheral blood-derived Vδ2+ve γδ T cells. More functional-based evidence was published by Sun's group (Cheng *et al.*, 2008), who showed antigen-specific proliferation of T cells following incubation with purified γδ T cells from the spleen and lymph nodes in mice. Recently, Brandes *et al.*, 2009, described that peripheral adult blood-derived γδ were able to cross-present soluble antigen to CD8 αβ T cells. Moreover, robust proliferation was obtained from naïve CD8 αβ T cells when using γδ T cells as stimulators. The evidence that γδ T cells can act as APCs was reinforced by Pistoia's group (Prigione *et al.*, 2009) when they published that Vδ2+ve cells pulsed with a *C. albicans* antigen promoted autologous CD4 T cell proliferation. Since these results suggest that γδ T cells can support a naïve T cell response in mice and adult humans it was, therefore, decided to investigate the APC potential of CB-derived γδ T cells.

The published literature for CB-derived γδ T cells is relatively scarce and focuses mostly on phenotypical characterisation and analysis of their cytotoxic/effector potential. One of the first papers describing γδ T cells in CB was Morita *et al.*, analysing the differences in Vγ and Vδ chain combinations between CB and adult samples and noting their reduced cytotoxicity when compared to adult (Morita *et al.*, 1994). Musha *et al.* described CB-derived γδ T cell expansion *in vitro* and reported a low percentage of Vγ+ve cells in CB even after expansion, in stark contrast with the results obtained in adults (Musha *et al.*, 1998). In 2005 Engelmann *et al.* studied the modulation of the immune response to *P. falciparum* during pregnancy and reported a higher percentage of CB-derived γδ T cells expressing CD25 and CD69 in samples treated for malarial infection during pregnancy compared to the control groups (placental infection at delivery and non-infected cohorts; Engelmann *et al.*, 2005). One year later the same group compared the phenotype of CB-derived γδ T cells with γδ T cells of maternal origin and found a decreased expression of HLA-DR, perforin and granzyme B, both *ex vivo* and following PMA/ionomycin stimulation, in the lymphocytes of CB origin (Engelmann *et al.*, 2006). Cairo *et al.* examined the responsiveness of CB-derived Vδ2+ve γδ T cells to either a phosphoantigen (pamidronate) or live BCG, reporting that as their naïve phenotype was rapidly changed to an effector one this suggested that γδ T cells are important responders to microbial infections in early life (Cairo *et al.*, 2008). Finally, Campos Alberto *et al.* characterised the IFN-γ secretion by CB-derived Vγ9+ve γδ T cells when stimulated with their specific ligand IPP and exogenous costimulatory cytokines (TNF-α and IL-12) (Campos Alberto *et al.*, 2009). CB-derived γδ T cells therefore, exist, although perhaps with some functional differences to adult cells, but prior to this study had not been assessed for APC function.

5.2 EXPERIMENTAL AIMS:

The work described in this chapter aims to assess the APC potential of the γδ T cell population in CB. In parallel, it was investigated whether there were any major

differences in terms of viability, numbers, and phenotype (HLA-DR, costimulatory markers, Vγ9 and Vδ2 chain repertoire) between γδ T cells derived from fresh and frozen CBMCs. While the main attention was on the CB phenotype, experiments assessing APC potential of γδ in adults were also carried out. The work described below was performed on healthy adult donor peripheral blood samples and compared with both fresh and frozen CB samples.

5.3 RESULTS:

5.3.1 CB γδ T CELL SELECTION AND KINETICS OF EXPANSION:

The first experiments were aimed at evaluating the overall percentage of γδ T cells present in the various types of samples (fresh adult PBMCs and fresh/frozen CBMCs) and, after this preliminary assessment, to determine what were the best options to be able to work with as pure a γδ T cell population as possible.

Figure 5.1, below, describes the percentages of γδ T cells at day 0 in CB (fresh and frozen) and adult peripheral blood samples, together with a representative example of the flow cytometry analysis at day 0 in both adult and CB.

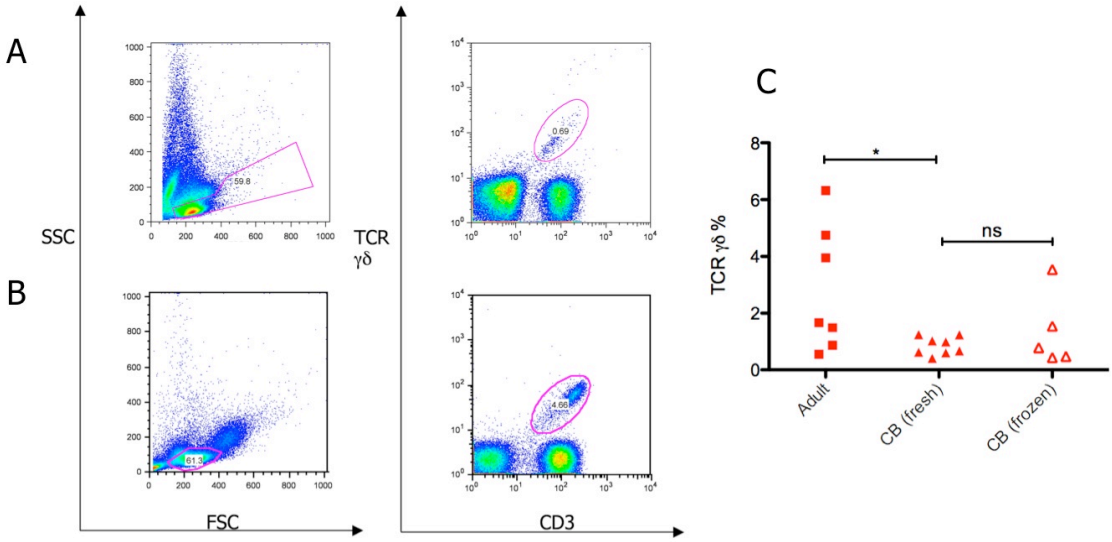

Figure 5.1: **flow cytometry analysis of γδ T cells at day 0, in adult and cord blood samples.** The lymphocyte population was selected according to FSC and SSC and within this gate the CD3+ve γδ+ve population was highlighted (A, frozen CB, B, fresh adult peripheral blood). C, γδ+ve percentage in all three set of samples. The student t-test was used (*P<0.05) and the relevant percentages are reported in the text as average ± standard deviation. Frozen CB N=5, fresh CB N=8, adult peripheral blood N= 7.

Figure 5.1A and 5.1B show the percentage of γδ T cells in representative unselected and untreated PBMCs (for adults) and CBMCs (for CB). 2.8±2.2% of the lymphocytes, in adult PBMCs, were γδ T cells whilst there was a significantly lower proportion in CB (1.3±0.6 and 0.8±0.1 for frozen and fresh CB respectively; Figure 5.1C). These findings are in line with the literature, which reports 1-5% of γδ T cells on the total lymphocytes in adults and significantly less in cord blood.

Of note, while the percentages of γδ T cells in fresh CB samples, and to a lesser degree in frozen ones, were quite similar, this was not the case for adults. In fact, it seemed that the γδ+ve T cell distribution in the adult samples under examination formed two populations; either <2% or 4% and above. The differences in γδ T cell percentages were significant between adult vs fresh CB samples but not between fresh vs frozen CB samples, suggesting that the freeze-thawing process did not have a significant impact on the percentage of γδ T cells in CB.

The principal aim of this chapter was to assess the antigen presenting potential of CB-derived γδ T cells. To achieve this, the ideal starting point would have been a pure γδ T cell population, to prevent any contamination from other cell types with professional antigen presentation functionality, such as B cells and monocytes, that might affect the results. Therefore, the possibility to select γδ T cells using a positive selection microbead kit (MILTENYI), from unexpanded PBMCs or CBMCs (i.e. immediately after ficoll or thawing) was explored. Figure 5.2, below, shows the purity obtained after TCRγδ positive selection with (5.2B) and without (5.2A) prior expansion.

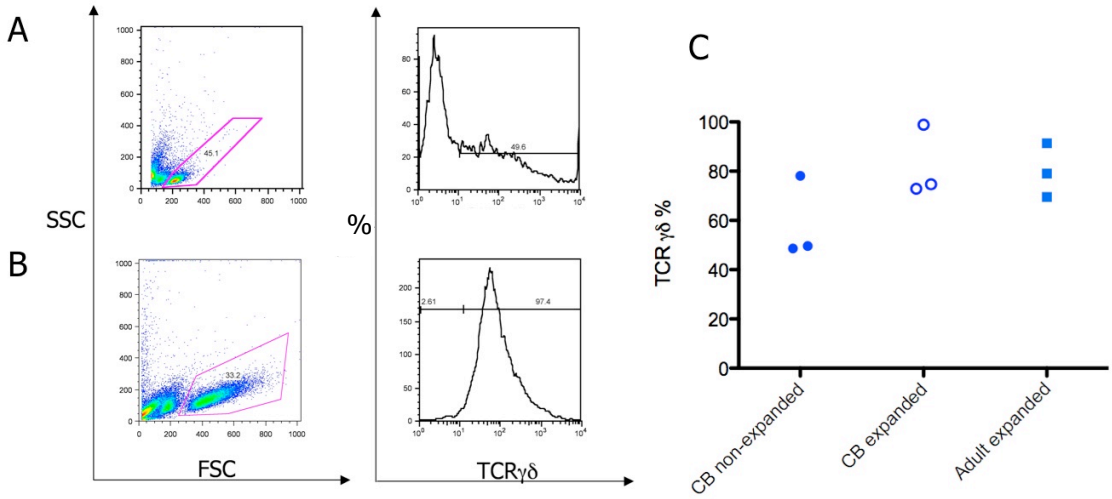

Figure 5.2: **flow cytometry analysis of γδ selection.** After microbeads selection, the lymphocyte population was gated according to FSC and SSC and the γδ+ve fraction was analysed within the lymphocyte gate (histograms). A, unexpanded and B, expanded CB sample. C, graph of γδ T cell purity after selection for CB and adult peripheral blood. Expanded and unexpanded CB and expanded adult peripheral blood N=3.

Figure 5.2A shows a typical selection from non-expanded CB samples and, as highlighted in the histogram, a purity of approx. 50% γδ T cells was observed for the positive fraction (a mean of 58.8±9.7% γδ T cells of lymphocytes was achieved from 3 unexpanded CB samples). Moreover, the yield of γδ T cells was extremely low for CB samples, in all cases ranging from 1-6 X 10^5 cells from whole cord blood samples (average size, 60-100 X 10^6 CBMCs) and in all cases less than expected judging from the percentage of γδ T cells present in any given CB sample (the maximum recovery of

γδ T cells was 50%). Overall, positive γδ T cell selection from non-expanded samples resulted in low yield and low purity.

Consequently, a γδ T cell expansion system was developed. Expansion of CBMCs and PBMCs was carried out in presence of 1000IU/ml of IL-2 immediately after ficoll/thawing. The initial percentage of γδ T cells was assessed at day 0, thereafter all the samples were assessed by flow cytometry at day 7 and day 14, while day 21 was maintained for frozen samples only (see Figure 5.3A-C). Cell expansion was carried out with the two objectives of expanding γδ T cells to ideally a minimum of 10-20% percentage of the total cell culture and to identify the optimal time point for microbead selection. Following this approach, Figure 5.2B shows a typical selection from expanded samples, where a much better purity was achieved in all cases (a mean of 82.2±8.3% and 80±6.3% γδ T cells of lymphocytes from expanded CB and adult samples, respectively; Figure 5.2C). Figure 5.2C summarises the γδ T cell selections in expanded and non-expanded samples, with a trend towards better purity when using expanded samples being observed, although statistical significance was not achieved with 3 samples.

Figure 5.3A-C, below, shows the kinetics of expansion for all the types of samples tested, while Figure 5.3D presents the graph for γδ T cells numbers in the frozen CB samples' group and Figure 5.3E shows the overall frozen CMBCs numbers across the expansion.

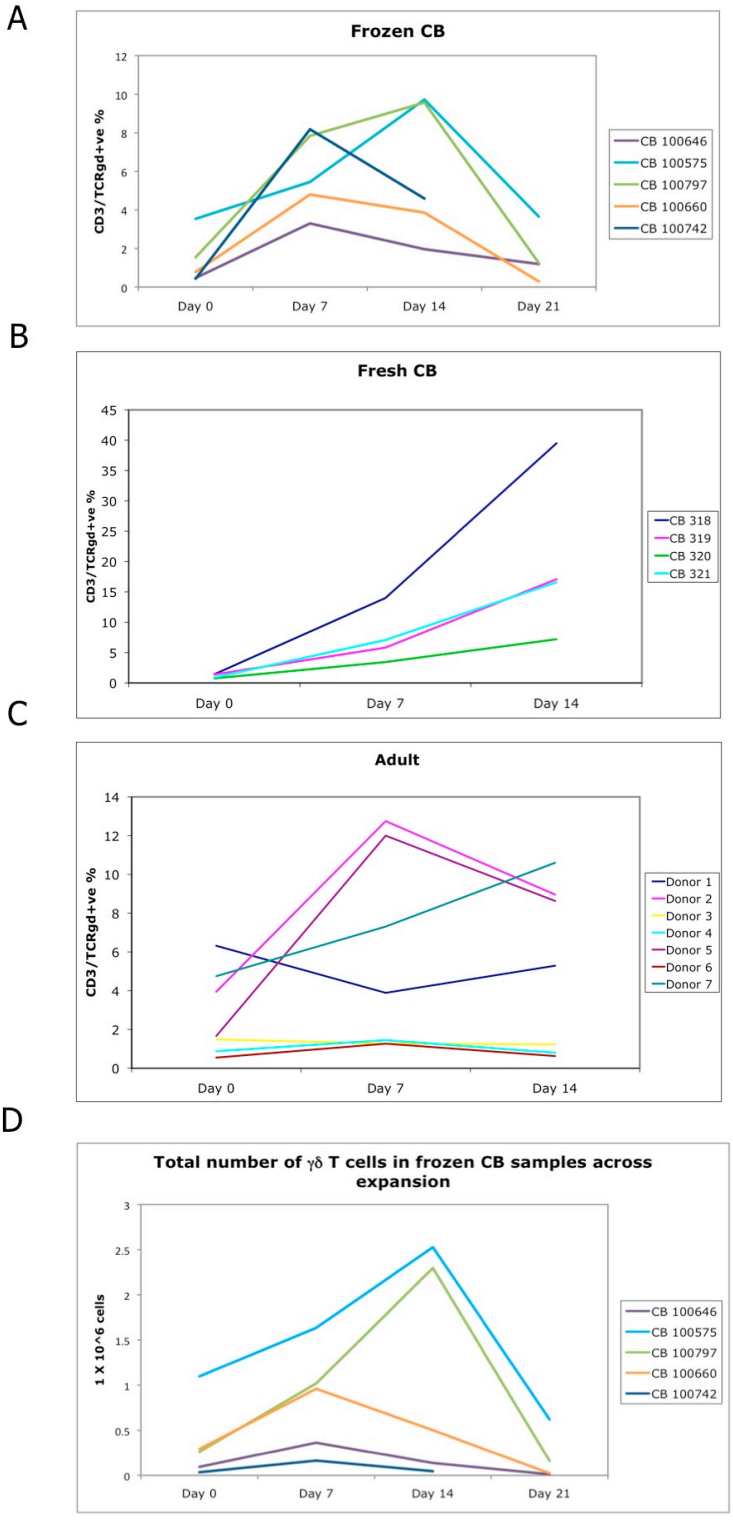

Figure 5.3A-D: kinetics of TCRγδ expansion from adult peripheral blood and CB samples and example of total number of cells during expansion. A, frozen CB, B, fresh CB and C, adult peripheral blood TCRγδ expansion over 2-3 weeks (the TCRγδ+ve population within the lymphocyte gate is plotted in the graphs above; frozen CB N=5, fresh CB N=4, adult peripheral blood N=7). D, Total number of TCRγδ+ve cells in the frozen samples across the 3-weeks expansion (N=5). All the data reported in the text are expressed as average ± standard deviation.

E

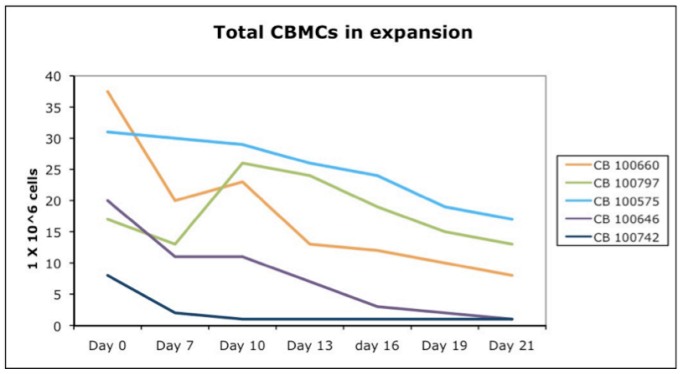

Figure 5.3E: total CBMCs over 3 weeks of TCRγδ expansion. N=5 frozen CB samples.

Figure 5.3A-C, above, shows the kinetics of γδ T cell expansion in IL-2- expanded CB and adult samples cultures. At day 7, the percentage of γδ T cells was 7.6±4.5% and 5.9±0.02% of gated lymphocytes in fresh and frozen CB samples and 5.7±5% in adults (while at day 0 these values were 1.11±0.34%, 1.35±0.01% and 2.8±2.2% respectively). At day 14, γδ T cells constituted 20.1±13.7% and 5.9±0.03% of the culture of fresh and frozen CBMCs respectively and 5.2±4.3% of the culture in adult PBMCs. For frozen samples only, the total number of γδ T cells in culture was followed as well, as shown in Figure 5.3D; three CB samples (CB 100646, 100660 and 100742) reached their highest number of γδ T cells at day 7 (range 1.63-9.6 X 10^5 cells), whilst in the other two CB samples (100575 and CB 100797) the maximum amount of γδ T cells was reached at day 14 (range 2.29-2.57 X 10^6 cells).

The results shown in Figure 5.3A-D suggested some preliminary conclusions. Firstly, the best moment for microbead selection (when the percentage of γδ T cells is highest) varied drastically according to the sample considered. In all frozen CB samples the highest γδ T cell proportion was clearly reached between day 7 and 14, as is in 6/7 adults donors. However, all the fresh CB cultures reached the highest percentage of γδ T cells at day 14. Adult PBMCs showed different kinetics of γδ T cell expansion compared to both fresh and frozen CB samples. Some of the adult samples (donors 3, 4, 6) maintained their initial low percentage (<2%) of γδ T cells throughout the expansion.

Whilst donors 2 and 5 showed expansion, donor 1 showed a slight decrease at week one, and then remained constant. 1 sample (donor 7) showed a clear expansion even after week two, when all cultures were stopped, much resembling the kinetics of fresh CB samples. Of the cultures, only one went above 10% γδ T cells for frozen CB whilst 15% was the best achieved for adult and fresh CB. The fresh CB sample 318 was a clear exception, but it was also the only sample among all the tested ones that showed such a remarkable expansion (>40% TCRγδ+ve cell after two weeks' expansion). In terms of total cell numbers in culture, Figure 5.3E shows a trend of constant and progressive decrease down to a very low total cell number for frozen CB samples. The same pattern was observed also in all but one of the fresh CB samples; CB 318 was again the exception to this decrease as its cell number and γδ T cells' percentage kept increasing until the culture was stopped.

To summarise these results, the data showed that the expansion of frozen CB and adult samples was quite variable and that the highest percentage of γδ T cells (around 10-12%) was usually reached between day 7 and 14. Fresh CB samples, instead, had a more homogeneous trend resulting in a continuous expansion and potentially reached higher percentages of γδ T cells (up to 40% in a single case).

5.3.2 CB γδ T CELL VIABILITY:

In addition to the overall γδ T cell expansion, the viability of the γδ T cells was also analysed during the expansion by co-staining γδ T cells with 7-AAD. Figure 5.4A and B, below, report the amount of γδ, 7-AAD double positive cells for frozen CB samples during the expansion (5.4A) and their percentage of the whole γδ T cell population (5.4B), while figure 5.4C shows a representative example of flow cytometry analysis for the incidence of cell death among the γδ+ve cell population during the expansion.

A

	1 week	2 weeks	3 weeks
CB 100660	0.22	0.95	1.42
CB 100575	0.7	1.45	1.27
CB 100797	0.52	2.74	2.81
CB 100646	0.31	1.74	1.42

B

	1 week	2 weeks	3 weeks
CB 100660	2.43	6.53	6.31
CB 100575	2.33	15.28	4.21
CB 100797	4.40	9.09	12.60
CB 100646	2.58	7.75	4.91

C

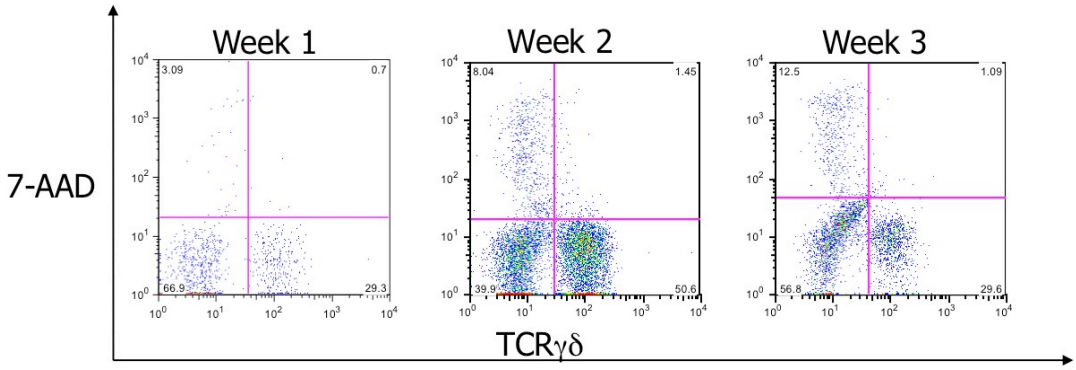

Figure 5.4: γδ T cells viability during expansion. A, table showing the values of γδ 7-AAD double +ve cells over the expansion and B, table showing the same parameter as percentage of 7-AAD+ve cells on the whole of the γδ+ve population. C. Flow cytometric analysis of the viability of the γδ T cell population. Shown is the labelling for TCRγδ and 7-AAD of events gated for lymphocytes and CD3 events. The flow cytometry results shown above are representative of N=4 independent experiments.

At no point during the expansion were a large proportion of γδ+ve 7-AAD+ve cells detected (figure 5.4B). Even after 3 weeks the majority of the γδ T cell population expanded from frozen CB samples remained 7-AAD-ve; the highest percentage of 7-AAD+ve cells of the γδ T cell population was approximately 15%, in CB 100575. However, the proportion of γδ+ve 7-AAD+ve cells increased in all the samples examined over the 3-week expansion (see Figure 5.4B). This finding, coupled with the decrease in cell number in the CB samples shown in Figure 5.3E and the decrease in γδ T cell percentage/numbers at day 21 (Figure 5.3A-5.3D), suggested that between day 7 and 21 there has been an overall reduction in the viability and absolute numbers of γδ+ve T cells in culture. These findings should be considered before setting up any new γδ+ve T cells expansion; the duration of the culture should be shortened in most cases, at least in frozen CB samples, and both viability and cell numbers should be used to determine when to stop an expansion to select the γδ+ve population.

5.3.3 CB γδ T CELL PHENOTYPE:

5.3.3.1 COSTIMULATORY PHENOTYPE:

During the γδ T cell expansion, a full characterisation for molecules relevant for antigen presentation (HLA-DR, CD80, CD86) was performed from week 1 onwards. The same characterisation at day 0 was not carried out, as the low γδ T cell number in the CB samples made a reliable staining impractical.

Figure 5.5, below, shows a representative flow cytometry analysis for each of the time points examined (adult and frozen CB samples only). TCRγδ+ve HLA-DR+ve cells are shown in Figure 5.5A, TCRγδ+ve CD80+ve cells in Figure 5.5B and TCRγδ+ve CD86+ve cells in Figure 5.5C. Flow cytometry analysis is shown at week one (left) and at week two (right).

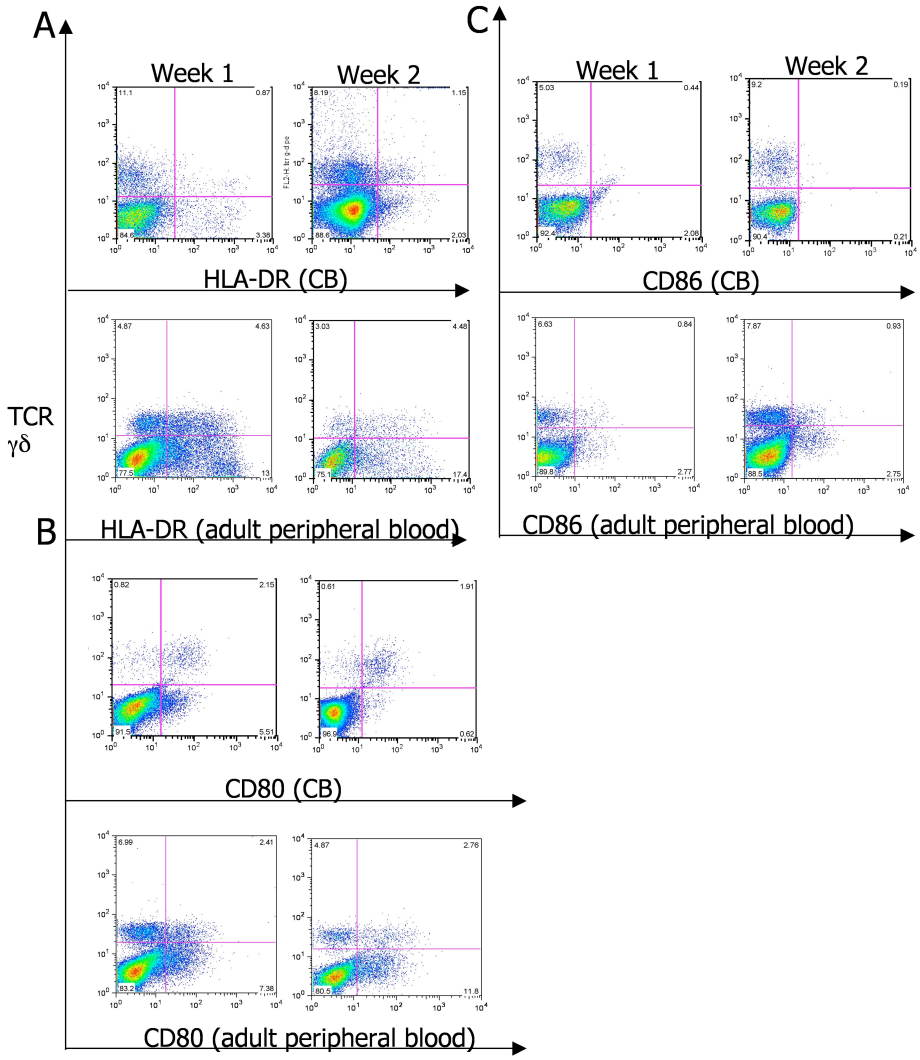

Figure 5.5: flow cytometry analysis during expansion. During expansion, the expression of APC-related markers was analysed in all set of samples. Cells were gated on lymphocytes, then the relevant markers (HLA-DR (A), CD80 (B) and CD86 (C)) were plotted against TCRγδ. The samples shown above are representative of 7 adult PBMCs samples and 4 (at week one)/5 (at week two) frozen CB samples.

As seen above, where a flow cytometry analysis from both a representative frozen CB and an adult sample is depicted, a TCRγδ+ve population is clearly present at all time points, however the co-expression with HLA-DR and co-stimulatory markers changes according to the type of sample and to the time point examined. While both HLA-DR and CD86 appear to be more co-expressed in adult TCRγδ+ve than in the same CB subset, the opposite is true for CD80 in the examples above. Figures 5.6 and 5.7 describe a fuller analysis of the TCRγδ+ve surface marker expression for the whole

group of samples (Figure 5.7), including the analysis of the MFI for each marker within the TCRγδ+ve population (Figure 5.6).

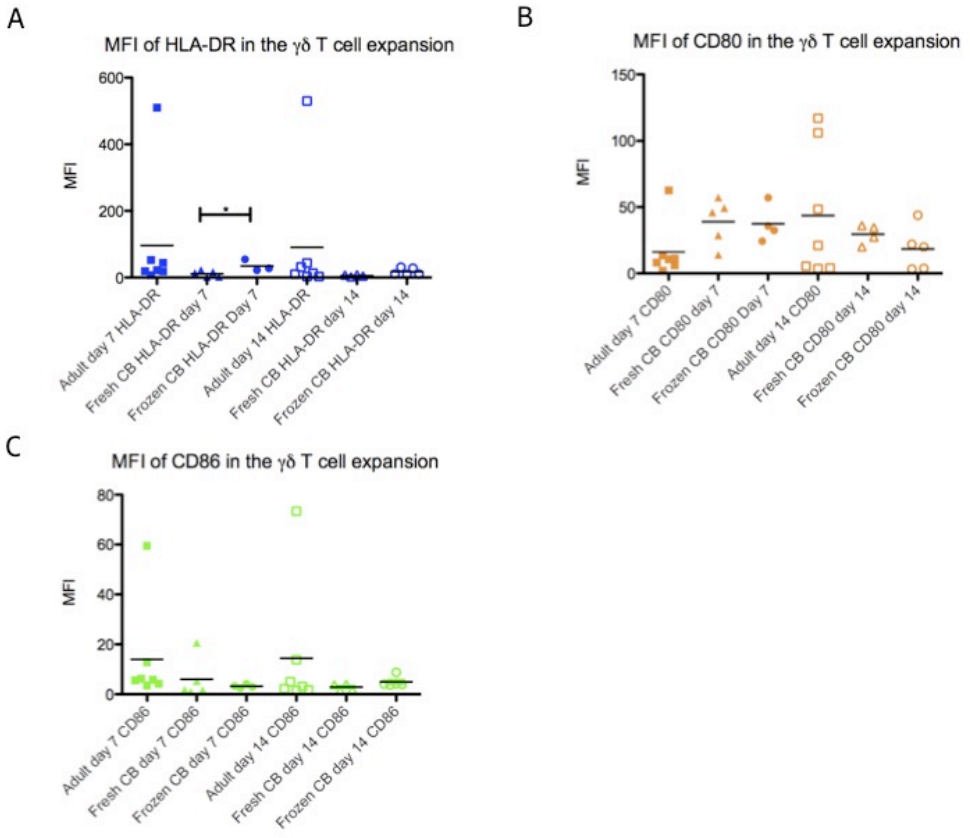

Figure 5.6: MFI analysis of HLA-DR, CD80 and CD86 within the TCRγδ+ve population. During expansion, the expression of APC-related markers was analysed in all the samples available at week 1 and 2. The plots above show the MFI for HLA-DR (A), CD80 (B) and CD86 (C) within the TCRγδ+ve population; the mean for each set of samples is shown as a black bar. The student t-test was used to analyse all the results presented above; values of *P<0.05 were considered significant and the MFI values are presented in the text as average of all the results for a specific marker/timepoint ± standard deviation. Adult samples N=7; fresh CB N=5 at day 7 and N=4 at day 14; frozen CB N=4 at day 7 (except for HLA-DR where N=3 due to a staining problem with one sample) and N=5 at day 14.

All the results shown above in Figure 5.6 were analysed using a student t-test; the paired t-test was used to compare the same subsets across the expansion, while the unpaired t-test was employed when comparing different subsets (for example, frozen CB samples and adult samples). Only the statistically significant results were shown in the figure. As a general conclusion, Figure 5.6 showed there was no significant

difference between the MFI values of CB and adults samples for any the markers used at any time point. There was, however, a significant difference (P=0.04) between the MFI of HLA-DR in fresh and frozen CB samples at week one.

The MFI values for each marker were examined separately, starting with HLA-DR. This is the most important marker among the ones examined as CD4 cells are HLA class II-restricted i.e, they only recognise peptides presented on HLA class II. The expression of HLA class II on a potential APC is fundamental, as without it CD4 T cells will never receive signal 1 activation. A double +ve (HLA-DR+ve TCRγδ+ve) population was observed in all samples at all time points, as seen in Figure 5.5A; differences in MFI between the various subsets were observed but they did not reach statistical relevance except in the case mentioned above (fresh vs frozen CB samples at week one). However, this is likely due to the small number of samples examined (especially for frozen CB); ideally, a larger number of CB samples would need to be examined for MFI of HLA-DR labelling while in expansion, to assess whether the difference seen in this work is genuinely dependent on the freeze-thaw status. At week one, TCRγδ+ve cells of adult origin had, on average, higher MFI values for labelling of HLA-DR than the equivalent cells in CB (96±69 in adults and 11±3 and 35±10 in fresh and frozen CB samples, respectively). The same trend was maintained at week two (MFI values were 90±70, 6±1.5 and 18±5 for adult, fresh and frozen CB sample respectively).

For CD80, a double +ve (CD80+ve TCRγδ+ve) population was present in all samples at all time points examined and the trend for this marker was slightly different from the one observed for HLA-DR. At week one, the MFI value for CD80 labelling within the TCRγδ+ve population of adult origin was minor than the same value in fresh and frozen CB samples, albeit not significantly (P*0.06, MFI values 16±8 vs 39±8 and 37±7, respectively). This trend was not maintained at week two, where the MFI for adult samples was higher than the same value for either fresh or frozen CB samples, (44±18 in adults versus 30±4 and 16±7 in fresh and frozen CB samples respectively).

In the case of CD86 a double +ve (CD86+ve TCRγδ+ve) population is present in all samples at all time points examined. The level of expression for this marker, as measured from MFI, was quite modest compared to HLA-DR and CD80, especially in CB samples. Both at week one and two the MFI for adult samples is slightly higher than the same value in CB samples, regardless fresh or frozen; moreover, the MFI of CD86 labelling in adult samples is very similar between week one and two (14±8 and 14±10 respectively). At week one the MFI of fresh CB samples is slightly higher than the same value in frozen CB samples, while the opposite is seen at week two. Overall, these results might suggest that adult cells express more markers of signal 1 (HLA-DR) and signal 2 (CD80 and CD86) of antigen presentation than the equivalent population in cord blood.

In addition to the MFI, the extent of co-expression of TCRγδ and HLA-DR, CD80 and CD86 was also examined. Figure 5.7, below, presents a plot of all the results summarised in Figure 5.5 and shows the percentages of TCRγδ+ve expressing HLA-DR+ve (5.7A), CD80+ve (5.7B) and CD86+ve cells (5.7C) at week one (on the left) and at week two (on the right).

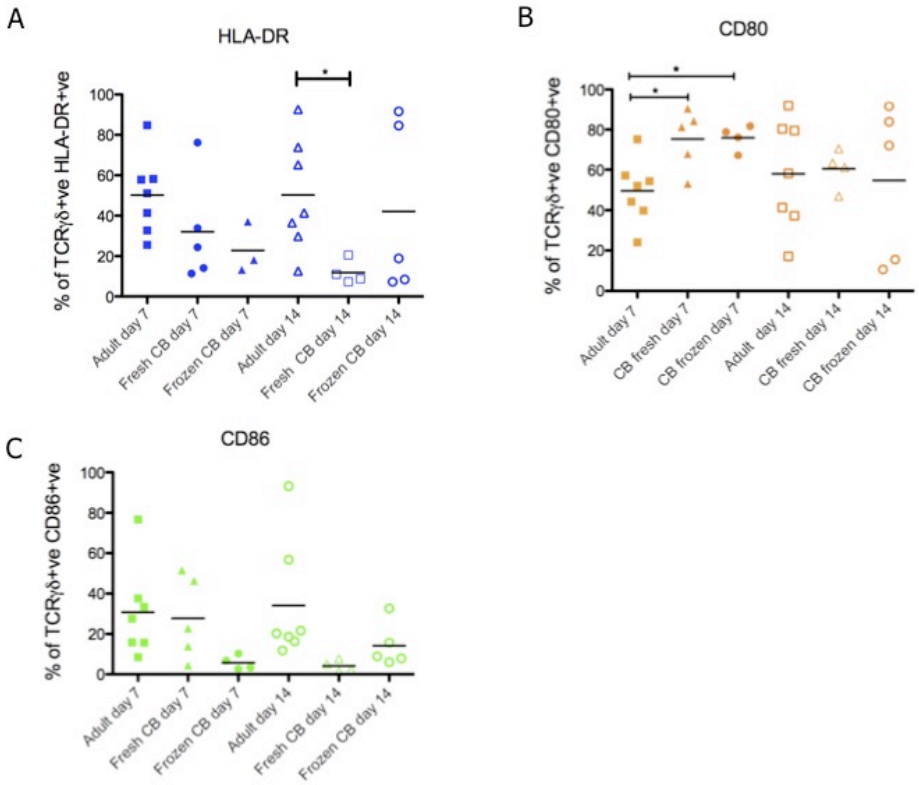

Figure 5.7: TCRγδ+ve cells phenotype during expansion. During expansion, the expression of APC-related markers was analysed for all the different conditions tested, at week one and two. The plots show the percentage of TCRγδ+ve cells expressing HLA-DR (A), CD80 (B) and CD86 (C), the mean for each set of samples is shown as a black bar. The student t-test was used to analyse the results and values of *P<0.05 were considered significant; percentages are presented in the text as average ± standard deviation. Adult samples N=7; frozen CB N=4 at day 7 (except for HLA-DR where N=3, as seen in Figure 5.6) and N=5 at day 14; fresh CB N=5 at day 7 and N=4 at day 14.

As seen for Figure 5.6, all the results shown above in Figure 5.7 were analysed using a student t-test; the paired t-test was used to compare the same subsets across the expansion, while the unpaired t-test was employed when comparing different subsets (for example, frozen CB samples and adult samples). Only the statistically significant results were shown in the figure. As general conclusion, Figure 5.7 showed that there is no significant difference between fresh and frozen CB samples for any of the markers examined at any of the time points considered. There were, however, differences in the expression of APC-related markers between adult and CB γδ T cells.

The phenotype of each of the three markers was examined separately, starting with HLA-DR. Within the TCRγδ+ve population, a reasonable HLA-DR+ve expression was

observed in the adult samples-50.2±7.4% at week one, 50.3±10.5% at week two, where the double +ve seemed to have split between a high and low HLA-DR population (either >60% or 40% and less as seen in Figure 5.7A, fourth column on the right). Within the TCRγδ+ve population, HLA-DR expression was significantly less in fresh CB samples than in adults at week two (11.9±3% in fresh CB samples vs 50.3±10.5% in adults, P*0.0261).

Within the TCRγδ+ve population, significantly more cells were expressing CD80 in CB (75.3±6.7% and 76±3% in fresh and frozen CB; P*0.0176 and 0.0122 respectively) than in adult samples at week one (49.5±6%). The same trend was also observed when examining the MFI for the same samples (see Figure 5.6B), even if in that case the difference was not significant. At week two, CD80 expression was generally maintained within the TCRγδ+ve population but the expression was more widespread and there were samples (both in adult and frozen CB samples) that had a large decrease in the percentage of CD80+ve cells (from around 80% to less than 20% in frozen CB samples). Moreover, at week two there was no significant difference in CD80 expression within the TCRγδ+ve population in any of the set of samples examined.

In the case of CD86 there was no significant difference in CD86 expression within the TCRγδ+ve population in any of the samples examined at any time point. At both weeks one and two CD86 expression was more noticeable in adult samples than in either CB subset. In particular, at week two the expression of CD86 within the TCRγδ+ve population in fresh and frozen CB was low (in both cases inferior to 20% on average); in this case as well the trend of coexpression of CD86 and TCRγδ mirrored the results obtained from MFI analysis (see Figure 5.6C), both in terms of low overall values and CB-adults ratio.

To summarise the phenotypic analysis performed so far, PBMCs-derived, IL-2 expanded γδ T cells express HLA-DR, CD80 and CD86 as reported in literature. CBMCs-derived, IL-2 expanded γδ T cells show as well the presence of APC-related

markers, even if their level of expression differs from their adult counterparts; in particular, the MFI for all three markers tends to be lower in CB than in adults samples (with the relevant exception of CD80 at week one) and had low values for CD86. The expression of the markers of interest was maintained throughout the culture, albeit being different when examined at different time points. While for HLA-DR and CD86 the level of expression was quite uniform within the same type of samples, for CD80 a higher degree of variability within the same group was noticed, especially at week two in adult samples. Taken together, these results would suggest that whilst the CB samples seem to be expressing the markers of APC function their expression levels trend towards lower levels than adult (again with the exception of CD80 at week one). This might comprise their function as APC.

5.3.3.2 INCREASING HLA-DR EXPRESSION:

While being cultured in IL-2, CB-derived γδ T cells showed only moderate expression of HLA-DR. As this is the most relevant marker for APC functionality, various stimulating conditions were attempted on CB-derived, TCRγδ+ve enriched culture to see if HLA-DR expression on γδ T cells could be increased. The conditions chosen were aimed to stimulate γδ T cells, as activation might lead to an increase in HLA-DR expression. IPP was used, as it is one of the best-known activating antigens for γδ T cells, and Dynabeads (anti-CD3CD28 beads) were also chosen as a non-specific T cell activator. Finally, K562 cells–a MHC-class I negative tumour cell line- were added to provide stress signals such as MICA and co-stimulation via NKG2D. Recognition of MICA by γδ TCR cells has been reported to be activating (Groh *et al.*, 1999) while also exerting a second-signal effect via engagement of NKG2D on the Vγ9Vδ2 subset (Casetti and Martino, 2008). Moreover, it was hypothesised that the lack of MHC class I on K562 cells may trigger activation via the CD94-NKG2A receptor, which the Vγ9Vδ2 subset of γδ T cells, at least, has been reported to express (Hayday, 2009). Results for this experiment are shown in Figure 5.8.

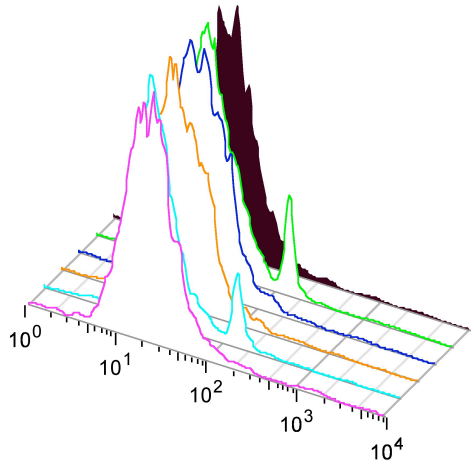

Figure 5.8: conditions tested to promote HLA-DR upregulation in CB samples. Different conditions were tested on a TCRγδ-enriched CB culture and HLA-DR expression was analysed. (—): -ve control (no stimulus). (—): cells incubated with K562 cells and Dynabeads. (—): cells incubated with K562 cells. (—): cells incubated with IPP and K562 cells. (—): cells incubated with Dynabeads only. (—): cells incubated with IPP only. Results are from one representative experiment out of two, the histograms refer to a TCRγδ+ve-gated population.

Following co-incubation of the γδ T cell-enriched cultures with the different stimuli, it appeared that only Dynabeads (anti-CD3CD28 beads) promoted an increase in HLA-DR expression in a small subset of the TCRγδ+ve gated population, as shown by the separate peaks in the two samples incubated with anti-CD3CD28 beads (green and turquoise line in Figure 5.8). Anti-CD3CD28 beads and K562 cells together had a slightly stronger effect on HLA-DR expression up-regulation than anti-CD3CD28 beads alone but no effect was seen when incubating the γδ T cell-enriched culture with K562 cells only. This prompts the conclusion that anti-CD3CD28 beads are the major stimulus and the presence of K562 alone cannot elicit any significant effect on its own. IPP, despite being one of the commonest physiological ligands for the γδTCR, did not up-regulate HLA-DR in CB derived cultures. It remains to be ascertained what particular stimulus, if any, could promote HLA-DR up-regulation in this system and this issue is currently under investigation by other members of the group. It cannot be excluded, for example, that other bisphosphonates such as HMBPP (that is around 100,000 times a stronger agonist than IPP) would be effective in promoting HLA-DR up-regulation.

5.3.3.3 Vγ9Vδ2 CELLS IN CB:

In addition to co-stimulatory molecules, another phenotype of interest across the cultures was the TCR chain combination and pairing, more specifically whether the Vγ9 and Vδ2 chains were co-expressed in the group of samples under examination and whether their co-expression level was similar to the published literature for CB and adult samples. The Vγ9Vδ2 double +ve population constitutes up to 80% of circulating TCR γδ in adult peripheral blood and has been reported to be present, albeit in small amounts, in cord blood too (Morita *et al.*, 1994 and Campos Alberto *et al.*, 2009).
Another goal was to observe whether a Vγ9Vδ2 double +ve population could be expanded from CB samples. Finally, if any APC phenotype was detected in CB, an important objective was to investigate if it correlated with the Vγ9Vδ2+ve population shown to have APC functionality in adults (Brandes *et al.*, 2005, and Brandes *et al.*, 2009). Figure 5.9A-C, below, shows the flow cytometry results obtained for CB (A) and adult samples (B) and the different percentages in Vγ9Vδ2 double +ve cells obtained in the samples under examination (C).

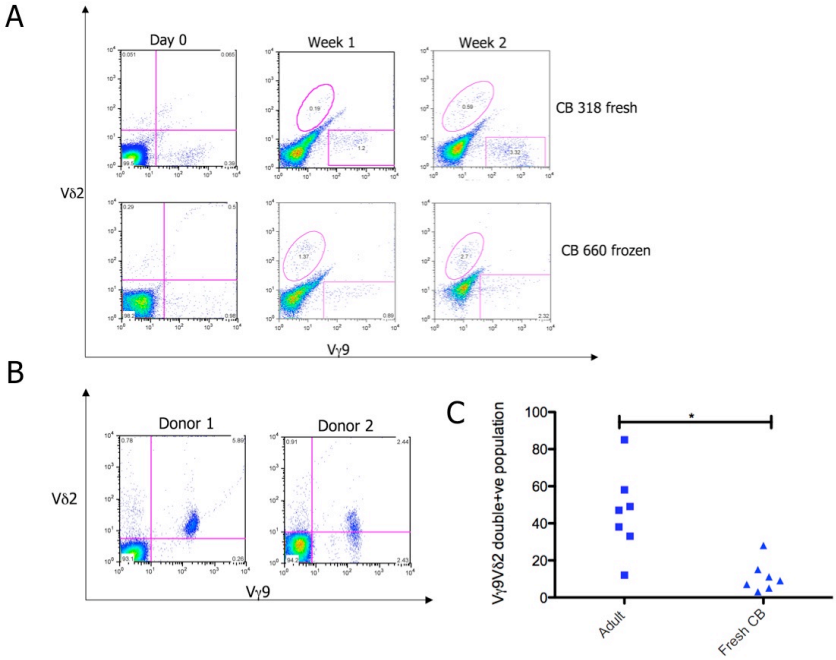

Figure 5.9: flow cytometry analysis of Vγ9Vδ2 double +ve population in CB and adult peripheral blood samples. A, Vγ9Vδ2 double +ve cells in fresh and frozen CB at day 0, week 1 and week 2 and B, Vγ9Vδ2 double +ve cells in adult at day 0. In all cases, cells were firstly gated for lymphocytes, then selected for CD3, then the Vγ9Vδ2 double +ve cells were plotted within the CD3+ve population. C, plot of the percentage of Vγ9Vδ2 population detected in fresh CB and adult peripheral blood samples calculated over the total population expressing either chain. An unpaired student t-test was performed; P*<0.01. Frozen CB N=5, fresh CB N=7, adult N=7.

The number of Vγ9Vδ2 double +ve cells in CB samples was examined and, as reported in literature, it was extremely low in all the fresh samples tested. Indeed, in the frozen CB samples, the Vγ9Vδ2 were undetectable (see 5.9A, above). In culture, at all time points past day 0, the Vγ9Vδ2 double +ve population became undetectable in both fresh and frozen samples (Figure 5.9A, for fresh and frozen CB sample). By contrast, using the same staining cocktail resulted in a well defined double +ve population in the adult samples (Figure 5.9B), precluding a technical issue as the explanation for the extremely low number of Vγ9Vδ2 double +ve cells in CB samples.

As shown in Figure 5.9C, in the fresh CB samples the percentage of Vγ9Vδ2 double +ve events (calculated on the total number of cells expressing either chain) was quite uniform and significantly lower than in adult samples (P*0.0024). In the adult samples a more widespread distribution was observed, with the majority of donors containing

between 40 and 60% of Vγ9Vδ2 double +ve cells, more in line with literature findings. The results in Figure 5.9C show the proportion of Vγ9Vδ2 double +ve cells of the whole CD3+ve population. Unfortunately it was not possible to assess the Vγ9Vδ2 labelling in the γδ +ve population, as currently there are not Abs available for these markers that are conjugated to different fluorochromes.

Some important conclusions were drawn from the results described in Figure 5.9. First of all it should be noted that even detection of Vγ9Vδ2 double +ve cells was quite difficult in all CB samples examined, regardless if they were fresh or frozen. Their low numbers made any characterisation for APC markers impossible, as event number would have been far too low to be meaningful. As such, the APC potential of Vγ9Vδ2 double +ve γδ cells was not assessed due to the very low numbers or absence of this subpopulation. It is possible that Vγ9Vδ2 double +ve cells became lost during cryo-preservation, as a small but detectable population was observed in all fresh CB samples examined but seemed to disappear during expansion in culture.

5.3.4 γδ T CELL SELECTION AFTER EXPANSION:

All the phenotype analyses explained above were performed during the γδ T cell expansion, which had the final aim of providing a large enough enrichment prior TCRγδ+ve selection. After expansion, total PBMCs-CBMCs numbers and γδ T cell enrichment were assessed within the cultures. The decision to select using the TCRγδ microbead kit was taken based on both criteria: in general, samples containing either less than 15 millions total PBMCs-CBMCs, or less than 10-15% of γδ T cells, were not selected, as the final yield in the +ve fraction would have been too low. These criteria unfortunately ruled out selection from all but one of the fresh CB samples, 4/7 adult samples and 3/5 of the frozen CB samples. In every TCRγδ positive selection performed, regardless of the source, the total number of cells in the positive fraction was below 7 X 10^5 cells. Following selection, a flow cytometry analysis was performed to check that the relevant APC phenotype was maintained, as shown in Figure 5.10.

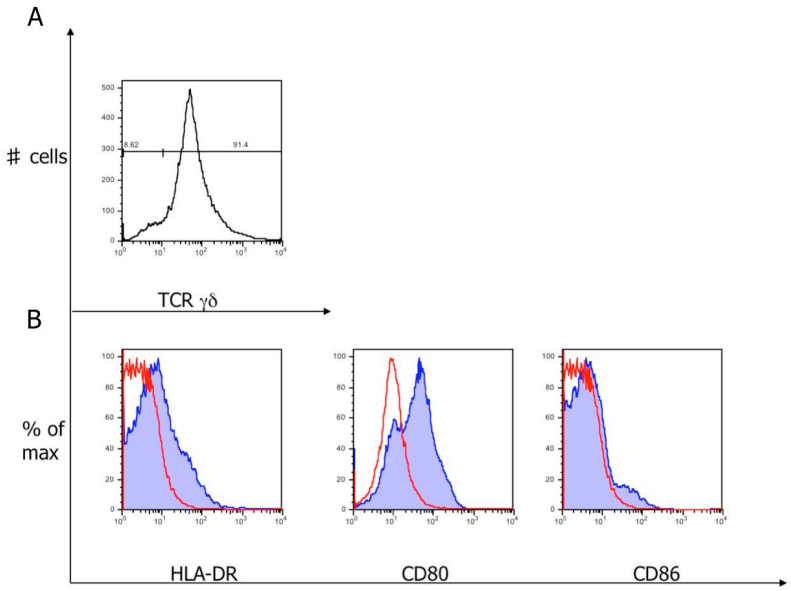

Figure 5.10: flow cytometry analysis of the APC phenotype of TCRγδ population after selection. A, TCRγδ purity after selection from a TCRγδ-enriched adult PBMC culture and B, level of expression of HLA-DR, CD80 and CD86 within the TCRγδ+ve fraction of the selected population. In both A, and B, cells were gated on lymphocytes; for B, (—) is double stained and (—) is TCRγδ+ve stained only (representative of 3 adult samples).

As shown above, the γδ T cell purity in the positive fraction was very good, at around 90% (Figure 5.10A). A clear CD80+ve population was observed in the selected population with a less well-defined HLA-DR+ve and CD86+ve populations also being present (5.10B, shaded histograms). Therefore, it was concluded that γδ T cells maintained their APC-related phenotype after positive selection.

Given the low numbers of γδ+ve T cells retrieved after selection from CB samples priority was given to the expansion of selected TCRγδ+ve cells. As a preliminary experiment using one cord blood sample (data not shown), the selected positive fraction was plated over an autologous feeder layer, with or without IPP. The rationale behind this was to provide a γδ–specific stimulus (IPP) to the γδ+ve T cells; moreover, it was thought that the feeder layer (frozen and irradiated cells derived from the negative fraction of the TCRγδ+ve selection) would provide the "stress" factor that is reported in literature to be an important element in activating TCRγδ+ve cells (Hayday, 2009). However, this approach was proved unsuccessful and no γδ T cell expansion was

detected in this experiment (data not shown).

5.4 DISCUSSION:

Various groups reported an APC activity for the specific subpopulation Vγ9Vδ2+ve of γδ T cells in adults (Brandes *et al.*, 2005, Moser and Brandes, 2006, and Brandes *et al.*, 2009). Recently, Prigione *et al.*, 2009 added additional evidence by reporting APC activity mediated by the Vδ2+ve fraction of γδ T cells in an autologous system. The original aim of the work performed in this chapter was to examine the APC potential in CB-derived γδ T cells, ideally in the same Vγ9Vδ2 subpopulation but also in the entire γδ pool, starting from the hypothesis that CB-derived γδ T cells possess the same APC properties as those seen in adult.

5.4.1 CELL YIELD:

At first, the rationale was to select γδ T cells from unexpanded cord and adult blood samples using a TCRγδ positive selection kit. This approach had to be re-evaluated as it was found that both yield (less than 0.5 X 10^6 cells on average) and purity (consistently less than 60%) of positively selected cells were too low, and a pre-selection expansion protocol was introduced.

Low yield and purity were not, however, the only factors that were taken into account in the decision not to perform a positive selection at the beginning of the culture and to shift this step further down in the protocol. It was also considered that the positive selection kit in use, whose microbeads recognize the whole of the γδTCR repertoire according to the manufacturer, could have an activating effect on the selected cells. It was speculated that the microbeads promote TCR engagement, in absence of secondary co-stimulation. This could lead either to undesired activation or even overstimulation and death or alternatively to anergy and unresponsiveness. Given that the low numbers of γδ T cells obtained from CB samples would mean an expansion step, it was

considered that such a risk should be avoided. Moreover, the ideal situation for analysis was to assess co-stimulatory molecule expression in conditions of activation that could be controlled exogenously (for example by adding phosphoantigens, or other stimuli, in the culture). By expanding the cells first to enrich for γδ T cells, it was hoped to prevent a possible selection-induced unregulated cell activation or anergy.

For selection purposes, absolute numbers of γδ T cells were low either starting from either adults or from CB. To overcome the yield issue, at least in adults, it should be noted that other adult tissues (for example tonsils, as used in Brandes *et al.*, 2005, or intestine) are much richer in γδ T cells than peripheral blood and as such might have been a more suitable cell source. However, the focus of this project was to characterise the APC potential of γδ T cells in cord blood. Therefore, adult peripheral blood-derived γδ T cells were judged the most comparable source of γδ T cells, especially since tonsil and blood derived γδ T cells have a different phenotype with regards to APC-related markers (Brandes *et al.*, 2005); while tonsillar γδ T cells show intrinsic expression of HLA-DR, CD80, CD86 and CD40, γδ T cells of blood origin express the same markers only following incubation with IPP.

The low number of cells obtained severely hampered the experiments that could be performed, however. Whilst a low yield was not so much of a problem during characterisation, small numbers of cells after expansion and selection limited the number and type of functional assays that could be performed. It was not possible, for example, to test a wide range of conditions for post-selection expansion, nor was it possible to perform MLR assays with CB-derived γδ T cells.

5.4.2 EXPANSION PROTOCOL RATIONALE:

Following the discovery of the low starting number of γδ T cells it was decided to try an enrichment protocol from unselected CBMCs/PBMCs. This rationale has a wide support in the literature (Musha *et al.*, 1998, Cipriani *et al.*, 2002, Brandes *et al.*, 2003,

Campos Alberto *et al.*, 2009 and Prigione *et al.*, 2009) and purity after selection became considerably better after IL-2 expansion in both adult and CB samples. γδ T cell expansion in the literature is usually performed using IPP, IL-2, or a mix of the two in various combinations (Cipriani *et al.*, 2002, Prigione *et al.*, 2009, Campos Alberto *et al.*, 2009, Vantourout *et al.*, 2009 and Salot *et al.*, 2009). Other protocols described in literature for γδ T cell proliferation involve the co-culture of PBMCs with IL-2 and PHA-P (Morita *et al.*, 1994), the use of other bisphosphonate-based compounds such as BrHPP (Braza *et al.*, and Ismaili *et al.*, 2002) and triphosphoric acid 1-adenosin-5-yl ester 3-(3-methylbut-3-enyl) ester (ApppI) (Vantourout *et al.*, 2009), and the use of zoledronate, a drug used in myeloma and osteoporosis treatment, both in combination with zoledronate-presenting cells (Roelofs *et al.*, 2009) or on its own (Kondo *et al.*, 2008, and Gruenbacher *et al.*, 2009). However, the lack of commercial availability of most bisphosphonates and the consequential requirement for custom-made preparation rendered them an unfeasible option in the present study.

For this project the simplest option of IL-2 only was chosen. In addition to its ease of use, it was also considered that the most readily available IPP formulation (Sigma) might affect the long-term viability of the culture as it is re-suspended in methanol and as such would be toxic to all eukaryotic cells. Besides the possible toxicity issue, it is one of the known ligands of the γδ TCR and therefore it might promote widespread activation prior to, or in contrast with, the expansion. At this stage, such an outcome would have been unfavourable. The ideal scenario instead would have been enrichment of γδ T cells from the expansion culture, followed by microbead-mediated positive selection, followed by activation of the positively selected fraction. This could then be attempted with a range of stimuli, both γδ-specific (including, at this point only, IPP) and general T cell activation (such as anti-CD3CD28 beads).

Co-cultures of γδ T cells with other cell types have also been effectively used to promote γδ T cell expansion (Brandes *et al.*, 2003 and Brandes *et al.*, 2005). More specifically, Brandes *et al.* used either IPP, HMBPP or bacterial lysate presented by

EBV-B cell lines (B-LCL) to achieve good γδ T cell expansion (Brandes *et al.*, 2005). There is, however, a major caveat against such an approach, despite its effectiveness; it results in a mixed culture. Given the very small number of cells involved, it would have been extremely difficult to separate the γδ+ve T cells from the feeder cell line after expansion. This would have lead to a mixture of cells in all downstream functional experiments, complicating the interpretation of the results. It was therefore a priority to maintain the post-selection γδ T cells as a pure population to avoid ambiguous results.

5.4.3 PHENOTYPE-COSTIMULATORY MOLECULES:

The initial aim of the work described in this chapter was to elucidate whether γδ T cells from CB samples could have an APC phenotype and exert APC functionality. While this project focused on the setting up of γδ T cells culture conditions and the phenotype analysis, other members of the group are currently investigating the APC functionality of these cells at the Anthony Nolan Research Institute.

As for APC phenotype, no statistically significant difference was detected between fresh and frozen CB samples for any of the phenotypic parameters examined (HLA-DR, CD80, CD86), with the exception of higher MFI of HLA-DR labelling at week one on frozen CB compared with fresh CB. However, a trend of lower MFI between CB samples (regardless of freezing status) and adults could be detected for all markers at all time points with the exception of CD80 at week one. The same trend was detected when assessing the co-expression of TCRγδ with another marker (HLA class II or co-stimulatory molecule), again with the exception of CD80 that was significantly more expressed in CB than in adults at week one. The overall lower expression level of HLA-DR and co-stimulatory molecules on CB cells compared to adults might suggest CB-derived cells would be a worse APC. The higher level of CD80 compared to CD86 might be indicative of a potential tolerogenic phenotype, as it is reported that CD80 is likely to be a better ligand for CTLA-4 than for CD28 (Collins *et al*., 2002). However, only functional tests would determine the effects, and eventual differences, of the phenotypes observed.

The data presented in this chapter for adult samples are in line with what was described by Moser's group (Brandes *et al.*, 2005), and any difference in HLA-DR and co-stimulatory molecules expression might be explained by the more specific stimulation (IPP in the published reference vs IL-2 only in this work).

As for the CB samples, the only two references in the literature to any APC-related marker expressed on CB-derived γδ T cells are by Engelmann *et al.*, 2006 and Prigione *et al.*, 2009. Prigione *et al.* reported around 27% expression of CD80 and around 42% expression of CD86 on CB-derived, *C. albicans*-stimulated γδ T cells (Prigione *et al.*, 2009). Their results are thus quite different from what obtained in this study, both in overall percentages for each marker and in CD86 being more highly expressed than CD80. However, such a difference could be explained with the different treatment the CB-derived γδ T cells underwent compared to our study; Prigione *et al.* established Vδ2+ve cell lines using IPP and used those in all subsequent experiments (Prigione *et al.*, 2009). The other paper (Engelmann *et al.*, 2006) described a very low (<1% in all cases) HLA-DR expression in γδ T cells in an African cohort, both *ex vivo* and following PMA/ionomycin stimulation. These results are also quite different from the ones presented in this work, however a direct comparison is difficult due to the fact that in this project staining for HLA class II and co-stimulatory molecules at day 0, for CB samples, was not performed, due to the scarcity of γδ T cells in CB. Also, the IL-2-mediated, prolonged expansion protocol used here for γδ T cells is quite different from the brief (4h) PMA/ionomycin stimulation performed by Engelmann *et al.*, 2006. As surface expression analysis for CB γδ T cells at day 0 was not taken due to the scarce amount of γδ T cells without expansion, it was decided to treat adult samples in the same way and follow up their expression during expansion comparing each time point.

5.4.4 PHENOTYPE- Vγ9Vδ2 CELLS:

Differences between fresh and frozen CB samples were detected with regards the presence or absence of Vγ9Vδ2+ve double +ve cells and in the kinetics of expansion. Whilst the difference in the kinetics of expansion was important in term of numbers, the Vγ9Vδ2 double +ve population was one of the main targets of this work so it will be examined first.

CB-derived Vγ9Vδ2+ve cells were first described in the mid 1990's (Morita *et al.*, 1994), when an average of 9.4% γδ T cells were reported to be Vγ9Vδ2+ve in CB. A more recent paper (Campos Alberto *et al.*, 2009) referred to a generically low percentage of Vγ9Vδ2+ve cells. In this project an average of 11.1% Vγ9Vδ2+ve cells was detected in fresh CB samples, which is consistent with the data presented in the literature.

In the group of samples used in this work, no detectable Vγ9Vδ2 double +ve population was observed in the frozen CB samples after thawing, in contrast to fresh samples examined at day 0. During this project, even in the case of fresh samples, the Vγ9Vδ2 double +ve populations detected by flow cytometry were so small that technical difficulties with flow cytometry staining and procedures were suspected. Vγ9Vδ2 double +ve cells were detected in adult samples, however, suggesting that a technical issue was not the explanation for the CB observations. The apparent lack of Vγ9Vδ2 double +ve cells in CB samples examined after day 0 has not been reported before and its significance is unclear. One possible hypothesis is that the antigens that drive the Vγ9Vδ2+ve expansion in adults were absent in the CB cultures performed in this project. Another possibility is that in CB Vγ9Vδ2 double +ve cells are dependent for their survival on DC help; it was recently published that CD56+ve DCs are important for γδ T cell expansion (Gruenbacher *et al.*, 2009). The lack of DCs in frozen CB samples, or in fresh CB samples after culture, could have had a negative effect on γδ T cell survival and expansion.

The very low number of Vγ9Vδ2 γδ T cells in CB samples suggested that they are likely not the source of the stimulatory and co-stimulatory molecular expression observed. Which γδ T cell subpopulation is responsible for the HLA-DR, CD80 and CD86 expression detected is still an open question. This issue could not be explored fully due to time constraints; moreover, the shortage of commercially available TCR single chain-specific antibodies would also have hampered clarification of this point, but this is definitely worthy of future assessment.

5.4.5 FRESH VS FROZEN SAMPLES' EXPANSION:

Differences in the kinetics of expansion were observed between fresh and frozen CB samples; cultures from fresh CB samples tended to contain a higher proportion of γδ+ve T cells. In both cases however the total cell number after expansion was very small, despite these differences. The definitive test to assess whether there is an intrinsic difference between chain combinations and proliferation potential for the TCRγδ T cell population in fresh and frozen CB would be to check the same CB sample for expansion before and after thawing. Unfortunately, this was not possible in the present study as frozen CB samples were received as whole cord blood and there were no accessible fresh aliquots for testing. However, it should also be considered that in a transplant setting the source of CB cells would be frozen CB units. Therefore, the phenotype and behaviour of γδ T cells derived from frozen CB units is likely to be the most applicable, even if the outcome is less satisfactory than that obtained in fresh CB.

5.4.6 CONCLUSIONS:

Taking into consideration all the data presented so far, γδ T cells from both CB and adults presented a phenotype that could be compatible with APC functionality. It was found that to obtain a sufficient number of γδ T cells for successful characterisation and selection experiments, an expansion step was required. Whilst functional assays, such as an MLR, were not performed, the increase of HLA-DR expression was considered an absolute priority before performing any APC-functional experiments using CB-derived

γδ T cells (other members of the group are actively exploring this issue). Finally, in addition to the topics explored in this chapter, some other questions emerged that need to be answered, namely: can γδ T cells from CB be expanded further *after* selection? If so, what would be the ideal protocol to do so? It still remains to be assessed whether CB-derived γδ T cells are true functional APC, in addition to displaying an APC-like phenotype, and if there are other functions, other than antigen presentation, that are compatible with the phenotype observed during this project.

CHAPTER 6:
FINAL DISCUSSION

6.0 INTRODUCTION:

This PhD project has focused on the development and characterisation of aAPCs as new immunotherapeutic tools, with a special interest in CMV infection, as it constitutes one of the major complications following HSCT. The design of the whole project focused around two key points. Firstly, the main target was to develop a flexible system that could be used in a variety of clinical settings for cellular immunotherapy. Within this objective, the major interest was the aspect of immunotherapy that was considered the main bottleneck in the successful generation of CMV-specific CD8+ve T cells ie., the availability of suitable APCs to generate an antigen specific response. At the moment the main immunotherapeutic options are patient-specific for both the APC and effector cell compartments; therefore, it was considered a priority to develop an alternative technique that could be used in many patients with minor adaptation. This would have been achievable with the liposome-based aAPC system.

In the following sections a summary will be presented of the main merits and disadvantages of each of the approaches that were employed, together with the main difficulties encountered and suggestions on how best to proceed with each approach if the project were to be taken further.

6.1 LIPOSOMES AND THEIR DEVELOPMENT AS aAPCs:

The development of a liposome-based aAPC was the first subproject carried out during the PhD; preliminary data on this topic were generated previously in the laboratory and published in De La Pena *et al*., 2009, during the course of this PhD. The establishment of liposome-based aAPCs in both human and murine models was the initial objective of this PhD project. It was considered that they would have suited the profile for the ideal aAPCs as presented in section 1.4.0 of the Introduction (flexible and biodegradable, non-toxic, non-tumorigenic, able to travel *in vivo*, traceable, capable of forming T cell synapses and of delivering adequate T cell activation signals).

Therefore, while it was not impossible to foresee some challenges ahead (in terms of biochemical standardisation and development of the liposomal aAPCs to suit different systems), it was considered that the final goal -the development of a truly flexible aAPCs- would have balanced out all the difficulties in setting up the model.

6.1.1 MAIN CHALLENGES:

At the very start of the project -at the stage of liposome loading and assessment- persisting difficulties were encountered. MHC loading on the liposome surface was stochastic and hard to reproduce; its clear detection, using all the means and techniques available, proved to be more challenging than expected. The optimisation of loading and particularly its detection had also been one of the most difficult elements in the previously published work (Prof Dodi, personal communication); therefore, more than one procedure (compared to just a dot blot in the published work, De la Peña et al., 2009) was employed. Consequently, this preliminary part took longer than envisaged in the general plan of the PhD.

Difficulties in reproducing the previously published results were also encountered in the tet-specific expansion experiment. Moreover, the framework of published references specific to the interaction of cells with liposomes is limited. When searching the literature for cell-liposome co-culture protocols, it was discovered that it was extremely hard to assess the precise amount/concentration of liposome used when co-cultured on cells, regardless of their final use (antigen delivery rather than stimulation, for example). In addition to De La Peña *et al.*, 2009, the only other reference stating a defined cell:liposome ratio was Marty and Schwendener, 2005. Since only in De La Peña *et al*., 2009, were liposomes used for the antigen-specific targeting of T cells, De La Peña *et al*., 2009 remained the chief reference for this part of the project.

One hypothesis for the difference in expansion seen between this project and the published data could be that the amounts of liposomes used in De la Pena *et al*., 2009, are only compatible with expansion in some donors and not in others. In other words, CD8+ve cells that are sensitive even to minimal antigenic stimulation could behave as seen in the published reference, while with cells from other donors, the presence of

liposomes could tilt the balance between expansion-inhibition of expansion towards toxicity promoted by the liposomes. As there are individual differences in the overall response to CMV (and, in general, antigenic stimulation) this could partly explain the disparity observed between the work presented in this thesis and the published reference. At this point in the project, the only way to completely clarify the discrepancy between the data presented in this thesis and the ones published in De La Pena *et al*., 2009, would have then been a new step-to-step optimisation starting from the very beginning (liposome formulation and loading, as detailed in Sections 2.1.1, 2.1.2.10 and 2.1.2.11). It was considered, however, that this move would have oriented the PhD towards a fully biochemical-based work. It was therefore decided to move away from this topic and to explore the potential for cellular-based aAPCs (see next sections).

The disadvantages of using liposomes (low reproducibility between different batches, stochastic MHC loading, difficulty to assess MHC loading efficiency and decrease in viability observed when co-incubating them with Buffy coats and presumably PBMCs) cannot, however, offset the one great advantage of liposome use in immunotherapy; their full biocompatibility *in vivo*. They are already used *in vivo*, albeit only in chemotherapy, to deliver therapeutic agents; therefore, once their standardization as aAPC was achieved, it is foreseeable their use in a clinical setting could be expedited.

6.1.2 NEXT EXPERIMENTAL STEPS:

In retrospect, and approaching the issue from a biochemical point of view, the challenges encountered in this subproject appear a small step towards the optimisation of a truly flexible, biocompatible, off-the-shelf aAPC to be used also *in vivo*. Were this project to be re-started, the right person to tackle the optimisation issues described above would be a biochemist with previous experience in liposomes. The first task would be assessing whether there is an “ideal” liposome formulation for aAPCs, testing as many protocols as possible; among the characteristics there should be the possibility of prolonging its survival *in vitro* and delaying uptake by cells *in vitro* and *in vivo*. Both

the lipid composition and the re-suspension buffer should be assessed independently. This objective should be achieved by evaluating various liposome compositions on PBMCs, Buffy coat and, ideally, immortalized cell lines (as these would enable comparison of the results obtained with the literature, where liposomes are mostly used on cell lines). Moreover, the work on primary cells should be performed in as wide a cohort as possible, to assess whether the viability issues seen in this project are a common trait or a feature regarding only a small subset of possible patients.

The second priority would be solving the loading issue; while the loading mediated via Cys-attachment still seems the only physiological method, a new way should be sought to optimize its detection. One possibility would be to prepare fluorescent or biotinylated (i.e trackable) MHC molecules (something akin to what has been showed in Prakken *et al.*, 2005); they would be loaded on the liposomes, as done in this project, but could allow a better detection (via specific fluorescence or streptavidin tagging) than an unlabelled protein. If fluorescence was used, fluorescent (or confocal) microscopy could be used to evaluate the degree of loading. While a possible objection could be that the presence of any foreign domain on the MHC protein could impair its tertiary conformation and Cys-loading, this appears to be an acceptable compromise between the need for a better loading detection and conformational stability. Once the detection was established in principle, unlabelled MHC molecules could then be used for experiments. Finally, to solve the lack of reproducibility in the expansion, one possibility would be to test more HLA-specific donors to assess in each case whether liposome presence impairs or not the tet-specific expansion. A further optimization of amount of liposome/protein concentration would be beneficial as well.

In the case of the murine model, it would be advisable to perform a separate optimization for the amount of liposomes/protein concentration to be added to the hybridoma cells. It is possible, in fact, that hybridoma cells are able to withstand higher amounts of liposomes/protein than PBMCs. The amount of peptide shown to be effective when pulsing the OT-1 spleen cells required for the +ve control of the system could provide a general indication of the amount of protein required. The optimisation

part of the murine system should be relatively easier and quicker than the one on the human system, as no change of the liposome formula is, in principle, required: therefore, it could be performed as a preliminary step. However, for clinical use, the data obtained in the human system would be more relevant as they would also reflect the heterogeneity of donors and patients compared to the uniform genetic background and strength of response obtained with the murine hybridoma.

6.2 CB-DERIVED DCs: ADVANTAGES AND DISADVANTAGES:

Following the decision to move to cellular-based aAPCs, the use of CB as source of cells for immunotherapy appeared a natural choice, given the growing importance it has in all roles of transplantation. Compared to liposomes, CB-derived DCs would have not been as flexible and would have not provided the "off-the-shelf" quality required; however, it was considered that they could have delivered a stronger and better activation signal to responder cells than any acellular aAPC currently available. Moreover, the use of CB as a cell source offered the possibility to develop a complete DC-CD8 responder system; while both components needed to be evaluated, this system would have provided the opportunity to develop all aspects of cellular immunotherapy in a well-defined model.

On the APC side, there was not a definite consensus in the literature on what the phenotype and functionality of a CB-derived DCs was; the references ranged from impaired phenotype and reduced functionality (compared to adults, see for example Liu *et al*., 2001, Langrish *et al*., 2002 and Naderi *et al*., 2009) to full APC potential and capability to generate antigen-specific CD8 cells (Salio *et al*., 2003, Park *et al*., 2006 and Hanley *et al*., 2009). Given this mixed evidence, it was fundamental to assess CB-derived aAPCs, in our hands, before setting up any functional experiment. This could have been a disadvantage in terms of a longer time required for setting up the system, but overall the full characterisation and comparison to adult DCs was beneficial in terms of valuable experience in DCs handling. Moreover, the wide literature

background provided a reference frame for CB DCs phenotype/functionality outcome (contrarily to what was available for the liposomes).

On the effector side there were two factors to be considered: the general naivety of CB T cells could have been both a general clinical advantage (as the use of CB material is correlated to less GvHD than adults) and a specific disadvantage for CMV-specific immunotherapy (as cells had to be primed to mount a response against CMV, and priming would have presumably been more difficult in CB than in adults). In the system presented in this thesis, it appears that stronger stimulation conditions should have been used to those that were employed, as it was not possible to detect peptide-specific expansion. However, before being able to address this challenge, viability issues concerning the frozen CB samples used emerged.

6.2.1 MAIN CHALLENGES AND FURTHER EXPERIMENTS:

While it was considered that CB-derived DCs could have provided a stronger stimulation than acellular aAPCs, thereby making them an attractive option, it was discovered that the use of frozen CB samples as DCs source presented considerable hurdles in terms of viability of starting material. These issues could have been solved, or at least bettered, using fresh rather than frozen CB. However, there is still the consideration that, to enable a perfect comparison with the samples used in clinic, frozen CB should be used exclusively.

Therefore, the first step to address the poor monocyte/DCs performance seen in this thesis would be comparing the viability data obtained here with the ones obtained by other CB banks, to see if they are similar. While it is generally acknowledged that the generation of DCs from frozen samples (regardless of the origin) is more difficult, this has been done at least once in the literature (Hanley *et al*., 2009) so it is not an impossible task. However, from the data presented here it appears that the problem with generating DCs from frozen samples might be the samples themselves, so this issue should be addressed before attempting any further DCs generation from CB. Another way to assess whether it is a sample-related problem would be getting frozen CB

samples from other CB banks, treat them as the samples described in this chapter and see whether different results are obtained. In addition to the analysis of viability data, the thawing of frozen CB samples from other CB banks should be useful to highlight the presence of a technical/handling issue. If a difference emerged in the general performance of frozen CB samples from other banks compared to the ones described here, then a protocol-related issue should be considered amongst the possible explanations. This hypothesis could be verified only by a thorough assessment of each step of the procedure used to thaw, select and differentiate monocytes into DCs. If, however, the poor viability persisted, then the most rational way ahead would either be the use of another APC or the use only of CB with the highest monocytes' percentage (as described in section 4.5). As all this part would not be aimed to peptide-specific CD8 T cell generation no typing would be required.

Once the monocyte/DCs viability issue was resolved, the next step would be to improve the efficiency of the antigen-specific CD8 expansion. The conditions used in this thesis (and taken from the published reference Salio *et al*., 2003) did not lead to a detectable tet+ve population. Therefore, stimulation conditions should be strengthened either via repeated administration of antigens, repeated rounds of stimulation with antigen-pulsed autologous cells as APCs (the ideal choice would be B-LCL, as mentioned in section 4.5), increased amount of IL-2 to boost any response, or a combination of all these factor together. A longer DC-responder co-incubation could be tested as well, however, this option should not be the first choice given the overall drop in cell number encountered in CB cultures longer than two weeks (see section 5.3.1).

6.3 THE MAIN CHALLENGES OF γδ T CELLS:

After the conclusion of the subproject on CB derived-DCs, it was decided to further explore CB as a source of APC and the choice was to focus on γδ T cells. The assessment of the APC potential of CB-derived γδ T cells seemed a very promising approach considered the strong published evidence for APC potential in the main γδ T cell subset in adult blood, which is termed Vγ9Vδ2 (Brandes *et al*., 2005 and 2009).

Moreover, while γδ T cells have been the focus of a large number of studies (see Hayday, 2009, for a recent review), their full characterization is still ongoing, especially in CB. It was also speculated that they would not be as affected by freeze-thawing as monocytes, therefore presenting the possibility of a more robust and viable APC subset. The full characterization of γδ T cells and the Vγ9Vδ2 subset in CB cells was however hampered by the extremely low number of these cells in CB, especially in frozen samples. In particular, the paucity of γδ T cells was the main hurdle against their immediate selection from the general PBMCs population without an expansion step and their full characterisation including functional experiments. Therefore, if the project were to be taken further all the efforts should be devoted initially to increase their number in CB-derived cultures.

6.3.1 γδ FUTURE EXPERIMENTS:

Two aspects should be the focus of further research on CB γδ T cells: the development of an effective, CB-specific protocol for γδ T cells expansion and the accurate determination of the chain repertoire dominant in CB, to see whether it matches any of the main populations in adults. The expansion would be the priority, in order to have enough γδ T cells to perform a full characterisation.

The objective of a γδ T cell-specific expansion from CBMCs should be to achieve ideally 1-2 X 10^6 of pure γδ T cells. This could be done in two ways; either by positive selection following expansion or after initial depletion and subsequent expansion. The first method would be recommended for small CB samples (50-100 X 10^6 CBMCs); in this case an IL-2-mediated expansion could be performed, as described in this thesis, however the use of phosphoantigens in the final stages of expansion could be considered. Their use in the beginning of the culture could promote widespread γδ T cell activation; such an outcome would not be favourable at that stage. A depletion (provided anti-CD56 antibodies are not present in the selection mix, as a subset of γδ T cells express CD56) would be an attractive option for large CB samples (above 200-300

X 10^6 CBMCs). Regardless of the protocol used, it is important to obtain as pure a (or as pure as possible, and in particular without any DCs or B cells) γδ T cell population as possible prior to its use in functional assays. If the aim is the assessment of APC activity, in fact, a moderate contamination with, for example, conventional T cells could be allowable, as they should not affect the final result. A DCs or B cells contamination would have more relevant, APC-related, effects.

After the increase of γδ T cell number, the next priority would be assessing their chain repertoire and to see if they match any of the known main subsets. Some of the papers that described their effector activity (Engelmann *et al*. 2005 and 2006) did not assess their repertoire; this information could be important for a general comparison between adult and CB-derived γδ T cells. As detailed at the end of chapter 5, the precise chain assessment is hampered by a general low cell number and by the lack of commercially available, non cross-reactive, chain specific, antibodies. While the repertoire assessment challenge could be overcome via RT-PCR, HLA-DR sorting and chain assessment with the antibodies currently available or limiting clonal dilution (see section 5.5.1 and 5.5.2), all these approaches would greatly benefit from a high cell number. Therefore, an optimised expansion protocol is still a priority.

Once a large, pure γδ T cell population has been achieved, the proper functional assessment could start. The preliminary data presented in this thesis shows that if there is an APC functionality by γδ T cells from CB this does not seem to belong to the Vγ9Vδ2 subset, as the number of these cells in CB samples is extremely low. It would then be relevant to know which repertoire correlated with the HLA-DR, CD80 and CD86-expressing γδ T cells. Functional assessment of antigen presentation by γδ T cells could include pulsing them with an antigen, followed by co-incubation with autologous, carboxyfluorescein diacetate succinimidyl ester (CFSE)-labelled responder cells and the evaluation of any antigen-processing capability (as done in Brandes *et al*., 2009).

Another important point to be elucidated would be the interaction between DCs and γδ T cells in CB. Gruenbacher *et al*., 2009, showed that DCs are important for γδ T cell activation in adults; therefore, it would be interesting to see whether this interaction is occurring in CB as well. Relevant data could be provided by a pure γδ T cell culture where autologous DC could be exogenously reintroduced. Any differences between DC-enriched and control cultures could then be assessed in terms of antigen-presenting capability and general functionality.

6.3 FINAL CONCLUSIONS:

The results presented in this thesis provide data on three different approaches to the development of APCs for immunotherapy in an HSCT setting. The merits and disadvantages of each of them have been discussed in this chapter. What is, however, the general direction of research for immunotherapy in HSCT? What approaches or strategies are predominant, and what will be the foreseeable advances in this field?

The greatest advantage of cellular immunotherapy over more conventional treatments such as chemotherapy is that it is disease-specific, targeting only the malignancy or the infection in a precise way. This is an invaluable advantage in the treatment of patients that are already debilitated by standard chemotherapy treatments. As the world of biomedicine is moving away from standard, “one-type-fits-all” treatments such as chemotherapy, it can be expected that the relevance of all applications of cellular immunotherapy will become greater and greater. In parallel, increasing progress in aAPC research is foreseeable, as the aAPC is a necessary requirement to generate the specific effector population needed. Within this field a steady, albeit slow, progression to clinical trials of more and more acellular aAPCs systems could be expected. In the meanwhile, cell-based aAPCs would fill the gap, so to speak, and become more and more standardised and widespread. The full potential of aAPCs generation and cellular immunotherapy is not been reached yet, therefore, it can be expected that substantial progress will be accomplished in the next few years. In this view, the work presented in this thesis can highlight some of the main difficulties on this path and help define where

to focus efforts (standardisation and interactions between liposomes and primary cells, for example) in future research.

BIBLIOGRAPHY

BIBLIOGRAPHY:

1968, structural chemistry and molecular biology (a volume dedicated to Linus Pauling by his students, colleagues and friends), W. H. Freeman and Co, San Francisco.

Ackerman, A. L., and P. Cresswell, 2004, Cellular mechanisms governing cross-presentation of exogenous antigens: Nat Immunol, v. 5, p. 678-84.

Ackerman, A. L., A. Giodini, and P. Cresswell, 2006, A role for the endoplasmic reticulum protein retrotranslocation machinery during crosspresentation by dendritic cells: Immunity, v. 25, p. 607-17.

Adams, E. J., P. Strop, S. Shin, Y. H. Chien, and K. C. Garcia, 2008, An autonomous CDR3delta is sufficient for recognition of the nonclassical MHC class I molecules T10 and T22 by gammadelta T cells: Nat Immunol, v. 9, p. 777-84.

Admyre, C., S. M. Johansson, S. Paulie, and S. Gabrielsson, 2006, Direct exosome stimulation of peripheral human T cells detected by ELISPOT: Eur J Immunol, v. 36, p. 1772-81.

Albert, M. L., B. Sauter, and N. Bhardwaj, 1998, Dendritic cells acquire antigen from apoptotic cells and induce class I-restricted CTLs: Nature, v. 392, p. 86-89.

Allen, T. M., 1994, The use of glycolipids and hydrophilic polymers in avoiding rapid uptake of liposomes by the mononuclear phagocyte system: Advanced Drug Delivery Review, v. 13, p. 285- 309.

Altin, J. G., and C. R. Parish, 2006, Liposomal vaccines--targeting the delivery of antigen: Methods, v. 40, p. 39-52.

Andre, F., N. Chaput, N. E. Schartz, C. Flament, N. Aubert, J. Bernard, F. Lemonnier, G. Raposo, B. Escudier, D. H. Hsu, T. Tursz, S. Amigorena, E. Angevin, and L. Zitvogel, 2004, Exosomes as potent cell-free peptide-based vaccine. I. Dendritic cell-derived exosomes transfer functional MHC class I/peptide complexes to dendritic cells: J Immunol, v. 172, p. 2126-36.

Archbold, J. K., 2009, To be gammadelta or not to be gammadelta? Signaling pathways in alphabeta versus gammadelta T cell maturation: Sci Signal, v. 2, p. 1-3.

Badovinac, V. P., B. B. Porter, and J. T. Harty, 2002, Programmed contraction of CD8(+) T cells after infection: Nat Immunol, v. 3, p. 619-26.

Badovinac, V. P., K. A. Messingham, A. Jabbari, J. S. Haring, and J. T. Harty, 2005, Accelerated CD8+ T-cell memory and prime-boost response after dendritic-cell vaccination: Nat Med, v. 11, p. 748-56.

Balan, S., V. P. Kale, and L. S. Limaye, 2009, A simple two-step culture system for the large-scale generation of mature and functional dendritic cells from umbilical cord blood CD34+ cells: Transfusion, v. 49, p. 2109-21.

Ballen, K. K., T. R. Spitzer, B. Y. Yeap, S. McAfee, B. R. Dey, E. Attar, R. Haspel, G. Kao, D. Liney, E. Alyea, S. Lee, C. Cutler, V. Ho, R. Soiffer, and J. H. Antin, 2007, Double unrelated reduced-intensity umbilical cord blood transplantation in adults: Biol Blood Marrow Transplant, v. 13, p. 82-9.

Banchereau, J., and R. M. Steinman, 1998, Dendritic cells and the control of immunity: Nature, v. 392, p. 245-52.

Banchereau, J., F. Briere, C. Caux, J. Davoust, S. Lebecque, Y. J. Liu, B. Pulendran, and K. Palucka, 2000, Immunobiology of dendritic cells: Annu Rev Immunol, v. 18, p. 767-811.

Barber, L. D., Jordan, S., Whitelegg, A. M., Madrigal, J. A., and Savage, P., 2006, HLA class I mono-specific APCs and target cells: a method to standardise in vitro CD8+ T cell expansion and functional assays, J Immunol Methods, v. 314, p. 147-52.

Baum, P., D. Muller, R. Ruger, and R. E. Kontermann, 2007, Single-chain Fv immunoliposomes for the targeting of fibroblast activation protein-expressing tumor stromal cells: J Drug Target, v. 15, p. 399-406.

Bautista, G., J. R. Cabrera, C. Regidor, R. Fores, J. A. Garcia-Marco, E. Ojeda, I. Sanjuan, E. Ruiz, I. Krsnik, B. Navarro, S. Gil, E. Magro, A. de Laiglesia, R. Gonzalo-Daganzo, T. Martin-Donaire, M. Rico, I. Millan, and M. N. Fernandez, 2009, Cord blood transplants supported by co-infusion of mobilized hematopoietic stem cells from a third-party donor: Bone Marrow Transplant, v. 43, p. 365-73.

Bjorkman, P. J., M. A. Saper, B. Samraoui, W. S. Bennett, J. L. Strominger, and D. C. Wiley, 1987, Structure of the human class I histocompatibility antigen, HLA-A2: Nature, v. 329, p. 506-12.

Blanchard, N., D. Lankar, F. Faure, A. Regnault, C. Dumont, G. Raposo, and C. Hivroz, 2002, TCR activation of human T cells induces the production of exosomes bearing the TCR/CD3/zeta complex: J Immunol, v. 168, p. 3235-41.

Boismenu, R., and W. L. Havran, 1998, Gammadelta T cells in host defense and epithelial cell biology: Clin Immunol Immunopathol, v. 86, p. 121-33.

Bousso, P., 2008, T-cell activation by dendritic cells in the lymph node: lessons from the movies: Nat Rev Immunol.

Bracho, F., C. van de Ven, E. Areman, R. M. Hughes, V. Davenport, M. B. Bradley, J. W. Cai, and M. S. Cairo, 2003, A comparison of *ex vivo* expanded DCs derived from cord blood and mobilized adult peripheral blood plastic-adherent mononuclear cells: decreased alloreactivity of cord blood DCs: Cytotherapy, v. 5, p. 349-61.

Brandes, M., K. Willimann, A. B. Lang, K. H. Nam, C. Jin, M. B. Brenner, C. T. Morita, and B. Moser, 2003, Flexible migration program regulates gamma delta T-cell involvement in humoral immunity: Blood, v. 102, p. 3693-701.

Brandes, M., K. Willimann, and B. Moser, 2005, Professional antigen-presentation function by human gammadelta T Cells: Science, v. 309, p. 264-8.

Brandes, M., K. Willimann, G. Bioley, N. Levy, M. Eberl, M. Luo, R. Tampe, F. Levy, P. Romero, and B. Moser, 2009, Cross-presenting human gammadelta T cells induce robust CD8+ alphabeta T cell responses: Proc Natl Acad Sci U S A, v. 106, p. 2307-12.

Braud, V. M., D. S. Allan, and A. J. McMichael, 1999, Functions of nonclassical MHC and non-MHC-encoded class I molecules: Curr Opin Immunol, v. 11, p. 100-8.

Braza, M. S., A. Caraux, T. Rousset, S. Lafaye de Micheaux, H. Sicard, P. Squiban, V. Costes, B. Klein, and J. F. Rossi, 2010, gammadelta T lymphocytes count is normal and expandable in peripheral blood of patients with follicular lymphoma, whereas it is decreased in tumor lymph nodes compared with inflammatory lymph nodes: J Immunol, v. 184, p. 134-40.

Brenner, M. B., J. McLean, D. P. Dialynas, J. L. Strominger, J. A. Smith, F. L. Owen, J. G. Seidman, S. Ip, F. Rosen, and M. S. Krangel, 1986, Identification of a putative second T-cell receptor: Nature, v. 322, p. 145-9.

Cairo, C., G. Mancino, G. Cappelli, C. D. Pauza, E. Galli, E. Brunetti, and V. Colizzi, 2008, Vdelta2 T-lymphocyte responses in cord blood samples from Italy and Cote d'Ivoire: Immunology, v. 124, p. 380-7.

Campos Alberto, E. J., N. Shimojo, M. Aoyagi, and Y. Kohno, 2009, Differential effects of tumor necrosis factor-alpha and interleukin-12 on isopentenyl pyrophosphate-stimulated interferon-gamma production by cord blood Vgamma9 T cells: Immunology, v. 127, p. 171-7.

Casetti, R., and A. Martino, 2008, The plasticity of gamma delta T cells: innate immunity, antigen presentation and new immunotherapy: Cell Mol Immunol, v. 5, p. 161-70.

Cemerski, S., J. Das, J. Locasale, P. Arnold, E. Giurisato, M. A. Markiewicz, D. Fremont, P. M. Allen, A. K. Chakraborty, and A. S. Shaw, 2007, The

stimulatory potency of T cell antigens is influenced by the formation of the immunological synapse: Immunity, v. 26, p. 345-55.

Cemerski, S., J. Das, E. Giurisato, M. A. Markiewicz, P. M. Allen, A. K. Chakraborty, and A. S. Shaw, 2008, The balance between T cell receptor signaling and degradation at the center of the immunological synapse is determined by antigen quality: Immunity, v. 29, p. 414-22.

Chang, S. C., F. Momburg, N. Bhutani, and A. L. Goldberg, 2005, The ER aminopeptidase, ERAP1, trims precursors to lengths of MHC class I peptides by a "molecular ruler" mechanism: Proc Natl Acad Sci U S A, v. 102, p. 17107-12.

Chaput, N., N. E. Schartz, F. Andre, J. Taieb, S. Novault, P. Bonnaventure, N. Aubert, J. Bernard, F. Lemonnier, M. Merad, G. Adema, M. Adams, M. Ferrantini, A. F. Carpentier, B. Escudier, T. Tursz, E. Angevin, and L. Zitvogel, 2004, Exosomes as potent cell-free peptide-based vaccine. II. Exosomes in CpG adjuvants efficiently prime naive Tc1 lymphocytes leading to tumor rejection: J Immunol, v. 172, p. 2137-46.

Chen, X., and P. E. Jensen, 2004, The expression of HLA-DO (H2-O) in B lymphocytes: Immunol Res, v. 29, p. 19-28.

Chen, X., and P. E. Jensen, 2008, The role of B lymphocytes as antigen-presenting cells: Arch Immunol Ther Exp (Warsz), v. 56, p. 77-83.

Cheng, L., Y. Cui, H. Shao, G. Han, L. Zhu, Y. Huang, R. L. O'Brien, W. K. Born, H. J. Kaplan, and D. Sun, 2008, Mouse gammadelta T cells are capable of expressing MHC class II molecules, and of functioning as antigen-presenting cells: J Neuroimmunol, v. 203, p. 3-11.

Cipriani, B., H. Knowles, L. Chen, L. Battistini, and C. F. Brosnan, 2002, Involvement of classical and novel protein kinase C isoforms in the response of human V gamma 9V delta 2 T cells to phosphate antigens: J Immunol, v. 169, p. 5761-70.

Cobbold M., N. Khan, B. Pourgheysari B, S. Tauro, D. McDonald, H. Osman, M. Assenmacher, L. Billingham, C. Steward, C. Crawley, E. Olavarria, J. Goldman, R. Chakraverty, P. Mahendra, C. Craddock, and P. A. Moss, 2005, Adoptive transfer of cytomegalovirus-specific CTL to stem cell transplant patients after selection by HLA-peptide tetramers: J Exp Med, v. 202, p. 379-86.

Collins, R. A., D. Werling, S. E. Duggan, A. P. Bland, K. R. Parsons, and C. J. Howard, 1998, Gammadelta T cells present antigen to CD4+ alphabeta T cells: J Leukoc Biol, v. 63, p. 707-14.

Collins, A. V., D. W. Brodie, R. J. Gilbert, A. Iaboni, R. Manso-Sancho, B. Walse, D. I. Stuart, P. A van der Merwe, and S. J. Davis, 2002, The interaction properties of costimulatory molecules revisited: Immunity, v. 17, p. 2010-10.

Colonna, M., G. Trinchieri, and Y. J. Liu, 2004, Plasmacytoid dendritic cells in immunity: Nat Immunol, v. 5, p. 1219-26.

Copelan, E. A., 2006, Hematopoietic stem-cell transplantation: N Engl J Med, v. 354, p. 1813-26.

Copland, M. J., M. A. Baird, T. Rades, J. L. McKenzie, B. Becker, F. Reck, P. C. Tyler, and N. M. Davies, 2003, Liposomal delivery of antigen to human dendritic cells: Vaccine, v. 21, p. 883-90.

Cui, Y., L. Kang, L. Cui, and W. He, 2009, Human gammadelta T cell recognition of lipid A is predominately presented by CD1b or CD1c on dendritic cells: Biol Direct, v. 4, p. 47.

Curtsinger, J., M. J. Deeths, P. Pease, and M. F. Mescher, 1997, Artificial cell surface constructs for studying receptor-ligand contributions to lymphocyte activation: J Immunol Methods, v. 209, p. 47-57.

Curtsinger, J. M., C. S. Schmidt, A. Mondino, D. C. Lins, R. M. Kedl, M. K. Jenkins, and M. F. Mescher, 1999, Inflammatory cytokines provide a third signal for activation of naive CD4+ and CD8+ T cells: J Immunol, v. 162, p. 3256-62.

Curtsinger, J. M., D. C. Lins, and M. F. Mescher, 2003, Signal 3 determines tolerance versus full activation of naive CD8 T cells: dissociating proliferation and development of effector function: J Exp Med, v. 197, p. 1141-51.

Curtsinger, J. M., J. O. Valenzuela, P. Agarwal, D. Lins, and M. F. Mescher, 2005, Type I IFNs provide a third signal to CD8 T cells to stimulate clonal expansion and differentiation: J Immunol, v. 174, p. 4465-9.

Cutler, C., S. Giri, S. Jeyapalan, D. Paniagua, A. Viswanathan, and J. H. Antin, 2001, Acute and chronic graft-versus-host disease after allogeneic peripheral-blood stem-cell and bone marrow transplantation: a meta-analysis: J Clin Oncol, v. 19, p. 3685-91.

Davis, M. M., and P. J. Bjorkman, 1988, T-cell antigen receptor genes and T-cell recognition: Nature, v. 334, p. 395-402.

De La Peña, H., J. A. Madrigal, S. Rusakiewicz, M. Bencsik, G. W. Cave, A. Selman, R. C. Rees, P. J. Travers, and I. A. Dodi, 2009, Artificial exosomes as tools for basic and clinical immunology: J Immunol Methods, v. 344, p. 121-32.

Deeths, M. J., and M. F. Mescher, 1997, B7-1-dependent co-stimulation results in qualitatively and quantitatively different responses by CD4+ and CD8+ T cells: Eur J Immunol, v. 27, p. 598-608.

Deeths, M. J., and M. F. Mescher, 1999, ICAM-1 and B7-1 provide similar but distinct costimulation for CD8+ T cells, while CD4+ T cells are poorly costimulated by ICAM-1: Eur J Immunol, v. 29, p. 45-53.

Delves, P. J., and I. M. Roitt, 2000a, The immune system. First of two parts: N Engl J Med, v. 343, p. 37-49.

Delves, P. J., and I. M. Roitt, 2000b, The immune system. Second of two parts: N Engl J Med, v. 343, p. 108-17.

Dick, T. P., N. Bangia, D. R. Peaper, and P. Cresswell, 2002, Disulfide bond isomerization and the assembly of MHC class I-peptide complexes: Immunity, v. 16, p. 87-98.

Dustin, M. L., 2008, T-cell activation through immunological synapses and kinapses: Immunol Rev, v. 221, p. 77-89.

Eberl, M., M. Hintz, A. Reichenberg, A. K. Kollas, J. Wiesner, and H. Jomaa, 2003, Microbial isoprenoid biosynthesis and human gammadelta T cell activation: FEBS Lett, v. 544, p. 4-10.

Einsele, H., E. Roosnek, N. Rufer, C. Sinzger, S. Riegler, J. Loffler, U. Grigoleit, A. Moris, H. G. Rammensee, L. Kanz, A. Kleihauer, F. Frank, G. Jahn, and H. Hebart, 2002, Infusion of cytomegalovirus (CMV)-specific T cells for the treatment of CMV infection not responding to antiviral chemotherapy: Blood, v. 99, p. 3916-22.

Engelhard, V. H., J. L. Strominger, M. Mescher, and S. Burakoff, 1978, Induction of secondary cytotoxic T lymphocytes by purified HLA-A and HLA-B antigens reconstituted into phospholipid vesicles: Proc Natl Acad Sci U S A, v. 75, p. 5688-91.

Engelmann, I., A. Santamaria, P. G. Kremsner, and A. J. Luty, 2005, Activation status of cord blood gamma delta T cells reflects *in utero* exposure to Plasmodium falciparum antigen: J Infect Dis, v. 191, p. 1612-22.

Engelmann, I., U. Moeller, A. Santamaria, P. G. Kremsner, and A. J. Luty, 2006, Differing activation status and immune effector molecule expression profiles of neonatal and maternal lymphocytes in an African population: Immunology, v. 119, p. 515-21.

Finberg, R., M. Mescher, and S. J. Burakoff, 1978, The induction of virus-specific

cytotoxic T lymphocytes with solubilized viral and membrane proteins: J Exp Med, v. 148, p. 1620-7.

Flutter, B., and B. Gao, 2004, MHC class I antigen presentation--recently trimmed and well presented: Cell Mol Immunol, v. 1, p. 22-30.

Fogg, D. K., C. Sibon, C. Miled, S. Jung, P. Aucouturier, D. R. Littman, A. Cumano, and F. Geissmann, 2006, A clonogenic bone marrow progenitor specific for macrophages and dendritic cells: Science, v. 311, p. 83-7.

Freiberg, B. A., H. Kupfer, W. Maslanik, J. Delli, J. Kappler, D. M. Zaller, and A. Kupfer, 2002, Staging and resetting T cell activation in SMACs: Nat Immunol, v. 3, p. 911-7.

Fremont, D. H., W. A. Hendrickson, P. Marrack, and J. Kappler, 1996, Structures of an MHC class II molecule with covalently bound single peptides: Science, v. 272, p. 1001-4.

Fu F., Y. Li, S. Qian, L. Lu, F. Chambers, T. E. Starzl, J. J. Fung, and A. W Thomson, 1996, Costimulatory molecule-deficient dendritic cell progenitors (MHC class II+, CD80 dim, CD86-) prolong cardiac allograft survival in nonimmunosuppressed recipients: Transpl, v. 62, p. 659–65.

Giannoni, F., J. Barnett, K. Bi, R. Samodal, P. Lanza, P. Marchese, R. Billetta, R. Vita, M. R. Klein, B. Prakken, W. W. Kwok, E. Sercarz, A. Altman, and S. Albani, 2005, Clustering of T cell ligands on artificial APC membranes influences T cell activation and protein kinase C theta translocation to the T cell plasma membrane: J Immunol, v. 174, p. 3204-11.

Gibbons, D. L., S. F. Haque, T. Silberzahn, K. Hamilton, C. Langford, P. Ellis, R. Carr, and A. C. Hayday, 2009, Neonates harbour highly active gammadelta T cells with selective impairments in preterm infants: Eur J Immunol, v. 39, p. 1794-806.

Giri, P. K., and J. S. Schorey, 2008, Exosomes derived from M. Bovis BCG infected macrophages activate antigen-specific CD4+ and CD8+ T cells in vitro and *in vivo*: PLoS One, v. 3, p. e2461.

Gluckman, E., H. A. Broxmeyer, A. D. Auerbach, H. S. Friedman, G. W. Douglas, A. Devergie, H. Esperou, D. Thierry, G. Socie, P. Lehn, and *et al.*, 1989, Hematopoietic reconstitution in a patient with Fanconi's anemia by means of umbilical-cord blood from an HLA-identical sibling: N Engl J Med, v. 321, p. 1174-8.

Gluckman, E., 2009, History of cord blood transplantation: Bone Marrow Transplant, v. 44, p. 621-6.

Goren, D., A. T. Horowitz, D. Tzemach, M. Tarshish, S. Zalipsky, and A. Gabizon, 2000, Nuclear delivery of doxorubicin via folate-targeted liposomes with bypass of multidrug-resistance efflux pump: Clin Cancer Res, v. 6, p. 1949-57.

Grakoui, A., S. K. Bromley, C. Sumen, M. M. Davis, A. S. Shaw, P. M. Allen, and M. L. Dustin, 1999, The immunological synapse: a molecular machine controlling T cell activation: Science, v. 285, p. 221-7.

Granucci, F., C. Vizzardelli, N. Pavelka, S. Feau, M. Persico, E. Virzi, M. Rescigno, G. Moro, and P. Ricciardi-Castagnoli, 2001, Inducible IL-2 production by dendritic cells revealed by global gene expression analysis: Nat Immunol, v. 2, p. 882-8.

Gregoriadis, G., 1976, The carrier potential of liposomes in biology and medicine (first of two parts): N Engl J Med, v. 295, p. 704-10.

Groh, V., S. Bahram, S. Bauer, A. Herman, M. Beauchamp, and T. Spies, 1996, Cell stress-regulated human major histocompatibility complex class I gene expressed in gastrointestinal epithelium: Proc Natl Acad Sci U S A, v. 93, p. 12445-50.

Groh, V., A. Steinle, S. Bauer, and T. Spies, 1998, Recognition of stress-induced MHC molecules by intestinal epithelial gammadelta T cells: Science, v. 279, p. 1737-40.

Groh, V., R. Rhinehart, H. Secrist, S. Bauer, K. H. Grabstein, and T. Spies, 1999, Broad tumor-associated expression and recognition by tumor-derived gamma delta T cells of MICA and MICB: Proc Natl Acad Sci U S A, v. 96, p. 6879-84.

Gruenbacher, G., H. Gander, A. Rahm, W. Nussbaumer, N. Romani, and M. Thurnher, 2009, CD56+ human blood dendritic cells effectively promote TH1-type gammadelta T-cell responses: Blood, v. 114, p. 4422-31.

Guermonprez, P., Valladeau, J., Zitvogel, L., Thery, C., and Amigorena, S., 2002, Antigen presentation and T cell stimulation by dendritic cells: Annu Rev Immunol, v. 20, p. 621-67.

Hanley, P. J., C. R. Cruz, B. Savoldo, A. M. Leen, M. Stanojevic, M. Khalil, W. Decker, J. J. Molldrem, H. Liu, A. P. Gee, C. M. Rooney, H. E. Heslop, G. Dotti, M. K. Brenner, E. J. Shpall, and C. M. Bollard, 2009, Functionally active virus-specific T cells that target CMV, adenovirus, and EBV can be expanded from naive T-cell populations in cord blood and will target a range of viral epitopes: Blood, v. 114, p. 1958-67.

Hansen, C. B., G. Y. Kao, E. H. Moase, S. Zalipsky, and T. M. Allen, 1995, Attachment of antibodies to sterically stabilized liposomes: evaluation, comparison and optimization of coupling procedures: Biochim Biophys Acta, v. 1239, p. 133-44.

Harty, J. T., A. R. Tvinnereim, and D. W. White, 2000, CD8+ T cell effector mechanisms in resistance to infection: Annu Rev Immunol, v. 18, p. 275-308.

Hayday, A. C., 2000, [gamma][delta] cells: a right time and a right place for a conserved third way of protection: Annu Rev Immunol, v. 18, p. 975-1026.

Hayday, A. C., 2009, Gammadelta T cells and the lymphoid stress-surveillance response: Immunity, v. 31, p. 184-96.

Hayes, S. M., L. Li, and P. E. Love, 2005, TCR signal strength influences alphabeta/gammadelta lineage fate: Immunity, v. 22, p. 583-93.

Hein, W. R., and C. R. Mackay, 1991, Prominence of gamma delta T cells in the ruminant immune system: Immunol Today, v. 12, p. 30-4.

Henrickson, S. E., and U. H. von Andrian, 2007, Single-cell dynamics of T-cell priming: Curr Opin Immunol, v. 19, p. 249-58.

Horowitz, M. M., R. P. Gale, P. M. Sondel, J. M. Goldman, J. Kersey, H. J. Kolb, A. A. Rimm, O. Ringden, C. Rozman, B. Speck, and *et al.*, 1990, Graft-versus-leukemia reactions after bone marrow transplantation: Blood, v. 75, p. 555-62.

Hussain, S., A. Pluckthun, T. M. Allen, and U. Zangemeister-Wittke, 2007, Antitumor activity of an epithelial cell adhesion molecule targeted nanovesicular drug delivery system: Mol Cancer Ther, v. 6, p. 3019-27.

Huth, U. S., R. Schubert, and R. Peschka-Suss, 2006, Investigating the uptake and intracellular fate of pH-sensitive liposomes by flow cytometry and spectral bio-imaging: J Control Release, v. 110, p. 490-504.

Iezzi, G., K. Karjalainen, and A. Lanzavecchia, 1998, The duration of antigenic stimulation determines the fate of naive and effector T cells: Immunity, v. 8, p. 89-95.

Ignatius, R., K. Mahnke, M. Rivera, K. Hong, F. Isdell, R. M. Steinman, M. Pope, and L. Stamatatos, 2000, Presentation of proteins encapsulated in sterically stabilized liposomes by dendritic cells initiates CD8(+) T-cell responses *in vivo*: Blood, v. 96, p. 3505-13.

Ikemizu, S., R. J. Gilbert, J. A. Fennelly, A. V. Collins, K. Harlos, E. Y. Jones, D. I Stuart, and S. J. Davis, 2000, Structure and dimerization of a soluble form of B7-1: Immunity, v. 12, p. 51-60.

Ismaili, J., V. Olislagers, R. Poupot, J. J. Fournie, and M. Goldman, 2002, Human gamma delta T cells induce dendritic cell maturation: Clin Immunol, v. 103, p. 296-302.

Janeway, C. A., Jr., B. Jones, and A. Hayday, 1988, Specificity and function of T cells bearing gamma delta receptors: Immunol Today, v. 9, p. 73-6.

Janeway, C. A., Jr., Travers, P., Walport, M., Schlomchik, M. J., 2005, Immunobiology-The immune system in health and disease, Garland Science.

Jenkins, M. K., and J. G. Johnson, 1993, Molecules involved in T-cell costimulation: Curr Opin Immunol, v. 5, p. 361-7.

Jensen, P. E., 2007, Recent advances in antigen processing and presentation: Nat Immunol, v. 8, p. 1041-8.

Jiang, X., X. Lu, R. Liu, F. Zhang, and H. Zhao, 2007, HLA Tetramer Based Artificial Antigen-Presenting Cells Efficiently Stimulate CTLs Specific for Malignant Glioma: Clin Cancer Res, v. 13, p. 7329-34.

Jonuleit, H., E. Schmitt, K. Steinbrink, and A. H. Enk, 2001, Dendritic cells as a tool to induce anergic and regulatory T cells: Trends Immunol, v. 22, p. 394-400.

Jorgensen, J. L., U. Esser, B. Fazekas de St Groth, P. A. Reay, and M. M. Davis, 1992, Mapping T-cell receptor-peptide contacts by variant peptide immunization of single-chain transgenics: Nature, v. 355, p. 224-30.

Kienast, A., M. Preuss, M. Winkler, and T. P. Dick, 2007, Redox regulation of peptide receptivity of major histocompatibility complex class I molecules by ERp57 and tapasin: Nat Immunol, v. 8, p. 864-72.

Kim, J. V., J. B. Latouche, I. Riviere, and M. Sadelain, 2004, The ABCs of artificial antigen presentation: Nat Biotechnol, v. 22, p. 403-10.

Kisielow, P. and H. von Boehmer, 1995, Deevelopment and selection of T cells: facts and puzzles: Adv Immunol, v. 58, p. 87-209.

Klibanov, A. L., K. Maruyama, V. P. Torchilin, and L. Huang, 1990, Amphipathic polyethyleneglycols effectively prolong the circulation time of liposomes: FEBS Lett, v. 268, p. 235-7.

Kloetzel, P. M., 2004, Generation of major histocompatibility complex class I antigens: functional interplay between proteasomes and TPPII: Nat Immunol, v. 5, p. 661-9.

Kobari, L., M. C. Giarratana, J. C. Gluckman, L. Douay, and M. Rosenzwajg, 2006, *Ex vivo* expansion does not alter the capacity of umbilical cord blood CD34+ cells to generate functional T lymphocytes and dendritic cells: Stem Cells, v. 24, p. 2150-7.

Kolb, H. J., J. Mittermuller, C. Clemm, E. Holler, G. Ledderose, G. Brehm, M. Heim, and W. Wilmanns, 1990, Donor leukocyte transfusions for treatment of recurrent chronic myelogenous leukemia in marrow transplant patients: Blood, v. 76, p. 2462-5.

Komanduri, K. V., L. S. St John, M. de Lima, J. McMannis, S. Rosinski, I. McNiece, S. G. Bryan, I. Kaur, S. Martin, E. D. Wieder, L. Worth, L. J. Cooper, D. Petropoulos, J. J. Molldrem, R. E. Champlin, and E. J. Shpall, 2007, Delayed immune reconstitution after cord blood transplantation is characterized by impaired thymopoiesis and late memory T-cell skewing: Blood, v. 110, p. 4543-51.

Koning, G. A., R. M. Schiffelers, M. H. Wauben, R. J. Kok, E. Mastrobattista, G. Molema, T. L. ten Hagen, and G. Storm, 2006, Targeting of angiogenic endothelial cells at sites of inflammation by dexamethasone phosphate-containing RGD peptide liposomes inhibits experimental arthritis: Arthritis Rheum, v. 54, p. 1198-208.

Kondo, M., K. Sakuta, A. Noguchi, N. Ariyoshi, K. Sato, S. Sato, K. Sato, A. Hosoi, J. Nakajima, Y. Yoshida, K. Shiraishi, K. Nakagawa, and K. Kakimi, 2008, Zoledronate facilitates large-scale *ex vivo* expansion of functional gammadelta T cells from cancer patients for use in adoptive immunotherapy: Cytotherapy, v. 10, p. 842-56.

Korbling, M., and P. Anderlini, 2001, Peripheral blood stem cell versus bone marrow allotransplantation: does the source of hematopoietic stem cells matter?: Blood, v. 98, p. 2900-8.

Kovacsovics-Bankowski, M., and K. L. Rock, 1995, A phagosome-to-cytosol pathway for exogenous antigens presented on MHC class I molecules: Science, v. 267, p. 243-6.

Kunzmann, V., E. Bauer, and M. Wilhelm, 1999, Gamma/delta T-cell stimulation by pamidronate: N Engl J Med, v. 340, p. 737-8.

Laffont, S., and F. Powrie, 2009, Immunology: Dendritic-cell genealogy: Nature, v. 462, p. 732-3.

Lamb, L. S., Jr., P. Musk, Z. Ye, F. van Rhee, S. S. Geier, J. J. Tong, K. M. King, and P. J. Henslee-Downey, 2001, Human gammadelta(+) T lymphocytes have in vitro graft vs leukemia activity in the absence of an allogeneic response: Bone Marrow Transplant, v. 27, p. 601-6.

Langenkamp, A., M. Messi, A. Lanzavecchia, and F. Sallusto, 2000, Kinetics of dendritic cell activation: impact on priming of TH1, TH2 and nonpolarized T cells: Nat Immunol, v. 4, p. 311-6.

Langrish, C. L., J. C. Buddle, A. J. Thrasher, and D. Goldblatt, 2002, Neonatal dendritic cells are intrinsically biased against Th-1 immune responses: Clin Exp Immunol, v. 128, p. 118-23.

Latouche, J. B., and M. Sadelain, 2000, Induction of human cytotoxic T lymphocytes by artificial antigen-presenting cells: Nat Biotechnol, v. 18, p. 405-9.

Lee, K. H., A. R. Dinner, C. Tu, G. Campi, S. Raychaudhuri, R. Varma, T. N. Sims, W. R. Burack, H. Wu, J. Wang, O. Kanagawa, M. Markiewicz, P. M. Allen, M. L. Dustin, A. K. Chakraborty, and A. S. Shaw, 2003, The immunological synapse balances T cell receptor signaling and degradation: Science, v. 302, p. 1218-22.

Leen, A. M., G. D. Myers, U. Sili, M. H. Huls, H. Weiss, K. S. Leung, G. Carrum, R. A. Krance, C. C. Chang, J. J. Molldrem, A. P. Gee, M. K. Brenner, H. E. Heslop, C. M. Rooney, and C. M. Bollard, 2006, Monoculture-derived T lymphocytes specific for multiple viruses expand and produce clinically relevant effects in immunocompromised individuals: Nat Med, v. 12, p. 1160-6.

Levine, B. L., W. B. Bernstein, M. Connors, N. Craighead, T. Lindsten, C. B. Thompson, and C. H. June, 1997, Effects of CD28 costimulation on long-term proliferation of CD4+ T cells in the absence of exogenous feeder cells: J Immunol, v. 159, p. 5921-30.

Li, L., and C. Y. Wu, 2008, CD4+ CD25+ Treg cells inhibit human memory gammadelta T cells to produce IFN-gamma in response to *M. tuberculosis* antigen ESAT-6: Blood, v. 111, p. 5629-36.

Liu, E., W. Tu, H. K. Law, and Y. L. Lau, 2001, Decreased yield, phenotypic expression and function of immature monocyte-derived dendritic cells in cord blood: Br J Haematol, v. 113, p. 240-6.

Malissen, M., J. Trucy, E. Jouvin-Marche, P. A. Cazenave, R. Scollay, and B. Malissen, 1992, Regulation of TCR alpha and beta gene allelic exclusion during T-cell development: Immunol Today, v. 13, p. 315-22.

Mamot, C., D. C. Drummond, K. Hong, D. B. Kirpotin, and J. W. Park, 2003, Liposome-based approaches to overcome anticancer drug resistance: Drug Resist Updat, v. 6, p. 271-9.

Mamot, C., D. C. Drummond, C. O. Noble, V. Kallab, Z. Guo, K. Hong, D. B. Kirpotin, and J. W. Park, 2005, Epidermal growth factor receptor-targeted immunoliposomes significantly enhance the efficacy of multiple anticancer drugs *in vivo*: Cancer Res, v. 65, p. 11631-8.

Martin-Donaire, T., M. Rico, G. Bautista, R. Gonzalo-Daganzo, C. Regidor, E. Ojeda, I. Sanjuan, R. Fores, E. Ruiz, I. Krsnik, B. Navarro, S. Gil, E. Magro, I. Millan, R.

Sanchez, N. Perez-Sanz, N. Panadero, J. A. Garcia-Marco, R. Cabrera, and M. N. Fernandez, 2009, Immune reconstitution after cord blood transplants supported by coinfusion of mobilized hematopoietic stem cells from a third party donor: Bone Marrow Transplant, v. 44, p. 213-25.

Martinez, F. O., L. Helming, and S. Gordon, 2009, Alternative activation of macrophages: an immunologic functional perspective: Annu Rev Immunol, v. 27, p. 451-83.

Marty, C., P. Scheidegger, K. Ballmer-Hofer, R. Klemenz, and R. A. Schwendener, 2001, Production of functionalized single-chain Fv antibody fragments binding to the ED-B domain of the B-isoform of fibronectin in Pichia pastoris: Protein Expr Purif, v. 21, p. 156-64.

Marty, C., B. Odermatt, H. Schott, D. Neri, K. Ballmer-Hofer, R. Klemenz, and R. A. Schwendener, 2002, Cytotoxic targeting of F9 teratocarcinoma tumors with anti-ED-B fibronectin scFv antibody modified liposomes: Br J Cancer, v. 87, p. 106-12.

Marty, C., and R. A. Schwendener, 2005, Cytotoxic tumor targeting with scFv antibody-modified liposomes: Methods Mol Med, v. 109, p. 389-402.

Maus, M. V., A. K. Thomas, D. G. Leonard, D. Allman, K. Addya, K. Schlienger, J. L. Riley, and C. H. June, 2002, *Ex vivo* expansion of polyclonal and antigen-specific cytotoxic T lymphocytes by artificial APCs expressing ligands for the T-cell receptor, CD28 and 4-1BB: Nat Biotechnol, v. 20, p. 143-8.

Maus, M. V., J. L. Riley, W. W. Kwok, G. T. Nepom, and C. H. June, 2003, HLA tetramer-based artificial antigen-presenting cells for stimulation of CD4+ T cells: Clin Immunol, v. 106, p. 16-22.

Mellman, I. and R. M. Steinman, 2001, Dendritic cells: specialized and regulated antigen processing machines: Cell, v. 106, p. 255-258.

Mempel, T. R., S. E. Henrickson, and U. H. Von Andrian, 2004a, T-cell priming by dendritic cells in lymph nodes occurs in three distinct phases: Nature, v. 427, p. 154-9.

Mempel, T. R., M. L. Scimone, J. R. Mora, and U. H. von Andrian, 2004b, *In vivo* imaging of leukocyte trafficking in blood vessels and tissues: Curr Opin Immunol, v. 16, p. 406-17.

Mercadal, M., J. C. Domingo, J. Petriz, J. Garcia, and M. A. de Madariaga, 1999, A novel strategy affords high-yield coupling of antibody to extremities of liposomal surface-grafted PEG chains: Biochim Biophys Acta, v. 1418, p. 232-8.

Merindol, N., A. J. Grenier, M. Caty, E. Charrier, A. Duval, M. Duval, M. A. Champagne, and H. Soudeyns, 2010, Umbilical cord blood T cells respond against the Melan-A/MART-1 tumor antigen and exhibit reduced alloreactivity as compared with adult blood-derived T cells: J Immunol, v. 185, p. 856-66.

Mesaeli, N., K. Nakamura, E. Zvaritch, P. Dickie, E. Dziak, K. H. Krause, M. Opas, D. H. MacLennan, and M. Michalak, 1999, Calreticulin is essential for cardiac development: J Cell Biol, v. 144, p. 857-68.

Mescher, M. F., 1992, Surface contact requirements for activation of cytotoxic T lymphocytes: J Immunol, v. 149, p. 2402-5.

Micklethwaite, K., A. Hansen, A. Foster, E. Snape, V. Antonenas, M. Sartor, P. Shaw, K. Bradstock and D. Gottlieb, 2007, Ex vivo expansion and prophylactic infusion of CMV-pp65 peptide-specific cytotoxic T-lymphocytes following allogeneic hematopoietic stem cell transplantation: Biol Blood Marrow Transplant, v. 13, p. 707-14.

Mignot, G., S. Roux, C. Thery, E. Segura, and L. Zitvogel, 2006, Prospects for exosomes in immunotherapy of cancer: J Cell Mol Med, v. 10, p. 376-88.

Miller, M. J., S. H. Wei, M. D. Cahalan, and I. Parker, 2003, Autonomous T cell trafficking examined *in vivo* with intravital two-photon microscopy: Proc Natl Acad Sci U S A, v. 100, p. 2604-9.

Mills, J. K., and D. Needham, 2004, The materials engineering of temperature-sensitive liposomes: Methods Enzymol, v. 387, p. 82-113.

Mitchell, M. S., D. Darrah, D. Yeung, S. Halpern, A. Wallace, J. Voland, V. Jones, and J. Kan-Mitchell, 2002, Phase I trial of adoptive immunotherapy with cytolytic T lymphocytes immunized against a tyrosinase epitope: J Clin Oncol, v. 20, p. 1075-86.

Mitchison, N. A., 1971, The carrier effect in the secondary response to hapten-protein conjugates. II. Cellular cooperation: Eur J Immunol, v. 1, p. 18-27.

Mocellin, S., S. Mandruzzato, V. Bronte, M. Lise, and D. Nitti, 2004, Part I: Vaccines for solid tumors: Lancet Oncol, v. 5, p. 681-9.

Monks, C. R., B. A. Freiberg, H. Kupfer, N. Sciaky, and A. Kupfer, 1998, Three-dimensional segregation of supramolecular activation clusters in T cells: Nature, v. 395, p. 82-6.

Morelli, A. E., and A. W. Thomson, 2007, Tolerogenic dendritic cells and the quest for transplant tolerance: Nat Rev Immunol, v. 7, p. 610-21.

Morita, C. T., C. M. Parker, M. B. Brenner, and H. Band, 1994, TCR usage and functional capabilities of human gamma delta T cells at birth: J Immunol, v. 153, p. 3979-88.

Moseman, E. A., X. Liang, A. J. Dawson, A. Panoskaltsis-Mortari, A. M. Krieg, Y. J. Liu, B. R. Blazar, and W. Chen, 2004, Human plasmacytoid dendritic cells activated by CpG oligodeoxynucleotides induce the generation of CD4+CD25+ regulatory T cells: J Immunok, v. 173, p. 4433-42.

Moser, B., and M. Brandes, 2006, Gammadelta T cells: an alternative type of professional APC: Trends Immunol, v. 27, p. 112-8.

Mosmann, T. R., H. Cherwinski, M. W. Bond, M. A. Giedlin, and R. L. Coffman, 1986, Two types of murine helper T cell clone. I. Definition according to profiles of lymphokine activities and secreted proteins: J. Immunol, v. 136, p. 2348-2357.

Mosmann, T. R., and R. L. Coffman, 1989, Th1 and Th2 cells: different patterns of lymphokine secresion lead to different functional properties: Annu Rev Immunol, v. 7, p. 145-173.

Mosmann, T. R., and Sad, S., 1996, The expanding universe of T-cell subsets: Th1, Th2 and more: Immunol today, v. 17, p. 138-146.

Musha, N., Y. Yoshida, S. Sugahara, S. Yamagiwa, T. Koya, H. Watanabe, K. Hatakeyama, and T. Abo, 1998, Expansion of CD56+ NK T and gamma delta T cells from cord blood of human neonates: Clin Exp Immunol, v. 113, p. 220-8.

Naderi, N., A. A. Pourfathollah, K. Alimoghaddam, and S. M. Moazzeni, 2009, Cord blood dendritic cells prevent the differentiation of naive T-helper cells towards Th1 irrespective of their subtype: Clin Exp Med, v. 9, p. 29-36.

Obar, J. J., and L. Lefrançois, 2010, Memory CB8+ T cell differentiation: Ann N Y Acad Sci., v. 1183, p. 251–266.

Odyniec, A. N., D. C. Barral, S. Garg, R. V. Tatituri, G. S. Besra, and M. B. Brenner, 2010, Regulation of CD1 antigen-presenting complex stability: J Biol Chem, v. 285, p. 11937-47.

Oelke, M., M. V. Maus, D. Didiano, C. H. June, A. Mackensen, and J. P. Schneck, 2003, *Ex vivo* induction and expansion of antigen-specific cytotoxic T cells by HLA-Ig-coated artificial antigen-presenting cells: Nat Med, v. 9, p. 619-24.

Oelke, M., C. Krueger, R. L. Giuntoli, 2nd, and J. P. Schneck, 2005, Artificial antigen-presenting cells: artificial solutions for real diseases: Trends Mol Med, v. 11, p. 412-20.

Oosten, L. E. M., E. Blokland, A. G. S. van Holteren, J. Curtsinger, M. F. Mescher, J. H. F. Falkenburg, T. Mutis and E. Goulmy, 2004, Artificial antigen0presenting constructs efficiently stimulate minor histocompatibility antigen-specific cytotoxic T lymphocytes: Blood, v. 104, p. 224-6.

Otto, M., R. C. Barfield, R. Iyengar, J. Gatewood, I. Muller, M. S. Holladay, J. Houston, W. Leung, and R. Handgretinger, 2005, Human gammadelta T cells from G-CSF-mobilized donors retain strong tumoricidal activity and produce immunomodulatory cytokines after clinical-scale isolation: J Immunother, v. 28, p. 73-8.

Pagnan, G., D. D. Stuart, F. Pastorino, L. Raffaghello, P. G. Montaldo, T. M. Allen, B. Calabretta, and M. Ponzoni, 2000, Delivery of c-myb antisense oligodeoxynucleotides to human neuroblastoma cells via disialoganglioside GD(2)-targeted immunoliposomes: antitumor effects: J Natl Cancer Inst, v. 92, p. 253-61.

Pan, B. T., K. Teng, C. Wu, M. Adam, and R. M. Johnstone, 1985, Electron microscopic evidence for externalization of the transferrin receptor in vesicular form in sheep reticulocytes: J Cell Biol, v. 101, p. 942-8.

Park, J. W., 2002, Liposome-based drug delivery in breast cancer treatment: Breast Cancer Res, v. 4, p. 95-9.

Park, K. D., L. Marti, J. Kurtzberg, and P. Szabolcs, 2006, In vitro priming and expansion of cytomegalovirus-specific Th1 and Tc1 T cells from naive cord blood lymphocytes: Blood, v. 108, p. 1770-3.

Pastorino, F., C. Brignole, D. Marimpietri, M. Cilli, C. Gambini, D. Ribatti, R. Longhi, T. M. Allen, A. Corti, and M. Ponzoni, 2003, Vascular damage and anti-angiogenic effects of tumor vessel-targeted liposomal chemotherapy: Cancer Res, v. 63, p. 7400-9.

Peggs, K., S. Verfuerth, and S. Mackinnon, 2001, Induction of cytomegalovirus (CMV)-specific T-cell responses using dendritic cells pulsed with CMV antigen: a novel culture system free of live CMV virions: Blood, v. 97, p. 994-1000.

Peggs, K. S., S. Verfuerth, A. Pizzey, N. Khan, M. Guiver, P. A. Moss, and S. Mackinnon, 2003, Adoptive cellular therapy for early cytomegalovirus infection after allogeneic stem-cell transplantation with virus-specific T-cell lines: Lancet, v. 362, p. 1375-7.

Peggs, K. S., 2009, Adoptive T cell immunotherapy for cytomegalovirus: Expert Opin Biol Ther, v. 9, p. 725-36.

Petrie, H. T., F. Livak, D. G. Schatz, A. Strasser, I. N. Crispe, and K. Shortman, 1993, Multiple rearrangements in T cell receptor alpha chain genes maximize the production of useful thymocytes: J Exp Med, v. 178, p. 615-22.

Pittet, M. J., D. Valmori, P. R. Dunbar, D. E. Speiser, D. Lienard, F. Lejeune, K. Fleischhauer, V. Cerundolo, J. C. Cerottini, and P. Romero, 1999, High frequencies of naive Melan-A/MART-1-specific CD8(+) T cells in a large proportion of human histocompatibility leukocyte antigen (HLA)-A2 individuals: J Exp Med, v. 190, p. 705-15.

Porcelli, S. A., 2005, Bird genes give new insights into the origins of lipid antigen presentation: Proc Natl Acad Sci U S A, v. 102, p 8399-400.

Pourgheysari, B., N. Khan, D. Best, R. Bruton, L. Nayak, and P. A. Moss, 2007, The cytomegalovirus-specific CD4+ T-cell response expands with age and markedly alters the CD4+ T-cell repertoire: J Virol, v. 81, p. 7759-65.

Prakken, B., M. Wauben, D. Genini, R. Samodal, J. Barnett, A. Mendivil, L. Leoni, and S. Albani, 2000, Artificial antigen-presenting cells as a tool to exploit the immune 'synapse': Nat Med, v. 6, p. 1406-10.

Prigione, I., F. Benvenuto, P. Bocca, L. Battistini, A. Uccelli, and V. Pistoia, 2009, Reciprocal interactions between human mesenchymal stem cells and gammadelta T cells or invariant natural killer T cells: Stem Cells, v. 27, p. 693-702.

Pulendran, B., J. L. Smith, G. Caspary, K. Brasel, D. Pettit, E. Maraskovsky, and C. R. Maliszewski, 1999, Distinct dendritic cell subsets differentially regulate the class of immune response *in vivo*: Proc Natl Acad Sci U S A, v. 96, p. 1036-41.

Querol, S., Capmany, G., Azqueta, C., Gabarro, M., Fornas, O., Martin-Henao, G. A., and Garcia, J., 2000, Direct immunomagnetic method for CD34+ cell selection from cryopreserved cord blood grafts for *ex vivo* expansion protocols, Transfusion, v. 40, p. 625-631.

Ramachandra, L., D. Simmons, and C. V. Harding, 2009, MHC molecules and microbial antigen processing in phagosomes: Curr Opin Immunol, v. 21, p. 98-104.

Rammensee, H-G., 1995, Chemistry of peptides associated with MHC class I and II molecules: Curr Opin Immunol, v. 7, p. 85-96.

Raposo, G., H. W. Nijman, W. Stoorvogel, R. Liejendekker, C. V. Harding, C. J. Melief, and H. J. Geuze, 1996, B lymphocytes secrete antigen-presenting vesicles: J Exp Med, v. 183, p. 1161-72.

Reddehase, M. J., F. Weiland, K. Munch, S. Jonjic, A. Luske, and U. H. Koszinowski, 1985, Interstitial murine cytomegalovirus pneumonia after irradiation: characterization of cells that limit viral replication during established infection of the lungs: J Virol, v. 55, p. 264-73.

Reis e Sousa, C., and R. N. Germain, 1995, Major histocompatibility complex class I presentation of peptides derived from soluble exogenous antigen by a subset of cells engaged in phagocytosis: J Exp Med, v. 182, p. 841-51.

Rescigno, M., M. Urbano, B. Valzasina, M. Francolini, G. Rotta, R. Bonasio, F. Granucci, J. P. Kraehenbuhl, and P. Ricciardi-Castagnoli, 2001, Dendritic cells express tight junction proteins and penetrate gut epithelial monolayers to sample bacteria: Nat Immunol, v. 2, p. 361-7.

Riddell, S. R., K. S. Watanabe, J. M. Goodrich, C. R. Li, M. E. Agha, and P. D. Greenberg, 1992, Restoration of viral immunity in immunodeficient humans by the adoptive transfer of T cell clones: Science, v. 257, p. 238-41.

Rocha, V., J. E. Wagner, Jr., K. A. Sobocinski, J. P. Klein, M. J. Zhang, M. M. Horowitz, and E. Gluckman, 2000, Graft-versus-host disease in children who have received a cord-blood or bone marrow transplant from an HLA-identical sibling. Eurocord and International Bone Marrow Transplant Registry Working Committee on Alternative Donor and Stem Cell Sources: N Engl J Med, v. 342, p. 1846-54.

Rocha, V., M. V. Carmagnat, S. Chevret, O. Flinois, H. Bittencourt, H. Esperou, F. Garnier, P. Ribaud, A. Devergie, G. Socie, L. Dal'Cortivo, J. P. Marolleau, D. Charron, E. Gluckman, and C. Rabian, 2001, Influence of bone marrow graft lymphocyte subsets on outcome after HLA-identical sibling transplants: Exp Hematol, v. 29, p. 1347-52.

Rock, K. L., and H. Kono, 2008, The inflammatory response to cell death: Annu Rev Pathol, v. 3, p. 99-126.

Rodriguez, A., A. Regnault, M. Kleijmeer, P. Ricciardi-Castagnoli, and S. Amigorena, 1999, Selective transport of internalized antigens to the cytosol for MHC class I presentation in dendritic cells: Nat Cell Biol, v. 1, p. 362-8.

Roelofs, A. J., M. Jauhiainen, H. Monkkonen, M. J. Rogers, J. Monkkonen, and K. Thompson, 2009, Peripheral blood monocytes are responsible for gammadelta T cell activation induced by zoledronic acid through accumulation of IPP/DMAPP: Br J Haematol, v. 144, p. 245-50.

Rossi, M., and Young, J. W., 2005, Human dendritic cells: potent antigen-presenting cells at the crossroads of innate and adaptive immunity: J Immunol, v. 175, p. 1373-81.

Sakaguchi, S., 2004, Naturally arising CD4+ regulatory T cells for immunologic self-tolerance and negative control on immune responses: Annu Rev Immunol, v. 22, p. 531-562.

Salio, M., N. Dulphy, J. Renneson, M. Herbert, A. McMichael, A. Marchant, and V. Cerundolo, 2003, Efficient priming of antigen-specific cytotoxic T lymphocytes by human cord blood dendritic cells: Int Immunol, v. 15, p. 1265-73.

Sallusto, F., and A. Lanzavecchia, 1994, Efficient presentation of soluble antigen by cultured human dendritic cells is maintained by granulocyte/macrophage colony-stimulating factor plus interleukin 4 and downregulated by tumor necrosis factor alpha: J Exp Med, v. 179, p. 1109-18.

Sallusto, F., J. Geginat, and A. Lanzavecchia, 2004, Central memory and effector memory T cell subsets: function, generation, and maintenance: Annu Rev Immunol, v. 22, p. 745-63.

Salot, S., S. Bercegeay, B. Dreno, S. Saiagh, V. Scaglione, C. Bonnafous, and H. Sicard, 2009, Large scale expansion of Vgamma9Vdelta2 T lymphocytes from human peripheral blood mononuclear cells after a positive selection using MACS "TCR gamma/delta+ T cell isolation kit": J Immunol Methods, v. 347, p. 12-8.

Sansom, D. M., C. N. Manzotti, and Y. Zheng, 2003, What's the difference between CD80 and CD86?: Trends in immunol, v. 24, p. 313-8.

Sato, K., H. Nagayama, and T. A. Takahashi, 1998, Generation of dendritic cells from fresh and frozen cord blood CD34+ cells: Cryobiology, v. 37, p. 362-71.

Sato, K., and S. Fujita, 2007, Dendritic cells: nature and classification: Allergol Int, v. 56, p. 183-91.

Saunderson, S. C., P. C. Schuberth, A. C. Dunn, L. Miller, B. D. Hock, P. A. MacKay, N. Koch, R. W. Jack, and A. D. McLellan, 2008, Induction of exosome release in primary B cells stimulated via CD40 and the IL-4 receptor: J Immunol, v. 180, p. 8146-52.

Savina, A., and S. Amigorena, 2007, Phagocytosis and antigen presentation in dendritic cells: Immunol Rev, v. 219, p. 143-56.

Schondelmaier, S., D. Wesch, K. Pechhold, and D. Kabelitz, 1993, V gamma gene usage in peripheral blood gamma delta T cells: Immunol Lett, v. 38, p. 121-6.

Schub, A., I. G. Schuster, W. Hammeschmidt, W., and Moosmann, A., 2009, CMV-specific TCR-transgenic T cells for immunotherapy: J Immunol, v. 183, p. 6819-30.

Shen, Z., G. Reznikoff, G. Dranoff, and K. L. Rock, 1997, Cloned dendritic cells can present exogenous antigens on both MHC class I and class II molecules: J Immunol, v. 158, p. 2723-30.

Shin J. S., M. Ebersold, M. Pypaert, L. Delamarre, A. Hartley, and I. Mellman, 2006, Surface expression of MHC class II in dendritic cells is controlled by regulated ubiquitination: Nature, v. 444, p. 115-8.

Shresta, S., C. T. Pham, D. A. Thomas, T. A. Graubert, and T. J. Ley, 1998, How do cytotoxic lymphocytes kill their targets?: Curr Opin Immunol, v. 10, p. 581-7.

Soderberg-Naucler, C., and J. Y. Nelson, 1999, Human cytomegalovirus latency and reactivation - a delicate balance between the virus and its host's immune system: Intervirology, v. 42, p. 314-21.

Solache, A., C. L. Morgan, A. I. Dodi, C. Morte, I. Scott, C. Baboonian, B. Zal, J. Goldman, J. E. Grundy, and J. A. Madrigal, 1999, Identification of three HLA-A*0201-restricted cytotoxic T cell epitopes in the cytomegalovirus protein pp65 that are conserved between eight strains of the virus: J Immunol, v. 163, p. 5512-8.

Song, J., F. T. Lei, X. Xiong, and R. Haque, 2008, Intracellular signals of T cell costimulation: Cell Mol Immunol, v. 5, p. 239-47.

Sotomayor, E. M., I. Borrello, F. M. Rattis, A. G. Cuenca, J. Abrams, K. Staveley-O'Carroll, and H. I. Levitsky, 2001, Cross-presentation of tumor antigens by bone marrow-derived antigen-presenting cells is the dominant mechanism in the induction of T-cell tolerance during B-cell lymphoma progression: Blood, v. 98, p. 1070-7.

Steenblock, E. R., and Fahmy, T. M, 2008, A comprehensive platform for *ex vivo* T-cell expansion based on biodegradable polymeric artificial antigen-presenting cells, Mol Ther, v. 16, p. 765-772.

Steenblock, E. R., S. H. Wrzesinski, R. A. Flavell, and T. M. Fahmy, 2009, Antigen presentation on artificial acellular substrates: modular systems for flexible, adaptable immunotherapy: Expert Opin Biol Ther, v. 9, p. 451-64.

Steinman, R. M., 1991, The dendritic cell system and its role in immunogenicity: Annu Rev Immunol, v. 9, p. 271-96.

Steinman, R. M., and M. C. Nussenzweig, 2002, Avoiding horror autotoxicus: the

importance of dendritic cells in peripheral T cell tolerance: Proc Natl Acad Sci U S A, v. 99, p. 351-8.

Steinman, R. M., and J. Banchereau, 2007, Taking dendritic cells into medicine: Nature, v. 449, p. 419-26.

Stemberger, C., M. Neuenhahn, V. R. Buchholz, and D. H. Busch, 2007, Origin of CD8+ effector and memory T cell subsets: Cell Mol Immunol, v. 4, p. 399-405.

Strid, J., S. J. Roberts, R. B. Filler, J. M. Lewis, B. Y. Kwong, W. Schpero, D. H. Kaplan, A. C. Hayday, and M. Girardi, 2008, Acute upregulation of an NKG2D ligand promotes rapid reorganization of a local immune compartment with pleiotropic effects on carcinogenesis: Nat Immunol, v. 9, p. 146-54.

Suchin, E. J., P. B. Langmuir, E. Palmer, M. H. Sayegh, A. D. Wells, and L.A. Turka, 2001, Quantifying the frequency of alloreactive T cells in vivo: new answers to an old question: J Immunol, v.166, p. 973–81.

Sullivan, K. M., H. J. Deeg, J. Sanders, A. Klosterman, D. Amos, H. Shulman, G. Sale, P. Martin, R. Witherspoon, F. Appelbaum, and *et al.*, 1986, Hyperacute graft-v-host disease in patients not given immunosuppression after allogeneic marrow transplantation: Blood, v. 67, p. 1172-5.

Sullivan, L. C., C. S. Clements, J. Rossjohn, and A. G. Brooks, 2008, The major histocompatibility complex class Ib molecule HLA-E at the interface between innate and adaptive immunity: Tissue Antigens, v. 72, p. 415-24.

Takahashi, S., J. Ooi, A. Tomonari, T. Konuma, N. Tsukada, M. Oiwa-Monna, K. Fukuno, M. Uchiyama, K. Takasugi, T. Iseki, A. Tojo, T. Yamaguchi, and S. Asano, 2007, Comparative single-institute analysis of cord blood transplantation from unrelated donors with bone marrow or peripheral blood stem-cell transplants from related donors in adult patients with hematologic malignancies after myeloablative conditioning regimen: Blood, v. 109, p. 1322-30.

Thery, C., A. Regnault, J. Garin, J. Wolfers, L. Zitvogel, P. Ricciardi-Castagnoli, G. Raposo, and S. Amigorena, 1999, Molecular characterization of dendritic cell-derived exosomes. Selective accumulation of the heat shock protein hsc73: J Cell Biol, v. 147, p. 599-610.

Thery, C., M. Boussac, P. Veron, P. Ricciardi-Castagnoli, G. Raposo, J. Garin, and S. Amigorena, 2001, Proteomic analysis of dendritic cell-derived exosomes: a secreted subcellular compartment distinct from apoptotic vesicles: J Immunol, v. 166, p. 7309-18.

Thery, C., L. Duban, E. Segura, P. Veron, O. Lantz, and S. Amigorena, 2002a, Indirect activation of naive CD4+ T cells by dendritic cell-derived exosomes: Nat Immunol, v. 3, p. 1156-62.

Thery, C., L. Zitvogel, and S. Amigorena, 2002b, Exosomes: composition, biogenesis and function: Nat Rev Immunol, v. 2, p. 569-79.

Thery, C., M. Ostrowski, and E. Segura, 2009, Membrane vesicles as conveyors of immune responses: Nat Rev Immunol, v. 9, p. 581-93.

Utsugi-Kobukai, S., H. Fujimaki, C. Hotta, M. Nakazawa, and M. Minami, 2003, MHC class I-mediated exogenous antigen presentation by exosomes secreted from immature and mature bone marrow derived dendritic cells: Immunol Lett, v. 89, p. 125-31.

Van den Bosch, G. A., P. Ponsaerts, G. Vanham, D. R. Van Bockstaele, Z. N. Berneman, and V. F. Van Tendeloo, 2006, Cellular immunotherapy for cytomegalovirus and HIV-1 infection: J Immunother, v. 29, p. 107-21.

Van der Merwe, P. A. and Davis, S. J., 2003, Molecular interactions mediating T cell antigen recognition: Annu Rev Immunol 2003, v 21, p. 659-84.

Vantourout, P., J. Mookerjee-Basu, C. Rolland, F. Pont, H. Martin, C. Davrinche, L. O. Martinez, B. Perret, X. Collet, C. Perigaud, S. Peyrottes, and E. Champagne, 2009, Specific requirements for Vgamma9Vdelta2 T cell stimulation by a natural adenylated phosphoantigen: J Immunol, v. 183, p. 3848-57.

Varma, R., G. Campi, T. Yokosuka, T. Saito, and M. L. Dustin, 2006, T cell receptor-proximal signals are sustained in peripheral microclusters and terminated in the central supramolecular activation cluster: Immunity, v. 25, p. 117-27.

Vemuri, S., and C. T. Rhodes, 1995, Preparation and characterization of liposomes as therapeutic delivery systems: a review: Pharm Acta Helv, v. 70, p. 95-111.

Villadangos, J. A., and L. Young, 2008, Antigen-presentation properties of plasmacytoid dendritic cells: Immunity, v. 29, p. 352-61.

von Andrian, U. H., and C. R. Mackay, 2000, T-cell function and migration. Two sides of the same coin: N Engl J Med, v. 343, p. 1020-34.

Vyas, J. M., Y. M. Kim, K. Artavanis-Tsakonas, J. C. Love, A. G. Van der Veen, and H. L. Ploegh, 2007, Tubulation of class II MHC compartments is microtubule dependent and involves multiple endolysosomal membrane proteins in primary dendritic cells: J Immunol, v. 178, p. 7199-210.

Vyas, J. M., A. G. Van der Veen, and H. L. Ploegh, 2008, The known unknowns of antigen processing and presentation: Nat Rev Immunol, v. 8, p. 607-18.

Wagner, J. E., J. S. Thompson, S. L. Carter, and N. A. Kernan, 2005, Effect of graft-versus-host disease prophylaxis on 3-year disease-free survival in recipients of unrelated donor bone marrow (T-cell Depletion Trial): a multi-centre, randomised phase II-III trial: Lancet, v. 366, p. 733-41.

Wagner, J. E., and E. Gluckman, 2010, Umbilical cord blood transplantation: the first 20 years: Semin Hematol, v. 47, p. 3-12.

Walker, J. D., C. L. Maier, and J. S. Pober, 2009, Cytomegalovirus-infected human endothelial cells can stimulate allogeneic CD4+ memory T cells by releasing antigenic exosomes: J Immunol, v. 182, p. 1548-59.

Wang, P., C. M. Munger, A. D. Joshi, S. J. Pirruccello, and S. S. Joshi, 2004, Cytotoxicity of cord blood derived Her2/neu-specific cytotoxic T lymphocytes against human breast cancer in vitro and *in vivo*: Breast Cancer Res Treat, v. 83, p. 15-23.

Watts, C., 2004, The exogenous pathway for antigen presentation on major histocompatibility complex class II and CD1 molecules: Nat Immunol, v. 5, p. 685-92.

Weaver, C. T., L. E. Harrington, P. R. Mangan, M. Gavrieli, and K. M. Murphy, 2006, Th17: an effector CD4 T cell lineage with regulatory T cell ties: Immunity, v. 24, p. 677-688.

Weinberger, O., S. H. Herrmann, J. L. Greenstein, M. F. Mescher, and S. J. Burakoff, 1985, The ability of Ia and H-2Kk-bearing membranes to replace the antigen-presenting cell in an H-2Kk allogeneic cytotoxic T cell response: Eur J Immunol, v. 15, p. 1013-8.

Whitelegg, A. M. E and L. D. Barber, 2004, The structural basis of allorecognition: Tissue Antigens, v. 63, p. 101-8.

Whitelegg, A. M. E., L. E. M. Oosten, S. Jordan, M. Kester, A. G. S. van Halteren, J. A. Madrigal, E. Goulmy and L. D. Barber, 2005, Investigation of peptide involvement in T cell allorecognition using recombinant MHC class I multimers: J Immunol, v. 1705, p. 1706-1714.

Williams, M. A., and M. J. Bevan, 2007, Effector and memory CTL differentiation: Annu Rev Immunol, v. 25, p. 171-92.

Witt, V., G. Fritsch, C. Peters, S. Matthes-Martin, R. Ladenstein, and H. Gadner, 1998, Resolution of early cytomegalovirus (CMV) infection after leukocyte

transfusion therapy from a CMV seropositive donor: Bone Marrow Transplant, v. 22, p. 289-92.

Wolfers, J., A. Lozier, G. Raposo, A. Regnault, C. Thery, C. Masurier, C. Flament, S. Pouzieux, F. Faure, T. Tursz, E. Angevin, S. Amigorena, and L. Zitvogel, 2001, Tumor-derived exosomes are a source of shared tumor rejection antigens for CTL cross-priming: Nat Med, v. 7, p. 297-303.

Zappasodi, R., M. Di Nicola, C. Carlo-Stella, R. Mortarini, A. Molla, C. Vegetti, S. Albani, A. Anichini, and A. M. Gianni, 2008, The effect of artificial antigen-presenting cells with preclustered anti-CD28/-CD3/-LFA-1 monoclonal antibodies on the induction of *ex vivo* expansion of functional human antitumor T cells: Haematologica, v. 93, p. 1523-34.

Zitvogel, L., A. Regnault, A. Lozier, J. Wolfers, C. Flament, D. Tenza, P. Ricciardi-Castagnoli, G. Raposo, and S. Amigorena, 1998, Eradication of established murine tumors using a novel cell-free vaccine: dendritic cell-derived exosomes: Nat Med, v. 4, p. 594-600.

Zhou, X. Y., Y. Yashiro-Otani, M. Nakahira, W. R. Park, R. Abe, T. Hamaoka, M. Naramura, H. Gu, and H. Fujiwara, 2002, Molecular mechanisms underlying differential contribution of CD28 versus non CD28 costimulatory molecules to IL-2 promoter activity: J Immunol, v. 168, p. 3847-3854.

Zhu, J. and W. E. Paul, 2008, CD4 T cells: fates, functions, and faults: Blood, v. 112, p. 1557-1569.

APPENDIX

Appendix 1: pDRIVE vector map

(courtesy of www.qiagen.com/products/cloning/pcrcloningsystem/qiagenpcrcloningkit.aspx#Tabs=t1)

Appendix 2: pET3d vector map

(courtesy of http://www.biovisualtech.com/bvplasmid/pET-3d.htm).